Développement d'un dispositif médical innovant pour la prise en charge prénatale de la hernie de coupole diaphragmatique

Nicolas Sananès

UNIVERSITÉ DE STRASBOURG

ÉCOLE DOCTORALE Physique et Chimie-Physique (ED 182)

Unité INSERM UMR-S 1121 « Biomatériaux et Bioingénierie »

THÈSE présentée par :

Nicolas SANANÈS

soutenue le : **9 juin 2017**

pour obtenir le grade de : **Docteur de l'université de Strasbourg**

Discipline/ Spécialité : Physique et Chimie-Physique

Développement d'un dispositif médical innovant pour la prise en charge prénatale de la hernie de coupole diaphragmatique

Development of a new device for the prenatal care of congenital diaphragmatic hernia

THÈSE dirigée par :

DEBRY Christian	Professeur, Université de Strasbourg
RUANO Rodrigo	Professor, Mayo Clinic (Rochester, USA)

RAPPORTEURS :

BENACHI Alexandra	Professeur, Université Paris Sud
DEPREST Jan	Professor, Katholieke Universiteit (Leuven, Belgium)

AUTRES MEMBRES DU JURY :

FAVRE Romain	Professeur, Hôpitaux Universitaires de Strasbourg
KUHN Pierre	Professeur, Université de Strasbourg
BECMEUR François	Professeur, Université de Strasbourg

Table of contents

RÉSUMÉ ÉTENDU DE LA THÈSE EN FRANÇAIS à partir de la page 178

Smart-

1. ACKNOWLEDGEMENTS

Professeur Christian Debry

Merci de m'avoir guidé au-delà des cordes vocales avec votre extraordinaire enthousiasme. Vous m'avez insufflé votre passion pour l'innovation mais aussi la conviction qu'on peut toujours y arriver.

Professeur Rodrigo Ruano

Obrigado por me guiando com sua sagacidade espumante e sua amizade benevolente. Trabalhar em Houston ao lado de alguém tão maravilhosa como você tem sido extraordinariamente gratificante para mim. Estou infinitamente grato a você por seu apoio.

Professeur Alexandra Benachi

Je me rends bien compte de l'immense honneur que tu me fais d'être rapporteur de mon travail de thèse. Tu as été la première à me montrer un utérus lorsque j'étais externe. Tu es aujourd'hui un modèle d'excellence scientifique.

Professeur Jan Deprest

Ik ben me bewust van de grote eer je hebt gedaan over mij oordelen mijn thesis. Je gemoedstoestand en relevantie hebben altijd gewekt mijn bewondering. Heel erg bedankt voor de interesse die u vriendelijk hebt gegeven aan mijn werk.

Professeur Romain Favre

Tu es à l'origine de ce projet comme de tant d'autres… Je mesure la chance que j'ai de travailler à tes côtés. La confiance que tu m'accordes, tes conseils justes et bienveillants, ont fait de moi le médecin que je suis aujourd'hui.

Professeur Becmeur

Comment ne pas être emporté dans ton tourbillon d'enthousiasme et de dynamisme ? Ton entrain passionné est communicatif et c'est un privilège de travailler à tes côtés. Merci d'avoir accepté de juger cette thèse.

Professeur Pierre Kuhn

Ta pertinence et ta sensibilité ont depuis toujours suscité mon admiration. Ton approche du soin est si juste, à la fois intelligente et bienveillante. Merci d'avoir accepté de juger mon travail de thèse.

Vous avez participé à ce projet…

Merci à l'unité INSERM UMR-S 1121 « Biomatériaux et Bioingéniérie » de l'Université de Strasbourg, et plus particulièrement Pierre Schaaf, Philippe Lavalle, Anne Schneider et Dominique Vautier. Vous m'avez accompagné depuis le début du projet jusqu'à ce jour. Nous continuerons l'aventure ensemble.

Merci à l'équipe de l'Institut de recherche contre les cancers de l'appareil digestif (IRCAD) et de l'Institut Hospitalo-Universitaire (IHU) de Strasbourg, et plus particulièrement Joël Leroy, Bruno Mutet, Juan Hernandez, Jean-Luc Dimarcq et Sophie Pernot. Vous m'avez donné les premières clés de l'innovation, vous m'avez aidé à définir le cahier des charges du ballon, vous avez participé à l'élaboration de la solution et au lancement du projet. Et vous avez également bouclé la boucle en quelque sorte, en accueillant les premiers tests animaux d'unplug !

Merci à Christian Goetz et Philippe Choquet. Vous avez participé à l'élaboration de la solution et accueilli avec beaucoup d'enthousiasme et d'ingéniosité les premiers tests au laboratoire d'imagerie préclinique des Hôpitaux Universitaires de Strasbourg.

Merci à la SATT-Conectus Alsace et plus particulièrement Anaïs Liegeon, Gabrielle Genet, Mariya Savinova et Mélany David. Vous m'avez aidé à constituer un dossier essentiel de valorisation et de transfert de technologie, vous avez financé la rédaction et le dépôt de brevet dont vous assurez la gestion aujourd'hui. Anaïs, merci infiniment d'avoir cru au projet, ton travail a été absolument déterminant. Gabrielle, merci pour tes conseils si judicieux par rapport aux questions de Brevet.

Merci à Guillaume Icre des Hôpitaux Universitaires de Strasbourg pour l'aide apportée quant aux questions de propriété intellectuelle.

Merci au cabinet Lavoix et plus particulièrement Damien Colombié pour la rédaction du brevet.

Merci à l'équipe de BS Medical Tech Industry (BS-MTI) et plus particulièrement Bertrand Basch, Raymond Basch et Valérie Lux. Vous avez participé à l'élaboration de la solution, vous avez mis au point avec beaucoup d'ingéniosité et d'enthousiasme le design du ballon et son système de pose, vous m'avez aidé à concevoir les tests, travaillé sur les aspects réglementaires et l'analyse de risques. Vous avez fait tellement… Et il nous reste tellement à faire encore ! Merci infiniment d'avoir cru à ce projet qui n'aurait jamais vu le jour sans vous. C'est un véritable plaisir de travailler avec vous. Une mention spéciale à Valérie Lux à qui je dois une partie de la rédaction de cette thèse…

Merci à Nicolas Séchet pour ses conseils de valorisation et de direction financière

Merci à l'Alsace Biovalley et plus particulièrement à Julie Freydière. Tu nous as aidé à consolider notre dossier, à recevoir le label Alsace Biovalley et à obtenir un financement sur un Partenariat Régional d'Innovation d'Alsace. Ton aide a été redoutablement efficace et déterminante.

Merci à Anne-Laure Bailly pour ses précieux conseils quant aux questions juridiques et réglementaires.

Merci à Daniel Vetter et Sébastien Molière pour m'avoir ouvert les portes de l'IRM et pour votre enthousiasme pour ce projet.

Merci à l'équipe du Centre de primatologie de l'Université de Strasbourg, et plus particulièrement Pierrick Regnard, Lyne Fellman, Yves Salmon, Laure Haelewyn et Fanélie Wanert. Vous nous avez aidé à développer le modèle du singe pour la foetoscopie et à réaliser les premières expérimentations du nouveau ballonnet. Merci pour votre compétence et votre enthousiasme. C'est chaque fois un grand plaisir de venir travailler avec vous au Fort Foch.

Merci Nicolas Mottet pour son aide et sa participation aux dernières expérimentations sur le singe.


UNIVERSITÉ DE STRASBOURG


Les Hôpitaux
Universitaires
de STRASBOURG

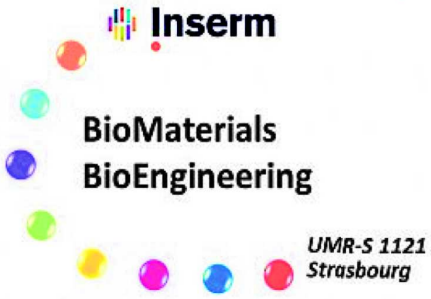
Inserm
BioMaterials
BioEngineering
UMR-S 1121
Strasbourg


ihu
STRASBOURG


ircad
France


CENTRE DE PRIMATOLOGIE


conectus
Alsace


Alsace
BioValley


BS MTI
Medical Tech Industry

Vous avez financé ce travail…

Merci à la Commission franco-américaine Fulbright d'avoir soutenu mon *research fellowship* au *Texas Children's Fetal Center* de Houston, ce qui m'a permis d'assister à des occlusions trachéales fœtales par endoscopie et de rédiger plusieurs articles en lien avec la hernie de coupole diaphragmatique.

Merci à la SATT-Conectus pour avoir financé la rédaction et le dépôt de brevet.

Merci à la Fondation de l'Avenir et au prix CASDEN du « jeune chercheur » pour avoir permis la réalisation d'un premier prototype.

Merci au Partenariat Régional d'Innovation d'Alsace qui finance la phase d'industrialisation de ce projet.

Merci au Ministère de la Santé et des Sports pour avoir soutenu le travail réalisé au Centre de Primatologie par le biais des Missions d'Intérêt Général et d'Aide à la Contractualisation

Je vous dédie cette thèse…

À Sarah. Sans toi il n'y aurait pas cette thèse mais surtout, avec toi, il y a tout.

À Axel, Romane et Charlie. Vous êtes notre synthèse. Je vous aime tellement.

À mes parents qui m'aiment tant et qui m'ont appris que l'on peut aimer tellement.

À ma famille. C'est si bon de vous avoir. Vous m'êtes essentiels.

À mes amis. Au nom du kif ! Vous êtes mon essence.

À mes collègues. Je vous dois énormément. Merci de votre soutien.

2. INTRODUCTION

2.1. Congenital diaphragmatic hernia (CDH)

2.1.1. Definition

The diaphragm develops during the 4th and 10th weeks of gestation. The septum transversum membrane growths anteriorly in order to separate the thoracic from the abdominal cavity. Then, the pleuroperitoneal fold will close posteriorly the pleuroperitoneal. Later, muscle fibers migrate into this membrane from anterior to posterior. (1-3). Due to the late closure of this membrane on the left side, left diaphragmatic hernias are more common (87% left versus 11% right, 2% are bilateral) and are predominantly posterior. Dorsal defects are called Bochdalek hernia, and anterior defects are named Morgagni hernia (4).

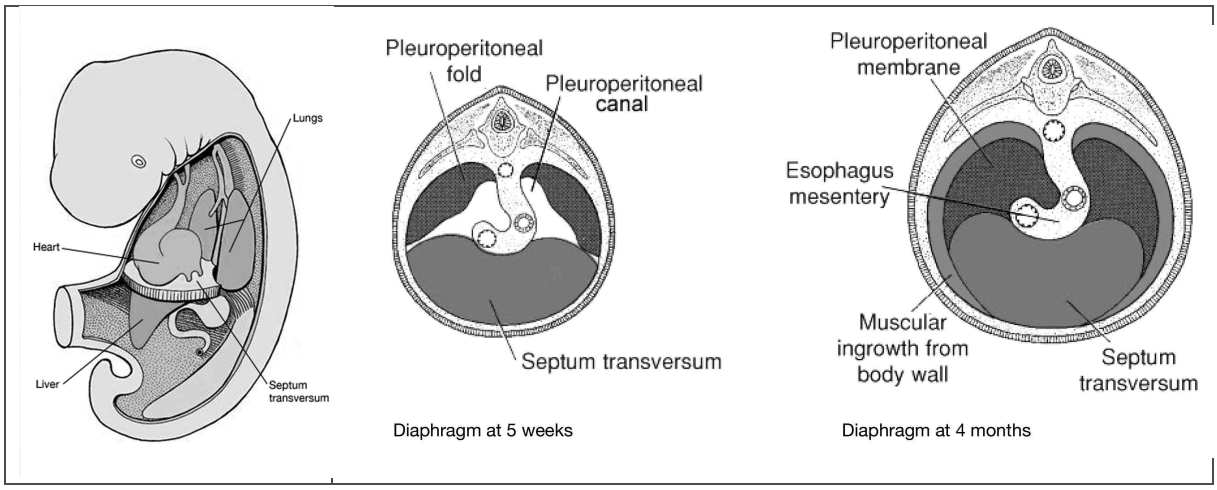

Figure 1: Embryology of the diaphragm (5)
http://www.bionalogy.com/respiratory_system.htm

2.1.2. Epidemiology

Congenital diaphragmatic hernia (CDH) is among the most common isolated fetal malformations. CDH occurs in 1/3000 to 1/5000 live births (6). This number doesn't include what has been called « hidden mortality » (7), such as stillbirths, medical termination of

pregnancy or neonatal death before transfer to a tertiary center. CDH affects about 542 to 2168 babies each year in Europe (8) and 1114 in the United States (9). Ultrasound screening programs have led to prenatal diagnosis in about 2 of 3 cases of CDH (10). 40% of cases have associated malformations, identified syndromes and/or genetic problems (11, 12). Theses associated anomalies require specific care and are independently correlated with a poor prognosis.

2.1.3. Outcomes

CDH is associated with hypoplasia of both lungs that affects airways and vessels with subsequent pulmonary hypertension. Pulmonary hypoplasia could be explained by two main mechanisms as postulated in the « dual-hit hypothesis » (13): primary affection of smooth muscles of both lungs that interfers with diaphragm development (14-16) and herniation of abdominal content into the thorax that interfers with ipsilateral lung development (17, 18). Anyhow, pulmonary hypoplasia leads to around 30 % of neonatal mortality in tertiary centers, even if CDH is a surgically correctable defect (19, 20). That's why fetal surgery is an area of interest, in order to promote lung growth during fetal life.

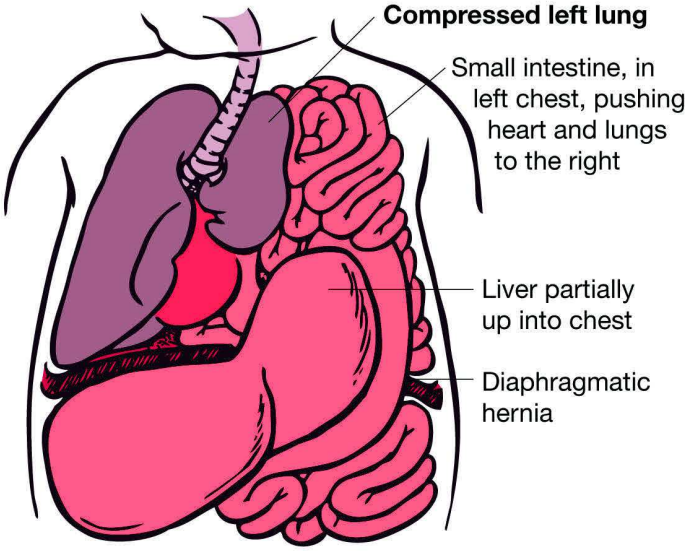

Figure 2: Illustration of CDH with lung compression (21)

https://fetus.ucsfmedicalcenter.org/cdh

2.1.4. Prenatal assessment

As prenatal intervention is a risky procedure, especially because of iatrogenic premature prelabor preterm rupture of membranes (PPROM) and early delivery, accurate evaluation is crucial to select worst cases eligible to fetal surgery. The principal prognosis factor is the lung-to-head ratio (LHR), that is the measurement of the controlateral lung quoted in relation to the head circumference (22). As the LHR depends on gestational age, it must be expressed as a function of what is expected in a gestational-age control (observed / expected): o/e LHR (23, 24). Estimation of lung size cane be done by ultrasound as well as magnetic resonance imaging (25, 26). The presence of liver herniation is also predictive (26, 27). Survival rates of fetuses with isolated left-sided CDH, depending on the measurement of the O/E LHR and the position of the liver are reported on figure 5 (28). Recently, evaluation of total lung volumes and pulmonary vascularization have been proposed for more accurate prediction of neonatal outcome (29). Lastly, fetuses with right-sided CDH seem to have a poorer outcome than that reported for fetuses with left-sided CDH with similar lung size before birth, but it's controversial (30-33).

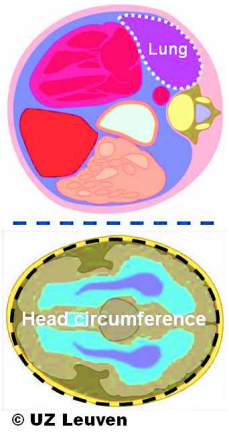

Figure 3: LHR (34)

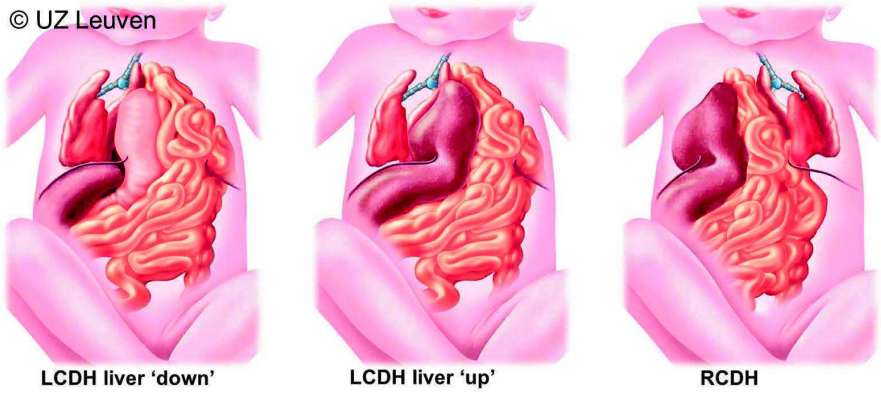

Figure 4: Illustration of liver position and CDH side (34)
http://www.totaltrial.eu/?id=13

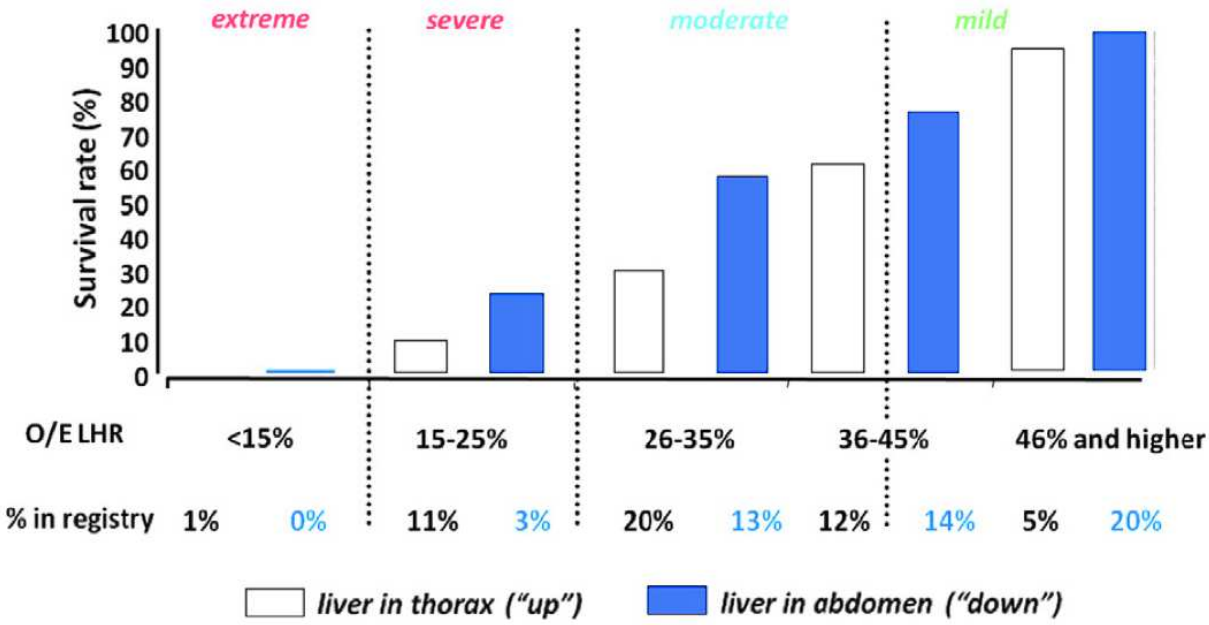

Figure 5: Survival rates of fetuses with isolated left-sided CDH, depending on the measurement of the O/E LHR and the position of the liver (28)

2.2. Fetal surgery

2.2.1. Evolution of fetal surgery

Anatomical repair of CDH in utero has been firstly attempted by Harrison *et al.* but open surgery with hysterotomy induced maternal morbidity and didn't improve newborn outcome (35, 36). Moreover, reducing CDH of fetuses with liver herniated into the thorax kinks the umbilical venous return and may lead to fetal death (37). Another approach was based on the fetal tracheal occlusion (TO). It prevents egress of lung fluid and increases airway pressure that leads to better growth of alveolar airspace and maturation of pulmonary vasculature (38-42). After experimentation on animal models (43-46), TO has been firstly performed in humans by open hysterotomy or endoscopic procedures involving maternal laparotomy (47). Minimally invasive approach has then been developed and has been called fetal endoscopic tracheal occlusion (FETO) (48). It combines percutaneous endoscopic surgery and ultrasound guidance.

2.2.2. Fetal Endoscopic Tracheal Occlusion (FETO): technical aspects

Technical aspects of FETO have been described by Deprest *et al* (49). At first, FETO was performed under general anesthesia but they moved to regional anesthesia with fetal sedation and immobilization. A thin endoscope is percutaneously introduced into the fetal trachea to position a detachable balloon between the carina and vocal cords, as illustrated by figure 6. Instrument specifications for FETO procedure are detailed in figure 7 and table 1. The balloon usually used for FETO is the Goldbal 2 detachable balloon, Balt (Montmorency, France) (off-label use), illustrated in figure 8.

Two multicenter international randomized controlled trials evaluating the interest of FETO in severe and moderate CDH are currently ongoing:

- Randomized trial of fetoscopic endoluminal tracheal occlusion (FETO) versus expectant management during pregnancy in fetuses with left sided and isolated congenital diaphragmatic hernia and severe pulmonary hypoplasia (NCT01240057).

- Randomized trial of fetoscopic endoluminal tracheal occlusion (FETO) versus expectant management during pregnancy in fetuses with left sided and isolated congenital diaphragmatic hernia and moderate pulmonary hypoplasia (NCT00763737).

  The acronym used is 'TOTAL' (Tracheal Occlusion To Accelerate Lung growth).

Severe pulmonary hypoplasia is defined by o/e LHR < 25% measured at the latest at 29 weeks and 5 days, whereas moderate hypoplasia is defined by o/e LHR between 25 and 35% (position of liver not relevant) or o/e LHR between 35 and 45% with liver in the chest.

In the severe cases, FETO is performed between 27 and 30 weeks, while in the moderate cases, FETO is performed between 30 and 32 weeks. Balloon removal is scheduled beyond 34 weeks. The tracheal release is a critical point and will be discussed further.

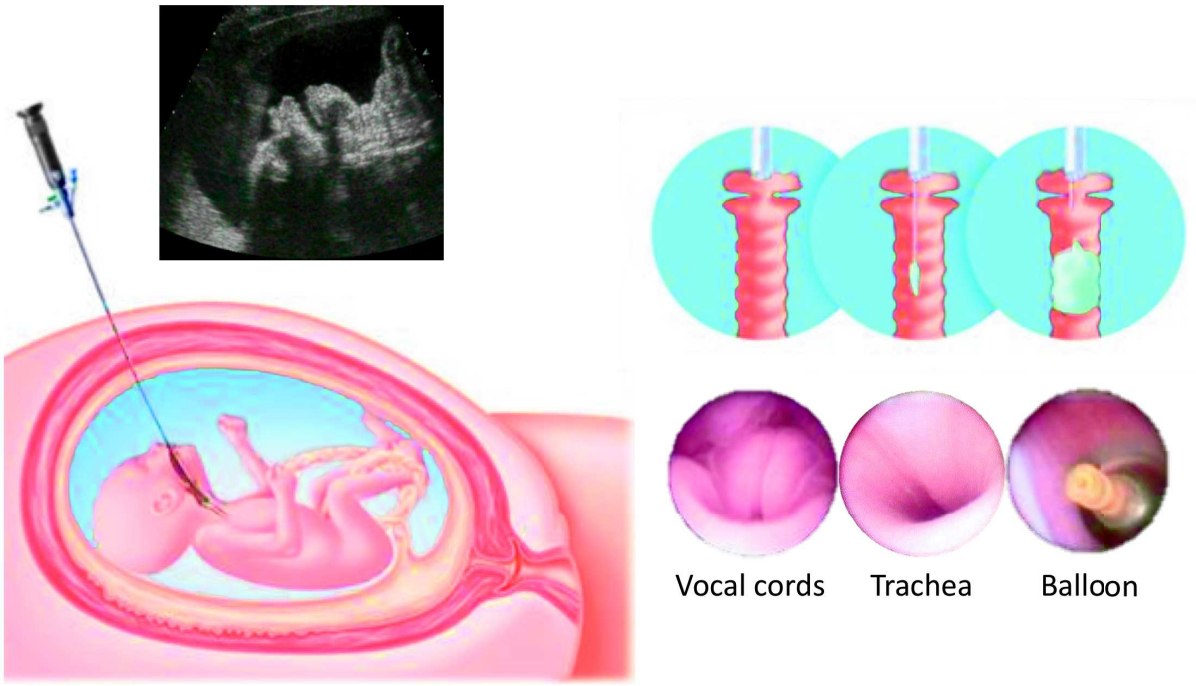

Figure 6: Illustration of FETO procedure (49)

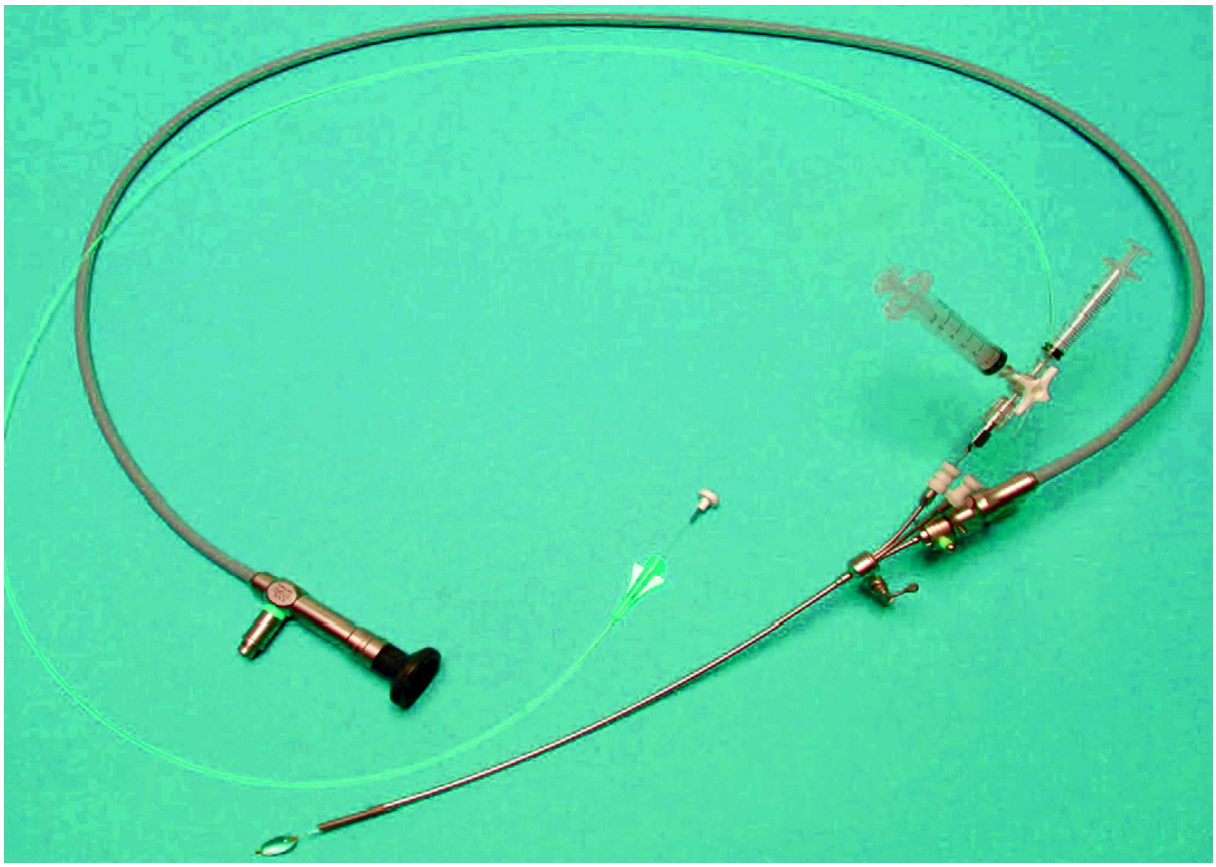

Figure 7: Instruments used for the FETO procedure (49)

Instrument	Physical properties	Other specific features
Insertion instruments		
Fetal tracheoscope, 11540AA, Karl Storz	Outer diameter = 1.3 mm Working length = 30.6 cm Opening angle = 70° Angle of view = 0° 17,000 pixels	Deported eye piece (lighter weight) Autoclavable Fiber optic endoscope (allows bending)
Tracheoscopic sheath with 3 side ports, 11540KE, Karl Storz	Outer diameter = 3.3 mm With 2 connections for instruments Working length = 30.6 cm Precurved 30°	Sandblasted tip for increased echogenicity Autoclavable Blunted tip to avoid direct trauma
Balloon removal instruments		
Inner sheath for postnatal tracheoscope, 26161CN, Karl Storz	Outer diameter = 4.3 mm Working channel = 1.7 mm, with stopcock and Luer lock connection	Together with outer sheath, it forms a continuous-flow sheath. Tip is blunted as to avoid trauma.
Continuous-flow fetoscope sheath, 26161CD, Karl Storz	Outer diameter = 5 mm With Luer lock connection	
Third-trimester tracheoscope, 26008FUA, Karl Storz	Outer diameter = 2.0 mm Opening angle = 60° Angle of view = 12° Working length = 26 cm	Autoclavable Rod lens telescope (comes also as 0° [26008AA] or 30° [26008BUA]
Retrieval forceps, 11510C, Karl Storz	Outer diameter = 1.0 mm Length = 35 cm	Semirigid Double-action jaws
Adjustable puncture stylet, 11506P, Karl Storz	Length = 50 cm Outer diameter = 0.4 mm Single use	Movable torquer allows adjustment of length to avoid overintroduction
Other instruments that are generic to fetoscopy		
Trocar, 11650TG	Pyramidal trocar, for introduction of cannula Length = 170 mm	For introduction of cannula
Cannula RCF-10.0, Check-Flo Performer Set, Cook	Outer diameter flexible cannula = 10 Fr Working length = 13 cm	
Single-use balloon and catheter systems (as used by the FETO consortium)		
GVB 16 detachable balloon, Nfocus Neuromedical (Palo Alto, CA) (off-label use)	Latex balloon, with radiopaque inclusion Outer diameter* = 1.5/8.0 mm Length* = 6.5/21 mm	Earlier marketed by Cathnet Science, and before by Nycomed. Recommended filling volume = 0.8 mL
Goldbal 2 detachable balloon, Balt (Montmorency, France) (off-label use)	Latex balloon, with radiopaque inclusion Outer diameter* = 1.5/7.0 mm Length* = 5.0/20.0 mm	Recommended filling volume = 0.6 mL
CIFN Mini-Torquer catheter, Nfocus Neuromedical (off-label use)	Length = 130 cm, tapered microcatheter supple section 20 cm Outer diameter = maximum, 0.X mm Tapered to ward the tip Guiding catheter inner diameter = 0.066"	Comes with mandrel and Toohy-Borst connection. Different lengths available
BALTACCI-BDPE catheter, Balt (off-label use)	Length = 160 cm, tapered microcatheter Outer diameter = maximum, 0.9 mm; minimum, 0.4 mm (tapered toward the tip) with guiding catheter	Comes with mandrel. Toohy-Borst (11510V, Karl Storz) Y- connection can be added. A coaxial double catheter system can be used as well.

Table 1: Instrument specifications for the FETO procedure (49)

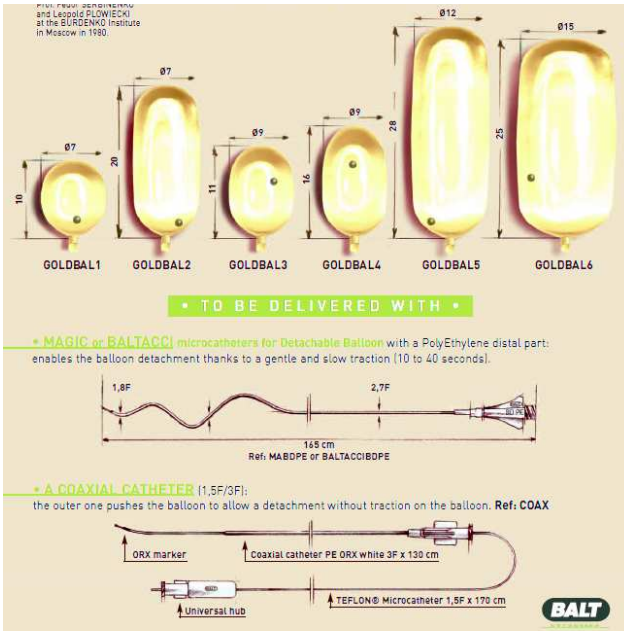

At first Balt manufactured tubes, as a subcontractor for the medical industry: tubes for catheters used in anaesthesiology, cardiology, gastrology, etc. In 1978, Professor Jean-Jacques Merlan, a pioneer in interventional radiology at Hôpital Lariboisiere in Paris, got in touch with Balt for a very special request: he required thin and supple tubes to enable the delivery of detachable balloons in cerebral arteries. At the time Balt was in the process of developing an extrusion technique to produce microcatheters with a unrivalled suppleness; It was thanks to this technology that BALT Extrusion entered the world of interventional neuroradiology. Pr. Serbinenko of the Burdenko Institute in Moscow was the inventor of the latex detachable balloon (used in treatment of aneurysms at that time). He asked Balt to develop a technology to enable mass-production of these balloons and the catheter systems necessary for their positionning. Léopold Plowiecki succeeded in producing them in 1980. Fortified by its successes, BALT began to develop its own range of products for interventional radiology: catheters for angiography, micro guidewires, valve introducers, stop-cocks, connectors and miscellaneous accessories

Figure 8: Illustration and history of Goldbal balloons (50)

2.2.3. Outcomes after tracheal occlusion

An European group published the results of the first 210 cases of severe CDH that underwent FETO (51). The median duration of FETO was 10 min and successful placement of the balloon at the first procedure was achieved in 96.7% of cases. Spontaneous PPROM occurred in 47.1% of cases and the median gestational age for delivery was at 35.3 weeks (before 34 weeks in 30.9% of cases). 97.1% of the babies were live born and 48.0% were discharged from the hospital alive. To be noted that there were 10 deaths directly related to difficulties with removal of the balloon. On the basis of the relationship between survival and o/e LHR in expectantly managed fetuses with CDH, authors estimated that in fetuses with left CDH treated with FETO the survival rate increased from 24.1% to 49.1%, and in right CDH survival increased from 0% to 35.3% ($P < 0.001$). Finally, their findings suggested that this technique may be associated with a substantial improvement in perinatal survival, with a low rate of complications. A similar increase in survival after TO has been observed in others series (52-54). *Ruano et al.* published the first randomized trial to comparing efficacy of FETO for the treatment of severe isolated CDH versus standard postnatal management alone, among 41 patients (55). Delivery occurred at 35.6 ± 2.4 weeks in the FETO group and at 37.4 ± 1.9 weeks in the controls ($P < 0.01$). In the intention-to-treat analysis, 50.0% of infants in the FETO group survived versus 4.8% in controls (relative risk (RR) 10.5, $P < 0.01$).

Two meta-analyses both showed that FETO improved survival in severe cases of CDH (56, 57). Results of the main studies are reported on table 2. Two multicenter international randomized controlled trials evaluating the interest of FETO in severe and moderate CDH are currently ongoing ('TOTAL' trial). Data on long-term morbidity is still lacking.

	Jani *et al*., 2009			**Peralta *et al.*, 2011**			**Ruano *et al.*, 2012**		
	FETO	Controls		FETO	Controls		FETO	Controls	
n	210	161		28	13		20	21	
Survival	49.1%	24.1%	p<0.001	36.0%	0%	p=0.012	50.0%	4.8%	p<0.01
Design	Cohort study			Non-randomized controlled trial			Randomized controlled trial		

Table 2: Results of the main studies evaluating survival after FETO in severe CDH

2.2.4. Balloon removal modalities

One of the major concerns about FETO procedure is the need of balloon removal. If it's feasible, fetal airway reestablishment has to be performed *in utero* for several reasons. First of all, removal of the balloon prior to delivery is crucial to achieve lung cellular maturation and therefore improve neonatal survival (49). Indeed, experimental studies have shown that TO-lungs are depleted of type II pneumocytes, which are responsible for surfactant synthesis and secretion, that leads to a lower lung compliance (58-61). Reversal of tracheal occlusion prior to delivery allows lung cellular make up recovery (62, 63). That's the reason why the « plug-unplug sequence » has been proposed and now became a standard (62, 64, 65). Moreover, there are additional secondary advantages of *in utero* removal such as the potential for vaginal delivery and above all, the easier neonatal management.

The restoration of airway potency is ideally accomplished prior to birth at 34 weeks of gestation, by either another fetal endoscopic procedure or, less frequently, by ultrasound-guided puncture (USGP) (28, 49, 51). The fetoscopy consists in a fetal tracheoscopy during which the balloon is punctured by a sharp stylet. A grasper forceps holds the tail of the balloon and allows its withdrawal. The balloon can also be punctured with a 20-G needle inserted through the maternal abdomen under ultrasound guidance. The balloon is then spontaneously washed out by the fluid coming out from the lungs.

Another scenario is that the patient presents earlier than planned, with threatening delivery, with or without ruptured membranes. Whenever clinically possible and safe, in utero removal of the balloon may be attempted. If not, the balloon can be extracted by tracheoscopy while the baby is still on the umbilical cord during conventional cesarean section under loco-regional anesthesia (49). To ensure appropriate and long-lasting placental circulation, the latter can also be done under deep inhalational anesthesia and several additional measures that allow a formal ex utero intrapartum treatment (EXIT) procedure (66, 67). The worst situation is the postnatal removal immediately after delivery on the resuscitation table by either tracheoscopy or puncture through the neck of the neonate (49).

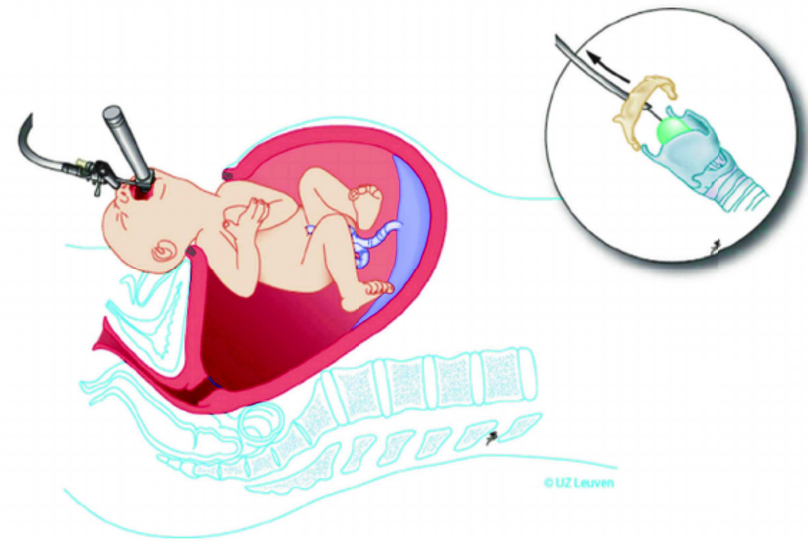

Figure 9: Removal of the balloon on placental circulation (UZ Leuven)

In the large historical series published by an European group, airway reestablishment following 210 consecutives cases of FETO was performed as followed: 69% *in utero* (50% by fetoscopy, 19% by USGP), 23% around the time of delivery (7% on placental circulation, 10% by postnatal tracheoscopy, 6% by postnatal puncture) and 8% no need for removal (failed insertion of the balloon, fetal death, termination of pregnancy, spontaneous deflation of the balloon) (49, 51). In 56% of the cases, removal of the balloon was an emergency procedure either prenatally or postnatally because of spontaneous preterm rupture of membranes, development of polyhydramnios or spontaneous preterm labor and delivery.

The experience with balloon removal of 3 centers has been recently published (68). A total of 302 in house balloon removal procedures were performed in 292 fetuses, including 10 patients where two attempts were needed (all balloons were eventually successfully removed). Techniques for removal according to the setting (elective or emergency) are reported in table 3. Airway reestablishment was performed as followed: 87.4% *in utero* (66.6% by fetoscopy, 20.8% by USGP), 12.3% around the time of delivery (11.3% on placental circulation, 1.3% postnatally). In 28.1% of the cases, removal of the balloon was performed in an emergency setting.

Balloon removal procedure	Elective (n=217; 71.9%)	Emergency (n=85; 28.1%)	Difference of proportions % (95% CI)	Total (n=302)
Ultrasound guided puncture	45 (20.7%)	18 (21.2%)	0.5 (-0.1-0.1)	**63 (20.8%)**
Fetoscopic	171 (78.8%)	30 (35.3%)	43.5 (0.3-0.5)	**201 (66.6%)**
On placental circulation	1 (0.5%)	33 (38.8%)	38.3 (0.3-0.5)	**34 (11.3%)**
Postnatal	0 (0%)	4 (4.7%)	4.8 (-0.03-0.09)	**4 (1.3%)**

Table 3: Techniques for removal according to the setting (elective or emergency) (68)

In nine cases the balloons were removed outside the FETO center: one electively by USGP, and eight emergency perinatal attempts. Four of these were removals on placental circulation and all were successful. In four cases, there was mention of primary removal in the postnatal period only. Three of them failed, with the consequent death of the newborn with the balloon still in situ.

2.2.5. Issues with balloon removal

First, balloon removal can be a difficult procedure. Among the 201 fetoscopic procedures from the study of Jimenez *et al.*, 26 attempts were categorized as difficult (12.9%) (68). The reasons why removal was classified as difficult are displayed in table 4. When the balloon could not be dislodged, operators intuitively resorted to puncture, at that time using a laser fiber. Based on that observation an adjustable stylet (Karl Storz, 11506P) was developed and introduced in 2008. Beyond that point, fetoscopic retrieval time significantly dropped, so as the number of attempts categorized as difficult (from 26.8% to 5.4%; difference 21.4%; 95% IC: 0.2 to 0.6; $P<0.05$). Due to the limited number of cases of USGP, there was no advanced analysis of difficulties.

Difficult fetoscopic removals	**26/201**
Criteria:	
Longer than 90th percentile	**21**
Difficult balloon traction/puncture	9
Difficult airway access	8
Fetal movements	3
Difficult access to amniotic cavity	1
Operator reporting as "difficult"	**5**
Difficult balloon traction/puncture	3
Fetal movements	1
Unable to remove	**1**

Table 4: Categorization of difficulties reported during fetoscopic balloon removal (68)

Second, balloon removal procedure can fail in some cases and then require a second attempt. In the series from 3 experienced centers, two attempts were needed in 10 cases out of 292 procedures (68). Moreover, even though fetal airway reestablishment should be performed ideally *in utero*, balloon removal may not be feasible by fetoscopy nor USGP and then require a removal on placental circulation or even postnatally in 12.6 to 24.7% of the cases (51, 68). Especially in an emergency setting, prenatal removal is not feasible in 41.3 to 43.5% (51, 68).

Third, balloon removal is performed in an emergency setting in 28.1 to 56% of the cases (51, 68). According to the study from Jimenez *et al*., emergency removal is not significantly associated with a higher risk of difficult procedure (68). However, airway reestablishment must be performed by a well-trained team with appropriate instrumentation and expertise, since a failure may lead to the death of the newborn, as in 3 cases out of the 9 removal outside the FETO center (68). In the series of 210 FETO from Jani *et al*., 10 cases of neonatal death (5%) were related to difficulties in removal of the balloon (51). That's why authors stated that parents should be advised to stay near or even in hospitals with expertise in balloon removal for the whole duration of fetal tracheal occlusion, since premature rupture of membranes or spontaneous premature labor can actually set off at any time. Unfortunately, such a policy would be unacceptable to most patients and it requires permanent availability of several fetal medicine or neonatal specialists.

Fourth, it is very difficult to assess the effect of in utero balloon removal but it may precipitate preterm delivery, which occured within 7 days of the procedure (*i.e.* most likely before 35 weeks of gestation) in about 25% of cases in the study from Jani *et al.* (51). This is of interest since a study suggested that neonatal survival rates after FETO were lower in infants born prematurely (43% versus 70%), particularly so in those born prior to 35 weeks of gestation compared to those born at 35 weeks of gestation or greater (18% versus 82%, p<0.001) (69). In the study from Jimenez *et al*., 23% of patients went into labor or ruptured their membranes within one week (68). To be noted however that in this series the mean gestational age at birth following elective removals was 36.6 weeks, that is one week later than what was reported in FETO patients expectantly managed using a strategy of balloon removal by EXIT (55).

Finally, there are several issues regarding the balloon removal, which are summarized in table 5.

Removal of the balloon is a difficult procedure which needs expertise
Prenatal balloon removal procedure can fail in 3.4% even in experienced centers
Balloon removal is not even feasible *in utero* in 12.6 to 24.7% of the cases
Balloon removal is performed in an emergency setting in 28.1 to 56% of the cases
Patients must stay close to a FETO center for the whole duration of the occlusion
Difficult removal of the balloon can lead to neonatal death in none well-trained centers
Prenatal removal of the balloon may induce delivery within 1 week in 25% of cases

Table 5: Issues with balloon removal

2.3. Objectives

2.3.1. Development of a new device for FETO

Our primary objective was to develop a new device for FETO in order to overcome the issues related to the unplug procedure. The development of this new device is presented in the chapter 4 'Development of a new balloon for FETO'.

2.3.2. Non-human primate model for FETO

Our secondary objective was to set-up a non-human primate model for tracheal occlusion that could be used to test the new device. This part is reported in the chapter 4 'Non-human primate model for FETO'.

2.3.3. Prediction of neonatal outcomes in case of CDH

Improving prenatal management of CDH includes the identification of the appropriate candidates for FETO. That's why we aimed to evaluate different prognostic factors and parameters related to developing lungs, liver herniation, and pulmonary vasculature. These studies are presented in the chapter 6 'Prediction of neonatal outcomes in case of CDH'.

2.3.4. Properties required for the postnatal prostheses

After birth, alive newborns with CDH require a surgical treatment that may include a diaphragmatic replacement. We aimed to determine the normal diaphragmatic growth from early childhood to adolescence in order to design a prosthesis with appropriate shape, size, and mechanical properties. This work is reported in chapter 7 'Properties required for the postnatal prostheses'

2.4. References

1. Labbe A, Coste K, Dechelotte PJ. [Congenital diaphragmatic hernia - mechanisms of pulmonary hypoplasia]. Rev Mal Respir. 2011;28(4):463-74.

2. Ackerman KG, Greer JJ. Development of the diaphragm and genetic mouse models of diaphragmatic defects. Am J Med Genet C Semin Med Genet. 2007;145C(2):109-16.

3. Babiuk RP, Zhang W, Clugston R, Allan DW, Greer JJ. Embryological origins and development of the rat diaphragm. J Comp Neurol. 2003;455(4):477-87.

4. Irish MS, Holm BA, Glick PL. Congenital diaphragmatic hernia. A historical review. Clin Perinatol. 1996;23(4):625-53.

5. Dryden R. Formation of respiratory system http://www.bionalogy.com/respiratory_system.htm.

6. Butler N, Claireaux AE. Congenital diaphragmatic hernia as a cause of perinatal mortality. Lancet. 1962;1(7231):659-63.

7. Harrison MR, Bjordal RI, Langmark F, Knutrud O. Congenital diaphragmatic hernia: the hidden mortality. J Pediatr Surg. 1978;13(3):227-30.

8. The EU-27 population continues to grow. [Internet]. Eurostat 2009. 2010.

9. Langham MR, Jr., Kays DW, Ledbetter DJ, Frentzen B, Sanford LL, Richards DS. Congenital diaphragmatic hernia. Epidemiology and outcome. Clin Perinatol. 1996;23(4):671-88.

10. Garne E, Haeusler M, Barisic I, Gjergja R, Stoll C, Clementi M. Congenital diaphragmatic hernia: evaluation of prenatal diagnosis in 20 European regions. Ultrasound Obstet Gynecol. 2002;19(4):329-33.

11. Slavotinek AM. The genetics of congenital diaphragmatic hernia. Semin Perinatol. 2005;29(2):77-85.

12. Stoll C, Alembik Y, Dott B, Roth MP. Associated malformations in cases with congenital diaphragmatic hernia. Genet Couns. 2008;19(3):331-9.

13. Keijzer R, Liu J, Deimling J, Tibboel D, Post M. Dual-hit hypothesis explains pulmonary hypoplasia in the nitrofen model of congenital diaphragmatic hernia. Am J Pathol. 2000;156(4):1299-306.

14. Featherstone NC, Connell MG, Fernig DG, Wray S, Burdyga TV, Losty PD, et al. Airway smooth muscle dysfunction precedes teratogenic congenital diaphragmatic hernia and may contribute to hypoplastic lung morphogenesis. Am J Respir Cell Mol Biol. 2006;35(5):571-8.

15. Jesudason EC, Smith NP, Connell MG, Spiller DG, White MR, Fernig DG, et al. Peristalsis of airway smooth muscle is developmentally regulated and uncoupled from hypoplastic lung growth. Am J Physiol Lung Cell Mol Physiol. 2006;291(4):L559-65.

16. Jesudason EC. Small lungs and suspect smooth muscle: congenital diaphragmatic hernia and the smooth muscle hypothesis. J Pediatr Surg. 2006;41(2):431-5.

17. Areechon W, Eid L. Hypoplasia of lung with congenital diaphragmatic hernia. Br Med J. 1963;1(5325):230-3.

18. Nakamura Y, Yamamoto I, Fukuda S, Hashimoto T. Pulmonary acinar development in diaphragmatic hernia. Arch Pathol Lab Med. 1991;115(4):372-6.

19. Gallot D, Boda C, Ughetto S, Perthus I, Robert-Gnansia E, Francannet C, et al. Prenatal detection and outcome of congenital diaphragmatic hernia: a French registry-based study. Ultrasound Obstet Gynecol. 2007;29(3):276-83.

20. Stege G, Fenton A, Jaffray B. Nihilism in the 1990s: the true mortality of congenital diaphragmatic hernia. Pediatrics. 2003;112(3 Pt 1):532-5.

21. University of California SF-TRotUoC. Congenital diaphragmatic hernia. In: https://fetus.ucsfmedicalcenter.org/sites/fetus.ucsfmedicalcenter.org/files/wysiwyg/cdh.jpg, editor. https://fetus.ucsfmedicalcenter.org/cdh2013

22. Metkus AP, Filly RA, Stringer MD, Harrison MR, Adzick NS. Sonographic predictors of survival in fetal diaphragmatic hernia. J Pediatr Surg. 1996;31(1):148-51; discussion 51-2.

23. Jani J, Nicolaides KH, Keller RL, Benachi A, Peralta CF, Favre R, et al. Observed to expected lung area to head circumference ratio in the prediction of survival in fetuses with isolated diaphragmatic hernia. Ultrasound Obstet Gynecol. 2007;30(1):67-71.

24. Jani JC, Benachi A, Nicolaides KH, Allegaert K, Gratacos E, Mazkereth R, et al. Prenatal prediction of neonatal morbidity in survivors with congenital diaphragmatic hernia: a multicenter study. Ultrasound Obstet Gynecol. 2009;33(1):64-9.

25. Knox E, Lissauer D, Khan K, Kilby M. Prenatal detection of pulmonary hypoplasia in fetuses with congenital diaphragmatic hernia: a systematic review and meta-analysis of diagnostic studies. J Matern Fetal Neona. 2010;23(7):579-88.

26. Mayer S, Klaritsch P, Petersen S, Done E, Sandaite I, Till H, et al. The correlation between lung volume and liver herniation measurements by fetal MRI in isolated congenital diaphragmatic hernia: a systematic review and meta-analysis of observational studies. Prenat Diagn. 2011;31(11):1086-96.

27. Cannie M, Jani J, Chaffiotte C, Vaast P, Deruelle P, Houfflin-Debarge V, et al. Quantification of intrathoracic liver herniation by magnetic resonance imaging and prediction of postnatal survival in fetuses with congenital diaphragmatic hernia. Ultrasound Obstet Gynecol. 2008;32(5):627-32.

28. Deprest J, De Coppi P. Antenatal management of isolated congenital diaphragmatic hernia today and tomorrow: ongoing collaborative research and development. Journal of Pediatric Surgery Lecture. J Pediatr Surg. 2012;47(2):282-90.

29. Ruano R, Takashi E, da Silva MM, Campos JA, Tannuri U, Zugaib M. Prediction and probability of neonatal outcome in isolated congenital diaphragmatic hernia using multiple ultrasound parameters. Ultrasound Obstet Gynecol. 2012;39(1):42-9.

30. Skari H, Bjornland K, Haugen G, Egeland T, Emblem R. Congenital diaphragmatic hernia: a meta-analysis of mortality factors. J Pediatr Surg. 2000;35(8):1187-97.

31. Nagata K, Usui N, Kanamori Y, Takahashi S, Hayakawa M, Okuyama H, et al. The current profile and outcome of congenital diaphragmatic hernia: a nationwide survey in Japan. J Pediatr Surg. 2013;48(4):738-44.

32. DeKoninck P, Toelen J, Zia S, Albersen M, Lories R, Coppi PD, et al. Routine isolation and expansion late mid trimester amniotic fluid derived mesenchymal stem cells in a cohort of fetuses with congenital diaphragmatic hernia. European journal of obstetrics, gynecology, and reproductive biology. 2014;178:157-62.

33. Bryner BS, Kim AC, Khouri JS, Drongowski RA, Bruch SW, Hirschl RB, et al. Right-sided congenital diaphragmatic hernia: high utilization of extracorporeal membrane oxygenation and high survival. J Pediatr Surg. 2009;44(5):883-7.

34. Leuven U. http://www.totaltrial.eu/.

35. Harrison MR, Adzick NS, Longaker MT, Goldberg JD, Rosen MA, Filly RA, et al. Successful repair in utero of a fetal diaphragmatic hernia after removal of herniated viscera from the left thorax. N Engl J Med. 1990;322(22):1582-4.

36. Harrison MR, Adzick NS, Bullard KM, Farrell JA, Howell LJ, Rosen MA, et al. Correction of congenital diaphragmatic hernia in utero VII: a prospective trial. J Pediatr Surg. 1997;32(11):1637-42.

37. Harrison MR, Adzick NS, Flake AW, Jennings RW, Estes JM, MacGillivray TE, et al. Correction of congenital diaphragmatic hernia in utero: VI. Hard-earned lessons. J Pediatr Surg. 1993;28(10):1411-7; discussion 7-8.

38. Khan PA, Cloutier M, Piedboeuf B. Tracheal occlusion: a review of obstructing fetal lungs to make them grow and mature. Am J Med Genet C Semin Med Genet. 2007;145C(2):125-38.

39. Luks FI, Wild YK, Piasecki GJ, De Paepe ME. Short-term tracheal occlusion corrects pulmonary vascular anomalies in the fetal lamb with diaphragmatic hernia. Surgery. 2000;128(2):266-72.

40. Kitano Y, Von Allmen D, Kanai M, Quinn TM, Davies P, Kitano Y, et al. Fetal lung growth after short-term tracheal occlusion is linearly related to intratracheal pressure. J Appl Physiol (1985). 2001;90(2):493-500.

41. Hashim E, Laberge JM, Chen MF, Quillen EW, Jr. Reversible tracheal obstruction in the fetal sheep: effects on tracheal fluid pressure and lung growth. J Pediatr Surg. 1995;30(8):1172-7.

42. Alcorn D, Adamson TM, Lambert TF, Maloney JE, Ritchie BC, Robinson PM. Morphological effects of chronic tracheal ligation and drainage in the fetal lamb lung. Journal of anatomy. 1977;123(Pt 3):649-60.

43. DiFiore JW, Fauza DO, Slavin R, Peters CA, Fackler JC, Wilson JM. Experimental fetal tracheal ligation reverses the structural and physiological effects of pulmonary hypoplasia in congenital diaphragmatic hernia. J Pediatr Surg. 1994;29(2):248-56; discussion 56-7.

44. Hedrick MH, Estes JM, Sullivan KM, Bealer JF, Kitterman JA, Flake AW, et al. Plug the lung until it grows (PLUG): a new method to treat congenital diaphragmatic hernia in utero. J Pediatr Surg. 1994;29(5):612-7.

45. Wilson JM, DiFiore JW, Peters CA. Experimental fetal tracheal ligation prevents the pulmonary hypoplasia associated with fetal nephrectomy: possible application for congenital diaphragmatic hernia. J Pediatr Surg. 1993;28(11):1433-9; discussion 9-40.

46. Benachi A, Dommergues M, Delezoide AL, Bourbon J, Dumez Y, Brunnelle F. Tracheal obstruction in experimental diaphragmatic hernia: an endoscopic approach in the fetal lamb. Prenat Diagn. 1997;17(7):629-34.

47. Harrison MR, Keller RL, Hawgood SB, Kitterman JA, Sandberg PL, Farmer DL, et al. A randomized trial of fetal endoscopic tracheal occlusion for severe fetal congenital diaphragmatic hernia. N Engl J Med. 2003;349(20):1916-24.

48. Deprest J, Gratacos E, Nicolaides KH. Fetoscopic tracheal occlusion (FETO) for severe congenital diaphragmatic hernia: evolution of a technique and preliminary results. Ultrasound Obstet Gynecol. 2004;24(2):121-6.

49. Deprest J, Nicolaides K, Done E, Lewi P, Barki G, Largen E, et al. Technical aspects of fetal endoscopic tracheal occlusion for congenital diaphragmatic hernia. J Pediatr Surg. 2011;46(1):22-32.

50. BALT. Goldballoon. In: BALT, editor.

51. Jani JC, Nicolaides KH, Gratacos E, Valencia CM, Done E, Martinez JM, et al. Severe diaphragmatic hernia treated by fetal endoscopic tracheal occlusion. Ultrasound Obstet Gynecol. 2009;34(3):304-10.

52. Ruano R, Duarte SA, Pimenta EJ, Takashi E, da Silva MM, Tannuri U, et al. Comparison between fetal endoscopic tracheal occlusion using a 1.0-mm fetoscope and prenatal expectant management in severe congenital diaphragmatic hernia. Fetal Diagn Ther. 2011;29(1):64-70.

53. Peralta CF, Sbragia L, Bennini JR, de Fatima Assuncao Braga A, Sampaio Rousselet M, Machado Rosa IR, et al. Fetoscopic endotracheal occlusion for severe isolated diaphragmatic hernia: initial experience from a single clinic in Brazil. Fetal Diagn Ther. 2011;29(1):71-7.

54. Kohl T, Gembruch U, Filsinger B, Hering R, Bruhn J, Tchatcheva K, et al. Encouraging early clinical experience with deliberately delayed temporary fetoscopic tracheal occlusion for the prenatal treatment of life-threatening right and left congenital diaphragmatic hernias. Fetal Diagn Ther. 2006;21(3):314-8.

55. Ruano R, Yoshisaki CT, da Silva MM, Ceccon ME, Grasi MS, Tannuri U, et al. A randomized controlled trial of fetal endoscopic tracheal occlusion versus postnatal management of severe isolated congenital diaphragmatic hernia. Ultrasound Obstet Gynecol. 2012;39(1):20-7.

56. Al-Maary J, Eastwood MP, Russo FM, Deprest JA, Keijzer R. Fetal Tracheal Occlusion for Severe Pulmonary Hypoplasia in Isolated Congenital Diaphragmatic Hernia: A Systematic Review and Meta-analysis of Survival. Ann Surg. 2016;264(6):929-33.

57. Junior EA, Tonni G, Martins WP, Ruano R. Procedure-Related Complications and Survival Following Fetoscopic Endotracheal Occlusion (FETO) for Severe Congenital Diaphragmatic Hernia: Systematic Review and Meta-Analysis in the FETO Era. Eur J Pediatr Surg. 2016.

58. Benachi A, Delezoide AL, Chailley-Heu B, Preece M, Bourbon JR, Ryder T. Ultrastructural evaluation of lung maturation in a sheep model of diaphragmatic hernia and tracheal occlusion. Am J Respir Cell Mol Biol. 1999;20(4):805-12.

59. Benachi A, Chailley-Heu B, Delezoide AL, Dommergues M, Brunelle F, Dumez Y, et al. Lung growth and maturation after tracheal occlusion in diaphragmatic hernia. Am J Respir Crit Care Med. 1998;157(3 Pt 1):921-7.

60. H IJ, Tibboel D. The lungs in congenital diaphragmatic hernia: do we understand? Pediatr Pulmonol. 1998;26(3):204-18.

61. Antunes MJ, Greenspan JS, Cullen JA, Holt WJ, Baumgart S, Spitzer AR. Prognosis with preoperative pulmonary function and lung volume assessment in infants with congenital diaphragmatic hernia. Pediatrics. 1995;96(6):1117-22.

62. Flageole H, Evrard VA, Piedboeuf B, Laberge JM, Lerut TE, Deprest JA. The plug-unplug sequence: an important step to achieve type II pneumocyte maturation in the fetal lamb model. J Pediatr Surg. 1998;33(2):299-303.

63. Bin Saddiq W, Piedboeuf B, Laberge JM, Gamache M, Petrov P, Hashim E, et al. The effects of tracheal occlusion and release on type II pneumocytes in fetal lambs. J Pediatr Surg. 1997;32(6):834-8.

64. Ruano R, Ali RA, Patel P, Cass D, Olutoye O, Belfort MA. Fetal endoscopic tracheal occlusion for congenital diaphragmatic hernia: indications, outcomes, and future directions. Obstetrical & gynecological survey. 2014;69(3):147-58.

65. Snowise S, Johnson A. Tracheal occlusion for fetal diaphragmatic hernia. American journal of perinatology. 2014;31(7):605-16.

66. Morris LM, Lim FY, Crombleholme TM. Ex utero intrapartum treatment procedure: a peripartum management strategy in particularly challenging cases. J Pediatr. 2009;154(1):126-31 e3.

67. Liechty KW. Ex-utero intrapartum therapy. Semin Fetal Neonatal Med. 2010;15(1):34-9.

68. Jimenez JA, Eixarch E, DeKoninck P, Bennini JR, Devlieger R, Peralta CF, et al. Balloon removal after fetoscopic endoluminal tracheal occlusion for congenital diaphragmatic hernia. Am J Obstet Gynecol. 2017.

69. Ali K, Grigoratos D, Cornelius V, Davenport M, Nicolaides K, Greenough A. Outcome of CDH infants following fetoscopic tracheal occlusion - influence of premature delivery. J Pediatr Surg. 2013;48(9):1831-6.

3. DEVELOPMENT OF A NEW BALLOON FOR FETO

3.1. Technical solution

3.1.1. Specifications

The first step was to define the specifications of the new device without any preconceived idea. These were defined as follow:

- Occlusion of a 7mm tube for a minimum duration of 6 weeks
- Insertion from a 1.5mm working channel of a tracheoscopic sheath.
- Non-invasive reversal occlusion.
- Easily triggered.
- Externally remote-controlled.

These specifications allowed to overcome every identified issue regarding the unplug.

Additionally, there were two different strategies. First, to develop a technology focused on prenatal treatment of CDH, which implies having limited development costs since the targeted market is small. Second, to develop a technology with other potential applications than prenatal treatment of CDH, allowing higher development costs since the targeted market is larger. Basically, the choice was to choose between a device allowing a one-time remotely controlled reversal occlusion (only useful for prenatal management of CDH) or cyclic remotely controlled occlusion (potentially useful in other conditions than CDH).

We've chosen the first strategy because our primary motivation was to improve the prenatal management of CDH and we wanted to focus on that. Moreover, we believe that developing a very small device allowing cyclic remotely controlled occlusion is technically challenging and may implies difficulties going through regulatory routes for a fetal use. For example, a US patent for a remote actuated valve implant has been filed in 2010 (US2010/0241241A). It brings into play an inductive source coil and, to be left inside the fetal trachea, a capacitor, a pick-up coil, a joule heater wire, and a thermally responsive polymer (see section 4.3.1 'Patentability study').

3.1.2. Evolution of ideas

The first idea was to develop a resorbable balloon. After analysis, this solution raised several issues. First, it was technically difficult to ensure an appropriate timing for resorption, neither too early (with no benefit from the occlusion) nor to late (no reversal of the occlusion before birth). Second, it raised the problem of fragments resulting from the degradation of the balloon that would be spread inside the tracheobronchial tree. At last, it did not fully meet the defined specifications since it did not offer a remote-controlled reversal occlusion. Indeed, this solution did not overcome the issue of the emergency setting when the patients go into labor or rupture their membranes whereas the balloon is not degraded yet. Finally, this technology has been fully abandoned.

The second idea was to develop a device incorporating the operating principle of artificial larynx ENTegral® (Protip, France). ENTegral® is an implantable device developed as a solution for patients indicated for total laryngectomy. The device partially replicates the natural functions of the larynx and the patient is again able to breathe through natural ways. The main operation system relies on a clap, which can open depending on the pressure on either side. We sought to develop a device that would allow the opening of valve only when the pressure inside the lung is high, i.e. after birth. The device would still need to be taken out afterwards but the newborn would be able to breath normally in the meantime. A potential advantage of this solution would have been to set the opening pressure in order to allow a cyclic occlusion *in utero* and restore breathing movements since early evidence suggests that it may be beneficial for lung maturity (1-3). Unfortunately, after analysis with the engineers from Protip, we realized that the development of such a device would be to challenging and was much more than a simple miniaturization process. We finally gave up this solution.

1. Nelson SM, Hajivassiliou CA, Haddock G, Cameron AD, Robertson L, Olver RE, Hume R. 2005. Rescue of the hypoplastic lung by prenatal cyclical strain. Am J Respir Crit Care Med 171:1395–1402.

2. Chapin CJ, Ertsey R, Yoshizawa J, Hara A, Sbragia L, Greer JJ, Kitterman JA. 2005. Congenital diaphragmatic hernia, tracheal occlusion, thyroid transcription factor-1, and fetal pulmonary epithelial maturation. Am J Physiol Lung Cell Mol Physiol 289: L44 – 52.

3. Muratore CS, Nguyen HT, Ziegler MM, Wilson JM. 2000. Stretch-induced upregulation of VEGF gene expression in murine pulmon- ary culture: A role for angiogenesis in lung development. J Pediatr Surg 35:906 – 912; Discussion 912–913.

The third idea was to develop a magnetic valve that would open thanks to a magnetic field. The valve would have been composed by to magnets and the permeability would have been ensured by the attraction between those. Then, the opening of the balloon would have been controlled by a magnetic field, which would have demagnetized the magnets and induced the balloon deflation. Two main mechanisms have been conceived and are illustrated in figure 10.

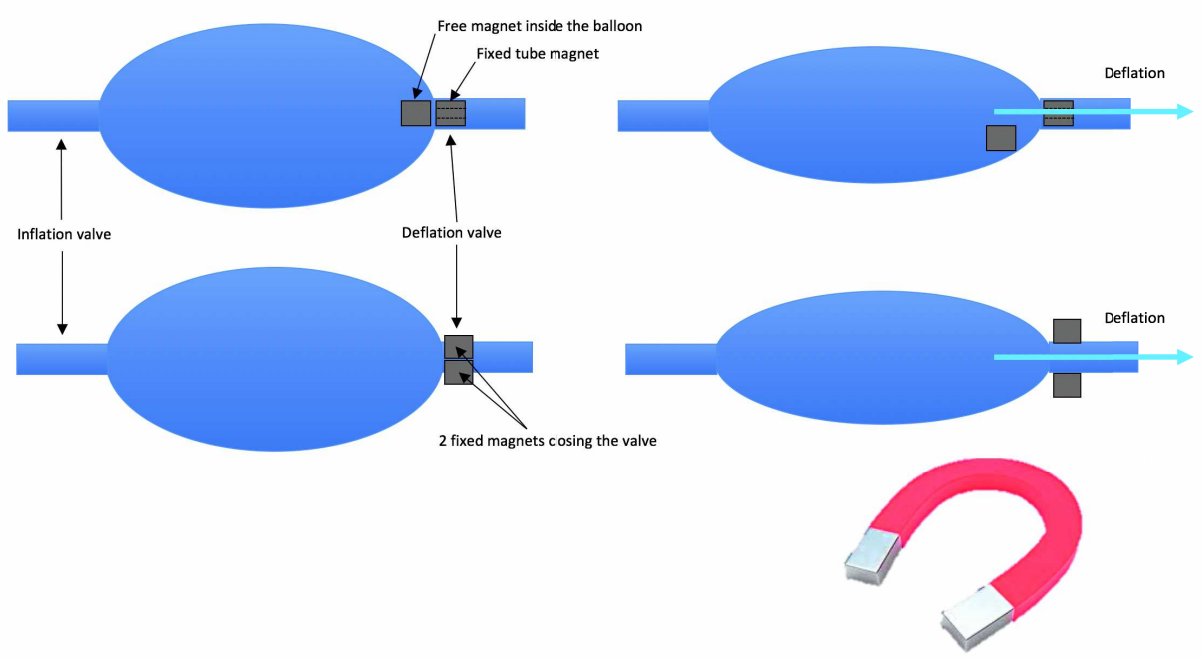

Figure 10: Principle of balloon deflation operating through demagnetization

So, we ran different tests in the preclinical imaging facility of Strasbourg University Hospital to evaluate the demagnetization induced by the fringe fields of an MRI machine. Unfortunately, we found that demagnetization was unsound because of the hysteresis phenomenon. In fact, magnet may have more than one possible magnetic moment in a given magnetic field, depending on how the field changed in the past.

Still, we decided to go on with the idea of a magnetic valve because we believe that the use of the fringe fields of an MRI machine is of interest since MRI machines are readily available in most of the hospitals. Moreover, it does not require the development of a specific controlled remote.

The fringe field is the peripheral magnetic field outside of the magnet core. Depending on the design of the magnet and the room a moderately large fringe may extend for several meters around, above, and below an MRI machine. Fields plots are available from each magnet manufacturer. To be noted that the fringe field operates near the MRI since the machine is on, with no need for an imaging acquisition. An example of fringe field is displayed in figure 11.

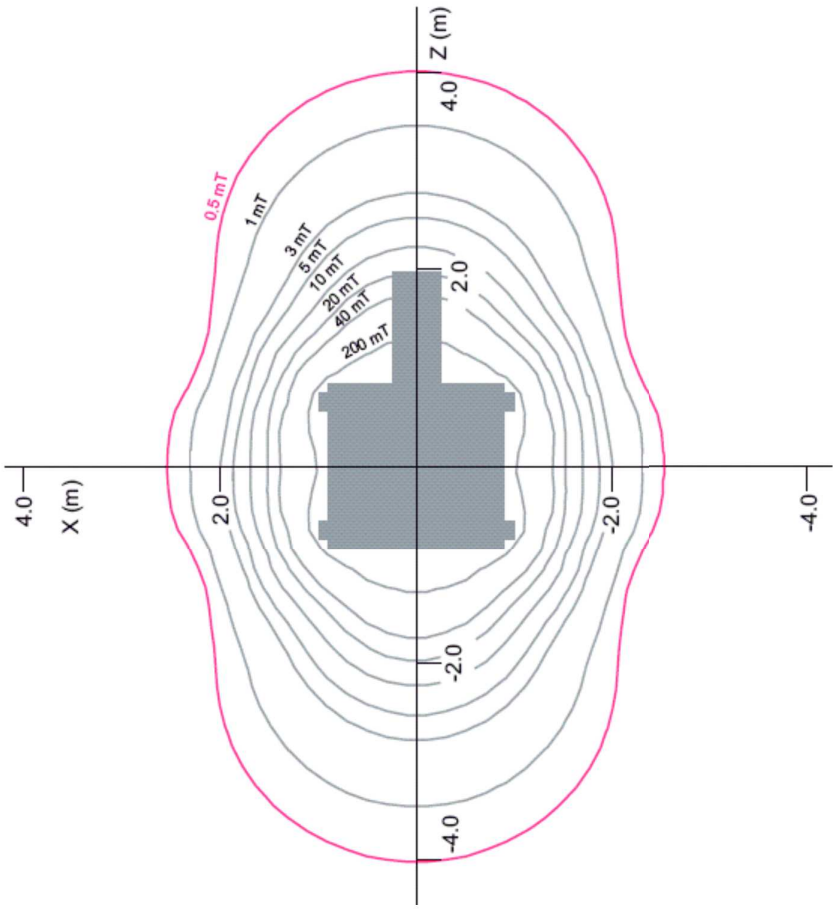

Figure 11: Fringe field of an MRI Siemens 1.5 T Avanto®

The fourth idea was to develop a magnetic valve whose opening would be operated by the attraction of a magnet, rather than a demagnetization process. At baseline, the balloon is inflated and the valve would be closed thanks to the magnetic attraction between a free of movement magnetic ball inside the balloon and a ferromagnetic ring fixed to the outer surface of the balloon. The magnetic ball would be attracted out of the ring when subjected to a magnetic field (*i.e.* the fringe field of an MRI machine) so the fluid can be released through the ring and the balloon gets deflated. Outlines of this balloon and its mechanisms are illustrated in figure 12.

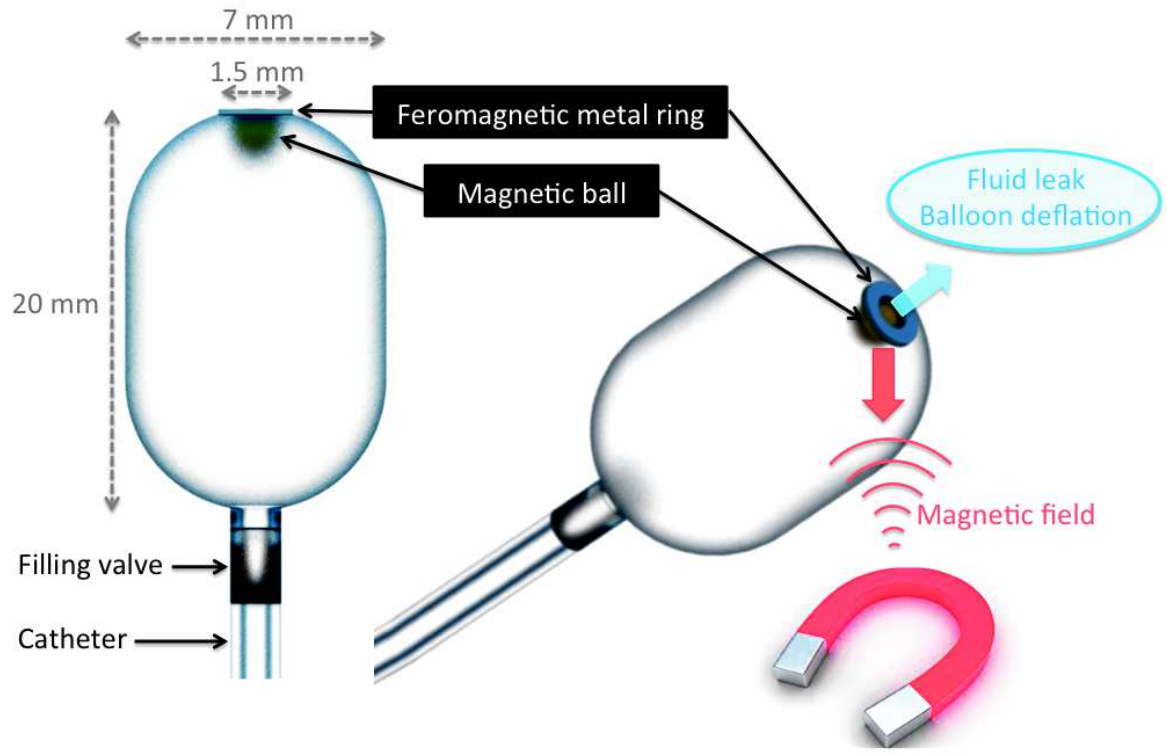

Figure 12: Principle of balloon deflation operating through magnetic attraction

The fifth and last idea was to design a balloon with a single magnetic valve allowing both inflation and deflation, according to the same operation principles. In this way, the risks related to the detachment of the ring so as several biocompatibility issues would be prevented. Finally, it would simplify as much as possible the device, which was one of our main concern.

3.1.3. Final concept

The final technical solution is as following. The single valve for both inflation and deflation is composed by an external ferromagnetic metal cylinder and a free of movement magnetic ball inside the balloon. Injection of saline through the valve moves away the ball thanks to the hydraulic pressure so the balloon can be filled. When filling is completed, the magnetic ball goes back against the metal cylinder and the impermeability is ensured by the interface of the balloon material. When the balloon is subjected to a magnetic field, the ball is attracted out of the cylinder, so the balloon gets deflated. Then, such as when the unplug is performed by ultrasound guided puncture, the balloon is then washed out by the fluid coming out from the lungs. The principle of the retained concept is displayed in figure 13.

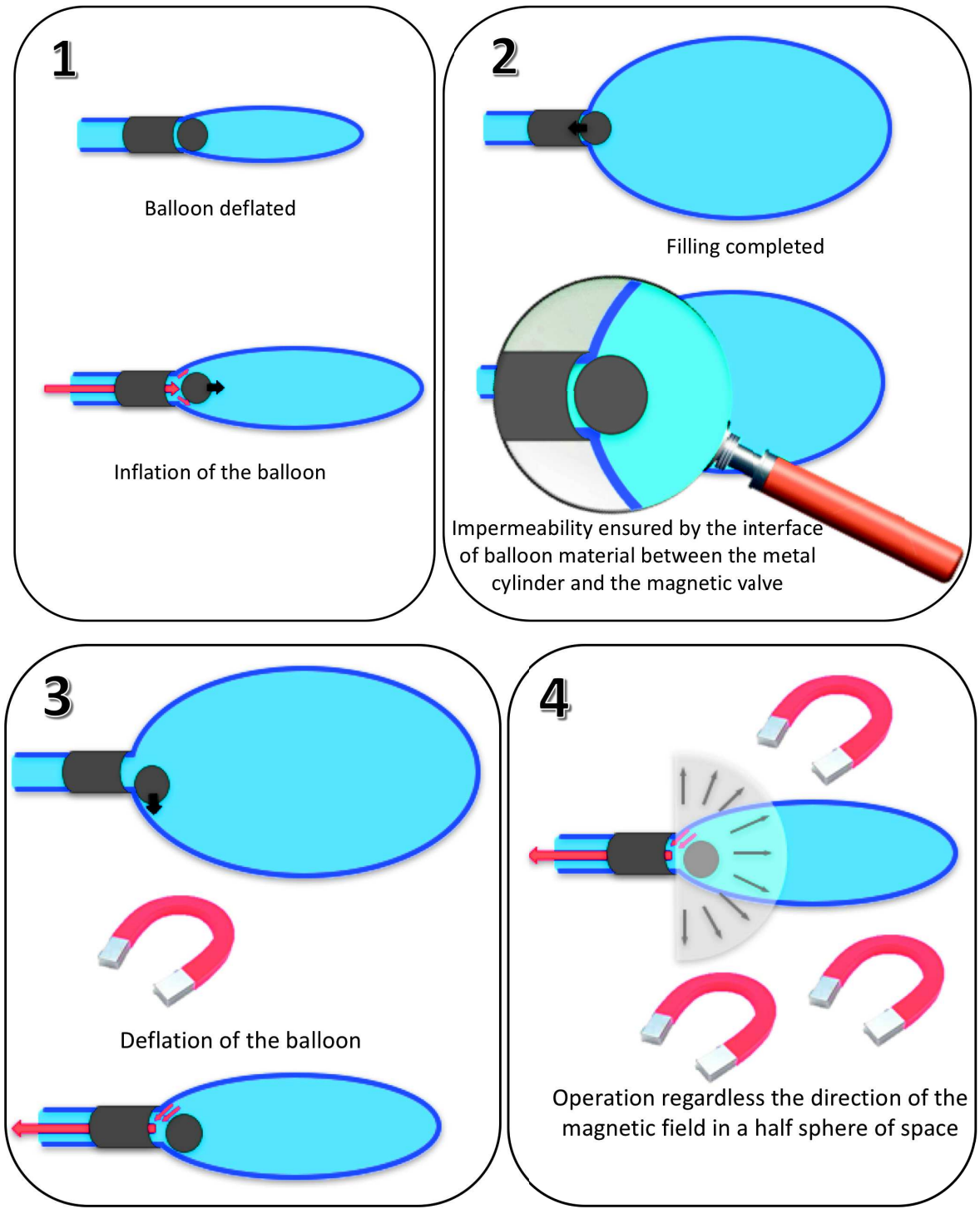

Figure 13: Principle of the retained concept for balloon operation

Finally, the retained concept is very simple since the valve is only composed by a metal cylinder and a magnetic ball, and operation only requires a fringe field of an MRI machine. To be noted that the deflation operates regardless the direction of the magnetic field in a half-sphere of space. This is a critical point, as the fetal position inside the uterus cannot be controlled. Regardless the fetal position, the valve may eventually open when the patient simply turns around the MRI machine.

3.1.4. First proof of concept

A first proof of concept has been performed in the preclinical imaging facility of Strasbourg University Hospital. A condom has been used as a balloon and was filled with air through a hole on its top. A deflation valve using a magnet and a metallic tube was arranged and the base of the condom. When subjected to a magnetic field of 60 mT, the magnet was attracted inducing the opening of the valve and the deflation of the balloon.

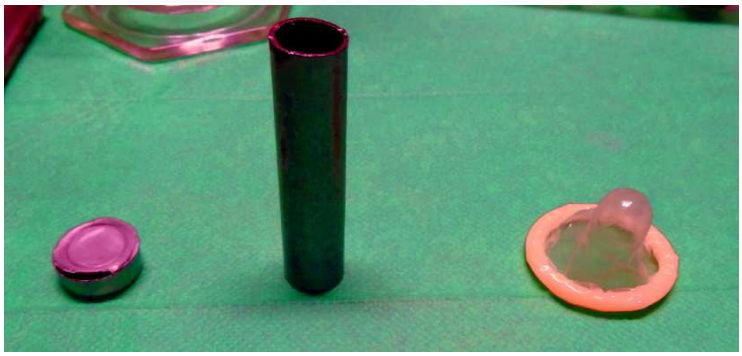

Material

Magnet / metallic tube / condom

Balloon with the valve

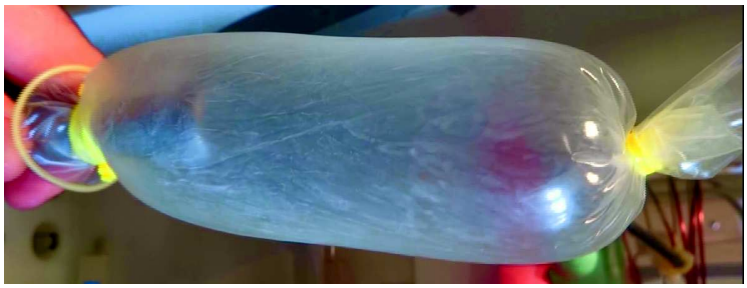

Away from the MRI,
the valve is closed.

Close to the MRI, the valve opens
allowing the deflation of the balloon

Figure 14: First proof of concept

3.2. Prototyping of the balloon

3.2.1. Identification of an industrialist

Several companies and industrialists have been approached and considered:

- 'Cousin biotech' develops and markets innovative products for visceral, spine, uro-gynecology and obesity surgery. This company is specialized in hand-manufactured implantable flexible medical devices.

- 'Protip' is a company specialized in implantable devices developed as a solution for patients indicated for total laryngectomy.

- 'Acclarent' develops and advances innovative technology for Otolaryngology. This company manufactures a balloon for sinuplasty.

- 'Sterne' is a company specialized in manufacturing and developing products made of silicone, elastomers and rubbers.

- 'Statice' transforms and develops bio-materials such as silicone moulding, plastics injection systems, bioresorbable injection, Ultrasound welding, and electrospinning.

Finally, the industrialist 'BS Medical Tech Industry' (BS-MTI) has been identified thanks to SATT-Conectus Alsace, which is a collaborative research and technology transfer company. BS-MTI is specialized in the design and the manufacturing of medical devices. The company has been created in 2008 and is located in the north of Alsace region in France. Several members of the team have over twenty years' experience in the field of single use medical devices. For the moment, BS-MTI mainly develops and produces medical devices for the field of urology and minimal invasive surgery.

One of the strengths of the company is the knowledge in the field of inflatable balloons (various raw material: polyurethane, polyisoprene, silicone,…) and catheter systems. Moreover, BS-MTI is also specialized in product development, prototyping and small scale production.

3.2.2. Choice of the material for the balloon

Several manufacturing processes and materials have been considered for the balloon itself: polyisoprene, latex-free material, and latex.

A first polyisoprene balloon was filled with saline solution. Dimensions and shape of the inflated balloon were correct. Then, the balloon was kept at room temperature for four weeks. At the end of that experiment, the balloon was totally damaged and detached from its support. Since this polyisoprene balloon was degraded really fast, polyisoprene was eliminated from the choice of balloon material.

Figure 15: Polyisoprene balloon 4 weeks after inflation with saline

A latex free material has also been tested in order to consider its use for Smart-TO balloon manufacturing. That material study was part of the process of non-allergic material search. One of the manufacturing process consisted in a distal end forming of the balloons by tube welding. Pieces of 5 cm long were cut from latex free tube. The distal end was then formed with a toss welding machine and the balloons were manufactured using the so obtained sealed tubes. When manufacturing these balloons, it was noticed that the material was really hard to introduce inside the metal cylinder as it had a tendency to break. Second, the latex free tubes walls had a tendency to stick together when manipulated thus making it hard to introduce the magnetic ball inside the tubes. Finally, it came out that in case this material and manufacturing methods were retained, the process had to be improved in terms of appearance.

Figure 16: Distal end forming of latex free balloons by tube welding

Another manufacturing process tested for latex free balloon distal end forming was point forming. Pieces of 8 cm long were cut from the 0.2 mm tube and a 0.9 mm diameter rod was then introduced inside the latex free tubes. The introduction of the rod inside the tube was hard as the tube form pleated. Tube and rod were then introduced into a glass form at a high temperature for a couple of seconds. The set was cooled down before the tube with formed point was extracted from glass tube and rod. Magnetic valve balloons were finally manufactured using the so obtained pointed tubes. However, none of the balloons could be filled as all the so formed distal end were leaking. As a consequence, even if that forming technique improved the appearance of the distal end of latex free balloons, the further permeability tests and mechanical measurements were performed on the tubes obtained with welding technique.

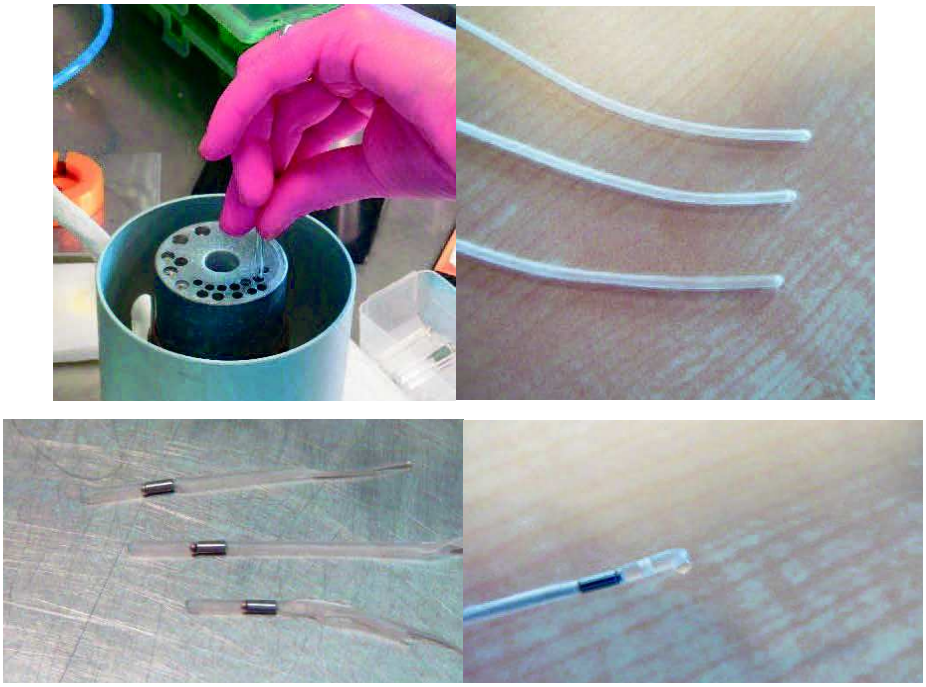

Figure 16: Distal end forming of latex free balloons by point forming

Permeability tests were conducted on latex free balloons formed by tube welding. They were filled with air or saline and were left out in ambient air or put in amniotic fluid. The balloon filled with saline and left in amniotic fluid was the closest to real circumstance of balloon use. That balloon has been observed for almost a month, and neither the length nor the diameter significantly decreased across time. Such observation lead to the conclusion that the latex free material had a good permeability function.

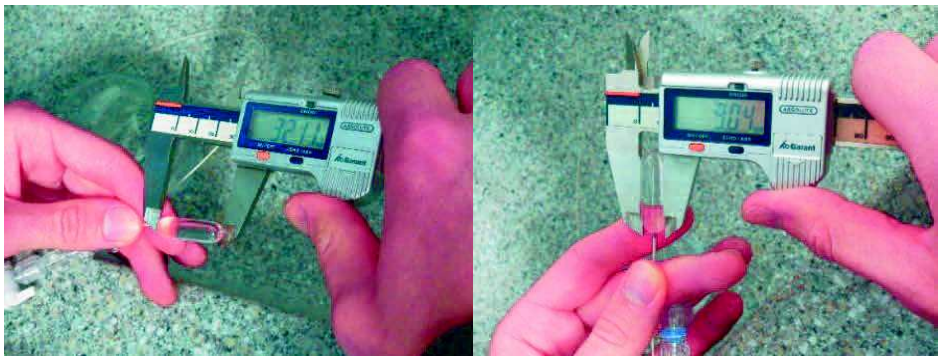

Figure 17: Measurements of the latex free balloon

Length (in cm)	Filled with air	Filled with saline in air	Filled with saline in amniotic fluid
02/03/2017	19.54	17.1	16.63
03/03/2017	7.67	15.89	16.2
06/03/2017	6.85	15.34	15.67
07/03/2017		14.6	15.56
10/03/2017		13.93	15.49
13/03/2017		13.51	15.46
22/03/2017		12.08	15.22
31/03/2017			15.2
07/04/2017			15.2
14/04/2017			15.2

Diameter (in cm)	Filled with air	Filled with saline in air	Filled with saline in amniotic fluid
02/03/2017	8	7.9	7.9
03/03/2017	3.2	8	8
06/03/2017	1.9	7.9	8
07/03/2017		7.8	8
10/03/2017		7.6	8
13/03/2017		7.4	8
22/03/2017		6.9	8
31/03/2017			8
07/04/2017			8
14/04/2017			8

Tables 6 and 7: Measurements of the latex free balloon across time

Mechanical tests were performed on latex free balloons formed by tube welding. They were carried out by over inflating the balloon with 3 mL of saline. It showed a good resistance and resistance at break. However, after deflation, the latex free balloon did not get back to its initial size and shape. Before the first inflation, the length and diameter were 6 and 1 mm, whereas they changed to 14 and 3 mm after inflation and deflation. That is a serious issue because before being used the balloons should be filled a first time in order to test their integrity. At that stage, if the balloon does not get back to its initial size and shape, one can't control final size and volume when inflating in trachea. On top of that, if the balloon does not get back to its initial size after inflation test, it won't be possible to back it up inside the endoscopic sheath. As a conclusion, that latex free material was no longer considered.

Finally, latex was chosen as the material for the balloon. Permeability and mechanical characteristics of latex are well known and we performed preliminary tests confirming that latex material fulfilled specifications required. Further tests along the product development route were performed to validate with larger scale protocols these preliminary development choices. They are reported further in chapters 4.5.1 'permeability tests' and 4.5.2 'occlusion tests'.

3.2.3. Choice of the materials for the metal tube and the magnetic ball

The material chosen for the metal tube is a ferritic stainless steel type 430. In comparison to austenitic steels, which have a face-centered cubic grain structure, ferritic steels are defined by a body-centered cubic grain structure. In other words, the crystal structure of such steels is comprised of a cubic atom cell with an atom in the center. This grain structure is typical of alpha iron and is what gives ferritic steels their magnetic properties.

Ferritic steels cannot be hardened or strengthened by heat treatment, but have good resistance to stress-corrosion cracking. They can be cold worked and softened by annealing. While not as strong or corrosion resistant as austenitic grades, the ferritic grades generally have better engineering properties. Though generally very weldable, some ferritic steel grades can be prone to sensitization of the weld heat-affected zone and weld metal hot cracking. Weldability limitations, therefore, restrict the use of these steels to thinner gauges.

The type 430 is the most commonly used ferritic steel. It has a higher chromium content and is, consequently, more resistant to corrosion by nitric acids, sulfur gasses and many organic and food acids.

The material chosen for the magnetic ball is neodymium, which is the strongest magnet material available. Neodym magnets are manufactured from rare powder materials under high pressure and are then coated with thin metal layers. Mostly these magnets are covered with a metallic coating which does not protect against corrosion in humid conditions. The magnetic ball we chose is coated with nickel, which is a sufficient protection against corrosion in dry ambients but not in humid conditions. We chose to perform an additional parylene coating as it's the only efficient protection (see chapter 4.2.4 'Choice for biocompatibility solution').

Tolerances : DIN ISO 2768-1m
ROHs (2011/65/EU) & REACh (2007/EU)
Outer diameter(D) = 1 mm
Material, Grade: Neodymium NdFeB / N35
Coating: Nickel
max.operation temperature = 80°C
Flux density inside the magnet 1.17 Tesla
Temperature coefficient flux = 0.11% per 1°K
Dead weight: 0.01 g
Holding force on a steel plate 0.2 Newton
Weight, which the magnet can lift: 0.02 kg

Table 8: Characteristics of the magnetic ball

3.2.4. Choice for biocompatibility solution

The biocompatibility of the metal tube and magnetic ball is ensured by a parylene coating. Parylene is a polymer film that is used as a protective coating for many metallic and non-metallic materials. It provides environmental and dielectric insolation in a variety of applications, including various medical devices. The most important properties of Parylene coating are uniformity and completeness of coverage and physical, electrical, chemical, mechanical and barrier properties. The thin films are of high optical quality, the mechanical characteristics are high tensile and yield strength, uniform thickness on all surfaces. Beyond preventing stiction due to its resistance to friction, a Parylene coating has many beneficial characteristics to ensure it works well with a wide variety of design requirements. The strong

particle retention is best for the upgrading of electronic and mechanical devices. For the Medical or Food and Beverage Industries, Parylene is FDA approved with a Class VI bio-compatibility rating.

Finally, as illustrated in figure 18, parylene is an excellent barrier to oxygen, moisture, chemicals, solvents, acids, carbon dioxide, fungus, bacteria, water vapor, and many other elements. It is bio-compatible, anti allergic and best suitable for medical applications. Parylene is light-weight, highly reliable, and has excellent adhesion properties. Due to its low coefficient of friction it is used as a dry film lubricant.

Figure 18: Characteristics of several coating solutions including parylene

3.2.5. Frozen design

The balloon is made of latex material and its dimensions are 1.42mm x 6mm when deflated and 7mm x 20mm when inflated with 0.7mL of saline. The magnetic ball is included inside the balloon and is free of movements. It is made of Neodymium NdFeB / N35 and its diameter is 1mm. The metal tube cylinder is made of ferritic stainless steel type 430 and its dimensions are 1.3mm x 3mm. At the balloon side, the impermeability is ensured by a chamfer hosting the magnetic ball with a latex interface. On the other side, there is a latex tube whose dimensions are 1.42mm x 2.5mm. The metal tube and the magnetic ball are both coated with parylene. Outlines of this final design are displayed in figure 19.

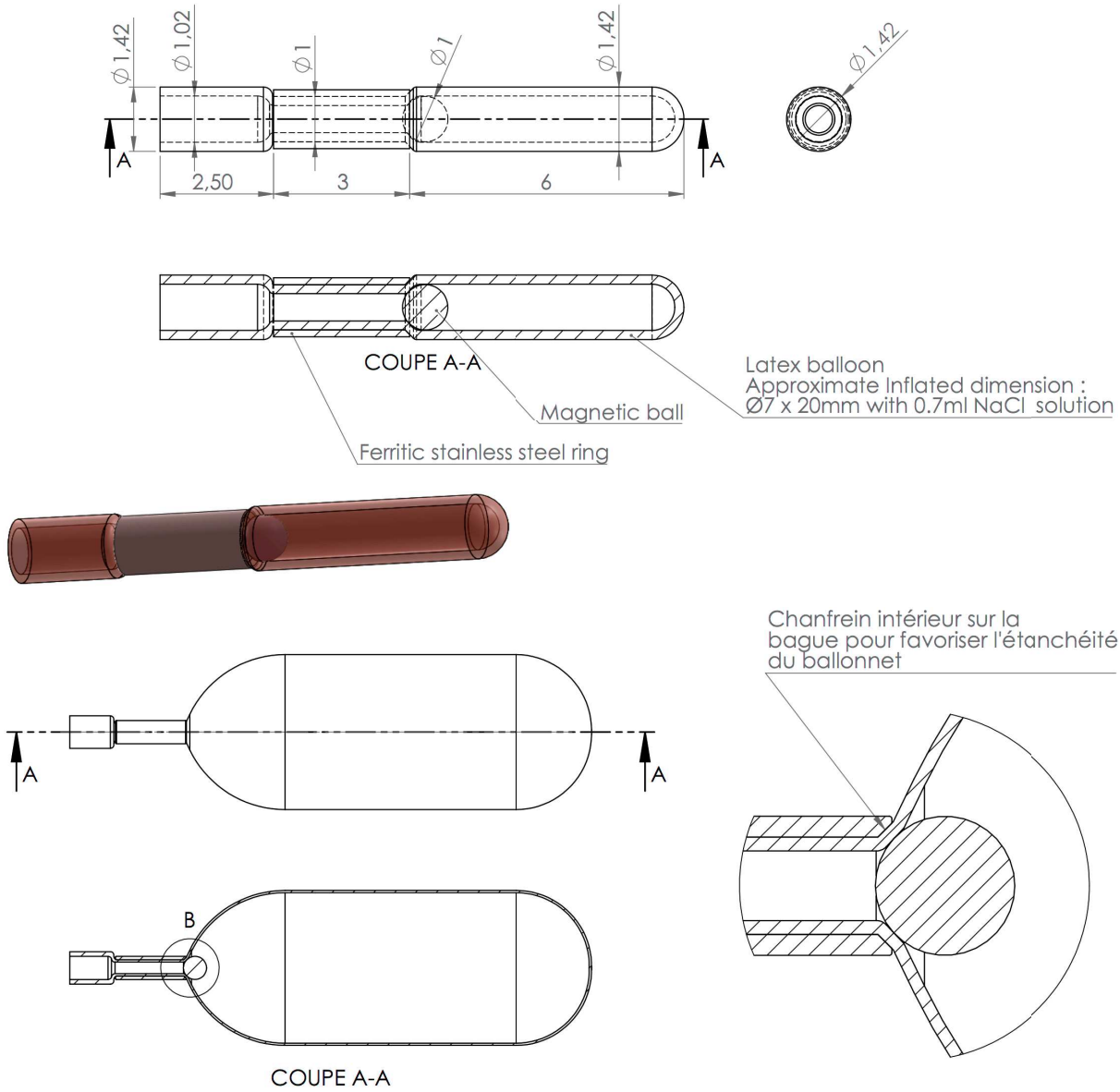

Figure 19: Outlines of the frozen design

3.2.6. Second proof of concept

The second proof of concept was conducted with a prototype scale 1/1, manufactured according to the frozen design presented above. This experiment took place in the imaging department of Strasbourg University Hospital, using 1.5 T and 2T MRI machines. The balloon was inflated inside a transparent tube of 7mm materializing the fetal trachea. The device was then moved towards the MRI machine and got deflated in seconds when subjected to a magnetic field of approximatively 0.4 T, *i.e.* 30 to 40 cm to the scanner tube depending on the MRI machine. Operation was reproducible when presenting the device with different angles.

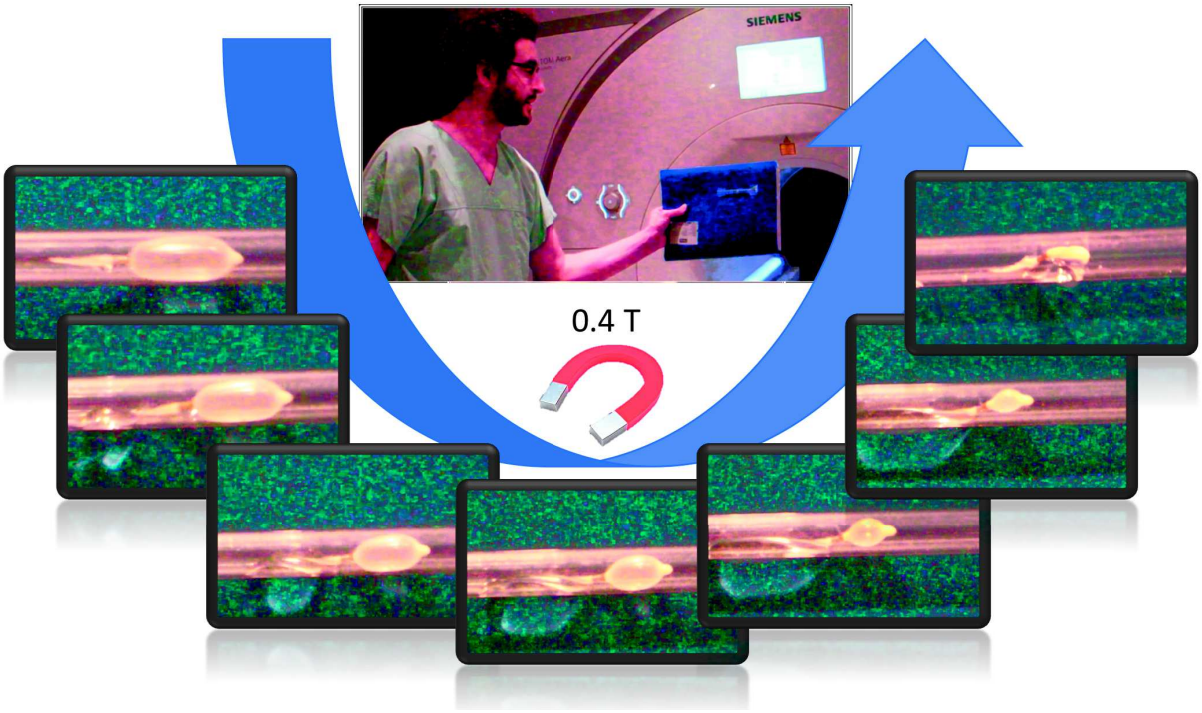

Figure 20: Second proof of concept with MRI machine

The prototype has also been tested with a high-fidelity simulator for FETO insertion and removal (Windrim R, Ryan G, Lebouthillier F, et al. Development and use of a high- fidelity simulator for fetal endotracheal balloon occlusion (FETO) insertion and removal. Prenat Diagn 2014;34:180e4.). We used a 1.3 mm endoscope (11540AA) and a 3.3 mm sheath (11540KE) manufactured by Karl Storz ®. The delivery catheter was pushed through a side port and the balloon was placed on its distal end. Then the delivery system was moved back in the fetoscope until the balloon is completely inside. The placement of the balloon in the trachea was performed according to the same principles than FETO technique. Finally, a 0.4 T magnet was positioned in front of the fetal neck and we could see the balloon get empty since we left the fetoscope inside the fetal trachea. This experiment is illustrated in figure 21.

Placement of the balloon on the catheter before moving back inside the fetoscope

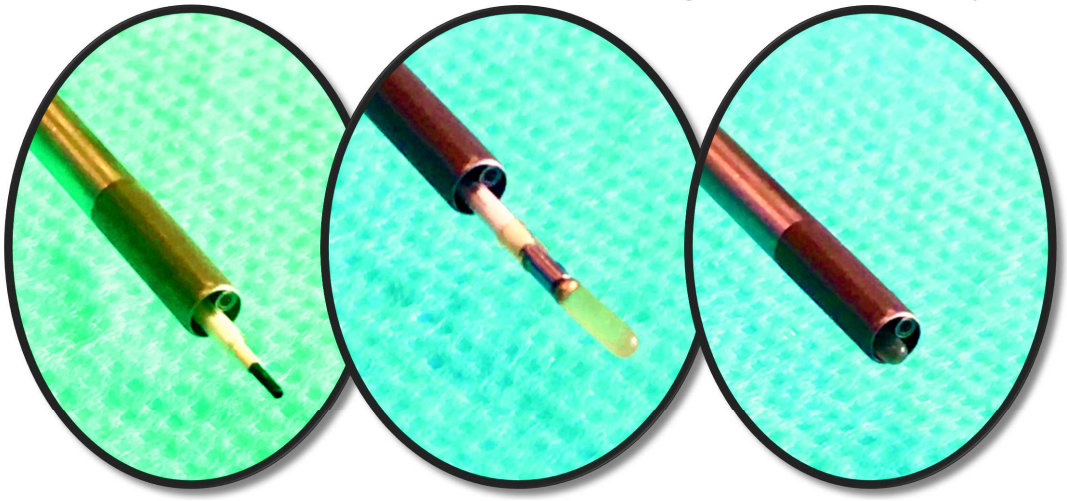

High-fidelity simulator for FETO, endoscopic instruments, balloon and delivery catheter

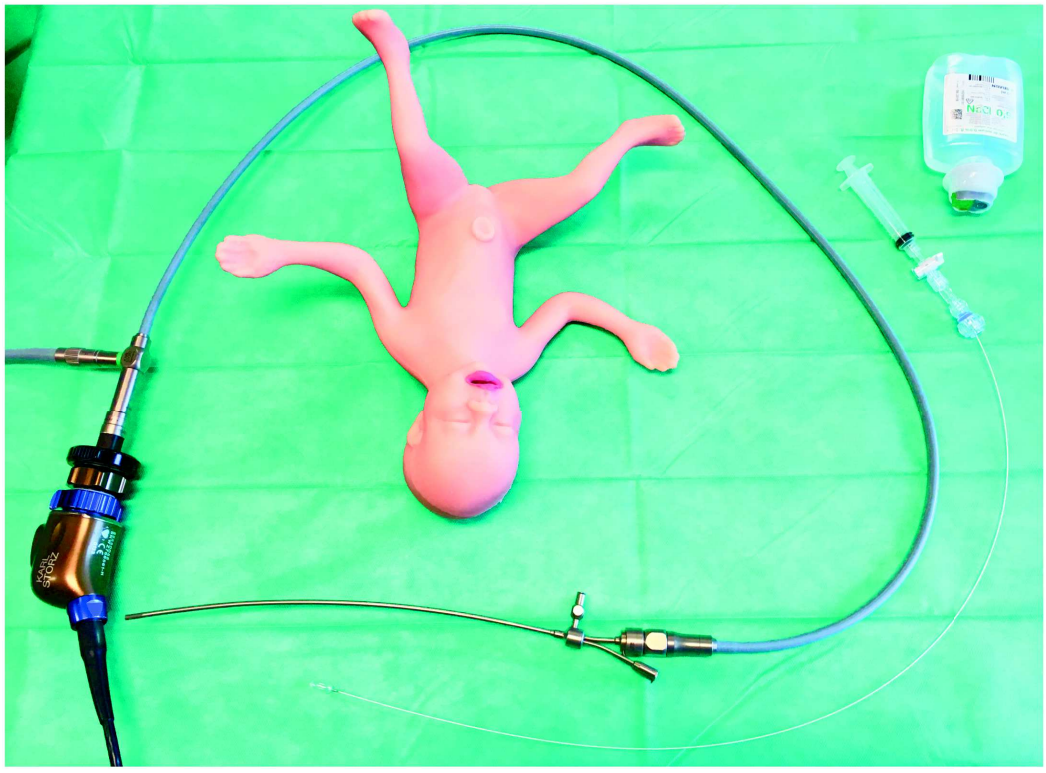

Balloon inflated inside the trachea

Saline coming out from the balloon

Balloon deflated inside the trachea

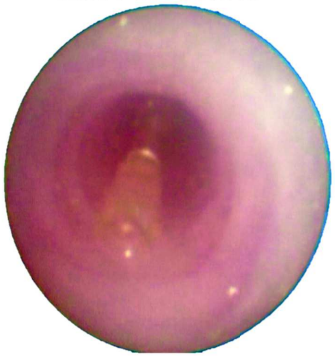

Figure 21: Second proof of concept with high-fidelity simulator for FETO

3.3. Prototyping of the delivery system

3.3.1. Development of the delivery system

The first delivery system was formed from a black peek tube inserted into a white peek tube, which internal diameter was slightly bigger than the external diameter from the black peek tube. These two peek tubes were glued at distal end, so that the black peek tube was 2.5 mm longer than the white peek tube. On the proximal end, the black tube was longer than the white tube. A male Luer Lock adapter and a female/female fitting were plugged so a syringe could be screwed.

The black peek tube enabled to infuse liquid into the balloon. Its small diameter allowed it to penetrate inside the latex balloon up to the internal part of the metal tube. The white peek tube glued 2.5 mm from the end of the black peek tube created a stop so that the black tube did not penetrate too far and push the magnetic ball away from the metal tube.

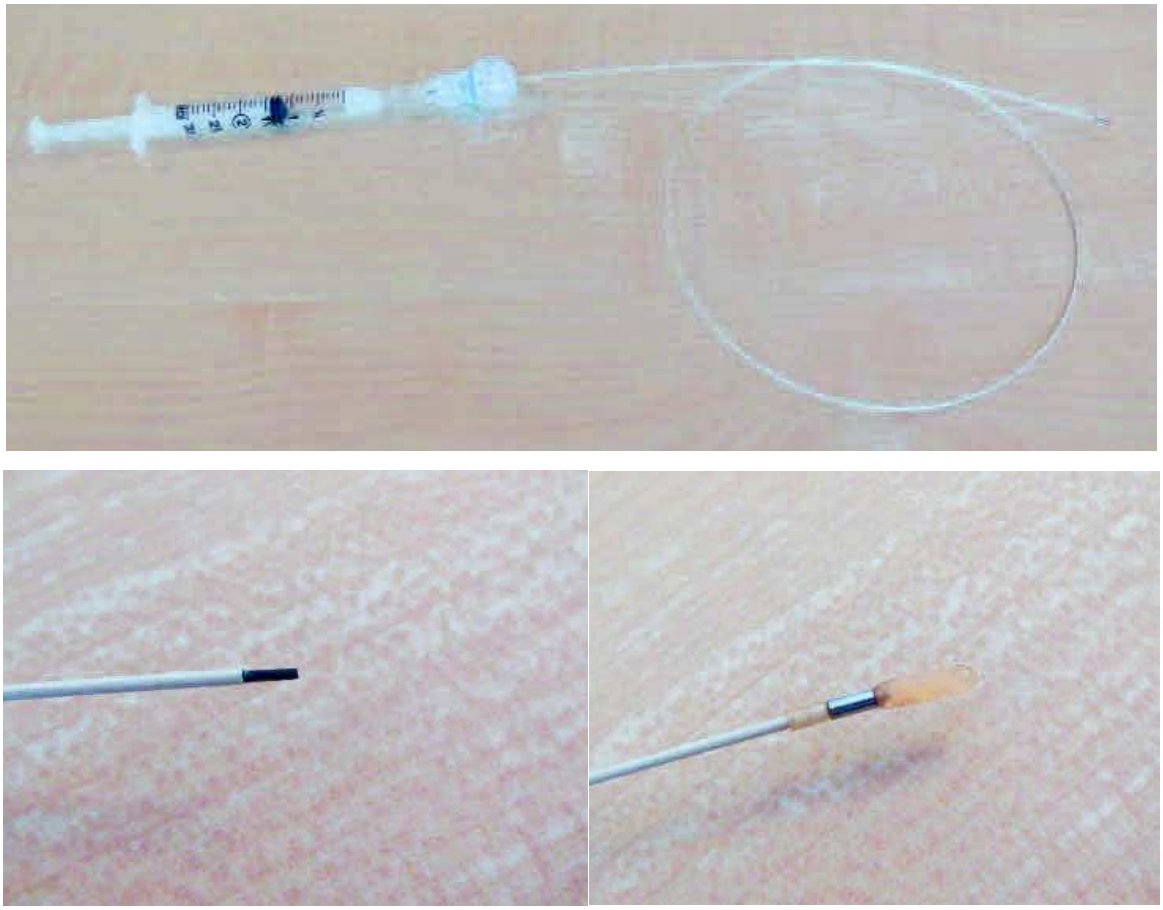

Figure 22: First delivery system

However, preliminary risks analysis pointed out that the balloon could unplug during the FETO procedure when operator moves back the delivery system inside the endoscopic sheath. Indeed, the diameter of the balloon was larger than the diameter of the delivery system. Delivery system had to be improved on the distal end to avoid this issue.

Moreover, before use of the balloon, the operator should be able to inflate the balloon to check its integrity, and therefore be able to deflate it. In the same way, it can be necessary to deflate the balloon during the surgery in case of inappropriate positioning in the fetal trachea. Finally, improvement of the delivery included the development of a stylet that could be inserted inside the black peek tube and allow the deflation of the balloon by pushing the magnetic ball away from the metal tube.

Regarding the development of the distal end of the delivery system in order to avoid accidental unplug, the solution of an external third tube over the black and white peek tubes was retained. This tube has the exact same diameter than the balloon, what prevents the risk of a hanging of the balloon when this one is moved back inside the endoscopic sheath.

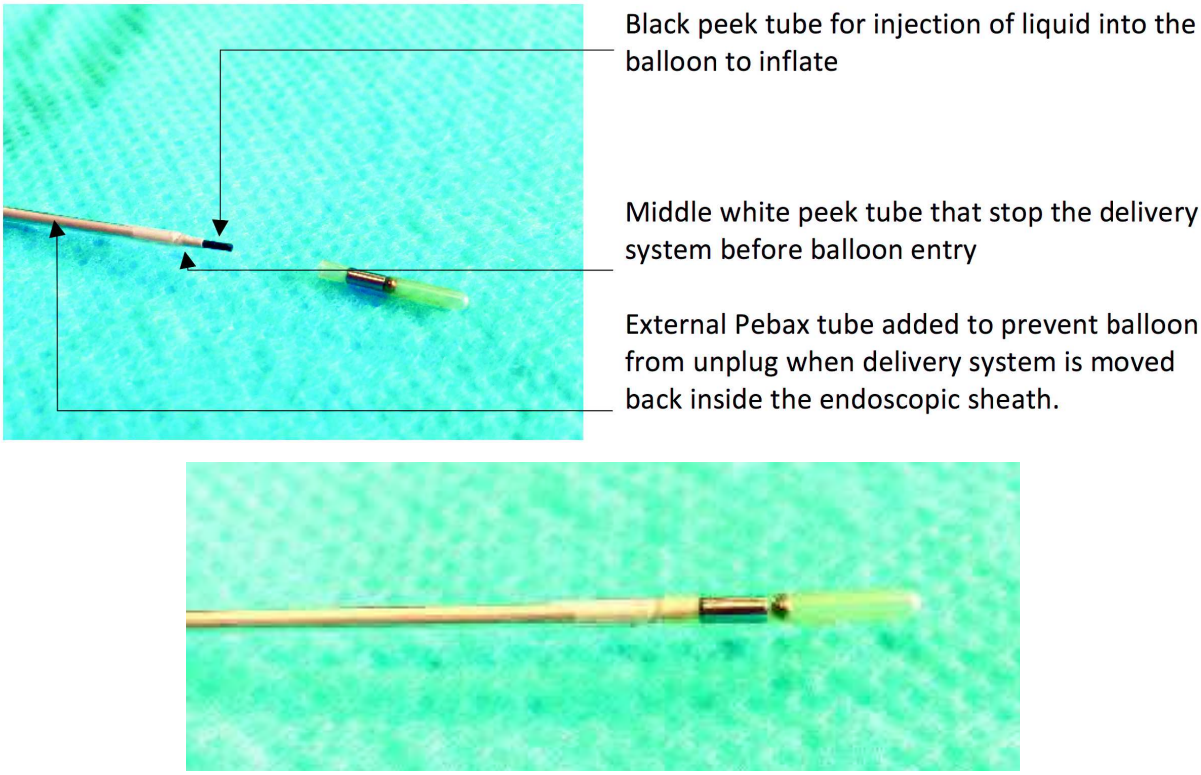

Figure 23: Improvement of the distal end of the delivery system

Regarding the development of a mechanical solution to deflate the balloon through the delivery system, a first stylet of 3mm of diameter was used. It has been observed that deflation time of a 0.7mL balloon using a 3mm stylet through the black peek tube of 0.42 mm could take up to 4 minutes. This deflation time would obviously be far too long. That's why we tried a 0.2mm stylet that allows a complete deflation of the balloon in 50 to 60 seconds. Therefore, the 0.2 mm stylet was retained as a solution for balloon deflation.

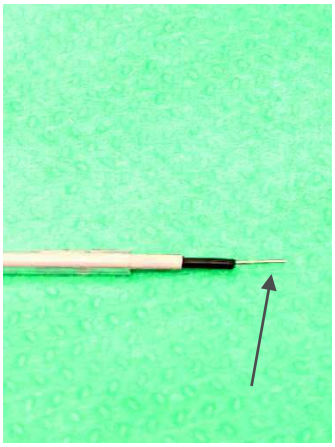

Stylet out of delivery system on distal end

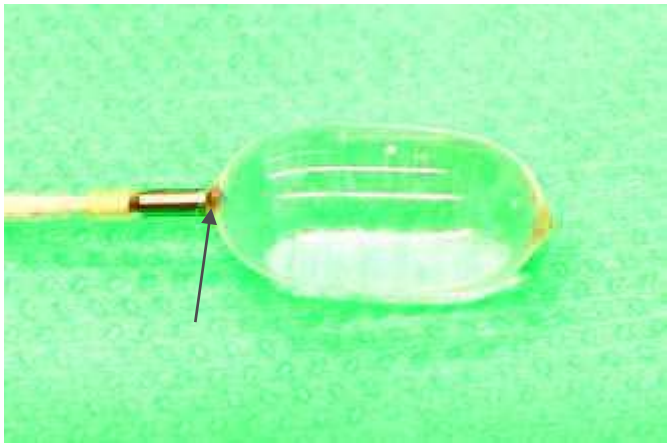

When the balloon is plugged at the distal end of the delivery system, the stylet moves slightly the magnetic ball on the side of the metal tube so the balloon deflates

Figure 24: Deflation of the balloon thanks to the internal stylet

Other improvements of the delivery system were developed: valve and fitting system on the proximal end, length of the delivery system, and syringe choice.

Regarding the valve and fitting system, the objective was to reduce the size of the valve and fitting on the proximal end, to make it easier to use and to allow the introduction of the stylet. The research was oriented toward a female valve so it will adapt to the Luer Lock syringe without a double LL female fitting. The white and green Tuohy Borst Female Luer lock cap answered the specification requests. The black peek tube was then adjusted so the tube goes through the valve and stops at 2 mm from the end of the white part of the valve. Therefore, the stylet can easily be inserted into the black peek tube to deflate the balloon before procedure or during surgery in case of incorrect positioning in the fetal trachea.

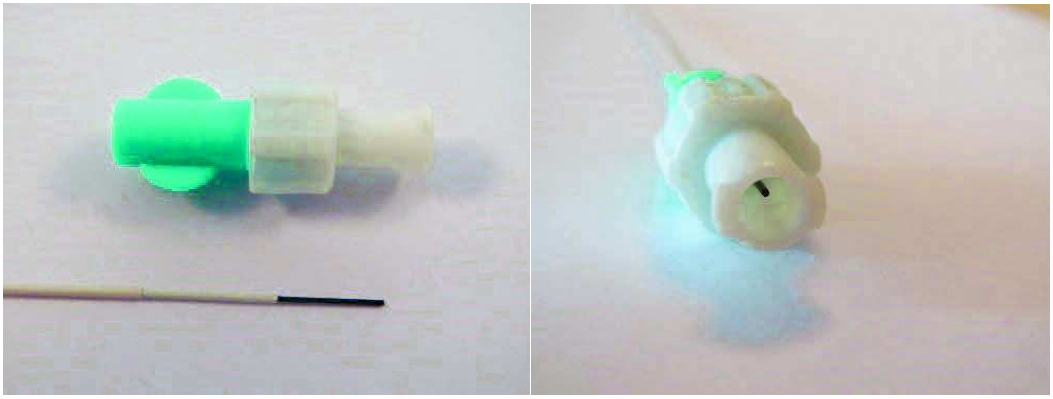

Figure 25: Convenient valve and fitting system allowing the stylet introduction

Regarding the length of the delivery system, knowing that the endoscopic sheath used for FETO is 33 cm long, two prototypes were assembled, which length were 90 cm for a long version and 40 cm for a shorter version. Tests were operated with an endoscope and a high-fidelity simulator for FETO. The longer delivery system was retained as it was long enough to allow the syringe to be conveniently laid on the operation field. The length of the stylet was then adapted so the stylet is long enough to push the magnetic ball away from the metal tube, but not too long so neither it pushes the magnetic ball too far from the ring nor it damages the balloon.

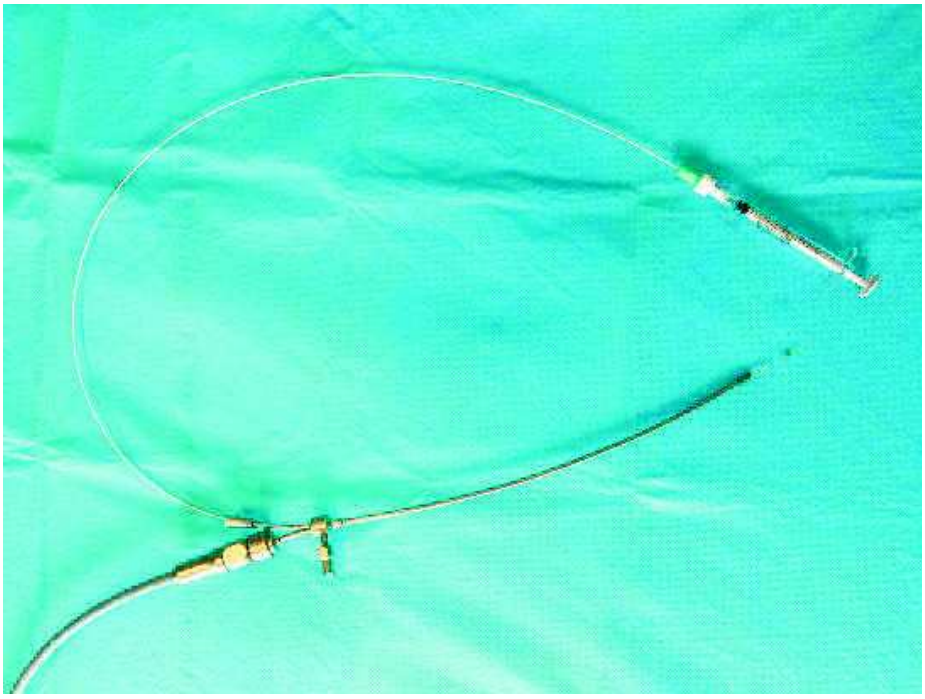

Figure 26: Delivery system inside the endoscopic sheath

Regarding the syringe choice, 4 syringes have been submitted to tests. The four of them were Luer Lock so they can be perfectly plugged to the delivery system. The syringe should have a volume suitable to flush the delivery system and fill the magnetic valve balloon. The calculation of the fluid volume necessary to flush a delivery system of 90 cm length and 0.42 mm of internal diameter was as follow: $900 \times \pi \times 0.2^2 = 0.125mL$. Therefore, a 1 ml syringe was appropriate to fill the balloon and flush the delivery system (0.7+0.125 = 0.825mL). The selected syringe was the Medallion Syringe. Indeed, it is perfectly adapted to the condition of use of the delivery system, and Its quality and volume make it an optimal choice.

3.3.2. Frozen design V1

Finally, the design of the delivery system has been frozen. It is composed by a three-layers tube: internal black peek tube for the injection of saline, middle white peek tube, and external transparent pebax tube to prevent balloon from unplug when delivery system is moved back inside the endoscopic sheath. A biocompatible glue is used to make those layers stick together. The length of the delivery system is 90cm. A 0.2 mm stylet can be easily introduced inside the delivery system so the balloon can be deflated. On the proximal end, a Tuohy Borst Valve (green with white cap Luer Lock blanc female) can be easily plugged with the Syringe Medallion (Male Luer Lock, white 1 ml, PC, ABS, Silicone).

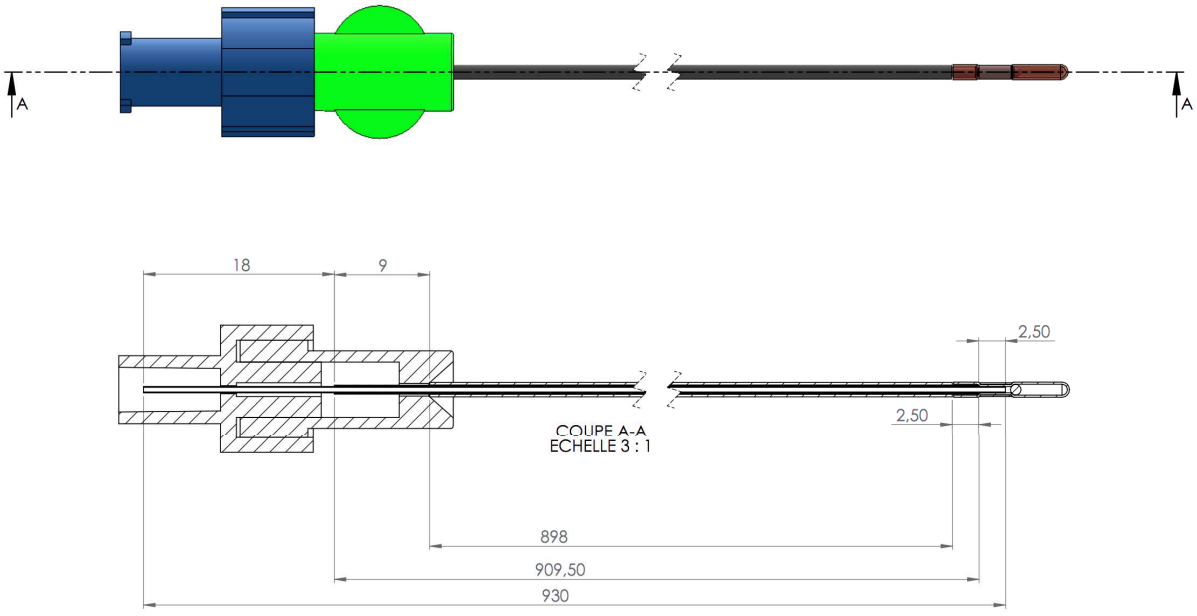

Figure 27: Outlines of the final delivery system

3.3.3. Ongoing development of the delivery system

At that stage of product development, the operator should pull gently on the delivery system to release the balloon. It has been questioned that there might be another way to release the balloon by exercising a regular and gentle pressure on its proximal end. An alternative delivery system is therefore under study and development.

On the distal end of the delivery system, the pebax tube would no longer be glued to the white and black peek tube so the pebax tube can slide on the peek tubes. On the proximal end, the simple valve would be replaced by a new fitting composed by three elements: a half LL female connector, a Tuohy Borst valve and a LL female tubing fit. The pebax tube would be glued to the LL female tubing fit.

When the female tubing fit is unscrewed, the pebax tube would slide along the peek tube. Therefore, when the balloon is connected at the distal end of the new delivery system, the unscrewing of the LL female tubing fit would make the pebax tube slide toward the distal end of delivery system, thus pushing the proximal end of the balloon. The LL female tubing fit should be unscrewed until the balloon is gently released.

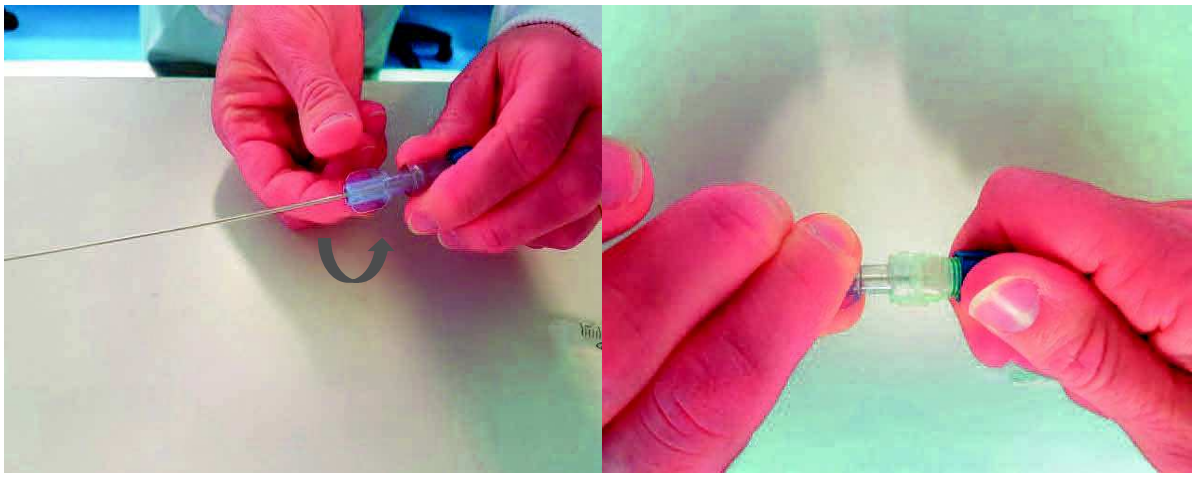

Figure 28: Unscrew of the female tubing fit

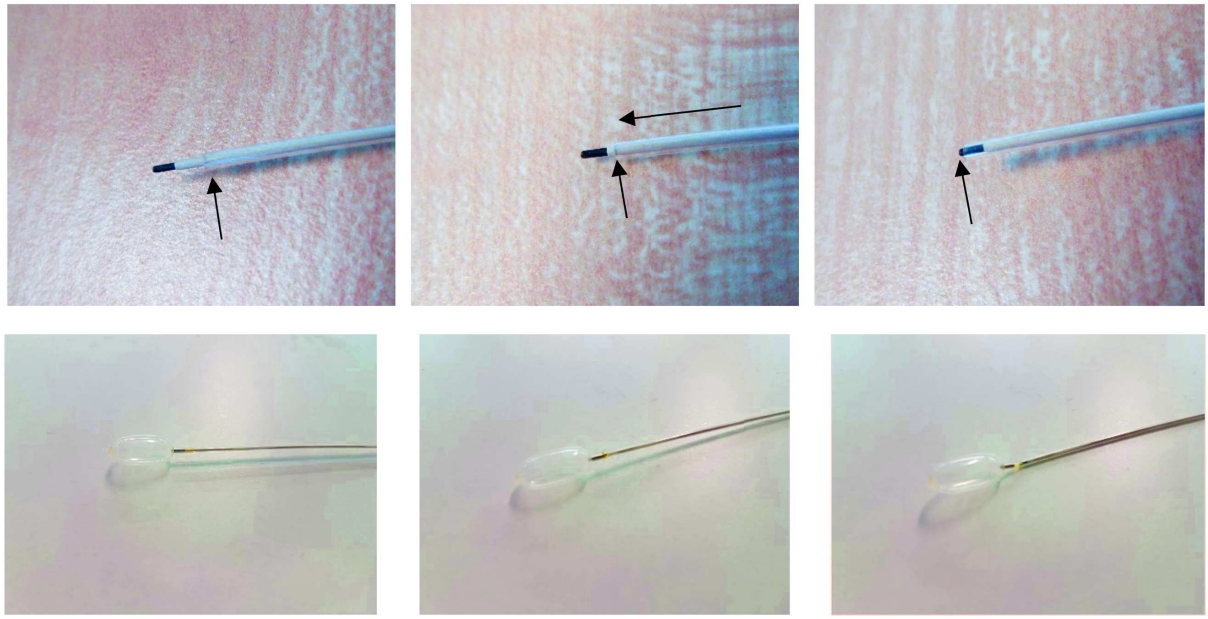

Figure 29: Release of the balloon

This delivery system is still under development. It shall be tested and further improved but could be the next generation of delivery system. This delivery system should be more convenient and reduce the risk of incorrect positioning of the balloon.

3.4. Intellectual property

3.4.1. Patentability study

A patentability study has been performed using the patents and publications databases.

There are two existing filed patents relative to an 'inflatable implant' (US 7632291B2) and a 'detachable balloon catheter apparatus and method' (US 4111146). These are not the subject of our innovation nor our claims.

There are three existing filed patents regarding different innovative techniques for noninvasive unplug after FETO procedure. They all share the same scientific background that our device but the technical solutions so as their claims are different than ours. Finally, it did not compromise the patentability of our device.

First, there is a patent on a 'remote actuated valve implant' (US2010/0241241A) (figure 30). This implant allows a remotely controlled cyclic occlusion, bringing into play an inductive source coil and, to be left inside the fetal trachea, a capacitor, a pick-up coil, a joule heater wire, and a thermally responsive polymer. Even though it's very interesting, we believe that developing such a device is technically challenging and may implies difficulties going through regulatory routes for a fetal use.

Second, there is a patent on a 'method and apparatus for delivery inside the fetal trachea' (US2012/0184808A1) (figure 31). In this technology, tracheal occlusion is provided by a polymerizable hydrogel that automatically dissolve during the fetal gestation period. Even though it's very interesting, it does not offer a remotely controlled reversal occlusion. Finally, this solution does not overcome the issue of the emergency setting when the patients go into labor or rupture their membranes whereas the polymer is not dissolved yet.

Third, there is a patent on a 'medical ultrasound system' (WO2013/146210A1) (figure 32). This technology relies on the utilization of high-density focused ultrasound to disrupt a balloon after tracheal occlusion. Even though it's very interesting, the reversal of the occlusion implies a specific expertise and the use of a specific ultrasound system. Moreover, the consequences of the balloon disruption on the fetal trachea and the tracheobronchial tree still need to be addressed.

(19) **United States**
(12) **Patent Application Publication** (10) **Pub. No.: US 2010/0241241 A1**
McKnight et al. (43) **Pub. Date: Sep. 23, 2010**

(54) **REMOTE ACTUATED VALVE IMPLANT**

(75) Inventors: **Timothy E. McKnight**, Greenback, TN (US); **Anthony Johnson**, Houston, TX (US); **Kenneth J. Moise, JR.**, Houston, TX (US); **Milton Nance Ericson**, Knoxville, TN (US); **Justin S. Baba**, Knoxville, TN (US); **John B. Wilgen**, Oak Ridge, TN (US); **Boyd Mccutchen Evans, III**, Oak Ridge, TN (US)

Correspondence Address:
Scully Scott Murphy & Presser PC
400 Garden City Plaza, Suite 300
Garden City, NY 11530 (US)

(73) Assignees: **UT-BATTELLE, LLC**, Oak Ridge, TN (US); **BAYLOR COLLEGE OF MEDICINE**, Houston, TX (US)

(21) Appl. No.: **12/729,671**

(22) Filed: **Mar. 23, 2010**

Related U.S. Application Data

(60) Provisional application No. 61/162,614, filed on Mar. 23, 2009.

Publication Classification

(51) **Int. Cl.**
A61F 2/04 (2006.01)
A61F 2/48 (2006.01)

(52) **U.S. Cl.** **623/23.68**; 623/24

(57) **ABSTRACT**

Valve implant systems positionable within a flow passage, the systems having an inlet, an outlet, and a remotely activatable valve between the inlet and outlet, with the valves being operable to provide intermittent occlusion of the flow path. A remote field is applied to provide thermal or magnetic activation of the valves.

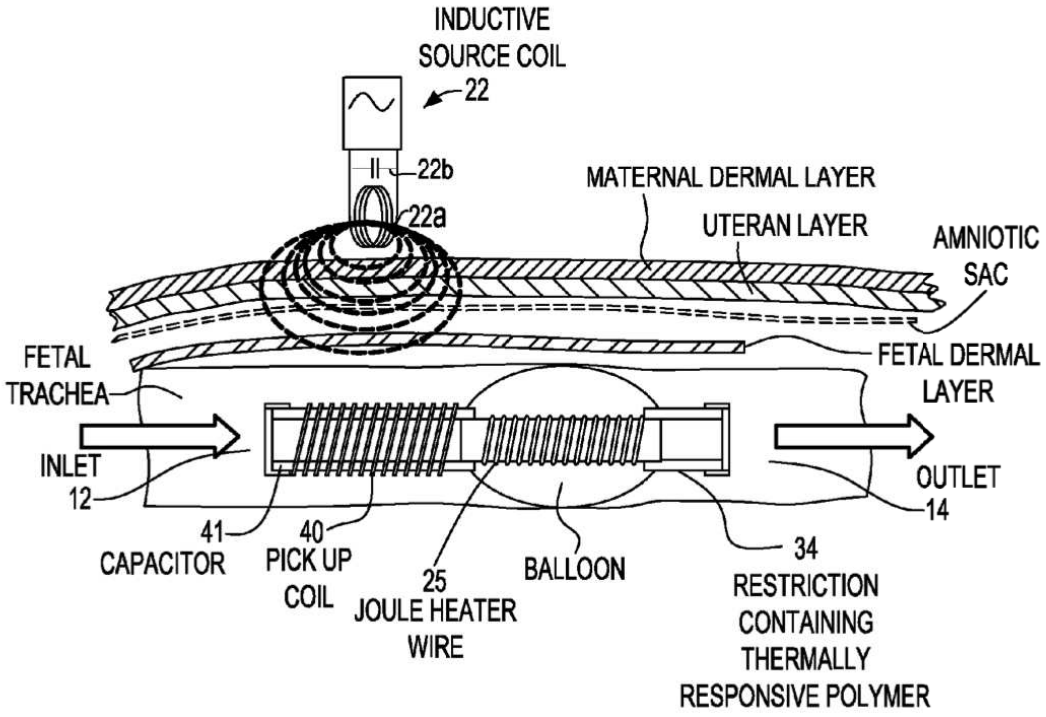

Figure 30: Patent US2010/0241241A 'remote actuated valve implant'

(19) **United States**
(12) **Patent Application Publication** (10) **Pub. No.: US 2012/0184808 A1**
Yang (43) **Pub. Date: Jul. 19, 2012**

(54) **METHOD AND APPARATUS FOR DELIVERY INTO THE FETAL TRACHEA**

(75) Inventor: **Edmund Y. Yang**, St. Louis, MO (US)

(73) Assignee: **SAINT LOUIS UNIVERSITY**, St. Louis, MO (US)

(21) Appl. No.: **13/352,466**

(22) Filed: **Jan. 18, 2012**

Related U.S. Application Data

(60) Provisional application No. 61/434,195, filed on Jan. 19, 2011.

Publication Classification

(51) **Int. Cl.**
A61B 1/018 (2006.01)

(52) **U.S. Cl.** **600/104**

(57) **ABSTRACT**

An method and apparatus for using polymerizable hydrogels to cause tracheal obstruction (TO) for treatment of pulmonary hypoplasia disorders to improve lung development in-utero. Use of the compound can cause effective TO for the purposes of inducing lung growth.

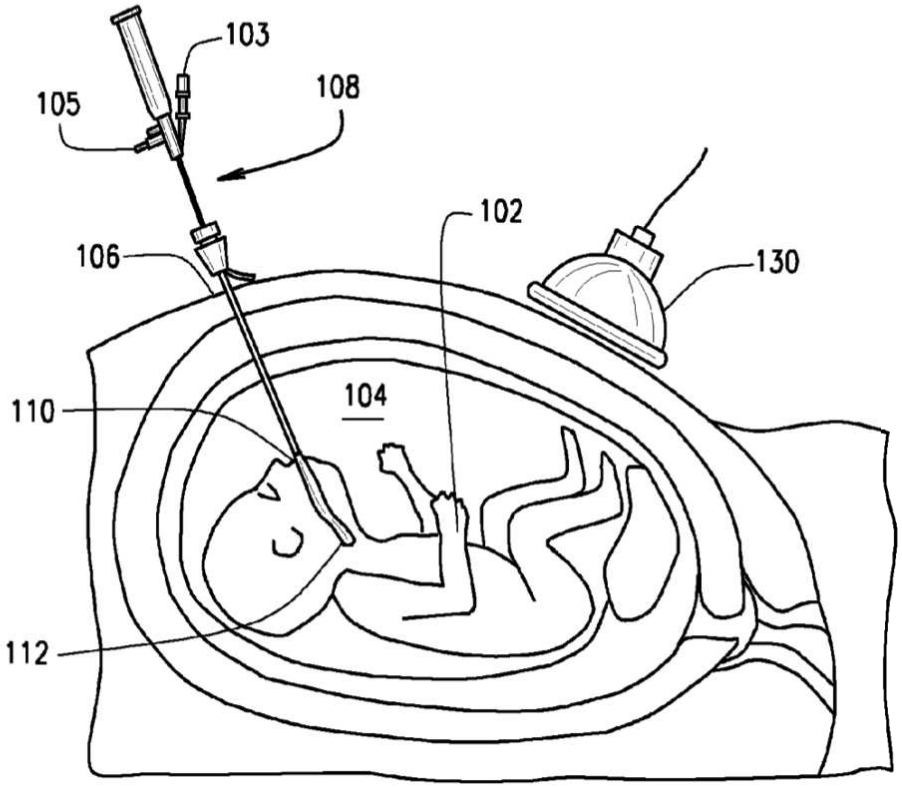

Figure 31: Patent US2012/0184808A1 'method and apparatus for delivery inside the fetal trachea'

(19) 世界知的所有権機関
国際事務局

(43) 国際公開日
2013 年 10 月 3 日(03.10.2013)

WIPO | PCT

(10) 国際公開番号
WO 2013/146210 A1

(51) 国際特許分類:
A61M 25/10 (2013.01) *A61B 17/24* (2006.01)

(21) 国際出願番号: PCT/JP2013/056614

(22) 国際出願日: 2013 年 3 月 11 日(11.03.2013)

(25) 国際出願の言語: 日本語

(26) 国際公開の言語: 日本語

(30) 優先権データ:
特願 2012-076107 2012 年 3 月 29 日(29.03.2012) JP

(71) 出願人: 日立アロカメディカル株式会社(HITACHI ALOKA MEDICAL, LTD.) [JP/JP]; 〒1818622 東京都三鷹市牟礼６丁目２２番１号 Tokyo (JP). 独立行政法人国立成育医療研究センター(NATIONAL CENTER FOR CHILD HEALTH AND DEVELOPMENT) [JP/JP]; 〒1578535 東京都世田谷区大蔵２－１０－１ Tokyo (JP).

(72) 発明者: 望月 剛 (MOCHIZUKI, Takeshi); 〒1818622 東京都三鷹市牟礼６丁目２２番１号 日立アロカメディカル株式会社内 Tokyo (JP). 千葉 敏雄(CHIBA, Toshio); 〒1578535 東京都世田谷区大蔵２－１０－１ 独立行政法人国立成育医療研究センター内 Tokyo (JP). 山下 紘正 (YAMASHITA, Hiromasa); 〒1578535 東京都世田谷区大蔵２－１０－１ 独立行政法人国立成育医療研究センター内 Tokyo (JP). 柿本 隆志 (KAKIMOTO, Takashi); 〒1578535 東京都世田谷区大蔵２－１０－１ 独立行政法人国立成育医療研究センター内 Tokyo (JP).

(74) 代理人: 特許業務法人ＹＫＩ国際特許事務所 (YKI PATENT ATTORNEYS); 〒1800004 東京都武蔵野市吉祥寺本町一丁目３４番１２号 Tokyo (JP).

(81) 指定国 (表示のない限り、全ての種類の国内保護が可能): AE, AG, AL, AM, AO, AT, AU, AZ, BA, BB, BG, BH, BN, BR, BW, BY, BZ, CA, CH, CL, CN, CO, CR, CU, CZ, DE, DK, DM, DO, DZ, EC, EE, EG, ES, FI, GB, GD, GE, GH, GM, GT, HN, HR, HU, ID, IL, IN, IS, KE, KG, KM, KN, KP, KR, KZ, LA, LC, LK, LR, LS,

[続葉有]

(54) **Title**: MEDICAL ULTRASOUND SYSTEM

(54) 発明の名称 : 超音波医用システム

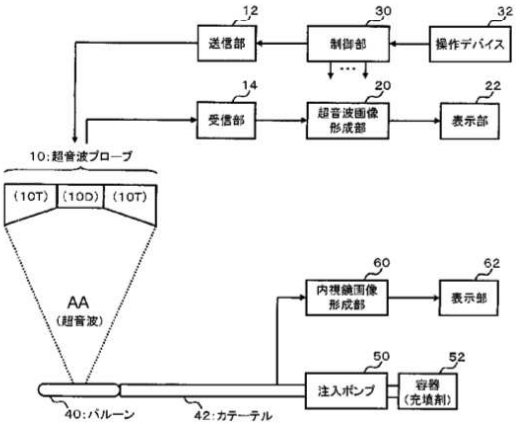

10 Ultrasound probe
12 Transmitter
14 Receiver
20 Ultrasound image-forming unit

(57) **Abstract**: The ultrasound probe (10) is configured from an image oscillator (10D) and a gasification oscillator (10T). The transmitter (12) forms a transmitting beam toward the position of the balloon (40) and controls the gasification oscillator (10T) of the ultrasound probe (10) so as to transmit a gasifying ultrasonic wave. A liquid filler is filled inside the balloon (40) and the balloon (40) occludes a tubular tissue in a living body. As a result of an ultrasonic wave being transmitted to the balloon (40), the liquid filler filled inside the balloon (40) is gasified by the ultrasonic wave and is discharged from inside the balloon (40), deflating the balloon (40) and releasing the occlusion of the tubular tissue.

(57) 要約: 超音波プローブ１０は、画像用振動子１０Ｄと気化用振動子１０Ｔで構成されている。送信部１２は、バルーン４０の位置に向けて送信ビームを形成して気化用の超音波を送波するように、超音波プローブ１０の気化用振動子１０Ｔを制御する。バルーン４０内には液状の充填剤が充填されており、バルーン４０が生体の管状組織を閉塞している。そのバルーン４０に超音波が送波されることにより、バルーン４０内に充填された液状の充填剤が超音波で気化させてバルーン４０内から排出され、バルーン４０が萎んで管状組織の閉塞が解除される。

Figure 32: Patent WO2013/146210A1 'medical ultrasound system'

There are three existing filed patents claiming an innovative magnetic valve technology. Even if those solutions were not developed for reversal tracheal occlusion, the relative patents had to be studied to ensure the patentability of our device.

First, there is a patent on a ‘magnetic retraction device’ (US2012/8303495B2) (figure 33). This technology relies on a magnetic agent, so it did not compromise the patentability of our device.

Second there are two patents for devices for urinary incontinence control: ‘female incontinence control device with magnetically operable valve and method’ (US1991/5030199) (figure 34), and ‘urethral indwelling catheter with magnetically controlled drainage valve and method’ (US1991/5041092) (figure 35). These techniques both rely on the operation of a magnetic valve thanks to the movement of a magnetic ball or cuff. However, these valves only allow the movement of the ball in a single longitudinal axis. In our technology, the opening of the valve operates regardless the direction of the magnetic field in a half-sphere of space, which is critical since the fetal position inside the uterus cannot be controlled. Finally, these two patents did not compromise the patentability of our device and one of our claims was that at least two axes of movement of the magnetic ball may operate the valve.

(12) **United States Patent**
Ducharme

(10) **Patent No.: US 8,303,495 B2**
(45) **Date of Patent: Nov. 6, 2012**

(54) **MAGNETIC RETRACTION DEVICE**

(75) Inventor: **Richard W. Ducharme**, Winston-Salem, NC (US)

(73) Assignee: **Cook Medical Technologies LLC**, Bloomington, IN (US)

(*) Notice: Subject to any disclaimer, the term of this patent is extended or adjusted under 35 U.S.C. 154(b) by 221 days.

(21) Appl. No.: **12/648,750**

(22) Filed: **Dec. 29, 2009**

(65) **Prior Publication Data**

US 2010/0168523 A1 Jul. 1, 2010

Related U.S. Application Data

(60) Provisional application No. 61/141,368, filed on Dec. 30, 2008.

(51) **Int. Cl.**
A61B 1/32 (2006.01)

(52) **U.S. Cl.** **600/207**; 600/12

(58) **Field of Classification Search** 600/12, 600/115, 116, 143, 206, 207, 208, 37; 606/191, 606/197–200, 203, 204, 206, 207, 208, 210, 606/215; 604/96.01–109; 623/1.11–1.12; 446/129, 137, 139
See application file for complete search history.

(56) **References Cited**

U.S. PATENT DOCUMENTS

7,163,506	B2	1/2007	Grise	
2007/0135685	A1	6/2007	Cuschieri	
2007/0244501	A1	10/2007	Horn	
2007/0270629	A1 *	11/2007	Charles	600/12
2008/0108860	A1 *	5/2008	Bell et al.	600/12
2008/0171907	A1	7/2008	Long et al.	

FOREIGN PATENT DOCUMENTS

GB	2 403 909	A	1/2005
WO	WO 00/66030		11/2000
WO	WO 2008/067317	A2	6/2008
WO	WO 2008/098166	A1	8/2008
WO	WO 2008/101077	A1	8/2008

* cited by examiner

Primary Examiner — Kevin T Truong
Assistant Examiner — Diana S Jones
(74) *Attorney, Agent, or Firm* — Brinks Hofer Gilson & Lione

(57) **ABSTRACT**

A magnetic retraction device is provided that may be used to manipulate organs and tissue. The device includes a magnetic agent, at least one inflatable member configured to contain the magnetic agent, and a magnetic device. The inflatable member can be disposed on an elongate member adapted for delivery into a patient lumen. The inflatable member can be interconnected with one or more additional inflatable members by a sling.

12 Claims, 8 Drawing Sheets

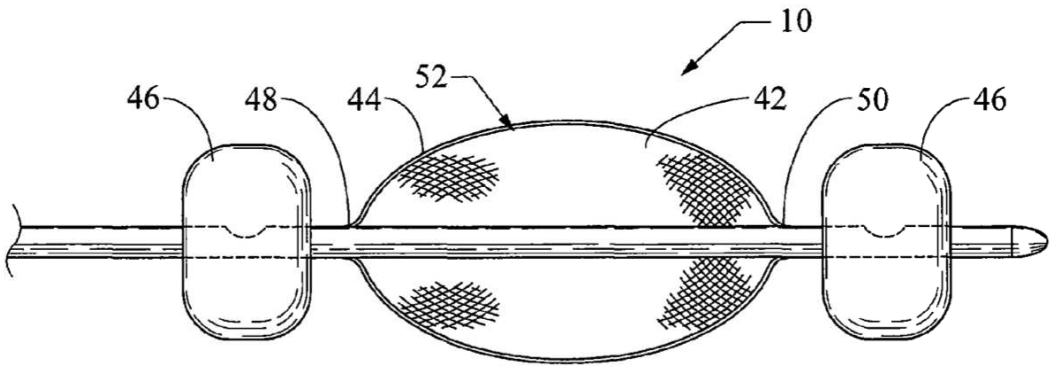

Figure 33: Patent US2012/8303495B2 'magnetic retraction device'

United States Patent [19]

Barwick et al.

[11] **Patent Number: 5,030,199**

[45] **Date of Patent: Jul. 9, 1991**

[54] **FEMALE INCONTINENCE CONTROL DEVICE WITH MAGNETICALLY OPERABLE VALVE AND METHOD**

[75] Inventors: **Carl B. Barwick**, Caledonia, Wis.; **Rebecca Y. Chin**, Mundelein, Ill.

[73] Assignee: **Medical Engineering Corporation**, Racine, Wis.

[21] Appl. No.: **448,496**

[22] Filed: **Dec. 11, 1989**

[51] **Int. Cl.**[5] **A61F 2/00**

[52] **U.S. Cl.** **600/29**; 128/DIG. 25; 604/54; 604/63; 604/96

[58] **Field of Search** 600/29-30; 604/54, 93, 96-99, 117, 246, 247; 251/65; 128/DIG. 25

[56] **References Cited**

U.S. PATENT DOCUMENTS

3,503,400	3/1970	Osthagen et al.	128/DIG. 25
3,642,004	2/1972	Osthagen et al.	128/DIG. 25
3,812,841	5/1944	Isaacson	600/29
3,841,304	10/1974	Jones	600/29
4,909,788	3/1990	Burton et al.	604/54

FOREIGN PATENT DOCUMENTS

2537506	3/1977	Fed. Rep. of Germany	128/DIG. 25
2624418	12/1977	Fed. Rep. of Germany	128/DIG. 25
2251302	7/1975	France	128/DIG. 25
526357	9/1976	U.S.S.R.	128/DIG. 25

Primary Examiner—Randall L. Green
Assistant Examiner—K. M. Reichle
Attorney, Agent, or Firm—Stuart E. Krieger

[57] **ABSTRACT**

A female incontinence control device includes a conduit having inlet and outlet openings for receiving, conducting and discharging urinary fluid. The device also includes stabilizing structure, which can be adjustable, for holding the conduit in its installed position relative to the urethra and bladder such that a drainage inlet opening can receive fluid from the bladder, and the outlet discharge opening is positioned outside the urethra. The conduit includes a magnetically actuatable drainage control valve adapted to be positioned between the urethral orifice and the labia majora. Magnetic actuation of the valve from a normally closed position to an open position is thus easily accomplished by manipulating a portable magnet at a distal end of the conduit outside the urethral opening to selectively control urinary flow through the conduit. The method of controlling female incontinence includes the steps of providing and positioning a conduit to receive the urinary fluid and magnetically actuating the valve in the conduit by manipulating a magnet proximal the conduit in the vicinity of the valve to open the valve and allow accumulated urinary fluids to be drained through the outlet opening. Removal of the magnet permits the valve to automatically close.

28 Claims, 5 Drawing Sheets

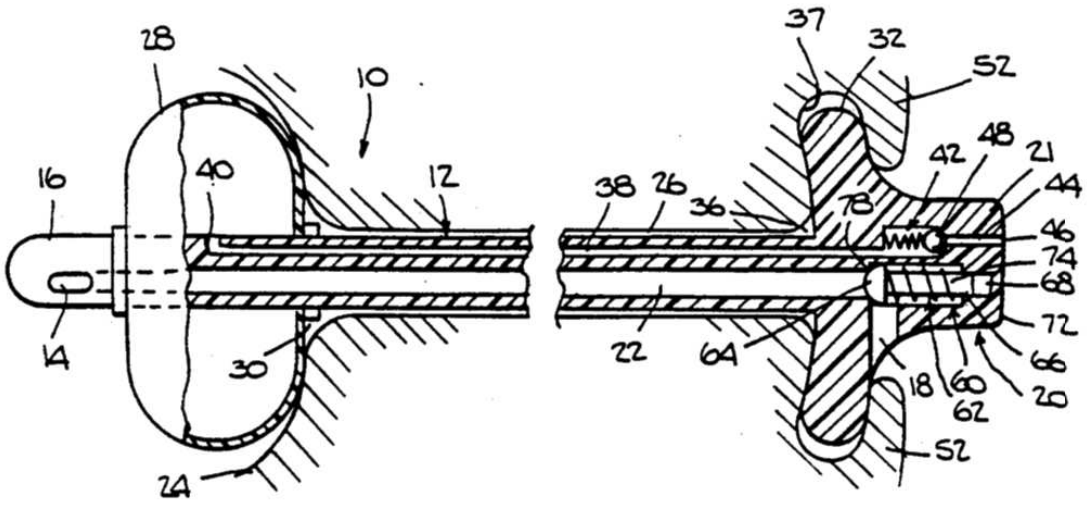

Figure 34: Patent US1991/5030199 'female incontinence control device with magnetically operable valve and method'

United States Patent [19]

Barwick

[11] **Patent Number: 5,041,092**

[45] **Date of Patent: Aug. 20, 1991**

[54] **URETHRAL INDWELLING CATHETER WITH MAGNETICALLY CONTROLLED DRAINAGE VALVE AND METHOD**

[75] Inventor: **Carl Barwick**, Caledonia, Wis.

[73] Assignee: **Medical Engineering Corporation**, Racine, Wis.

[21] Appl. No.: **608,605**

[22] Filed: **Oct. 30, 1990**

Related U.S. Application Data

[63] Continuation of Ser. No. 400,194, Aug. 29, 1989, abandoned.

[51] **Int. Cl.**[5] **A61M 29/00**; A61F 2/00

[52] **U.S. Cl.** **604/104**; 604/246; 128/DIG. 25; 600/29

[58] **Field of Search** 604/8, 9, 65, 96, 97, 604/99, 101, 246, 247, 280; 128/DIG. 25; 600/12, 29–31; 251/65

[56] **References Cited**

U.S. PATENT DOCUMENTS

3,354,898	11/1967	Barnes	251/65
3,419,008	12/1968	Plishner	251/65
3,503,400	3/1970	Ostagen et al.	128/DIG. 25
3,642,004	2/1972	Ostagen et al.	128/DIG. 25
3,731,670	5/1973	Loe	600/30
3,812,841	5/1974	Isaacson	128/DIG. 25
4,850,963	7/1989	Sparks et al.	128/DIG. 25
4,932,938	6/1990	Goldberg et al.	604/96

FOREIGN PATENT DOCUMENTS

2537506	3/1977	Fed. Rep. of Germany	128/DIG. 25
1194358	6/1970	United Kingdom	600/30

Primary Examiner—John D. Yasko
Assistant Examiner—Anthony Gutowski
Attorney, Agent, or Firm—S. Krieger

[57] **ABSTRACT**

The catheter includes a user controlled incontinence portion that is combinable with a combination inflation/drainage member. The inflation/drainage member can be detached from the incontinence portion to provide a user controlled device. A magnetic valve is incorporated in the user controlled incontinence portion for magnetic actuation with an external magnet. The valve is normally closed and magnetically actuatable to an open condition. Removal of the external magnet from proximity to the penis enables the valve to assume its normally closed position. In one embodiment of the invention the valve includes a pressure relief feature. In another embodiment of the invention there is no pressure relief feature.

18 Claims, 5 Drawing Sheets

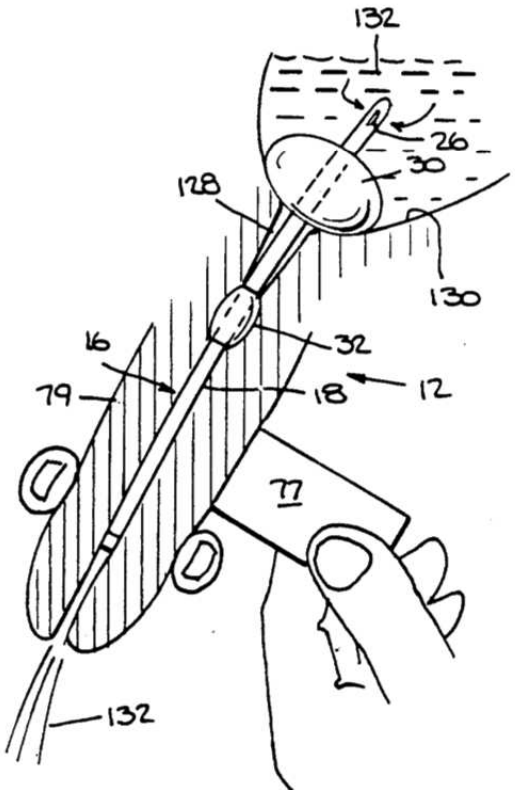

Figure 35: Patent US1991/5041092 'urethral indwelling catheter with magnetically controlled drainage valve and method'

3.4.2. Patent filling

A patent application has been filed on May 2nd 2016 (request #1653954 / submission #1000345616): 'BALLONNET GONFLABLE ET DÉTACHABLE, DESTINÉ À ÊTRE IMPLANTÉ DANS UNE CAVITÉ CORPORELLE, NÉCESSAIRE DE TRAITEMENT ET PROCÉDÉ DE VIDANGE ASSOCIÉS'.

The patent and related figures are displayed in Appendix 9.1 'Patent filed'. Claims are structured in several parts:

- Claims 1 and 13 present the general aspect of the medical device, its functional parts and materials.
- Claims 2 to 9 describe the closing and permeability principles of the magnetic valve.
- Claim 10 describes the balloon material itself.
- Claim 11 presents the inflation of the balloon using the catheter.
- Claims 14 and 15 present the procedure of unplug using a magnetic field.

The National Institute for intellectual property (INPI) validated all the claims of our patent except the claims 14 and 15 regarding the deflation process, because they consider it was a surgical procedure and it's not possible to claim a surgical method according to the European legislation. We submitted additional information arguing that deflation process should not be considered as a surgical procedure since it's totally noninvasive. We are currently waiting for the answer. To be noted that in United States for example, surgical methods are not excluded from patentability.

We applied for an international extension of our patent on May 2017.

3.4.3. Infringement risk

Infringement risks are very low with CE marking on medical devices. The balloon structure will have well-defined morphologies. Therefore, a simple analysis can detect a potential infringement. As medical devices are partly reimbursed by health agencies ('Sécurité Sociale', etc.), their origins and qualities are better controlled. Finally, we are confident that no mass infringement shall disturb the commercialization of this device.

3.5. Tests

3.5.1. Impermeability tests

Impermeability tests were conducted on non-coated valve and also on parylene coated valve.

A latex balloon equipped with non-coated magnetic valve was filled with saline. It was placed into water and after three days, placed in amniotic fluid. The sample was kept in a close container, at room temperature, protected from light. The size of that balloon was documented over time. The length was measured with a caliper and the diameter with a hole gauge.

Figure 36: Methods for measurements of length and diameter of the balloon

During the observation period, the diameter of the magnetic valve balloon did not change. Over the four months' observation, its value has been constant with 7.2mm as controlled with the hole gauge.

The length of the balloon decreased by 1.5mm the first month and then the length has stabilized for more than three months, as presented in the following graph displayed in figure 37.

The duration of observation for that balloon was much higher than the practical need for fetal tracheal occlusion. However, it enabled us to study its behavior and to confirm its impermeability over time. Finally, these first dimensional measurements of the latex magnetic valve balloon over the time were promising.

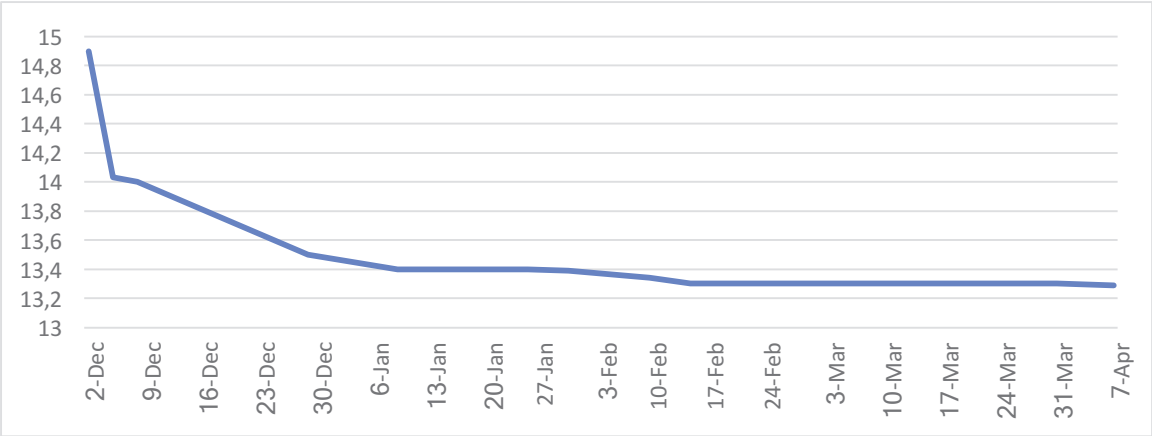

Figure 37: Length of the balloon with non-coated valve over time

A latex balloon equipped with a parylene coated magnetic valve was filled with saline. It was placed in amniotic fluid. The sample was kept in a close container, at room temperature, protected from light. The size of that balloon was documented over time. The length and the diameter were measured according to the same methods than previously described.

This test is still ongoing, but during the observation period of one month, the diameter of the magnetic valve balloon did not change. Its value has been constant with 7.6 mm as controlled with the hole gauge.

The length of the balloon decreased continuously over time, by 0.8mm in one month, as presented in the following graph displayed in figure 38.

Even though that test is still ongoing, the duration of the observation roughly corresponds to the clinical need for fetal tracheal occlusion. Finally, these first dimensional measurements of the latex parylene coated magnetic valve over time were promising. Even if a small decrease of length has been recorded, the diameter does not change over time. As the function of the balloon is its occlusion capacity, the diameter consistency is a key factor.

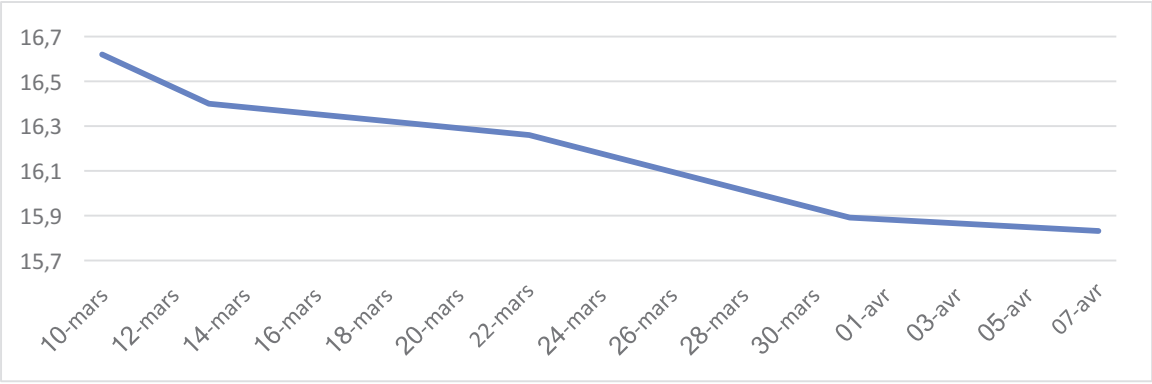

Figure 38: Length of the balloon with parylene coated valve over time

The impermeability testing still requires a study on a larger scale (30 samples are planned) in order to collect meaningful values from a statistical point of view. This larger scale study will be carried out in a 37°C controlled temperature water bath, where the samples will be kept in test tubes filled with amniotic fluid. On top of that, the larger scale study will include measurements and documentation of weight variation (±0.001mg) of balloons over the time.

3.5.2. Occlusion tests

The sample batch for occlusion tests consisted in 10 latex balloons equipped with parylene coated valve and 10 latex free balloons equipped with parylene coated valve. Latex free balloons were manufactured by welding the distal end of a latex free tube, as previously described in the chapter 4.2.2 'Choice of the material for the balloon'. The objective of that test was to study the behavior of magnetic valve balloon in occlusion conditions.

A glass tube with an inner diameter of 7 mm materialized here the fetal trachea. Balloons were inflated as they were in the glass tube so the occluded the tube. For that batch of samples, the primary judgement criterion was the occlusion function of the balloon in the glass tube. At the end of the protocol, deflation of balloon was tested by subjecting the device to a magnetic field.

The batch of samples was prepared as follow. The empty balloons were inserted inside glass tubes of 7mm internal diameter and that are open on both sides. Balloons were then filled with 0.7mL saline, thus applying the balloons sides against the open tubes. A mark was drawn on the tube glass at the chamfered position of the metal cylinder. Finally, the tubes and balloons were placed into 8.5mm test tubes filled with amniotic fluid. Test tubes containing samples were protected from light and kept in a 37°C water bath during 8 weeks (still ongoing).

Tubes were shaken daily. Once a day, a visual control was performed and the position of the balloon inside the 7mm diameter glass tube was documented. Temperature of water bath was controlled daily and documented. The color of the balloon, the presence of crystals or external coloration of samples were documented, so as eventual corrosion on metallic parts.

Once a week, the balloons length was recorded. The balloons were left in the glass tubes they occlude but removed from the test tube with amniotic fluid. Balloons length was then measured with a caliper through the glass tube.

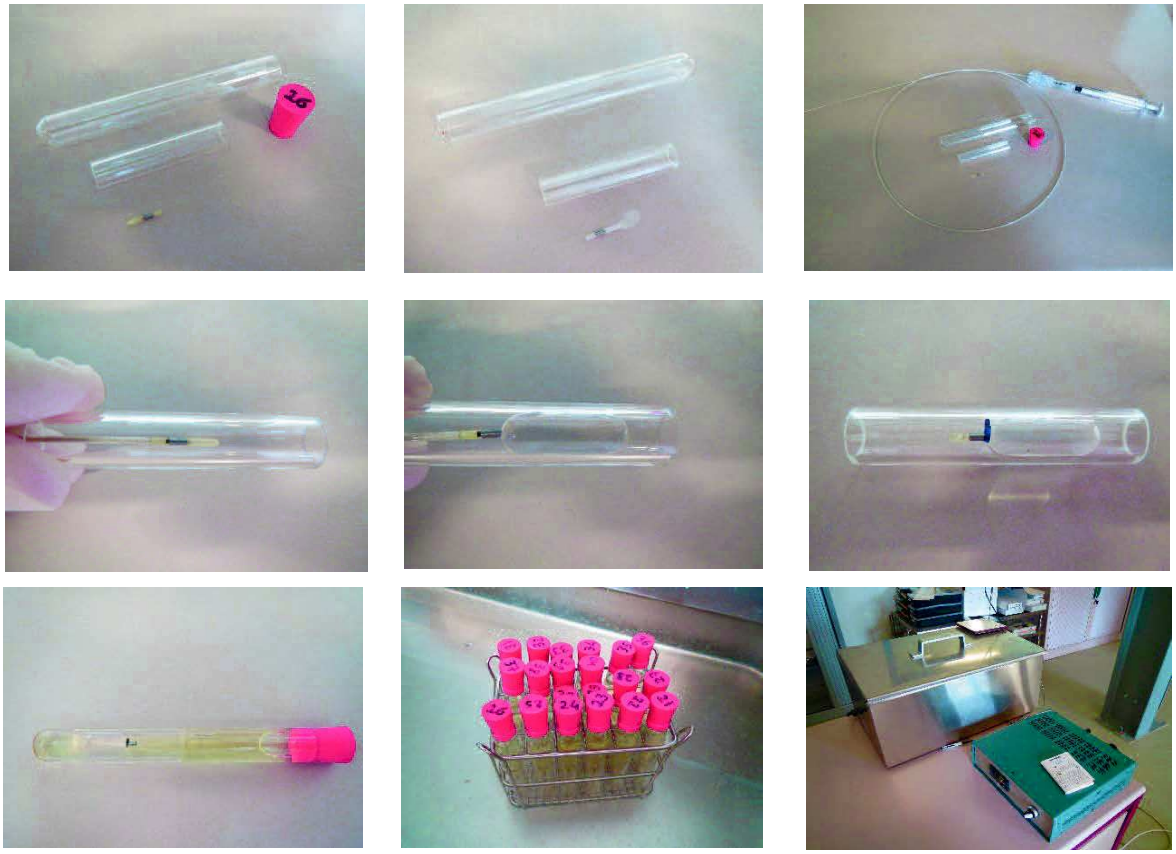

Figure 39: Illustration for the occlusion tests methods

These occlusion tests are still ongoing. Still, three weeks after the beginning, none of the balloons lost its occlusion functionality. The visual aspect of the balloons did not change. There was no sign of corrosion on metal tube nor on magnetic balls. These preliminary results were promising. There might be additional tests to forecast involving mechanical squeeze on balloons walls to simulate non-static constrain as in a fetal trachea subjected to fetal respiratory movements.

3.5.3. Prospects of other in vitro tests

Additional tests are planned on the latex balloon (mechanical resistance, sealing, traction test…), on the valve (corrosion), and on the finished product (releasable, aging, and sterilization protocol).

3.5.4. Operation tests

The objective of these tests was to define what position and/or movement should be done by the patient in front of the MRI machine to open the magnetic valve, thus deflating the balloon, with a 100% achievement regardless the position of the fetus. These investigations were conducted in the Imaging department of Strasbourg University Hospital, using a Philipps Ingenia 1.5T Omega HP.

Former investigations and a couple of tests have been conducted in order to appropriately design the operation tests.

First, when a filled balloon is presented in front of the MRI, the balloon may deflate in seconds but it does not operate systematically, obviously because of the polarity of the magnetic ball, which you cannot predict. If we perform a gentle 180° rotation according to the longitudinal axis of the balloon, a 100% valve opening seems to be achieved.

Second, the fringe field necessary to open the valve seems to be between 0.2 and 0.4T as measured with a gaussmeter, *i.e.* 10 to 50cm from the entrance of the MRI tunnel.

Third, we performed measurements of magnetic field in front of an MRI scanner, with or without the interposition of an individual between the gaussmeter and the MRI. The values of the magnetic was not dependent on the presence of a human body. This observation suggests that the magnetic field measured during these operation tests would be identical or very similar to the magnetic field of which the magnetic ball is subjected while inside the fetal trachea.

Fourth, we observed that the balloons did not deflate when placed longitudinally inside the MRI tunnel. Even though the strongest magnetic field is inside the core of the MRI scanner, the magnetic field is parallel to the set formed by the metallic tube and the magnetic ball, thus not disjoining the two elements and not opening the valve. This observation suggest that the positioning of the patient lying on the MRI table is not likely to open the valve and to deflate the balloon.

Finally, the operation tests were conducted with 10 samples of latex balloons equipped with parylene coated magnetic valves. Balloons were inserted inside 7mm diameter glass tubes and filled with 0.7mL of saline. Tubes were then set on a 3D rotating device.

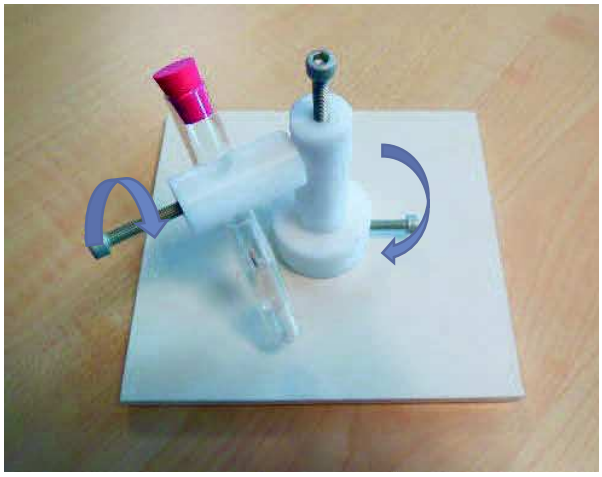

Figure 40: 3D rotating device for operation tests

The rotating device was placed on the rails on the MRI patient table. Samples were set at 90 cm from ground level.

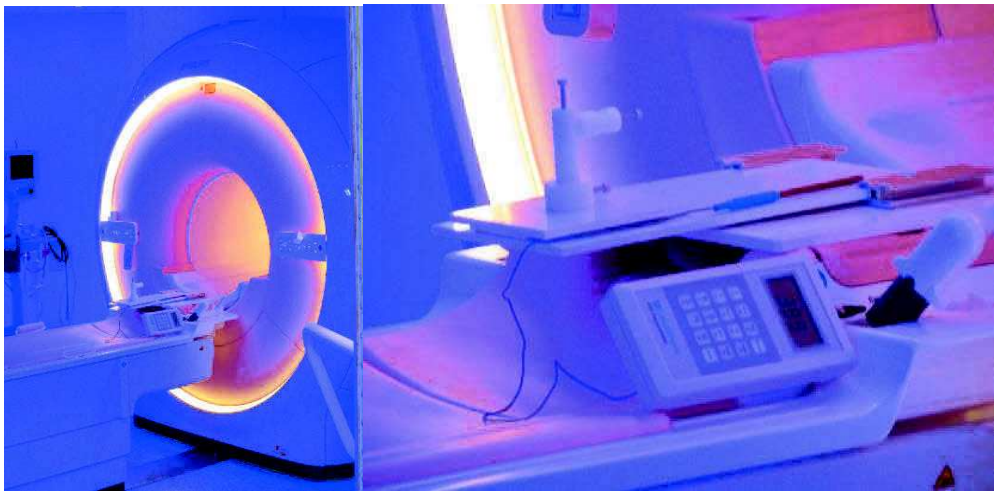

Figure 41: MRI setting for operation tests

The studied parameters were the impact of the inclination angle and the distance of the balloon from the MRI on valve opening. Regarding the angles, α was the horizontal rotation angle (zero was set along the rail axis, facing the magnet of the MRI) and β was the vertical rotation angle (zero was set perpendicular to the rail axis).

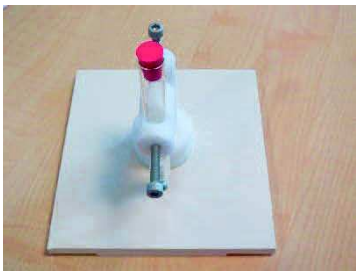

α = 0° – β =0°

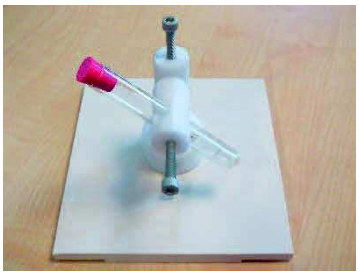

α = 0° - β =45°

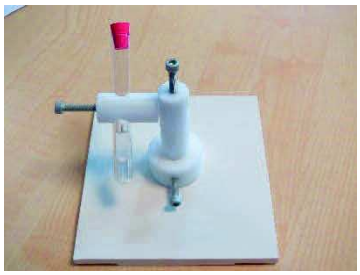

α =90° - β =45°

Figure 42: Examples of different angles tested thanks to the rotating device

It has been formerly tested that a variation of α from 0° to 90°and then 180° (thus corresponding to the patient presenting its face, profile and back to the MRI) allowed the deflation of the balloon. β would then be considered for the values between 0 and 90°, for every increment angle of 30°, thus covering the different possible presentations of the fetus trachea in the uterus (β=0° being the vertical position of the trachea).

The tests consisted in presenting the filled balloons set in the rotating device with β=0°, 30°, 60°, and 90°, and apply if necessary a rotation so α = 90° and 180°. In case the balloon did not deflate, it was removed from the fringe field and presented a second time according to the same protocol. For each position of the rotating device at the moment the balloon deflated, the distance between the rotating device and the MRI was documented, as well as the intensity of the magnetic field indicated by the gaussmeter. All these measurements are reported in table 9.

Even though deflation of the balloon was achieved in all cases, we found that neither the distance nor the angle operating deflation where consistent. Moreover, it was necessary in most cases to remove the balloon from the fringe field and to present it a second time in order to complete the deflation of the balloon.

β (°)	sample	α (°)	Distance to MRI (cm)	Magnetic field (Tesla)	First or second presenting
0	1	90	17	0.4	1
	2	0	36	0.18	2
	3	180	21	0.34	1
	4	0	36	0.18	1
	5	90	17	0.4	1
30	1	0	13	0.45	2
	2	180	21	0.34	1
	3	0	36	0.18	2
	4	0	36	0.18	2
	5	0	36	0.18	2
60	1	180	21	0.34	1
	2	0	36	0.18	2
	3	0	36	0.18	2
	4	0	36	0.18	2
	5	0	36	0.18	2
90	1	0	36	0.18	2
	2	180	21	0.34	1
	3	0	13	0.45	1
	4	0	36	0.18	2
	5	0	36	0.18	2

Table 9: Distance, angle and magnetic field to obtain balloon deflation

A second raw of tests was then conducted. The filled balloons occluding the 0.7mm diameter glass tubes and placed in test tubes were carried by an experimenter at his abdomen level. The experimenter had to walk up to the front of the MRI machine, exposing his abdomen as close as possible from the entrance of the tunnel. After doing a quarter turn in front of the tunnel, he had to walk all around the MRI machine before leaving the room. A total of 40 tests have been conducted, with the tubes held at different abdomen levels and with different angles (β=0°, 30°, 60°, and 90°).

Deflation of the balloon was achieved in 100% of the cases. On top of that, the deflation was already completed half-way from the walk around the MRI machine and a complete turn was necessary in only one case.

Finally, the deflation protocol for the patient could then be described as follow. It takes place in an MRI examination room. To be noted that the fringe field operates near the MRI since the machine is on, with no need for an imaging acquisition. The patient must be positioned in front of the MRI scanner, with her abdomen facing the tunnel. Then she needs to make a quarter turn on herself in front of the middle of the tunnel and turn around the MRI scanner staying close to the machine. On the other side of the machine, once again she will need to position her abdomen facing the tunnel, make a quarter turn in front of the middle of the tunnel and turn around the MRI machine on the other side until the other side of the tunnel. The patient shall then leave the MRI room. The illustration of this protocol is displayed in figure 43.

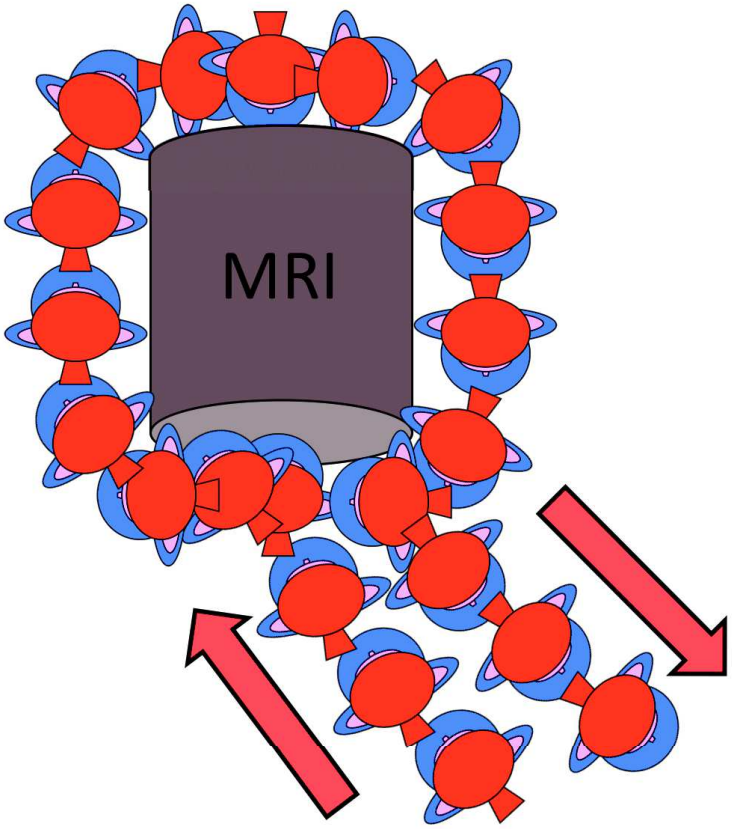

Figure 43: Balloon deflation protocol

3.5.5. Animal tests

One first experiment on a rhesus monkey (Macaca mulata) has been performed and two others are planned. The monkeys are group-housed in indoor/outdoor facilities in SILABE plate- form (Simian Laboratory Europe). They live in social groups (1 or 2 adult males and 4 to 10 females) in indoor/outdoor facilities of approximately 40 to 85 m3 for the indoor facility (depending on the animal facility and group) and 40 to 50 m3 for the outdoor facility. Water and food are distributed *ad libitum*. Animals are captured regularly in order to perform ultrasound to detect pregnancy and establish the gestational age. The timing of surgery was determined by ultrasound measurement of the biparietal diameter of the fetus in early pregnancy (Voluson E GE®). The pregnant female was captured on the day of the surgery. After surgery, the monkey was isolated until the following morning and was then returned to its social group. The Regional Ethics Committee on Animal Experimentation (CREMEAS) at Strasbourg University, France (number A6732636) approved this study in 2013. Guidelines for the care and use of the monkeys approved by this institution were followed.

The pregnant rhesus monkey underwent FETO procedure with the smart-TO balloon at 139 days of gestation. The monkey was first sedated with ketamine (10 mg/kg, IM) before general anesthesia with propofol (5 mg/kg, IV) and 1 to 2.5% isoflurane after tracheal intubation. Ventilation was controlled by assisted mechanical respiration after tracheal intubation. Maternal breath frequency, electrocardiogram, PO2/PCO2 measurement, halogenated gas and temperature were continually monitored and a heating blanket was applied to maintain body temperature. Maternal blood pressure was monitored with a sphygmomanometer. A single dose of 2% marbocyl was given (Marbofloxacin 2 mg/kg, IM) prior to surgery. No tocolytic was administered.

Before surgery, fetal monkey curarization was performed by an intra-muscular injection of 0.20mg cisatracurium in the fetal leg, under ultrasound guidance. After localization of the fetal head and placenta in order to determine the optimal entry site, 5 ml 2% xylocaine was injected percutaneously into the myometrium of the pregnant monkey in order to provide additional local anesthesia.

Endoscopic access was performed using the modified Seldinger technique under continuous ultrasound guidance. A 17G needle was first introduced into the uterine cavity and an amnioinfusion of 300 mL saline administered. A guide wire was then introduced through the needle and a 10 French-gauge arterial introducer set placed over this guide. Instrument specifications for FETO procedure followed the usual recommendations. A 1.3 mm fetal tracheoscope was inserted through a 3.3 mm sheath 30°-precurved with 3 side ports (11540AA and 11540KE, Karl Storz, Tuttlingen, Germany). Amnioinfusion of saline was performed during the procedure in order to open the fetal mouth and vocal cords. A Smart-TO detachable balloon (BS-MTI, Niederroedern, France) was used for TO. Excessive amount of the infused fluid was drained through the trocar after surgery, under ultrasound guidance.

At the end of the procedure, the balloon could be nicely visualized in the fetal trachea and its dimensions were 17.3 x 6.7mm. One week later, the dimensions of the balloon did not change significantly.

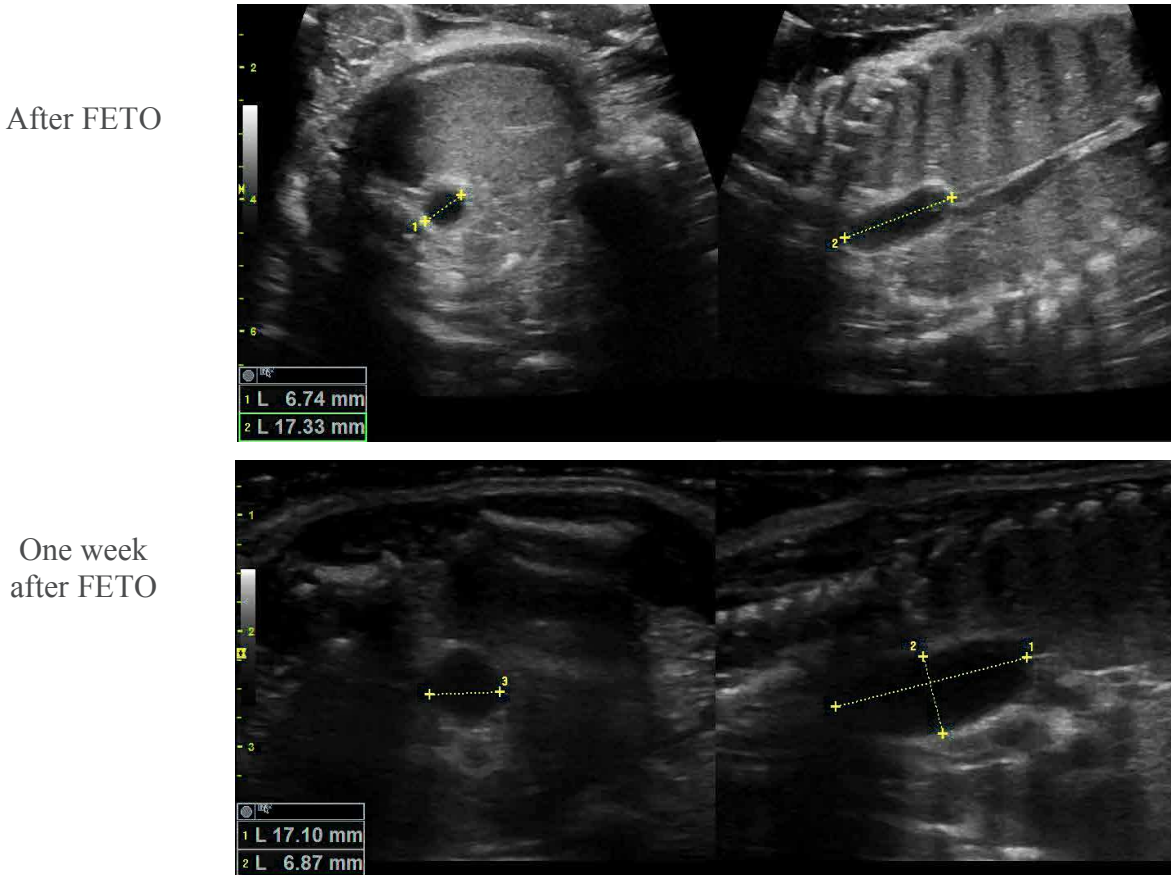

Figure 44: Balloon in the trachea after the FETO procedure and one week after

One week after the FETO procedure, at 146 days of gestation, the pregnant monkey was sedated with ketamine and was carried in front of an MRI machine Siemens MAGNETOM Aera 1.5T, in the imaging facility of University Hospital Institute, Strasbourg. After that, the control ultrasound scan could not visualize the balloon anymore. A control X-ray showed that the balloon was in the amniotic fluid, out of the fetal trachea, *i.e.* the balloon was washed out in the pulmonary secretions.

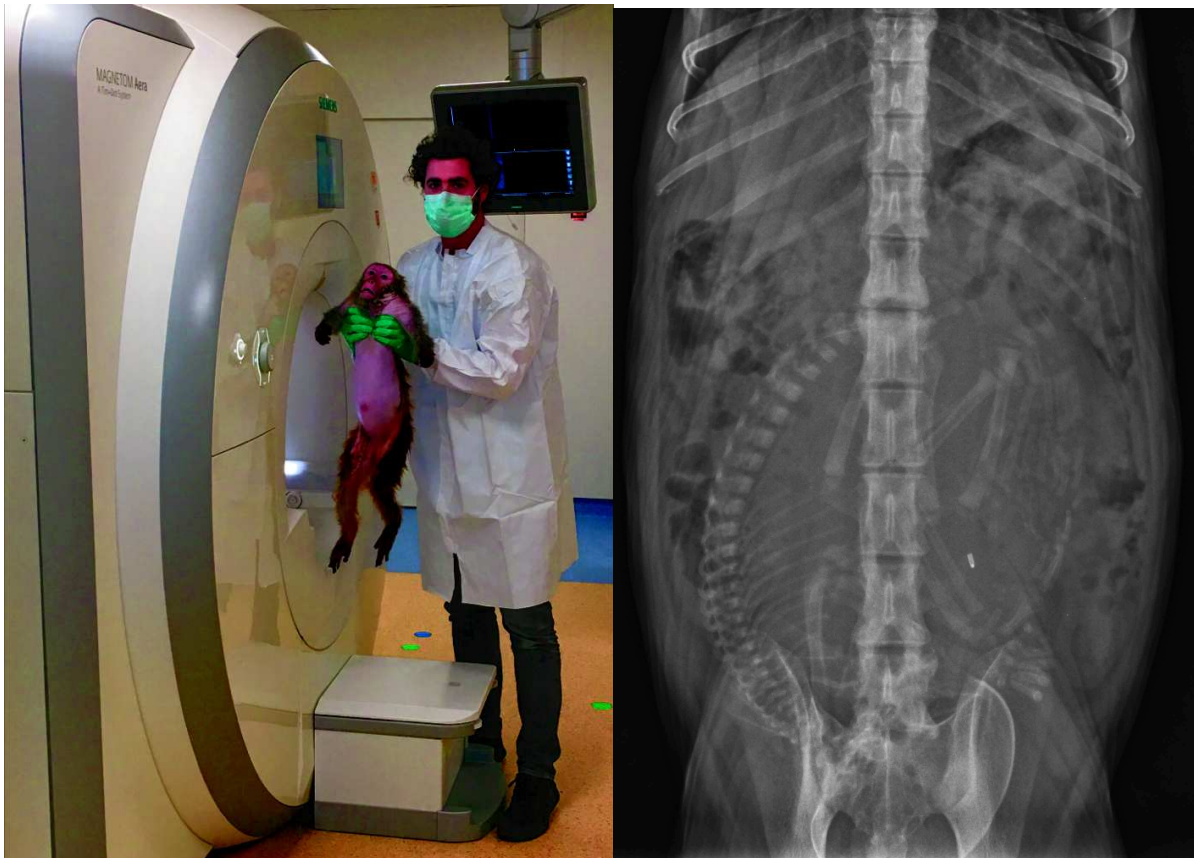

Figure 45: Monkey in front of the MRI machine and X-ray control

The tracheal occlusion duration was only one week but the lung sizes seemed to be a bit larger, according to the LHR measurements before the plug and after the unplug, as shown in the figure 46: 1.6 and 2.6 for the right LHR, and 1.8 and 1.6 for left LHR.

Finally, this first experiment was promising since the smart-TO balloon remained inflated during one week, it was deflated thanks the magnetic fringe field of an MRI, and could be washed out thanks to the pulmonary fluid. Two others experiments are planned on the monkey model.

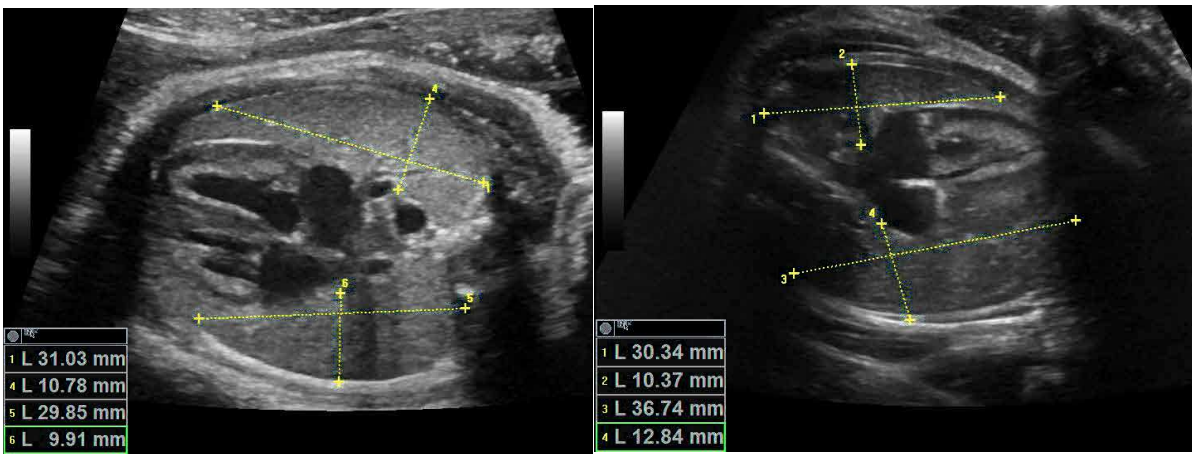

Figure 46: LHR measurements before plug and after unplug

3.6. Industrial process

3.6.1. Balloon manufacturing technique

The present chapter describes the different steps that are followed to assemble the magnetic valve occlusion system balloon and delivery system. Before assembly, metallic parts require a coating to guaranty biocompatibility. Assembly of the different parts require a precise and meticulous process.

3.6.2. Control of metal cylinder and magnetic ball

When delivered from the supplier, the metal tubes must be controlled. First the metal tube is observed under a microscope. The chamfered side of the cylinder must be regular and it can't be crushed, striped or irregular. If the chamfered side of the tube does is not in line with above expectations, the tube is rejected and excluded from production process. Once all the tubes have been observed and controlled under the microscope, the batch of tubes is cleaned and made ready for ultrasound bath treatment. After ultrasound cleaning, the rings are rinsed and dried before performing parylene coating treatment. After parylene coating treatment, the metal tubes batch is again quality controlled, with a magnifying glass to detect any irregularity in the coating layer.

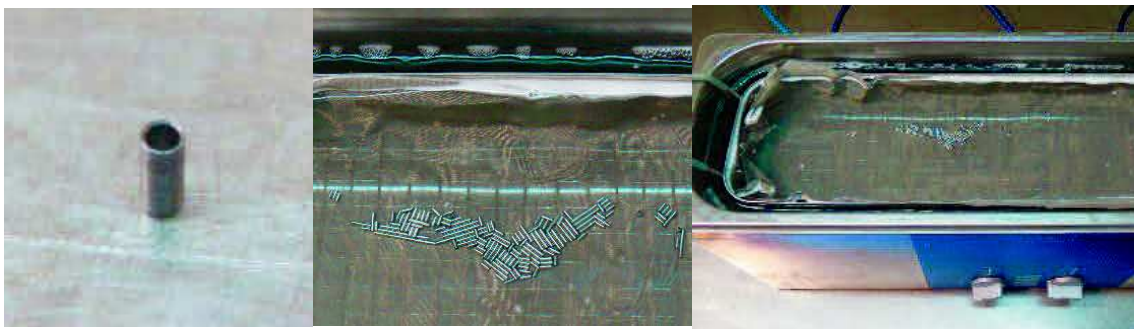

Figure 47: Control of the metal cylinders

When delivered from the supplier, the magnetic balls must be quality controlled under microscope. Once the magnetic ball is set alone, it must be cleaned from the dust and eventual tiny metal parts that could have been attracted by the magnetism of the ball. The surface must be clean (no tiny metal parts), round (not excrescences), and regular (no breaks). If the surface does is not in line with expectations (excrescences or breaks), the magnetic ball is rejected and excluded from production process. If the surface is not clean (tiny parts on the surface), the ball must be cleaned again until control under microscope confirms it is completely clean. When the magnetic ball has been qualified as clean, it is stored individually for ultrasound bath cleaning. Once the ultrasound cleaning is finished, magnetic balls are rinsed and dried. They are set in a parylene treatment device, where they are separated from each other, and not attracted by each other so they are free of movement. Therefore, parylene coating will be uniform and ensure a complete coverage of the magnetic balls. After parylene coating treatment, the magnetic balls are again quality controlled under microscope to detect any irregularity in the coating layer and to remove any metal dust contamination if necessary.

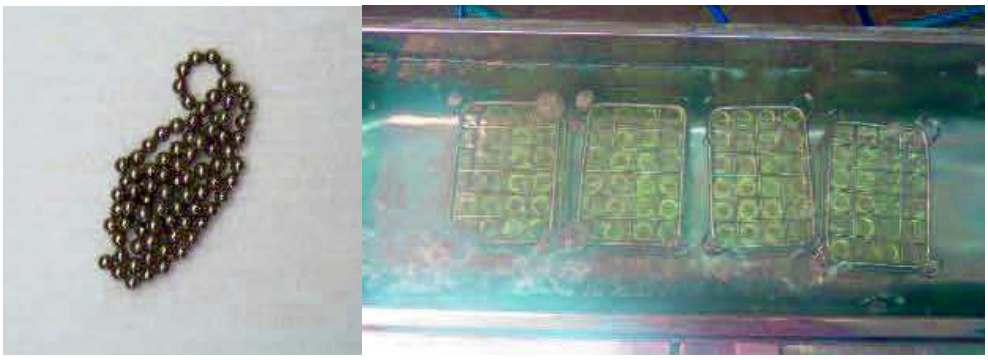

Figure 48: Control of the magnetic balls

3.6.3. Parylene coating

For the metal tubes, the parylene treatment consists in a bulk treatment. Tubes are stored in a rotating cylinder in which the parylene loaded gas circulates, thus covering the rings with a thin layer of parylene.

Balls being magnetic, they attract each other, so they are set in a specific parylene treatment device. That device is equipped with holes each receiving a ball. The holes are distant so the balls are not attracted by each other during the treatment. The device is pierced from part to part so that the parylene loaded gas can penetrate and circulate around the balls to ensure their regular and entire coating. The device is closed to ensure the balls stay in their individual cells during treatment.

3.6.4. Assembly of the balloon and delivery system

Latex balloons are washed so the talc is removed. It also allows to detect any leaky balloons. After that, the balloons must be carefully dried, especially in their internal part. The magnetic ball is then inserted in the balloon and pushed to the distal end of balloon. The balloon containing the magnetic ball is then inserted into the metal tube through the chamfered side of the tube. The tube is positioned at the appropriate distance from the back of the balloon. At last, the final balloon equipped with magnetic valve is measured and the proximal end of the balloon is cut to final size.

Figure 49: Assembly of the balloon

The delivery system is composed of three different types and size tubes. The pebax tube, the black peek tube and the white peek tube are cut to their final length. The black peek tube is introduced into the white peek tube and they are glued together in appropriate position. The so obtained set is then inserted into the pebax tube and glue in its final position. At proximal end, a white and green Luer Lock valve is positioned against the Pebax tube and tighten.

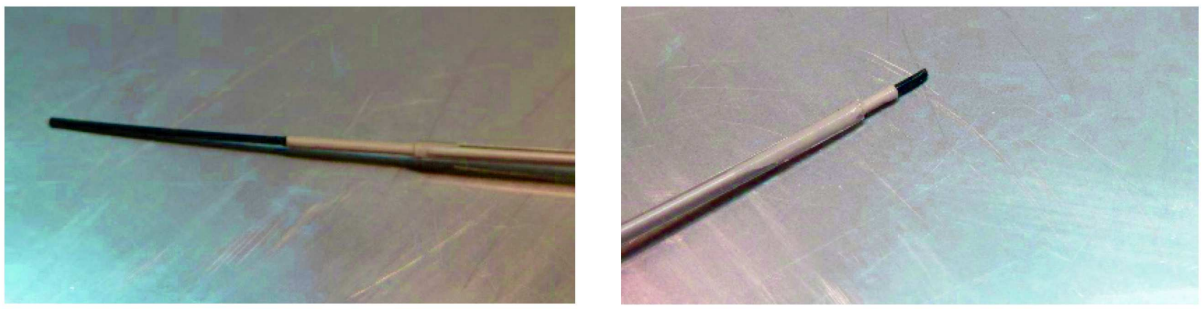

Figure 50: Assembly of the delivery system

At last, the 0.2mm diameter stylet is inserted and glued into a black peek tube piece and a pod.

3.6.5. Industrial testing

Before packaging, Smart-TO balloon and delivery system are paired to guaranty a perfect plug and disconnect functionality at the distal end. The balloon is then inflated and deflated to check its integrity and operation.

3.6.6. Sterilization methods

Ethylene Oxide (EtO) sterilization is used to sterilize Smart-TO balloon an delivery system as it is mainly used to sterilize medical and pharmaceutical products that cannot support conventional high temperature steam sterilization. A protocol will be implemented later to validate the sterilization cycle adapted to the product and delivery system.

3.6.7. Deliverable description and packaging

The balloon is placed into a little pealing bag, which is weld and cut to final size. The delivery system is inserted into a circular dispenser with angled clip. The stylet into circular dispenser with straightener guide wire. The balloon in its small bag, the stylet in its dispenser, the delivery system in its dispenser, and the syringe are placed in a large pealing bag.

Finally, the Smart-TO balloon and delivery system include different components:

- Smart-TO balloon equipped with magnetic valve, Ø 7 x 20 mm delivered in a dedicated pouch
- Delivery system (length 935 mm) equipped with Luer Lock valve and delivered in a dispenser
- Stylet Ø 0.2 mm x 937 mm equipped with a pod and delivered in a dispenser
- Luer Lock 1 ml Syringe

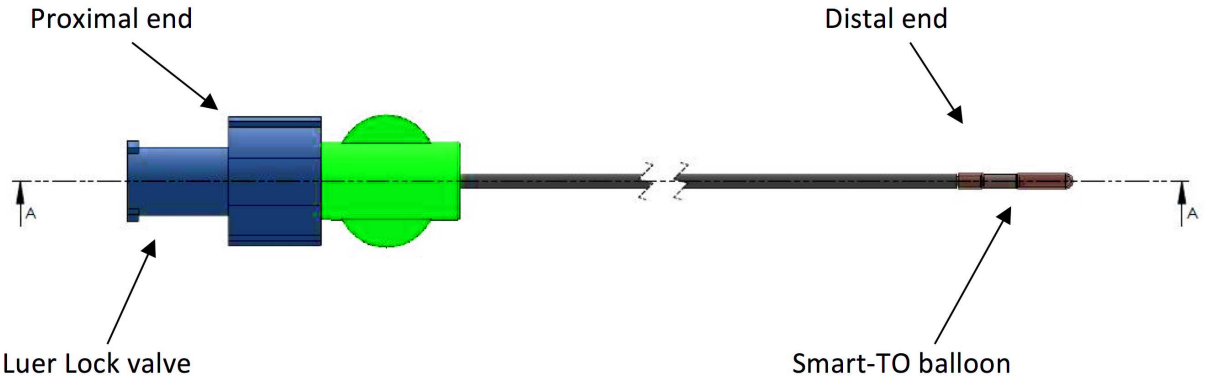

Figure 51: Outlines of the deliverable

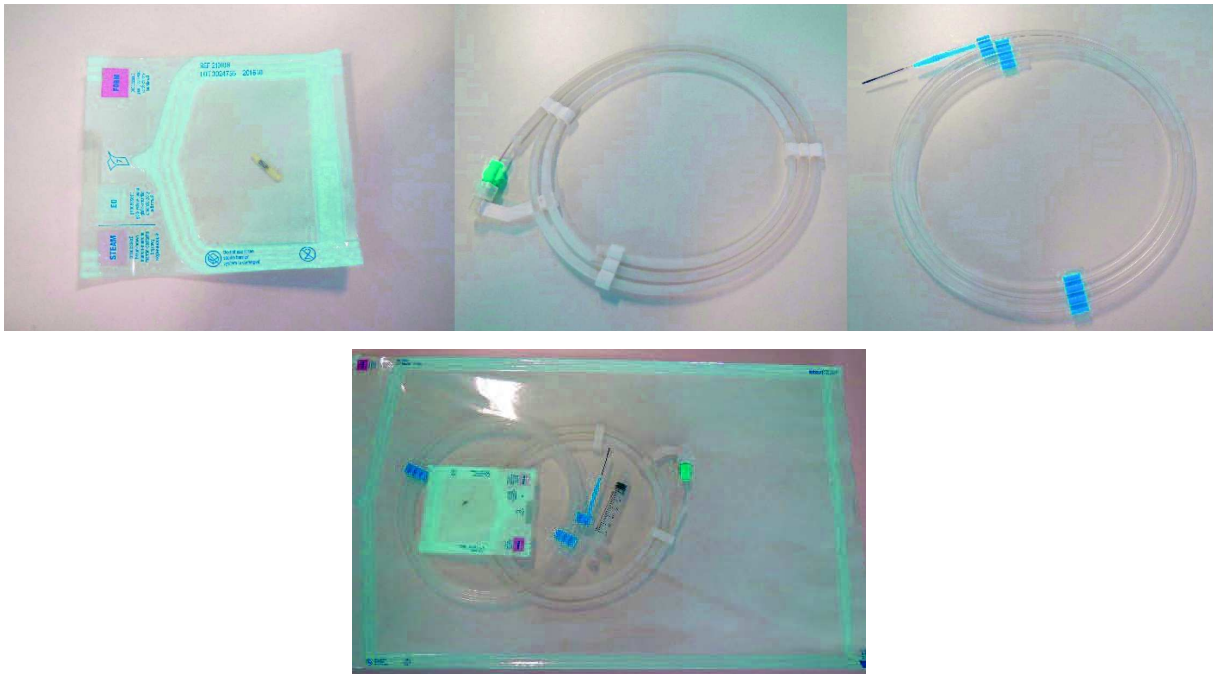

Figure 52: Pictures of the deliverable

3.6.8. Instruction for use

See Appendix 9.2. ‘Instruction for use’

3.7. Risk analysis

A preliminary risk analysis has been performed from a clinical point of view based on the dedicated diagrams and the definitions for severity and probability reported below.

The risk analysis itself is displayed in table 11.

Risk Diagramm

		Severity levels S				
		Negligible	Minor	Serious	Critical	Catastrophic
		S1	**S2**	**S3**	**S4**	**S5**
Probability level P						
Frequent	**P6**	III	I	I	I	I
Probable	**P5**	III	I	I	I	I
Occasional	**P4**	III	III	I	I	I
Remote	**P3**	III	III	III	I	I
Improbable	**P2**	III	III	III	III	III
Unimaginable	**P1**	III	III	III	III	III

Severity levels S		
Catastrophic	S5	When the risk of death or serious injury could be induced, associated with longer stay in hospital or in intensive care or else could generate physical damages. Product specific example: non sterile product
Critical	S4	When the risk of an injury could be induced, associated with hospital stay or the environment might be highly contaminated or side physical damage could be generated. Product specific example: Rupture of implant, Components insufficiently screwed together.
Serious	S3	When the chance of a minor physical damage exists, that require a doctor consultation, or a minor physical damage, or a temporary environmenta contamination with no lasting consequence. Product specific example: Set a bone back after luxation.
Minor	S2	When smaller physical damage could be induced, that does not require a doctor consultation, a negligible physical damage with no environmental contamination. Product specific example: resintering of a component
Negligible	S1	No risk of injury or no physical damage Product specific example:

Probability level P		
Frequent	P6	The incident occurs frequently during the life cycle of the product
Probable	P5	The incident could be expected each time during the life cycle of the product
Occasional	P4	The incident could be expected occasionally during the life cycle of the product.
Remote	P3	The incident is not excluded during the life cycle of the product
Improbable	P2	By normal use, the incident is not expected during the life cycle of the product. It is vaguely conceivable that the incident occurs.
Unimaginable	P1	The incident does not occur during the life cycle of the product. (defect prevention), Preventive measures have been taken to restrain danger (Safety system).

Risk table before actions

		Negligible S1	Minor S2	Serious S3	Critical S4	Catastrophic S5
Frequent	P6	0	0	0	0	0
Probable	P5	0	0	2	0	0
Occasional	P4	0	0	4	0	0
Remote	P3	0	0	4	4	0
Improbable	P2	0	0	1	2	0
Unimaginable	P1	0	0	0	0	0

Subsequent actions (corrective actions)

		Negligible S1	Minor S2	Serious S3	Critical S4	Catastrophic S5
Frequent	P6	0	0	0	0	0
Probable	P5	2	0	0	0	0
Occasional	P4	1	3	0	0	0
Remote	P3	1	4	3	0	0
Improbable	P2	2	0	1	0	0
Unimaginable	P1	0	0	0	0	0

Table 10: Diagrams for risk analysis

1	2	3	4	5	6	7	8	9	10	11	12	13	14
Hazard	Probable causes	Accident event (what, where, when)	Possible harm	Acts on	S	P	R	Contingencies/Preventive actions	ID	Verification/Documented evidence	S	P	R
Preliminary Risk Analysis / Clinical point of view													
Product is non-sterile	Damaged packaging	Shipping / Storage	Infection Need to use a new kit as the former one has lost steriity		4	3	I 43	To be written on the packaging label as well as on IFU: The material (kit) shall not be used in case of damaged packaging Trained staff		IFU Label	4	2	III 42
Product is non-sterile	Non convenient packaging/ non appropriate packaging; when opening the kit, some or all parts can fall on the floor	Mishandling	Infection Need to use a new kit as the former one has lost steriity		4	3	I 43	Packaging design Shipping validation IFU Trained staff		IFU Shipping validation report	4	2	III 42
Magnetic valve balloon is hard to place (fit) on the device	Too high mounting force needed –>Tolerance not adapted	Delivery system is damaged	Need to use a new kit		2	3	III 23	Product design 100% Control IFU : Balloon has to be humidified before assembly		IFU Monitoring form	2	1	III 21
The balloon is released during being introduced into the foetoscope (outside the patient body)	Balloon not correctly mounted Balloon makes contact with the foetoscope shaft	Balloon can fall on the floor	Need to use a new kit		2	4	III 24	Product design : Need a mark or a mechanical stop to place the balloon in its optimum position / tolerance Trained staff		Drawing	2	1	III 21
The balloon is released too early inside the foetus body during inflation or positionning	Balloon not correctly mounted Too low mounting force	Need to extract the balloon with a clamp Need to extract the foetoscope with clamp and balloon	Need to use a new kit Increase the surgery duration		3	4	I 34	Product design : Need a mark or a mechanical stop to place the balloon in its optimum position / / tolerance Trained staff 100% Control		Drawing Monitoring form	3	2	III 32
The balloon is released too early inside the foetus body during positionning or at begining of inflation	Balloon not correctly mounted Too low mounting force	Risk is that the balloon is lost. It is deflated and gone too far in the trachea or in bronchi	Need to use a new kit Increase the surgery duration. No consequence on the imediate fetus development, but an intervention will have to be scheduled to retreive it by bonchoscopy within two days after baby's birth.		3	4	I 34	Product design : Need a mark or a mechanical stop to place the balloon in its optimum position / tolerance Trained staff 100% Control		Drawing Monitoring form	3	2	III 32
The balloon is released when only partially field	Balloon not correctly mounted Too low mounting force	Need to extract the balloon with a clamp Need to extract the foetoscope with clamp and balloon. Need to pierce the balloon in some case.	Need to use a new kit Increase the surgery length.		3	4	I 34	Product design : Need a mark or a mechanical stop to place the balloon in its optimum position / tolerance Trained staff 100% Control		Drawing Monitoring form	3	2	III 32
The balloon burst	The balloon is over-inflated	Need to recover all the different tiny parts (magnetic ball, metal ring + balloon)	Increase the surgery length. Need to use a new kit No consequence on the imediate fetus development, but an intervention will have to be scheduled to retreive it by bonchoscopy within two days after baby's birth.		4	3	I 43	Product design : Material choice Trained staff A 1 mL max. syringe will be placed into the kit IFU : max volume in balloon 0,7ml		Destruction test report	4	1	III 41
The mounting device press on the magnetic ball thus preventing the valve from closing	Delivery system or ballon is non conform	Need to extract the balloon with a clamp Need to extract the foetoscope with clamp and balloon.	Need to use a new kit Increase the surgery length.		3	3	III 33	Product design 100% Control		Monitoring form	3	1	III 31
The balloon is filled totally with air instead of of physiological serum	Syringue filled with air	Risk to loose volume quickly (bad effect on permeability performance)	Consequence on the fetus development New intervention have to be planed to place a new balloo		5	3	I 53	Trained staff IFU		IFU	5	1	III 51
The balloon is filled partially with air (0,1ml) instead of physiological serum	Draining of the delivery system is not well done	Risk to loose a little volume during implementation time	No consequence on the fetus development		2	4	III 24	Trained staff IFU : draining procedure		IFU	2	3	III 23
Balloon is directly permeable	Balloon damaged Valve is not closed because the magnetic ball is not in contact with the metalic ring	Need to extract the balloon with a clamp Need to extract the foetoscope with clamp and balloon.	Need to use a new kit Increase the surgery lengh.		3	4	I 34	100% Control Trained staff IFU : control the position of the magnetic ball		IFU Monitoring form	3	3	III 33
Balloon is permeable within few minutes or days	Pinhole in the balloon / valve is not 100% tight	when the lung is not well developed yet, need to plan/schedule a new surgery for a second balloon placement	Consequence on the fetus development. Need contol the volume and efficency of the balloon by regular echography. 5% of Balt balloons were deflated New intervention have to be paned to place a new		5	3	I 53	Permeability test 100% Control		Permeability test report Monitoring form	5	1	III 51
Balloon is difficult to release. The position of the balloon is modified	Too high release force is needed → Tolerance	Placement of the balloon can be wrong and move up to the vocal cords or else the mouth. Balloon needs to be extracted with a clamp, some times deflated with a needle.	Need to extract the foetoscope with clamp and balloon Need to use a new kit Increase the surgery lengh.		3	3	III 33	Product design 100% Control		Drawing Monitoring form	3	2	III 32
The magnetic valve balloon does not deflate when submited to MRI	Incrustation of the magnetic ball		A second surgery needs to be performed to deflate the balloon with a needle - actual method - loss of all benefits of the new magnetic device		4	3	I 43	Deflation test		Deflation test report	4	2	III 42
Balloon deflates when submited to MRI, but is not spit by the fœtus			In the two days following the birth, a surgery has to be paned/scheduled to retrieve the balloon		3	3	III 33				3	3	III 33
Balloon deflates when submited to MRI but MRI's attraction prevents the balloon to be carried out by the pressure accumulated into the lung	MRI's attraction > pressure in lung		In the two days following the birth, a surgery has to be planed/scheduled to retrieve the balloon		3	3	III 33				3	3	III 33

Table 11: Risk analysis from a clinical point of view

3.8. Regulatory routes

3.8.1. EU legislation

The directive 93/42/CEE relating to medical devices was adopted in 1993. It guarantees that medical devices should provide patients as well as users “a high level of protection and attain the performance levels attributed to them by the manufacturer.” This directive imposes EC marking of medical devices for their marketing. This EC marking means that the medical device is in conformity with the “Essential Requirements” defined by the directive, and which are in fact the technical conditions which the medical devices must satisfy in order to be placed on the market. Their respect ensures both quality and reproducible safety for the user.

The directive 93/42/CEE defines as medical devices ‘any instrument, apparatus, appliance, material or other article whether used alone or in combination, including the software necessary for its proper application, intended by the manufacturer to be used for human beings for the purpose of’:

- diagnosis, prevention, monitoring, treatment or alleviation of disease,
- diagnosis, prevention, monitoring, treatment or alleviation of or compensation for an injury or handicap,
- investigation, replacement or modification of the anatomy or a physiological process,
- control of conception, and which does not achieve its principal intended action in or on the human body by pharmacological, immunological or metabolic means, but which may be assisted in its function by such means.

The medical devices thus defined are divided into four classes: I, IIa, IIb and III. The rules of classification defined by the European directive are based on:

- the duration of use
- whether or not the device is invasive and the type of invasivity
- whether or not the device may be reused
- the therapeutic or diagnostic aim
- whether the device is active (dependent on a source of energy)
- the part of the body in contact with the medical device.

According to the legislation, Smart-TO device is implanted for an average of 6 weeks in the fetus using a surgical procedure. Smart-TO is therefore considered a class IIb medical device.

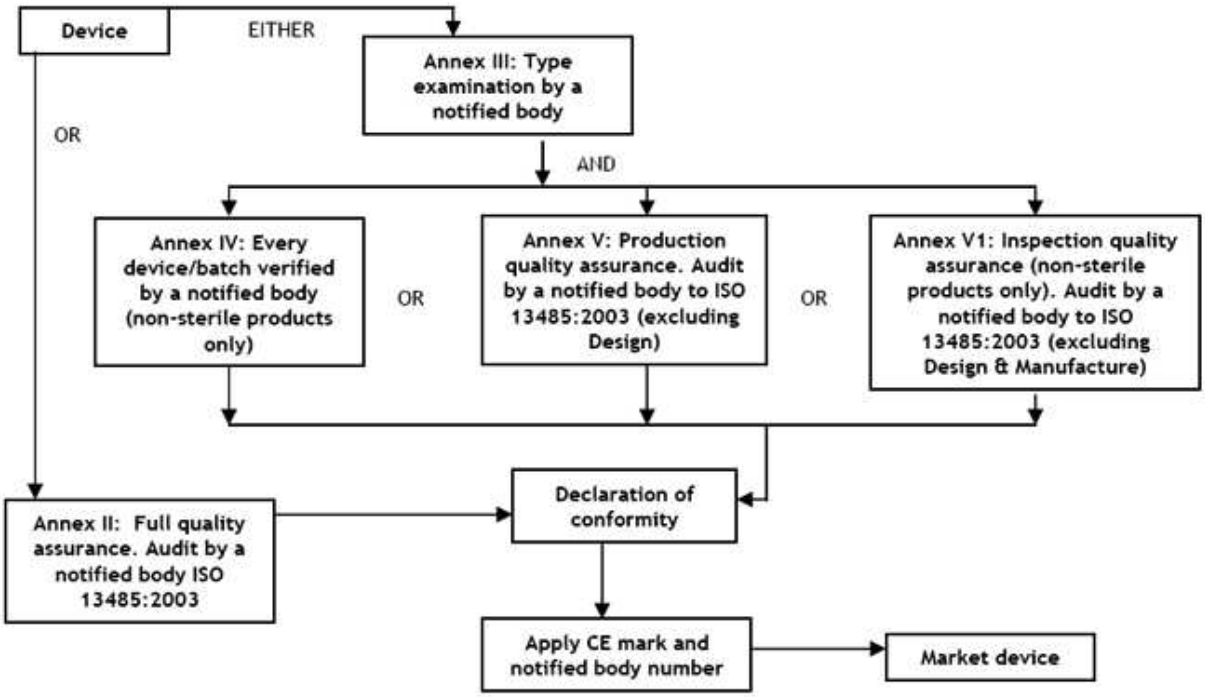

Figure 53: CE marking route for class IIB medical devices

3.8.2. US legislation

The FDA Office of Orphan Products Development (OOPD) mission is to advance the evaluation and development of products (drugs, biologics, devices, or medical foods) that demonstrate promise for the diagnosis and/or treatment of rare diseases or conditions. In fulfilling that task, OOPD evaluates scientific and clinical data submissions from sponsors to identify and designate products as promising for rare diseases and to further advance scientific development of such promising medical products. The office also works on rare disease issues with the medical and research communities, professional organizations, academia, governmental agencies, industry, and rare disease patient groups.

The Humanitarian Use Device (HUD) program designates a device that is intended to benefit patients by treating or diagnosing a disease or condition that affects fewer than 4,000 individuals in the United States per year as per 21 CFR 814.3(n). The HUD marketing pathway is a marketing approval process that under certain conditions will allow medical devices for the treatment of rare disease/conditions to be commercialized if they meet safety and probable benefit criteria.

There are approximately 6 million pregnancies every year throughout the United States, and taking into account the frequency of CDH, Smart-TO could therefore classified as a humanitarian device which lightens the process of marketing. To obtain approval for an HUD, a humanitarian device exemption (HDE) application is submitted to FDA. An HDE is similar in both form and content to a premarket approval (PMA) application, but is exempt from the effectiveness requirements of a PMA. An HDE application is not required to contain the results of scientifically valid clinical investigations demonstrating that the device is effective for its intended purpose. The application, however, must contain sufficient information for FDA to determine that the device does not pose an unreasonable or significant risk of illness or injury and that the probable benefit to health outweighs the risk of injury or illness from its use, taking into account the probable risks and benefits of currently available devices or alternative forms of treatment. Although the agency acknowledges the challenges of obtaining a large sample for a clinical study of an HUD, there is nevertheless a requirement for demonstration of safety and probable benefit. In most cases, these can only be fully demonstrated with clinical data of some kind. This should be easy as the use of a balloon for TO has already proven to be efficient in promoting lung growth and thus improving survival. Additionally, the applicant must demonstrate that no comparable devices are available to treat or diagnose the disease or condition, and that they could not otherwise bring the device to market. To that we could argue that the actual solution could be improved in term of results of fetal survival and is also used off-record.

Currently, as part of the TOTAL trial, there is an Investigational Device Exemption for the Goldbal detachable balloon, Balt (Montmorency, France).

3.9. Market and socio-economical context

3.9.1. Benefits offered by the new balloon

The innovative balloon has the same functional occlusive characteristics as the Goldbal® balloon, Balt (Montmorency, France). Additionally, it offers a simple and remotely controlled noninvasive removal. Not only it avoids a surgical procedure, but it also avoids organizational issues and complications related to the airway reestablishment.

3.9.2. Size of the targeted market

CDH is among the most common isolated fetal malformations. It occurs in 1/3000 to 1/5000 live births but these numbers don't include what has been called the « hidden mortality », such as stillbirths, medical terminations of pregnancy or neonatal deaths before transfer to a tertiary center (1, 2). Finally, it is usually estimated that the prevalence of CDH is around 1/2200 live births (3, 4). Maternal ultrasound screening programs have led to prenatal diagnosis in about 2 on 3 cases as evaluated in a large multicenter study in 2002, but detection rate can even be raised to 90% (5, 6). We can therefore estimate that 80% of CDH are diagnosed prenatally. Approximately 40% of CDH cases have associated malformations, identified syndromes and/or genetic problems (7-9). These associated anomalies require specific care and are independently correlated with a poor prognosis. At last, proportions of severe, moderate, and mild CDH can be respectively estimated as 25%, 35%, and 40% (10,11).

Finally, if we consider 5 131 500 live births in Europe each year (Eurostat data 2014), there would be a total of 2 333 CDH cases (1/2200), among which 1 866 with prenatal diagnosis (80%), among which 1 120 isolated (60%), among which 280 severe (25%) and 392 moderate CDH cases (35%). With the same calculation methods, if we consider 3 988 076 live births in US each year (US Department of Health data 2014), there would be 218 severe and 305 moderate CDH cases each year.

1. Butler N, Claireaux AE. Congenital diaphragmatic hernia as a cause of perinatal mortality. Lancet. 1962;1(7231):659-63.

2. Harrison MR, Bjordal RI, Langmark F, Knutrud O. Congenital diaphragmatic hernia: the hidden mortality. J Pediatr Surg. 1978;13(3):227-30.

3. Deprest JA, Nicolaides K, Gratacos E. Fetal surgery for congenital diaphragmatic hernia is back from never gone. Fetal Diagn Ther. 2011;29(1):6-17.

4. Langham MR, Jr., Kays DW, Ledbetter DJ, Frentzen B, Sanford LL, Richards DS. Congenital diaphragmatic hernia. Epidemiology and outcome. Clin Perinatol. 1996;23(4):671-88.

5. Guibaud L, Filiatrault D, Garel L, Grignon A, Dubois J, Miron MC, et al. Fetal congenital diaphragmatic hernia: accuracy of sonography in the diagnosis and prediction of the outcome after birth. AJR Am J Roentgenol. 1996;166(5):1195-202.

6. Garne E, Haeusler M, Barisic I, Gjergja R, Stoll C, Clementi M. Congenital diaphragmatic hernia: evaluation of prenatal diagnosis in 20 European regions. Ultrasound Obstet Gynecol. 2002;19(4):329-33.

7. Slavotinek AM. The genetics of congenital diaphragmatic hernia. Semin Perinatol. 2005;29(2):77-85.

8. Stoll C, Alembik Y, Dott B, Roth MP. Associated malformations in cases with congenital diaphragmatic hernia. Genet Couns. 2008;19(3):331-9.

9. Fauza DO, Wilson JM. Congenital diaphragmatic hernia and associated anomalies: their incidence, identification, and impact on prognosis. J Pediatr Surg. 1994;29(8):1113-7.

10. Jani JC, Nicolaides KH, Gratacos E, Vandecruys H, Deprest JA, Group FT. Fetal lung-to-head ratio in the prediction of survival in severe left-sided diaphragmatic hernia treated by fetal endoscopic tracheal occlusion (FETO). Am J Obstet Gynecol. 2006;195(6):1646-50.

11. Jani J, Cannie M, Sonigo P, Robert Y, Moreno O, Benachi A, et al. Value of prenatal magnetic resonance imaging in the prediction of postnatal outcome in fetuses with diaphragmatic hernia. Ultrasound Obstet Gynecol. 2008;32(6):793-9.

3.9.3. Market trends and penetration

Fetal surgery is a new and expanding market, which has greatly developed since the nineties. To our knowledge, there are currently around 20 FETO centers in the world: Paris (2), Leuven, Brussels, Barcelona, London, Milano-Roma, Bonn, Hamburg, Giessen, Toronto, Houston (2), Philadelphia, San-Francisco, Denver, Cincinnati, Baltimore, Rochester, and Brisbane. We can estimate that approximately a mean of 10 FETO procedures are performed each year in each center. However, the number of potential candidates is much larger, as detailed above.

Two multicenter international randomized controlled trials evaluating the interest of FETO in severe (NCT01240057) and moderate (NCT00763737) CDH are currently ongoing. The acronym used is 'TOTAL' (Tracheal Occlusion To Accelerate Lung growth). The development of the market will depend on the results of this trial.

If the TOTAL trial shows that FETO improves survival for severe and/or moderate CDH, the FETO procedure will have to be offered to patients with a prenatally diagnosed CDH. Indeed, this trial will provide results with the highest level of evidence. We can assume therefore that the number of FETO will increase the same way as the number of laser procedures for twin-to-twin transfusion syndrome (TTTS) increased after the randomized trial published in 2004 (Senat MV, Deprest J, Boulvain M, Paupe A, Winer N, Ville Y. Endoscopic laser surgery versus serial amnioreduction for severe twin-to-twin transfusion syndrome. N Engl J Med. 2004;351(2):136-44). In a world-wide survey on laser surgery published in 2014, 106 fetal surgery centers offering laser procedures for TTTS have been identified (Akkermans J1, Peeters SH, Middeldorp JM, Klumper FJ, Lopriore E, Ryan G, Oepkes D. A world-wide survey on laser surgery for twin-twin transfusion syndrome. Ultrasound Obstet Gynecol. 2014 Sep 23. doi: 10.1002/uog.14670). A total of 76 centers answered the survey and the total number of laser procedures performed by those centers was approximately 1 500. If we consider the centers that did not answer the survey, we can therefore estimate that more than 2000 laser procedures are performed each year in the world. To be noted that not only the Smart-TO balloon would avoid complications related to unplug, but in addition it could participate in the diffusion of the technique. Indeed, it would not be necessary that the patients stay close to a FETO center for the whole duration of the fetal tracheal occlusion, what is a practical limitation the diffusion of FETO procedure.

If the TOTAL trial shows that FETO does not improve survival for severe and/or moderate CDH, the Smart-TO balloon would still be of interest. Indeed, since the fetal morbidity and mortality of plug-unplug sequence are partially due to issues related to airway reestablishment, the use of Smart-TO balloon might improve outcomes of CDH cases treated by FETO. Moreover, since Smart-TO offers a non-invasive reversal occlusion, the timing for the unplug so the timing for the plug could be performed later in the pregnancy, thus limiting the risk of premature delivery associated with the FETO procedure.

3.9.4. Valorization scheme

Satt-Conectus has been mandated to manage the intellectual property on behalf of the patent owners. It is recognized to grant an exclusive license in the fetal surgery field to the company BS-Medical Tech Industry (BS-MTI) which is the historical industrial projects partner. The licensing contracts are now being finalized.

After obtaining the CE-marking, BS-MTI will start to sale the Smart-TO device. A monetary restitution will be operated to the industrial property owners once a year. It's also possible to grant another license to an industrial partner who could operate in another medical field.

The aim is to replace the off-label Balt balloon by the 'BS-MTI – Smart-TO' device. Unlike to the current device, Smart TO has been specifically developed for FETO which involves a lot of costs and surely increase the current purchase price for the hospitals. The clinical benefits, the patient comfort, and the expected reduction costs for the hospitals will be the principal arguments to penetrate the market and to justify an increased purchasing price.

BS-Medical Tech Industry will have the opportunity to operate in a small niche market which is generally not 'major players goal'. For such a company, a niche market is often very profitable. For the clinician, the advantage will be to have a supplier which will remain attentive to the clinical needs. We are in this case in a win-win context which may guarantee the success of Smart-TO.

3.10. Partnership and funding

3.10.1. Partners

Several institutional partners and companies have been involved in the development of this innovative device:

- Strasbourg University Hospital.
- Strasbourg University.
- INSERM UMR-S 1121 'Biomaterials and Bioengineering'.
- Simian Laboratory Europe (SILABE).
- Research Institute against Digestive Cancer (IRCAD).
- Institute of image-guided surgery (IHU Strasbourg).
- SATT-Conectus Alsace.
- Lavoix Intellectual Property Company.
- Alsace BioValley (the project obtained the 'Alsace BioValley label').
- BS Medical Tech Industry (BS-MTI).

3.10.2. Funders

Several funders have contributed to the development of this innovative device:

- Franco-American Fulbright Commission.
- SATT-Conectus Alsace.
- Fondation de l'avenir.
- Banque populaire CASDEN
- French Ministry of Health.
- Regional Innovation Partnership.

Development is now under the responsibility of BS Medical Tech Industry (BS-MTI).

3.11. Conclusion and prospects

We developed a new balloon for Fetal Endoscopic Tracheal Occlusion (FETO) which allows an easy, remotely controlled, and non-invasive reversal occlusion. This 'Smart-TO' balloon allows to overcome issues related to the airway reestablishment. The technology solution is based on a magnetic valve whose opening is actuated by the fringe field of an MRI scanner. The opening of the valve induces the deflation of the balloon, which is then washed out by the fluid coming out from the lungs.

The impermeability, occlusion, and operation tests are promising. A very first experimentation on the monkey model showed appropriate functionality and operation of the 'Smart-TO' balloon. Further *in vitro* and animal tests are planned. A patent has been filed in 2016.

Preliminary risk analysis, regulatory routes exploration, and market study have been started but are still ongoing.

Regarding the testing of the 'Smart-TO' device, further impermeability, occlusion, and operation tests are planned, so as tests on the latex balloon itself (mechanical resistance, sealing, traction test…), on the magnetic valve (corrosion), and on the finished product (releasable, aging, and sterilization protocol). Two other experiments are planned on the monkey model. Thanks to a collaboration with Pr Jan Deprest, we also plan to test the 'Smart-TO' balloon on the sheep model. This is of interest since there is an existing sheep model of congenital diaphragmatic hernia (CDH), in contrast to the monkey model.

The use of 'Smart-TO' balloon in human will depend on the results of the TOTAL trial, which evaluates the interest of FETO in severe and moderate CDH.

The use of 'Smart-TO' balloon might improve outcomes of CDH cases treated by FETO since the fetal morbidity and mortality of plug-unplug sequence are partially due to issues related to airway reestablishment. Moreover, since Smart-TO offers a non-invasive reversal occlusion, the timing for the unplug so the timing for the plug could be performed later in the pregnancy, thus limiting the risk of premature delivery associated with the FETO procedure.

Not only the 'Smart-TO' balloon may avoid complications related to unplug, but in addition it could participate in the diffusion of the FETO technique. Indeed, it would not be necessary that the patients stay close to a FETO center for the whole duration of the fetal tracheal occlusion, what is a current practical limitation the diffusion of FETO procedure.

4. NON-HUMAN PRIMATE MODEL FOR FETO

Experimental fetal endoscopic tracheal occlusion in rhesus and cynomolgus monkeys: nonhuman primate models.

Sananès N, Ruano R, Weingertner AS, Regnard P, Salmon Y, Kohler A, Miry C, Mager C, Guerra F, Schneider A, Becmeur F, Leroy J, Dimarcq JL, Debry C, Favre R.

J Matern Fetal Neonatal Med. 2015;28(15):1822-7.

THE JOURNAL OF MATERNAL-FETAL & NEONATAL MEDICINE

http://informahealthcare.com/jmf
ISSN: 1476-7058 (print), 1476-4954 (electronic)

J Matern Fetal Neonatal Med, 2015; 28(15): 1822–1827
 DOI: 10.3109/14767058.2014.969234

informa healthcare

ORIGINAL ARTICLE

Experimental fetal endoscopic tracheal occlusion in rhesus and cynomolgus monkeys: nonhuman primate models

Nicolas Sananès[1,2], Rodrigo Ruano[3], Anne-Sophie Weingertner[1], Pierrick Regnard[4], Yves Salmon[4], Anne Kohler[1], Claire Miry[1], Cécile Mager[1], Fernando Guerra[1], Anne Schneider[5], François Becmeur[5], Joël Leroy[6], Jean-Luc Dimarcq[7], Christian Debry[8], and Romain Favre[1]

[1]Department of Fetal Medicine, Strasbourg Teaching Hospital, France, [2]INSERM, UMR-S, "Biomatériaux et Bioingénierie", Strasbourg Cedex, France, [3]Texas Children's Fetal Center and Baylor College of Medicine, USA, [4]SILABE – ADUEIS Platform, Niederhausbergen, France, [5]Department of Pediatric Surgery, Strasbourg Teaching Hospital, France, [6]IRCAD – EITS, Strasbourg Teaching Hospital, France, [7]Scientific foundation IHU Strasbourg, France, and [8]Department of Ear, Nose and Throat, Strasbourg Teaching Hospital, France

ABSTRACT

Objective: The monkey model is the best model to investigate some physiological response to the fetal transitory tracheal occlusion but it has never been described in *Macaca* monkeys. The aim of this study was to evaluate the feasibility of fetal endoscopic tracheal occlusion (FETO) in a non-human primate model.
Methods: Pregnant rhesus monkeys and cynomolgus were tested as a potential experimental model for FETO in the third trimester of pregnancy, by performing fetal tracheoscopies with and without tracheal occlusion.
Results: A total of 22 pregnancies were followed in 16 monkeys and underwent fetal surgery. Percutaneous endoscopic access to the uterine cavity was possible in 20 cases (91%). Of these 20 pregnant monkeys, fetal tracheoscopy could be achieved in 15 cases (75%). In rhesus monkeys, the time between the onset of endoscopy and tracheal penetration decreases as operator experience increases. Neither maternal morbidity nor mortality was related to surgery. Two fetal losses were possibly due to the procedure.
Conclusion: FETO is feasible in the non-human primate, which closely reflects procedures in humans. The non-human primate model for FETO, specially the rhesus monkeys, may be useful for future studies concerning the mechanisms related to the lung growth after transitory fetal tracheal occlusion.

Keywords

Cynomolgus monkey, endoscopic surgery, fetal endoscopic tracheal occlusion, non-human primate, rhesus monkey

History

Received 24 May 2014
Accepted 22 September 2014
Published online 9 October 2014

Introduction

Congenital diaphragmatic hernia (CDH) is one of the most common isolated fetal malformations. CDH occurs in 1/3000 to 1/5000 live births [1]. CDH is associated with hypoplasia of both lungs, which affects airways and vessels with subsequent pulmonary hypertension. This leads to approximately 30% neonatal mortality in tertiary centres, even though CDH is a surgically correctable defect [2]. Promoting lung growth during fetal life is therefore of benefit.

Fetal tracheal occlusion (TO) increases airway pressure and prevents egress of lung fluid, leading to improved growth of the alveolar airspace and maturation of the pulmonary vasculature [3]. A minimally invasive approach has been developed which is known as fetal endoscopic tracheal occlusion (FETO) [4,5]. A thin endoscope is percutaneously introduced into the fetal trachea in order to position a detachable balloon between the carina and vocal cords at between 27 and 30 weeks. The balloon is ideally removed prenatally by fetal tracheoscopy or punctured by ultrasound-guided needle at around 34 weeks. Several studies have shown an improvement of neonatal survival in severe cases [6,7].

Different animal models have been used to study the effect of TO on lung growth: sheep (*Ovis aries*), rabbits (*Oryctolagus cuniculus*), rats (*Rattus norvegicus*) and mice (*Mus musculus*). Every model has strengths and weaknesses which vary depending on ethical issues, cost, animal and lung size, surgical difficulty, abortion rates, alveolarization timing, genome knowledge, and availability of genes and protein sequences [3]. For this purpose, the sheep model has been used for endoscopic TO, but unfortunately this model does not represent entirely the same condition observed in humans [8,9]. A non-human primate model may be a relevant translational model for fetal surgery, especially FETO, because both anatomy and physiology are closed to humans [3,10]. There are only few studies evaluating fetal surgery in monkeys and only three cases of FETO in baboons (*Papio* spp) have been recently reported [11–14]. In addition, to our

Address for correspondence: Dr. Nicolas Sananès, Service de Gynécologie Obstétrique, Hôpitaux Universitaires de Strasbourg, 67091 Strasbourg cedex, France. Tel: +33 3 88 12 78 39. E-mail: nicolas.sananes@chru-strasbourg.fr

knowledge, there is no study evaluating different types of monkey foetuses would be adequate as a FETO experimental model. Therefore, the objective of this study was to evaluate the feasibility of fetal surgery in non-human primates using exclusively percutaneous fetoscopy by testing two different models.

Methods

The monkeys (16 females from 6 reproduction groups) were group-housed in indoor/outdoor facilities in SILABE plateform (Simian Laboratory Europe). They lived in social groups (1 or 2 adult males and 4 to 10 females) in indoor/outdoor facilities of approximately 40 to 85 m^3 for the indoor facility (depending on the animal facility and group) and 40 to 50 m^3 for the outdoor facility. Water and food were distributed *ad libitum*. Animals were captured regularly in order to perform ultrasound to detect pregnancy and establish the gestational age. The timing of surgery was determined by ultrasound measurement of the biparietal diameter of the fetus in early pregnancy (Voluson E GE®). Pregnant rhesus monkeys (*Macaca mulata*) and cynomolgus (*Macaca fascicularis*) underwent fetal surgery in the last third trimester of pregnancy . Pregnant female were captured on the day of the surgery. After surgery, they were isolated until the following morning and were then returned to their social group. The Regional Ethics Committee on Animal Experimentation (CREMEAS) at Strasbourg University, France (number AL/02/03/03/09) approved this study. Guidelines for the care and use of the monkeys approved by this institution were followed.

A total of 22 pregnancies (12 in rhesus and 10 in cynomolgus monkeys) were followed in 16 monkeys and subsequently underwent fetal surgery. Gestational dates were interpreted by ultrasound measurement of the biparietal diameter on average at 66 ± 15 days' gestation (40 to 110). Surgery took place on average at 133 ± 5 days' gestation (124 to 144): 135 days in rhesus and 131 days in cynomolgus, representing 81.8% of the gestational period in rhesus and 79.9% in cynomolgus monkeys, assuming gestational lengths of 165 and 164 days respectively [15].

The pregnant monkey was first sedated with ketamine (10 mg/kg, IM) before general anesthesia with propofol (5 mg/kg, IV) and 1 to 2.5% isoflurane after tracheal intubation. Ventilation was controlled by assisted mechanical respiration after tracheal intubation. Maternal breath frequency, electrocardiogram, PO_2/PCO_2 measurement, halogenated gas and temperature were continually monitored and a heating blanket was applied to maintain body temperature. Maternal blood pressure was monitored with a sphygmomanometer. A single dose of 2% marbocyl was given (Marbofloxacin 2 mg/kg, IM) prior to surgery. No tocolytic was administered.

Before surgery, fetal monkey curarization was performed by an intra-muscular injection of 0.15 to 0.20 mg cisatracurium in the fetal leg, under ultrasound guidance. After localization of the fetal head and placenta in order to determine the optimal entry site, 5 ml 2% xylocaine was injected percutaneously into the myometrium of the pregnant monkey in order to provide additional local anesthesia. Endoscopic access was performed using the modified Seldinger technique under continuous ultrasound guidance [16,17]. A 17G needle was first introduced into the uterine cavity and an amnioinfusion of 200 to 300 mL saline administered. A guide wire was then introduced through the needle and a 10 French-gauge arterial introducer set placed over this guide. Instrument specifications for FETO procedure followed the usual recommendations [5]. A 1.3 mm fetal tracheoscope was inserted through a 3.3 mm sheath 30°-precurved with 3 side ports (11540AA and 11540KE, Karl Storz, Tuttlingen, Germany). A Goldbal 2 detachable balloon (Balt, Montmorency, France) was used for TO. Retrieval forceps (11510C, Karl Storz) and adjustable puncture stylet (11506P, Karl Storz) were used for balloon removal. Amnioinfusion of saline was performed during the procedure in order to open the fetal mouth and vocal cords.

Surgical procedures involved fetal tracheoscopies, with or without TO. When TO was performed, balloon removal was done in the same surgery session. A single operator performed all surgical procedures. Excessive amount of the infused fluid was drained through the trocar after surgery, under ultrasound guidance.

Results

Percutaneous endoscopic access inside the uterine cavity could be performed in 20 cases (91%). Of these 20 pregnant monkeys, fetal tracheoscopy was feasible in 15 cases (75%): 9 rhesus (90%) and 6 cynomolgus monkeys (60%). TO was attempted in 3 rhesus monkeys; it took place without incident, as well as the unplugging procedure.

The duration between onset of endoscopy and tracheal penetration was on average 19 ± 9 min (4 to 34): 17 ± 10 min in rhesus (4 to 35) and 22 ± 5 min in cynomolgus (13 to 28) monkeys. In rhesus monkeys, this duration decreased with increasing operator experience (Figure 1). This correlation was not replicated in the cynomolgus monkey (Figure 2).

The fetal monkey model reflects very closely human fetal anatomy. Figure 3 shows endoscopic views of the fetal monkey.

Gestational age at delivery was on average 158 ± 14 days (131 to 203). One mother died during delivery because of fetal malpresentation (arm dystocia). No other maternal mortality or morbidity was observed. There were 6 cases of

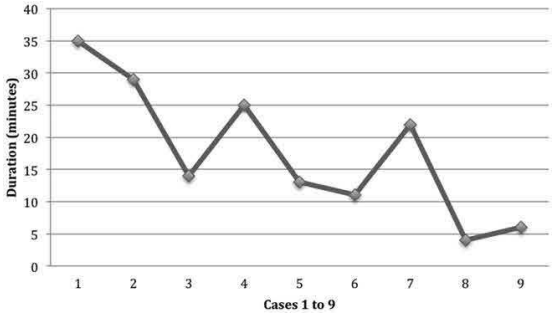

Figure 1. Duration between the beginning of endoscopy and the penetration into the trachea in fetal rhesus monkeys (first to ninth case). In rhesus monkeys, the duration between onset of endoscopy decreased with increasing operator experience.

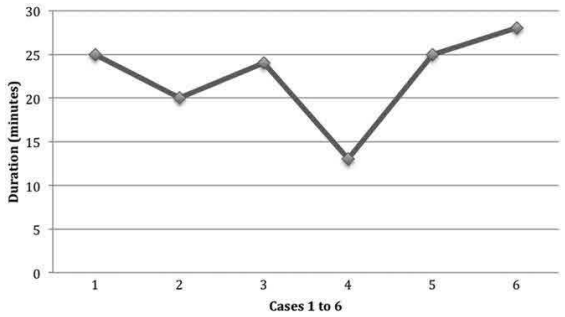

Figure 2. Duration between the beginning of endoscopy and the penetration into the trachea in fetal cynomolgus monkeys (first to sixth case). In cynomolgus monkeys, the duration between onset of endoscopy doesn't decrease with operator experience.

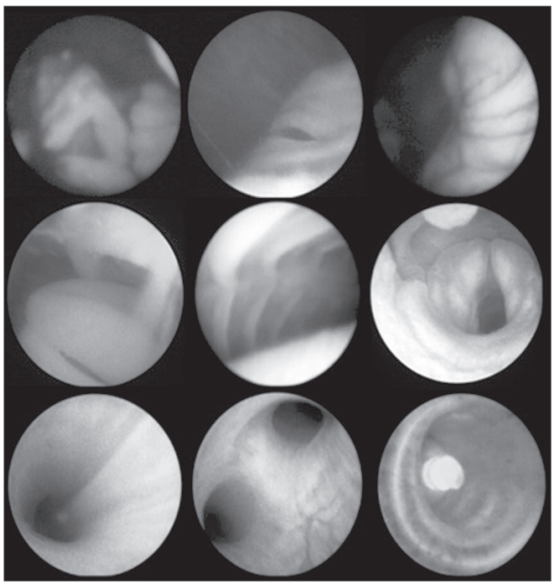

Hand	Eye	Profile
Mouth and tongue	Palate	Vocal cords
Trachea	Bifurcation	Balloon

The monkey model reflects closely human fetal anatomy

Figure 3. Endoscopic views of the fetal monkey.

poor neonatal outcome (27%): 2 intra-uterine fetal deaths and 4 perinatal deaths. Among these cases, only 2 fetal losses were possibly due to the surgery (9%): one intra-uterine fetal death in which fetal reversion was attempted during surgery and one perinatal death for which the only possible detected cause was *Staphylococcus aureus* in the neonatal lungs.

Characteristics of the animals, surgical details and outcomes are displayed in Table 1. Comparison between the two non-human primate models for FETO is displayed in Table 2.

Discussion

Principal findings

Our study demonstrated that non-human primate model is feasible to preform FETO, by showing that FETO was successfully performed by a single port access in all cases. Moreover, the present model, specially the Rhesus monkey, reflected anatomy on fetoscopic views very close to the human fetuses. In addition, FETO was performed mimicking the human surgery by using the same instruments. We believe that this model may be useful for future experimental studies that will investigate (1) the mechanisms related to the fetal growth after FETO [18], (2) the effects of early FETO [19], and (3) the tracheal and pulmonary effects on FETO.

Exclusive percutaneous endoscopic access to the fetal monkey with a single trocar was possible in most cases. However, in spite of the thinness of the subcutaneous layer and uterine wall in monkeys, percutaneous access is not that straightforward due to tissue elasticity. The needle has to be introduced directly, in one smooth motion, under ultrasound guidance. Amnioinfusion of saline is necessary because amniotic liquid is scanty in pregnant monkeys, especially in the last third of pregnancy.

Tracheoscopy was successful in three-quarters of our cases. It was much easier in rhesus monkeys than in cynomolgus ones, because the larynx and trachea are wider. When endoscopic access to the uterine cavity was successful in rhesus monkeys, tracheoscopy failed in only one case because of a problem of visibility due to bleeding. In contrast, most failed tracheoscopy attempts in cynomolgus monkeys were attributed to anatomical issues. It should be noted that the cynomolgus is still an interesting model for fetal surgery because of its non-seasonal breeding.

When TO was attempted it took place without incident. It should be noted that balloon removal was performed in the same surgery session, since the aim of this study was to evaluate the feasibility of TO in the fetal monkey, not the effect of TO on lung growth. We would suggest that other animal models are more suitable for this purpose.

All fetal losses occurred in the cynomolgus group. We assume that this mortality is partly due to a colony issue. Indeed, this group was mostly composed of relatively elder female primigravidas (around 10 years' old). Three fetal losses occurred in mature primigravidas and 2 fetal losses in females who had had a prior fetal loss. Moreover, in a control group of 6 monkeys from the same cynomolgus colony, rates of poor neonatal outcome were even higher: 50% of fetal losses and 83% of early neonatal mortality (before 7 days' life).

Finally, in our series, only 2 fetal losses occurred, which were possibly due to the surgery. It should be noted that in order to avoid premature births, surgery was scheduled for the last third trimester of pregnancy as suggested before by other investigators using the non-human primate model for other fetal surgical procedures [13,20].

Table 1. Characteristics of animals and surgeries.

Cases	Macaque ID	Subspecies	Age (years)	Weight (kg)	Parity	Previous fetal loss	GA at surgery (days)	Surgical procedure	Time to trachea (min)	GA at birth (days)	Fetal outcome	Maternal outcome	Comments
1	1	Rhesus	14.8	7.7	1	0	130	Failure of fetoscopic access	NA	173	Alive	Alive	
2	2	Rhesus	6.0	6.2	2	0	129	Foetoscopy/tracheoscopy	35	149	Alive	Alive	
3	3	Rhesus	3.0	7.1	0	0	134	Foetoscopy/tracheoscopy	29	155	Alive	Alive	
4	4	Rhesus	18.0	6.7	5	0	139	Foetoscopy/tracheoscopy	14	164	Alive	Alive	
5	5	Cynomolgus	12.0	5.9	0	0	127	Foetoscopy	NA	131	Perinatal death	Death	Arm dystocia
6	6	Cynomolgus	11.3	5.3	0	0	127	Foetoscopy/tracheoscopy	25	145	Alive	Alive	
7	7	Cynomolgus	9.3	5.0	0	0	132	Foetoscopy	NA	158	IUFD	Alive	Reversion of fetus during surgery
8	8	Cynomolgus	10.6	6.3	0	0	127	Foetoscopy/tracheoscopy	20	145	Perinatal death	Alive	No maceration of the new-born
9	3	Rhesus	4.0	7.1	1	0	144	Foetoscopy	NA	155	Alive	Alive	
10	6	Cynomolgus	12.0	5.3	1	0	124	Foetoscopy	NA	145	Perinatal death	Alive	Cephalic subcutaneous hematoma
11	1	Rhesus	16.0	7.7	2	0	132	Foetoscopy/tracheoscopy	25	163	Alive	Alive	
12	7	Cynomolgus	10.0	5.0	1	1	135	Foetoscopy/tracheoscopy	24	158	Alive	Alive	
13	9	Rhesus	10.8	9.1	6	2	138	Failure of fetoscopic access	NA	162	Alive	Alive	
14	10	Rhesus	3.9	6.1	0	0	136	Foetoscopy/tracheoscopy	13	153	Alive	Alive	
15	11	Rhesus	13.2	9.0	6	0	138	Foetoscopy/tracheoscopy/plug	11	163	Alive	Alive	
16	12	Rhesus	12.1	7.8	3	0	135	Foetoscopy/tracheoscopy	22	166	Alive	Alive	
17	6	Cynomolgus	12.7	5.3	2	1	139	Foetoscopy	NA	156	Alive	Alive	
18	13	Cynomolgus	8.8	5.7	2	1	134	Foetoscopy/tracheoscopy	13	203	IUFD	Alive	Post-term pregnancy
19	14	Cynomolgus	13.7	6.5	1	1	133	Foetoscopy/tracheoscopy	25	159	Perinatal death	Alive	*Staphylococcus aureus* in neonate lungs
20	15	Rhesus	12.5	7.3	1	0	132	Foetoscopy/tracheoscopy/plug	4	159	Alive	Alive	
21	16	Cynomolgus	13.2	7.7	2	0	136	Foetoscopy/tracheoscopy	28	162	Alive	Alive	
22	9	Rhesus	12.9	9.1	7	2	134	Foetoscopy/tracheoscopy/plug	6	143	Alive	Alive	

NA: not applicable; GA: gestational age; IUFD: intra-uterine fetal death.

Table 2. Comparison between the two non-human primate models for FETO.

	Rhesus monkeys $n = 12$	Cynomolgus monkeys $n = 10$
Age: years (mean ± SD)	10.6 ± 5.1	11.4 ± 1.7
Weight: kg (mean ± SD)	7.6 ± 1.0	5.8 ± 0.8
Previous fetal loss (n, %)	2 (17%)	4 (40%)
GA at surgery: days (mean ± SD)	136 (±4)	131 (±5)
Tracheoscopy (*n*, %)	9 (75%)	6 (60%)
Time to trachea: min (mean ± SD)	17 ± 10	22 ± 5
GA at birth (mean ± SD)	159 ± 8	156 ± 19
IUFD or perinatal death (n)	0 (0%)	6 (60%)
Maternal death (n)	0 (0%)	1 (10%)

SD: standard deviation; GA: gestational age; IUFD: intra-uterine fetal death.

Previous publications

Open fetal surgery with hysterotomy in primates was developed in the 1980s [21–23]. Several operations have been attempted: cystotomy, suprapubic catheterization, relief of urethral obstruction and perineal dissection [22]. Various topics have been studied: scar formation [24], brain development [25] and stem cell and bone transplantation [26–28].

Endoscopic access in fetal monkey model was evaluated in the 1990s [11–13]. However, this did not involve percutaneous endoscopic access, as it is deployed in most current human endoscopic fetal surgical procedures: midline abdominal incision and partial uterine mobilization from the abdominal cavity were performed before endoscopic access.

Experiments on congenital diaphragmatic hernia using the monkey model involved *in utero* repair of the diaphragm [29]. This technique has been abandoned because of failure to improve the newborn outcome and hysterotomy-induced maternal morbidity [30].

Three cases of FETO in baboons (*Papio* spp) have been recently reported [14]. Baboons have the same type of placentation than human but these monkeys have long dog-like muzzles that could be an issue for practicing FETO [10]. Beyond theses cases, no data have been published on exclusively percutaneous endoscopic access for FETO using the fetal monkey model. Only the sheep model has been used for endoscopic FETO [8,9]. The monkey model more closely reflects human fetal anatomy, especially in respect of the fetal face, mouth, vocal cords and trachea.

Conclusions

Experimental FETO is feasible using a monkey model specially using the rhesus *Macaca*. This non-human primate model seems to be very similar to humans, which allows future studies related to the anatomy and consequences of the fetal transitory tracheal occlusion to the lung growth.

Acknowledgements

The authors thank Karl Storz for the laparoscopic unit.

Declaration of interest

This study was funded by the French Ministry of Health MIGAC research fund (Missions of General Interest and Assistance to Contracting) to the Fetal Medicine Department, Strasbourg, France.

References

1. Butler N, Claireaux AE. Congenital diaphragmatic hernia as a cause of perinatal mortality. Lancet 1962;1:659–63.
2. Gallot D, Boda C, Ughetto S, et al. Prenatal detection and outcome of congenital diaphragmatic hernia: a French registry-based study. Ultrasound Obstet Gynecol 2007;29:276–83.
3. Khan PA, Cloutier M, Piedboeuf B. Tracheal occlusion: a review of obstructing fetal lungs to make them grow and mature. Am J Med Genet C Semin Med Genet 2007;145C:125–38.
4. Deprest J, Gratacos E, Nicolaides KH. Fetoscopic tracheal occlusion (FETO) for severe congenital diaphragmatic hernia: evolution of a technique and preliminary results. Ultrasound Obstet Gynecol 2004;24:121–6.
5. Deprest J, Nicolaides K, Done E, et al. Technical aspects of fetal endoscopic tracheal occlusion for congenital diaphragmatic hernia. J Pediatr Surg 2011;46:22–32.
6. Jani JC, Nicolaides KH, Gratacos E, et al. Severe diaphragmatic hernia treated by fetal endoscopic tracheal occlusion. Ultrasound Obstet Gynecol 2009;34:304–10.
7. Ruano R, Yoshisaki CT, da Silva MM, et al. A randomized controlled trial of fetal endoscopic tracheal occlusion versus postnatal management of severe isolated congenital diaphragmatic hernia. Ultrasound Obstet Gynecol 2012;39:20–7.
8. Flageole H, Evrard VA, Vandenberghe K, et al. Tracheoscopic endotracheal occlusion in the ovine model: technique and pulmonary effects. J Pediatr Surg 1997;32:1328–31.
9. Evrard VA, Verbeken EA, Vandenberghe K, et al. Endoscopic In Utero Tracheal Plugging in the Fetal Lamb to Treat Congenital Diaphragmatic Hernia. J Am Assoc Gynecol Laparosc 1996;3:S11.
10. Schlabritz-Loutsevitch NE, Lopez-Alvarenga JC, Comuzzie AG, et al. The prolonged effect of repeated maternal glucocorticoid exposure on the maternal and fetal leptin/insulin-like growth factor axis in Papio species. Reprod Sci 2009;16:308–19.
11. van der Wildt B, Luks FI, Steegers EA, et al. Absence of electrical uterine activity after endoscopic access for fetal surgery in the rhesus monkey. Eur J Obstet Gynecol Reprod Biol 1995;58:213–14.
12. Feitz WF, Steegers EA, Aarnink RG, et al. Endoscopic intrauterine fetal therapy: a monkey model. Urology 1996;47:118–19.
13. Feitz WF, Steegers EA, de Gier RP, et al. Feasibility of minimally invasive intrauterine fetal access in a monkey model. J Urol 1999;161:281–5.
14. Mari G, Deprest J, Schenone M, et al. A novel translational model of percutaneous fetoscopic endoluminal tracheal occlusion – baboons (*Papio* spp.). Fetal Diagn Ther 2014;35:92–100.
15. Abee CR, Mansfield K, Tardif S, Morris T. Nonhuman Primates in Biomedical Research: Biology and Management. London, UK: Academic Press; 2012.
16. Hajivassiliou CA, Nelson SM, Dunkley PD, et al. Evolution of a percutaneous fetoscopic access system for single-port tracheal occlusion. J Pediatr Surg 2003;38:45–50 (discussion 45–50).
17. Luks FI, Deprest JA, Gilchrist BF, et al. Access techniques in endoscopic fetal surgery. Eur J Pediatr Surg 1997;7:131–4.
18. Ruano R, da Silva MM, Campos JA, et al. Fetal pulmonary response after fetoscopic tracheal occlusion for severe isolated congenital diaphragmatic hernia. Obstet Gynecol 2012;119:93–101.
19. Ruano R, Peiro JL, da Silva MM, et al. Early fetoscopic tracheal occlusion for extremely severe pulmonary hypoplasia in isolated congenital diaphragmatic hernia: preliminary results. Ultrasound Obstet Gynecol 2013;42:70–6.
20. Silk JSJ, Roberts J, Kusnitz J. Gestation length in Rhesus macaques (*Macaca mulatta*). Int J Primatol 1993;14:95–104.

21. Michejda M, Bacher J, Johnson D. Surgical approaches in fetal radiography and the study of skeletal age in Macaca mulatta. J Med Primatol 1980;9:50–61.
22. Harrison MR, Anderson J, Rosen MA, et al. Fetal surgery in the primate I. Anesthetic, surgical, and tocolytic management to maximize fetal-neonatal survival. J Pediatr Surg 1982;17: 115–22.
23. Adzick NS, Harrison MR, Glick PL, et al. Fetal surgery in the primate. III. Maternal outcome after fetal surgery. J Pediatr Surg 1986;21:477–80.
24. Lorenz HP, Whitby DJ, Longaker MT, et al. Fetal wound healing. The ontogeny of scar formation in the non-human primate. Ann Surg 1993;217:391–6.
25. Michejda M, Bacher J. Functional and anatomic recovery in the monkey brain following excision of fetal encephalocele. Pediatr Neurosci 1985;12:90–5.
26. Cowan MJ, Chou SH, Tarantal AF. Tolerance induction post in utero stem cell transplantation. Ernst Schering Res Found Workshop 2001;145–71.
27. Mychaliska GB, Rice HE, Tarantal AF, et al. In utero hematopoietic stem cell transplants prolong survival of postnatal kidney transplantation in monkeys. J Pediatr Surg 1997; 32:976–81.
28. Michejda M, Bacher J, Kuwabara T, et al. In utero allogeneic bone transplantation in primates: roentgenographic and histological observations. Transplantation 1981;32:96–100.
29. Esteve C, Toubas F, Gaudiche O, et al. Evaluation of 5 years of experimental in utero surgery for the repair of diaphragmatic hernia. Ann Fr Anesth Reanim 1992;11:193–200.
30. Harrison MR, Adzick NS, Bullard KM, et al. Correction of congenital diaphragmatic hernia in utero VII: a prospective trial. J Pediatr Surg 1997;32:1637–42.

5. PREDICTION OF NEONATAL OUTCOMES IN CASE OF CDH

5.1. Standardization of LHR measurements

Standardization of sonographic Lung-to-Head Ratio Measurements in Isolated Congenital Diaphragmatic Hernia: Impact on the Reproducibility and Efficacy to Predict Outcomes.

Britto IS, Sananes N, Olutoye OO, Cass DL, Sangi-Haghpeykar H, Lee TC, Cassady CI, Mehollin-Ray A, Welty S, Fernandes C, Belfort MA, Lee W, Ruano R. Standardization of

J Ultrasound Med. 2015 Oct;34(10):1721-7.

Standardization of Sonographic Lung-to-Head Ratio Measurements in Isolated Congenital Diaphragmatic Hernia

Impact on the Reproducibility and Efficacy to Predict Outcomes

Ingrid Schwach Werneck Britto, MD, PhD, Nicolas Sananes, MD, Oluyinka O. Olutoye, MD, PhD, Darrell L. Cass, MD, Haleh Sangi-Haghpeykar, PhD, Timothy C. Lee, MD, Christopher I. Cassady, MD, Amy Mehollin-Ray, MD, Stephen Welty, MD, Caraciolo Fernandes, MD, Michael A. Belfort, MD, PhD, Wesley Lee, MD, Rodrigo Ruano, MD, PhD

Received November 25, 2014, from the Texas Children's Fetal Center, Houston, Texas USA (I.S.W.B., N.S., O.O.O., D.L.C., T.C.L., C.I.C., A.M.-R., S.W., C.F., M.A.B., W.L., R.R.); and Department of Obstetrics and Gynecology (I.S.W.B., N.S., H.S.-H., M.A.B., W.L., R.R.), Michael E. DeBakey Department of Surgery (O.O.O., D.L.C., T.C.L.), Department of Radiology (C.I.C., A.M.-R.), and Department of Pediatrics, Section of Neonatology (S.W., C.F.), Baylor College of Medicine, Houston, Texas USA. Revision requested December 10, 2014. Revised manuscript accepted for publication December 16, 2014.

Dr Britto is a recipient of a postdoctoral scholarship grant from the Fundação de Amparo à Pesquisa do Estado de São Paulo (process number 2013/12493-1), and Dr Sananes is a recipient of a scholarship grant from the Fulbright Franco-American Commission for Education Exchange (process number 68141003).

Address correspondence to Rodrigo Ruano, MD, PhD, Pavilion for Women, Texas Children's Fetal Center, 6651 Main St, Suite F1020, Houston, TX 77030 USA.

E-mail: ruano@bcm.edu, rodrigoruano@hotmail.com

Abbreviations

AUC, area under the curve; CDH, congenital diaphragmatic hernia; CI, confidence interval; ECMO, extracorporeal membrane oxygenation; MRI, magnetic resonance imaging; 3D, 3-dimensional; 2D, 2-dimensional

doi:10.7863/ultra.15.14.11064

Objectives—The purpose of this study was to evaluate the impact of standardization of the lung-to-head ratio measurements in isolated congenital diaphragmatic hernia on prediction of neonatal outcomes and reproducibility.

Methods—We conducted a retrospective cohort study of 77 cases of isolated congenital diaphragmatic hernia managed in a single center between 2004 and 2012. We compared lung-to-head ratio measurements that were performed prospectively in our institution without standardization to standardized measurements performed according to a defined protocol.

Results—The standardized lung-to-head ratio measurements were statistically more accurate than the nonstandardized measurements for predicting neonatal mortality (area under the receiver operating characteristic curve, 0.85 versus 0.732; $P = .003$). After standardization, there were no statistical differences in accuracy between measurements regardless of whether we considered observed-to-expected values ($P > .05$). Standardization of the lung-to-head ratio did not improve prediction of the need for extracorporeal membrane oxygenation ($P > .05$). Both intraoperator and interoperator reproducibility were good for the standardized lung-to-head ratio (intraclass correlation coefficient, 0.98 [95% confidence interval, 0.97–0.99]; bias, 0.02 [limits of agreement, –0.11 to +0.15], respectively).

Conclusions—Standardization of lung-to-head ratio measurements improves prediction of neonatal outcomes. Further studies are needed to confirm these results and to assess the utility of standardization of other prognostic parameters.

Key Words—congenital diaphragmatic hernia; fetal lung; lung-to-head ratio; obstetric ultrasound; pulmonary hypoplasia; standardization

Congenital diaphragmatic hernia (CDH) occurs in approximately 1 per 2500 live births and is associated with high morbidity and mortality depending on the severity of pulmonary hypoplasia and pulmonary arterial hypertension.[1–5] Accurate prenatal assessment in fetuses with isolated CDH is of interest because it can guide appropriate counseling and prenatal care (fetal endoscopic tracheal occlusion, expectant management, or termination of pregnancy).[6–9] The most widely used prognostic factor is

the sonographic measurement of the lung-to-head ratio, which was first described for left-sided CDH before 25 weeks' gestation.[10] Its efficacy in predicting outcomes varies substantially in different studies.[10–13] Recently, Jani et al[14] suggested that conflicting results might occur from using different methods of measuring the lung-to-head ratio. These investigators proposed the need for standardization of lung-to-head ratio measurements based on adequate imaging, operator training, and correction for gestational age. However, so far, there is a paucity of data that have examined the impact of lung-to-head ratio standardization on clinical outcomes.

Our hypothesis was that standardization of lung-to-head ratio measurements would improve the accuracy of predicting outcomes of fetuses with isolated CDH and improve intraoperator and interoperator reproducibility. The primary and secondary objectives of this study were to evaluate the impact of standardization of lung-to-head ratio measurements on prediction of neonatal outcomes and reproducibility of these standardized measurements, respectively.

Materials and Methods

Study Design

We conducted a retrospective cohort study of all patients who underwent at least 1 prenatal sonographic scan for fetal isolated CDH and who delivered at Texas Children's Hospital and were at least 6 months of life between January 2004 and July 2012. In this cohort of patients, there was no infant 6 months or older who underwent fetal endoscopic tracheal occlusion. Two operators (I.S.W.B. and R.R.), who were blinded to the neonatal outcome and each operator's measurements, reviewed all video clips from comprehensive fetal sonography and measured the contralateral lung areas and the lung-to-head ratios. The study was approved (H-29006) by the Institutional Review Board of Baylor College of Medicine.

Sonographic Measurements

We compared the lung-to-head ratio measurements that were performed prospectively at our institution (nonstandardized lung-to-head ratio) during clinical evaluation of the patients to the lung-to-head ratio measurements that we performed by reviewing the video clips and after adjusting the images according to the proposal of Jani et al[14] (standardized lung-to-head ratio measurements) for the same fetus at the same gestational age. Only 1 sonographic examination per patient (the first examination) was considered for analysis in this study.

The nonstandardized lung-to-head ratio measurements were performed by maternal-fetal medicine specialists, radiologists, and sonographers. The lung area was estimated by multiplication of the longest diameter of the lung by its longest perpendicular diameter. Then, the area of the lung was divided by the head circumference (in millimeters).[10] The observed-to-expected lung-to-head ratio values were calculated by using nomograms reported by Peralta et al.[15]

The standardized lung-to-head ratio measurements were performed according to the following protocol described by Jani et al[14]: (1) lung measurements should be obtained in an axial view at the level of the 4-chamber view of the fetal heart, with the lung contralateral to the diaphragmatic defect close to the probe, avoiding shadows produced by the ribs; (2) the image should be frozen before final magnification to ensure that all landmarks are clearly visible, and the image should then be magnified so that the axial view of the fetal thorax occupies the whole screen; and (3) the calipers should be placed according to the method being used to measure the lung area. For each fetus, the lung area was estimated by 3 different techniques and divided by the head circumference to calculate the lung-to-head ratio: by multiplying the 2 longest perpendicular diameters, by multiplying the anteroposterior diameter by the perpendicular diameter located at the midpoint, and by manually tracing the area around the lung. These 3 methods are illustrated in Figure 1. All images were obtained from video clips of the axial view of the fetal chest with the contralateral lung close to the ultrasound probe. The images were then frozen and magnified before measurements. The observed-to-expected lung-to-head ratio was calculated by using nomograms reported by Jani et al[14] and Britto et al.[16]

Perinatal Management

In this study, there was no case of termination of pregnancy based on state law. Therefore, the lung-to-head ratio was not used to guide prenatal management in these cases. All neonates were treated according to a standard perinatal protocol.[17] All neonates underwent immediate endotracheal intubation with orogastric decompression and avoidance of bag-mask ventilation by a staff neonatologist. Gentle mechanical ventilation using a permissive hypercapnia protocol was used. Escalation of ventilatory support to a maximal peak inspiratory pressure and positive end-expiratory pressure of 30 and 6 cm H_2O, respectively, and use of high-frequency oscillatory ventilation to a maximum mean airway pressure of 15 cm H_2O were based on preestablished criteria. The need for extracorporeal membrane

oxygenation (ECMO) was determined by the presence of persistent hypoxia (preductal oxygen saturation <80%), persistent acidosis (pH <7.2), or inadequate tissue perfusion. The timing of surgical repair was managed according to the infant's physiologic stability.

Statistical Analysis

Results were reported as mean ± standard deviation unless otherwise specified. Each method for obtaining the lung-to-head ratio measurement was assessed as a potential predictor of 6-month neonatal mortality and need for ECMO (primary outcome). The performances of the different predictors were evaluated by receiver operating characteristic curve analysis, with estimation of areas under the curves (AUCs) with 95% confidence interval (CI) and sensitivity and specificity for the best cutoffs. Statistical comparisons between the AUCs of the different predictors were performed according to the methods of DeLong et al[18] and Hanley et al.[19,20] The intraoperator reproducibility and interoperator reproducibility were analyzed by the intraclass correlation test and Bland-Altman analysis, respectively. $P < .05$ was considered statistically significant. The SPSS version 19.0 statistical software package (IBM Corporation, Armonk, NY) was used for all data analyses, except for comparisons of AUCs, for which MedCalc version 11.6 software (MedCalc, Mariakerke, Belgium) was used.

Results

A total of 80 patients were identified, but 3 cases were excluded because of inability to assess the images and video clips adequately. Therefore, 77 fetuses with isolated CDH were included in the study. Patients' demographics and characteristics were previously reported[21]: the mean maternal age ± SD was 27.5 ± 5.8 years; and mean gestational ages at diagnosis and delivery were 21.9 ± 5.8 and 38.2 ± 1.9 weeks, respectively. The 6-month mortality rate was 20.7% (16 of 77). Extracorporeal membrane oxygenation was used in 35.5% of neonates (27 of 76); 1 fetus died in utero.

Table 1 demonstrates that all lung-to-head ratio measurements were statistically associated with mortality and the need for ECMO. Figures 2 and 3 show receiver operating characteristic curves for standardized and nonstandardized measurements to predict mortality and the need for ECMO, respectively.

Receiver operating characteristic analyses are shown in Table 2. In considering prediction of mortality (Figure 2), the standardized longest and observed-to-expected longest lung-to-head ratio measurements were statistically more

Figure 1. **A**, Two-dimensional sonogram of the longest right lung area in a fetus with right CDH. **B**, Two-dimensional sonogram of the antero-posterior right lung area in a fetus with right CDH. **C**, Two-dimensional sonogram of the tracing right lung area in a fetus with right CDH.

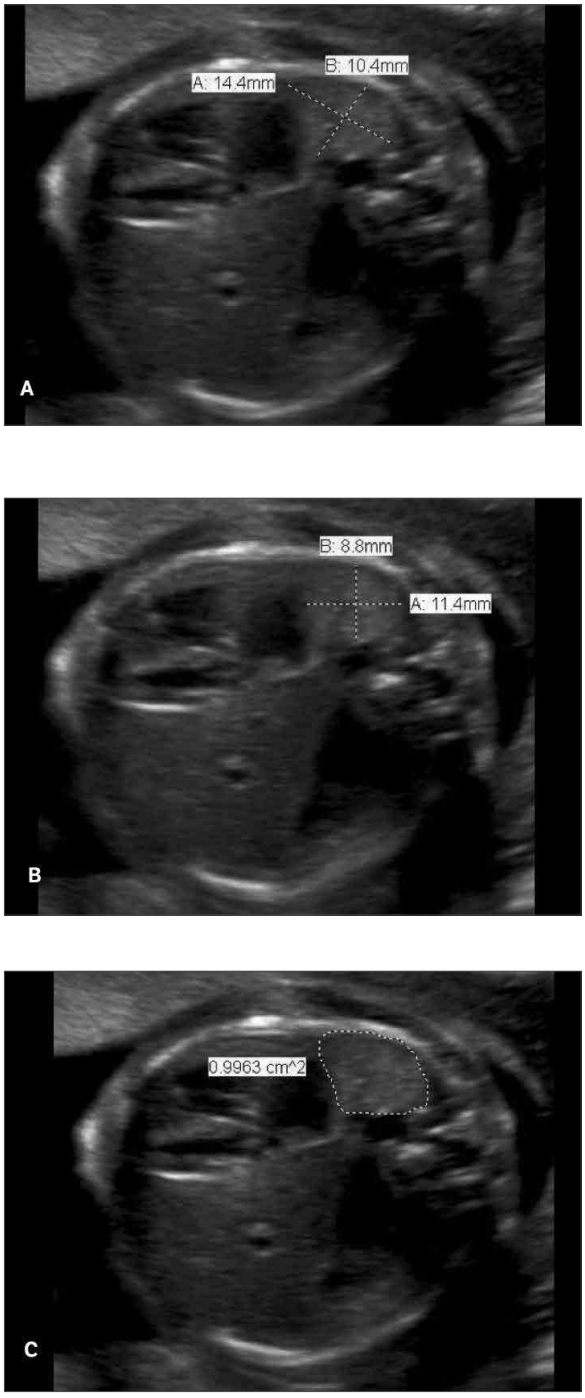

accurate than the nonstandardized measurements (P = .003; P = .024). After standardization, there was no statistical difference among the measurements regardless of whether the lung-to-head ratio was adjusted for gestational age by using the observed-to-expected lung-to-head ratio (standardized ratio versus standardized observed-to-expected ratio according to Jani et al[14] and Britto et al[16]; P = .711) or the method of measuring the contralateral lung area (standardized longest diameter versus standardized anteroposterior diameter versus standardized tracing area; P > .05).

Regarding prediction of the need for ECMO, standardization of the lung-to-head ratio measurements improved the accuracy from an AUC of 0.67 to an AUC of 0.74. However, those differences were not statistically significant (P > .05; Table 2 and Figure 3).

Good intraoperator reproducibility was observed for the standardized lung-to-head ratio measurements (anteroposterior diameter: intraclass correlation coefficient, 0.97 [95% CI, 0.95–0.98]; longest diameter: intraclass correlation coefficient, 0.98 [95% CI, 0.97–0.99]; and tracing area: intraclass correlation coefficient, 0.99 [95% CI,

Table 1. Sample Characteristics and Results Related to Mortality and Need for ECMO in 77 Fetuses With Isolated CDH

	Mortality			Need for ECMO		
Characteristic	Alive (n = 60)	Death (n = 16)	*P*	No (n = 49)	Yes (n = 27)	*P*
Maternal age, y	27.3 ± 5.6	28.1 ± 6.8	.62	27.2 ± 6.7	27.2 ± 5.7	.97
GA at diagnosis, wk	22.4 ± 5.4	22.5 ± 5.9	.75	22.4 ± 6.1	23.0 ± 6.4	.79
Side of CDH, n						
Left	53	15		44	23	
Right	8	1	.68	5	4	.48
Nonstandardized longest LHR	1.82 ± 0.68	1.31 ± 0.53	<.01	1.85 ± 0.69	1.49 ± 0.60	.24
Standardized longest LHR	1.91 ± 0.70	1.15 ± 0.40	<.01	1.92 ± 0.70	1.45 ± 0.65	<.01
Standardized anteroposterior LHR	1.40 ± 0.49	0.90 ± 0.36	<.01	1.41 ± 0.49	1.11 ± 0.49	.01
Standardized tracing area LHR	1.34 ± 0.53	0.86 ± 0.37	<.01	1.35 ± 0.53	10.8 ± 0.48	.03
Nonstandardized observed-to-expected LHR (Peralta et al[15])	0.51 ± 0.19	0.38 ± 0.19	<.01	0.51 ± 0.19	0.44 ± 0.19	.12
Standardized observed-to-expected LHR (Jani et al[14])	0.51 ± 0.15	0.32 ± 0.12	<.01	0.52 ± 0.15	0.40 ± 0.15	<.01
Standardized observed-to-expected LHR (Britto et al[16])	0.45 ± 0.13	0.28 ± 0.11	<.01	0.47 ± 0.14	0.35 ± 0.13	<.01
GA at birth, wk	37.0 ± 1.9	38.1 ± 1.2	.32	37.4 ± 1.5	37.9 ± 2.8	.64
Newborn weight, g	3208.0 ± 740.9	3154.2 ± 493.5	.75	3154.1 ± 713.3	3067.1 ± 497.8	.75
Age at repair, d	3 (2–8)	8 (2–18)	.17	3 (1–8)	10 (2–25)	.01

Data are presented as mean ± SD and median (range) where applicable. GA indicates gestational age, and LHR, lung-to-head ratio.

Figure 2. **A**, Receiver operating characteristic curves for prediction of 6-month neonatal mortality for standardized and nonstandardized lung-to-head ratio (LHR) measurement methods. **B**, Receiver operating characteristic curves for prediction of 6-month neonatal mortality for the 3 standardized lung-to-head ratio measurement methods. Diagonal segments are produced by ties; AP indicates anteroposterior; and o/e, observed-to-expected.

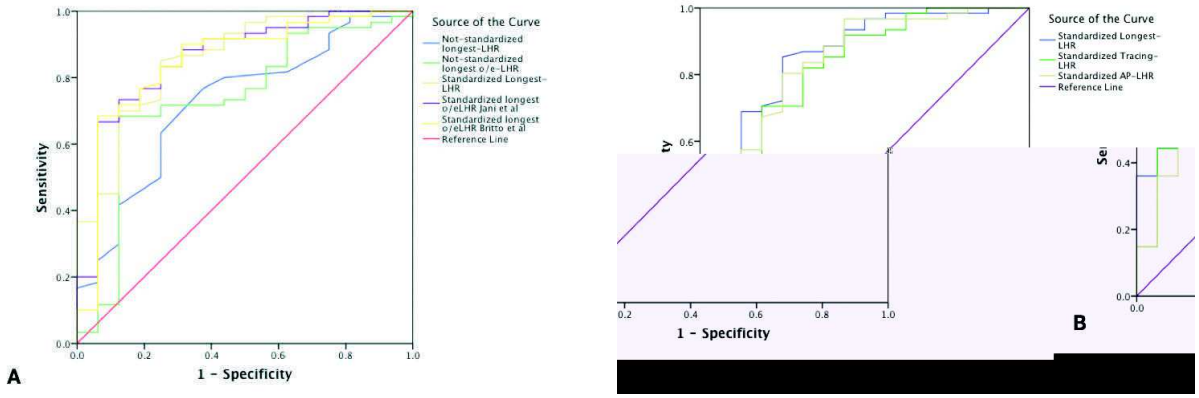

0.98–0.99]). Good interoperator reproducibility was also observed for the standardized measurements (anteroposterior diameter: bias, –0.01 [absolute limits of agreement, –0.16 to +0.15]; longest diameter: bias, 0.02 [absolute limits of agreement, –0.11 to +0.15]; and tracing area: bias, –0.01 [absolute limits of agreement, –0.12 to +0.10]).

Discussion

Our study demonstrates that standardization of lung-to-head ratio measurements as proposed by Jani et al[14] significantly improves prediction of mortality at 6 months of life, independently from the method of measuring the contralateral lung area (anteroposterior diameter versus longest diameter versus tracing area). The standardized observed-to-expected lung-to-head ratio measurements were slightly more accurate in predicting the need for ECMO than the standardized lung-to-head ratio measurements (without adjusting the expected value for specific gestational age), albeit the difference did not reach statistical significance. To our knowledge, a study evaluating the utility of a standardization protocol for measuring the lung-to-head ratio has not been reported previously.

Prediction of the prognosis in CDH assists in counseling parents, helps in the selection of cases that may benefit from fetal surgery, and determines the choice of a specialized medical center for delivery and neonatal care.[22] Neonatal mortality is associated with severe pulmonary hypoplasia; therefore, it is important to measure fetal lung size by 2-dimensional sonography, 3-dimensional sonography, or magnetic resonance imaging (MRI).

Three-dimensional sonographic and MRI measurements of total fetal lung volumes might predict outcomes more accurately than the lung-to-head ratio and other 2D sonographic ratios.[23–25] Both 3D sonography and MRI have their own advantages: 3D sonography is less expensive and allows longitudinal monitoring, whereas MRI may be less operator dependent and may allow a better evaluation of liver-related parameters. However, 2D sonography is still of interest, as it is more frequently available.

The most widely used 2D sonographic prognostic factor is the lung-to-head ratio, but its efficacy in predicting outcome varies in different studies.[10–13] Therefore, stan-

Figure 3. Receiver operating characteristic curves for prediction of the need for ECMO for standardized and nonstandardized lung-to-head ratio (LHR) measurement methods. Diagonal segments are produced by ties; o/e indicates observed-to-expected.

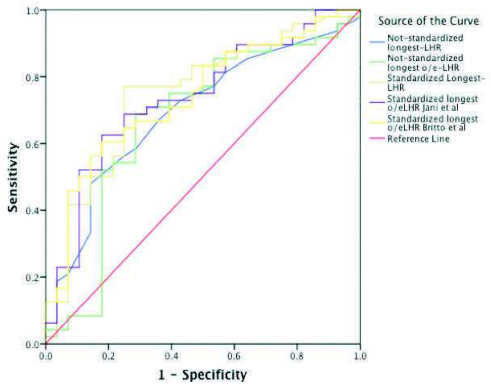

Table 2. Sensitivity, Specificity, and AUC for Each Lung-to-Head Ratio Measurement Method

Measurement Method	Sensitivity/Specificity, %	AUC (95% CI)
6-mo mortality		
Nonstandardized longest LHR	62.5/76.7	0.72 (0.59–0.86)
Nonstandardized observed-to-expected longest LHR (Peralta et al[15])	87.5/67.2	0.73 (0.59–0.88)
Standardized Longest LHR	75.0/85.2	0.85 (0.75–0.96)
Standardized observed-to-expected longest LHR (Jani et al[14])	87.5/72.1	0.86 (0.75–0.97)
Standardized observed-to-expected longest LHR (Britto et al[16])	93.7/68.9	0.85 (0.73–0.96)
Standardized anteroposterior LHR	75.0/80.3	0.82 (0.69–0.95)
Standardized tracing area LHR	81.2/70.5	0.81 (0.68–0.94)
Need for ECMO		
Nonstandardized longest LHR	85.2/67.9	0.69 (0.57–0.81)
Nonstandardized observed-to-expected longest LHR (Peralta et al[15])	70.4/67.3	0.67 (0.54–0.81)
Standardized longest LHR	74.1/75.5	0.75 (0.63–0.86)
Standardized observed-to-expected longest LHR (Jani et al[14])	81.5/61.2	0.74 (0.62–0.85)
Standardized observed-to-expected longest LHR (Britto et al[16])	81.5/59.2	0.74 (0.63–0.85)
Standardized anteroposterior LHR	77.8/61.2	0.72 (0.60–0.84)
Standardized tracing area LHR	70.4/73.5	0.71 (0.59–0.83)

LHR indicates lung-to-head ratio.

dardization of the lung-to-head ratio measurement technique is of interest.[14] Our study demonstrates that standardization significantly improves prediction of mortality. Interestingly, we found that standardization mattered even more than the choice of the lung-to-head ratio measurement technique itself. Indeed, there was no difference in the mortality predictions made by each method (anteroposterior diameter versus longest diameter versus tracing area).

Some studies in the literature have suggested that the lung-to-head ratio varies throughout gestational age; therefore, the use of an observed-to-expected ratio has been proposed.[15,26] However, our study demonstrated that there was no statistical difference in predicting outcomes among the standardized measurements regardless of whether we considered the observed-to-expected measurements. In addition, longitudinal studies demonstrated that even the observed-to-expected lung-to-head ratio seems to vary throughout gestational age, suggesting that there is no need to adjust the measurements for gestational age.[27,28] Additionally, it seems that evaluating the fetal total lung volumes (observed-to-expected total fetal lung volume ratio) has better accuracy for predicting outcomes (mortality and need for ECMO) than 2D sonographic measurements.[23,29]

In this study, standardization of the lung-to-head ratio did not improve prediction of the need for ECMO. Evidently, measurement of lung size does not accurately predict the use of ECMO. This idea might be explained by the fact that, regardless of the method by which lung size is evaluated, we are not considering future lung function or pulmonary arterial hypertension. Evaluation of vasculature and pulmonary arterial hypertension with 2D and 3D Doppler studies may be a better option for predicting pulmonary arterial hypertension, as some authors have proposed.[30–32]

Among the different methods for measuring the lung area using 2D sonography, tracing has been considered the most reproducible.[33] However, in our experience, all 3 methods for measuring the lung-to-head ratio (longest diameter versus anteroposterior diameter versus tracing area) had similar predictive values and reproducibility after standardization in our cohort of fetuses, suggesting that they can be used with similar results. In our opinion, we think that the tracing area seems to be easier to perform, since it can provide the area value directly, and it may be more reproducible in a larger population.

The strength of this study was that we tested the hypothesis that standardized lung-to-head ratio measurements might improve the reproducibility and accuracy of predicting outcome in fetuses with isolated CDH. However, this study's limitations include the retrospective design. Despite the retrospective nature of the study, we were able to obtain adequate images from video clips, since acquisition of a video clip of the fetal chest in an axial view is part of the standard sonographic examination in our center. To avoid bias, the operator measured the lung sizes on images from video clips without knowing the outcomes of any of the fetuses.

In conclusion, we have shown that standardization of lung-to-head ratio measurements improves prediction of neonatal outcomes. Further prospective studies are necessary to confirm these results in other patient cohorts and to assess the utility of standardization of other prognostic parameters.

References

1. Cannie MM, Jani JC, De Keyzer F, Allegaert K, Dymarkowski S, Deprest J. Evidence and patterns in lung response after fetal tracheal occlusion: clinical controlled study. *Radiology* 2009; 252:526–533.
2. Gucciardo L, Deprest J, Done E, et al. Prediction of outcome in isolated congenital diaphragmatic hernia and its consequences for fetal therapy. *Best Pract Res Clin Obstet Gynaecol* 2008; 22:123–138.
3. Langham MR Jr, Kays DW, Ledbetter DJ, Frentzen B, Sanford LL, Richards DS. Congenital diaphragmatic hernia: epidemiology and outcome. *Clin Perinatol* 1996; 23:671–688.
4. Jani JC, Benachi A, Nicolaides KH, et al. Prenatal prediction of neonatal morbidity in survivors with congenital diaphragmatic hernia: a multicenter study. *Ultrasound Obstet Gynecol* 2009; 33:64–69.
5. Ruano R, Aubry MC, Barthe B, Mitanchez D, Dumez Y, Benachi A. Predicting perinatal outcome in isolated congenital diaphragmatic hernia using fetal pulmonary artery diameters. *J Pediatr Surg* 2008; 43:606–611.
6. Jani JC, Nicolaides KH, Gratacos E, et al. Severe diaphragmatic hernia treated by fetal endoscopic tracheal occlusion. *Ultrasound Obstet Gynecol* 2009; 34:304–310.
7. Peralta CF, Jani JC, Van Schoubroeck D, Nicolaides KH, Deprest JA. Fetal lung volume after endoscopic tracheal occlusion in the prediction of postnatal outcome. *Am J Obstet Gynecol* 2008; 198:60.e1–60.e5.
8. Ruano R, da Silva MM, Campos JA, et al. Fetal pulmonary response after fetoscopic tracheal occlusion for severe isolated congenital diaphragmatic hernia. *Obstet Gynecol* 2012; 119:93–101.
9. Ruano R, Duarte SA, Pimenta EJ, et al. Comparison between fetal endoscopic tracheal occlusion using a 1.0-mm fetoscope and prenatal expectant management in severe congenital diaphragmatic hernia. *Fetal Diagn Ther* 2011; 29:64–70.
10. Metkus AP, Filly RA, Stringer MD, Harrison MR, Adzick NS. Sonographic predictors of survival in fetal diaphragmatic hernia. *J Pediatr Surg* 1996; 31:148–152.
11. Arkovitz MS, Russo M, Devine P, Budhorick N, Stolar CJ. Fetal lung-head ratio is not related to outcome for antenatal diagnosed congenital diaphragmatic hernia. *J Pediatr Surg* 2007; 42:107-111.

12. Laudy JA, Van Gucht M, Van Dooren MF, Wladimiroff JW, Tibboel D. Congenital diaphragmatic hernia: an evaluation of the prognostic value of the lung-to-head ratio and other prenatal parameters. *Prenat Diagn* 2003; 23:634–639.
13. Lipshutz GS, Albanese CT, Feldstein VA, et al. Prospective analysis of lung-to-head ratio predicts survival for patients with prenatally diagnosed congenital diaphragmatic hernia. *J Pediatr Surg* 1997; 32:1634–1636.
14. Jani JC, Peralta CF, Nicolaides KH. Lung-to-head ratio: a need to unify the technique. *Ultrasound Obstet Gynecol* 2012; 39:2–6.
15. Peralta CF, Cavoretto P, Csapo B, Vandecruys H, Nicolaides KH. Assessment of lung area in normal fetuses at 12–32 weeks. *Ultrasound Obstet Gynecol* 2005; 26:718–724.
16. Britto IS, Araujo Júnior E, Sangi-Haghpeykar H, et al. Reference ranges for 2-dimensional sonographic lung measurements in healthy fetuses: a longitudinal study. *J Ultrasound Med* 2014; 33:1917–1923.
17. Lazar DA, Cass DL, Rodriguez MA, et al. Impact of prenatal evaluation and protocol-based perinatal management on congenital diaphragmatic hernia outcomes. *J Pediatr Surg* 2011; 46:808–813.
18. DeLong ER, DeLong DM, Clarke-Pearson DL. Comparing the areas under two or more correlated receiver operating characteristic curves: a nonparametric approach. *Biometrics* 1988; 44:837–845.
19. Hanley JA, McNeil BJ. A method of comparing the areas under receiver operating characteristic curves derived from the same cases. *Radiology* 1983; 148:839–843.
20. McNeil BJ, Hanley JA, Funkenstein HH, Wallman J. Paired receiver operating characteristic curves and the effect of history on radiographic interpretation: CT of the head as a case study. *Radiology* 1983; 149:75–77.
21. Ruano R, Lazar DA, Cass DL, et al. Fetal lung volume and quantification of liver herniation by magnetic resonance imaging in isolated congenital diaphragmatic hernia. *Ultrasound Obstet Gynecol* 2014; 43:662–669.
22. Ruano R, Yoshisaki CT, da Silva MM, et al. A randomized controlled trial of fetal endoscopic tracheal occlusion versus postnatal management of severe isolated congenital diaphragmatic hernia. *Ultrasound Obstet Gynecol* 2012; 39:20–27.
23. Ruano R, Takashi E, da Silva MM, Haeri S, Tannuri U, Zugaib M. Quantitative lung index, contralateral lung area, or lung-to-head ratio to predict the neonatal outcome in isolated congenital diaphragmatic hernia? *J Ultrasound Med* 2013; 32:413–417.
24. Victoria T, Bebbington MW, Danzer E, et al. Use of magnetic resonance imaging in prenatal prognosis of the fetus with isolated left congenital diaphragmatic hernia. *Prenat Diagn* 2012; 32:715–723.
25. Kehl S, Kalk AL, Eckert S, et al. Assessment of lung volume by 3-dimensional sonography and magnetic resonance imaging in fetuses with congenital diaphragmatic hernias. *J Ultrasound Med* 2011; 30:1539–1545.
26. Jani J, Nicolaides KH, Keller RL, et al. Observed to expected lung area to head circumference ratio in the prediction of survival in fetuses with isolated diaphragmatic hernia. *Ultrasound Obstet Gynecol* 2007; 30:67–71.
27. Ruano R, Takashi E, da Silva MM, Campos JA, Tannuri U, Zugaib M. Prediction and probability of neonatal outcome in isolated congenital diaphragmatic hernia using multiple ultrasound parameters. *Ultrasound Obstet Gynecol* 2012; 39:42–49.
28. Ruano R, Britto IS, Sangi-Haghpeykar H, et al. Longitudinal assessment of lung area measurements by two-dimensional ultrasound in fetuses with isolated left-sided congenital diaphragmatic hernia. *Ultrasound Obstet Gynecol* 2015; 45:566–571.
29. Ruano R, Joubin L, Sonigo P, et al. Fetal lung volume estimated by 3-dimensional ultrasonography and magnetic resonance imaging in cases with isolated congenital diaphragmatic hernia. *J Ultrasound Med* 2004; 23:353–358.
30. Ruano R, Aubry MC, Barthe B, Mitanchez D, Dumez Y, Benachi A. Quantitative analysis of fetal pulmonary vasculature by 3-dimensional power Doppler ultrasonography in isolated congenital diaphragmatic hernia. *Am J Obstet Gynecol* 2006; 195:1720–1728.
31. Cruz-Martinez R, Hernandez-Andrade E, Moreno-Alvarez O, Done E, Deprest J, Gratacos E. Prognostic value of pulmonary Doppler to predict response to tracheal occlusion in fetuses with congenital diaphragmatic hernia. *Fetal Diagn Ther* 2011; 29:18–24.
32. Mahieu-Caputo D, Aubry MC, El Sayed M, Joubin L, Thalabard JC, Dommergues M. Evaluation of fetal pulmonary vasculature by power Doppler imaging in congenital diaphragmatic hernia. *J Ultrasound Med* 2004; 23:1011–1017.
33. Jani JC, Cordier AG, Martinovic J, et al. Antenatal ultrasound prediction of pulmonary hypoplasia in congenital diaphragmatic hernia: correlation with pathology. *Ultrasound Obstet Gynecol* 2011; 38:344–349.

5.2. Growth patterns of fetal lung volumes

Growth Patterns of Fetal Lung Volumes in Healthy Fetuses and Fetuses with Isolated Left-Sided Congenital Diaphragmatic Hernia

Ruano R, Britto IS, Sananes N, Lee W, Sangi-Haghpeykar H, Deter RL.

J Ultrasound Med. 2016 Jun;35(6):1159-66.

Growth Patterns of Fetal Lung Volumes in Healthy Fetuses and Fetuses With Isolated Left-Sided Congenital Diaphragmatic Hernia

Rodrigo Ruano, MD, PhD, Ingrid Schwach Werneck Britto, MD, PhD, Nicolas Sananes, MD, Wesley Lee, MD, Haleh Sangi-Haghpeykar, PhD, Russell L. Deter, MD

Objectives—To evaluate fetal lung growth using 3-dimensional sonography in healthy fetuses and those with congenital diaphragmatic hernia (CDH).

Methods—Right and total lung volumes were serially evaluated by 3-dimensional sonography in 66 healthy fetuses and 52 fetuses with left-sided CDH between 20 and 37 weeks' menstrual age. Functions fitted to these parameters were compared for 2 groups: (1) healthy versus those with CDH; and (2) fetuses with CHD who survived versus those who died.

Results—Fetal right and total lung volumes as well as fetal observed-to-expected right and total lung volume ratios were significantly lower in fetuses with CDH than healthy fetuses ($P < .001$) and in those fetuses with CDH who died ($P < .001$). The observed-to-expected right and total lung volume ratios did not vary with menstrual age in healthy fetuses or in those with CDH (independent of outcome).

Conclusions—Lung volume rates were lower in fetuses with left-sided CDH compared to healthy fetuses, as well as in fetuses with CDH who died compared to those who survived. The observed-to-expected right and total lung volume ratios were relatively constant throughout menstrual age in fetuses with left-sided CDH, suggesting that the origin of their lung growth abnormalities occurred before 20 weeks and did not progress. The observed-to-expected ratios may be useful in predicting the outcome in fetuses with CDH independent of menstrual age.

Key Words—congenital diaphragmatic hernia; fetal lung; fetal lung volume; obstetric ultrasound; prenatal diagnosis; pulmonary hypoplasia; 3-dimensional sonography

Received August 3, 2015, from the Department of Obstetrics and Gynecology, Baylor College of Medicine and Texas Children's Hospital Fetal Center, Houston, Texas USA (R.R., I.S.W.B., N.S., W.L., H.S.-H., and R.L.D.); Department of Obstetrics and Gynecology, Medical Science College of Santa Casa of São Paulo, São Paulo, Brazil (I.S.W.B.). Revision requested August 25, 2015. Revised manuscript accepted for publication August 31, 2015.

Address correspondence to Rodrigo Ruano, MD, PhD, Pavilion for Women, Texas Children's Hospital Fetal Center, 6651 Main St, Suite F1020, Houston, TX 77030 USA.

E-mail: ruano@bcm.edu, rodrigoruano@hotmail.com

Abbreviations

CDH, congenital diaphragmatic hernia; ECMO, extracorporeal membrane oxygenation; 3D, 3-dimensional

doi:10.7863/ultra.15.08005

Congenital diaphragmatic hernia (CDH) occurs in approximately 1 per 2550 live births and can be accurately diagnosed by second-trimester sonography.[1,2] Neonatal mortality and morbidity in cases with isolated CDH depend on the severity of pulmonary hypoplasia and pulmonary arterial hypertension. Fetal tracheal occlusion has been proposed to prevent these complications in severe forms of the disease, increasing neonatal survival.[3–9]

Since pulmonary hypoplasia is defined as a decrease in the size of the lungs, different methods for evaluating fetal lung size have been used to predict outcomes in fetuses with CDH.[10–20] The most frequently used measurement is the lung-to-head ratio, determined by 2-dimensional sonography, in which the contralateral lung area is divided by the head circumference.[8,21–23] However, lung-to-head ratio measurements vary with menstrual age in healthy fetuses and

those with CDH; therefore, investigators suggested the use of observed-to-expected lung-to-head ratio measurements to avoid the influence of menstrual age.[15] In contrast, our recent longitudinal study demonstrated that both lung-to-head ratio measurements and observed-to-expected lung-to-head ratio measurements varied differently with menstrual age when healthy fetuses were compared to those with CDH.[24]

The fetal lung size can also be measured by calculating the total fetal lung volumes using 3-dimensional (3D) sonography or magnetic resonance imaging and can also be expressed as an observed-to-expected ratio in order to avoid the influence of the menstrual age (observed-to-expected fetal lung volume). To date, a few studies evaluated 2 fetal lung volume measurements (second and third trimesters), but to our knowledge, there are no published studies that have evaluated lung volume growth patterns in fetuses with CDH in comparison to healthy fetuses with longitudinal consecutive measurements in the same fetus. Our study investigated the growth patterns of fetal lung volumes in isolated cases of left-sided CDH compared to healthy control fetuses with respect to severity and mortality, considering longitudinal measurements of fetal lung volumes.

Materials and Methods

Sample

Fetal lung volumes were measured in 66 randomly selected healthy fetuses and 52 consecutive fetuses with isolated left-sided CDH every 2 or 4 weeks, depending on maternal availability, between 20 and 37 weeks' menstrual age (January 2004 and December 2010). No fetal surgery was performed in those patients. Inclusion criteria were as follows: (1) singleton pregnancy; (2) live fetus with normal fetal morphologic findings or diagnosis of isolated left-sided CDH (normal fetal karyotype and absence of other structural anomalies); (3) no fetal surgery; (4) more than 3 lung sonographic examinations with intervals varying from 2 to 4 weeks; and (5) menstrual age confirmed by first-trimester measurement of the crown-rump length.[25] Only fetuses with left-sided CDH who had more than 3 sonographic examinations starting in the second trimester were included from 108 fetuses with prenatal diagnosis of CDH previously reported.[8] All healthy fetuses had normal weights at birth. The Institutional Review Board approved this study. Pregnant patients were informed that study results would not be used to modify their perinatal management. The perinatologists, sonographers, and surgeons in charge were not given information on lung evaluations.

Sonographic Evaluation

Each fetus was evaluated every 2 or 4 weeks (depending on patients' availability) by 3D sonography using a Voluson E8 system (GE Healthcare, Milwaukee, WI) with a 4–8-MHz transabdominal transducer. Right and total fetal lung volumes were measured by Virtual Organ Computer-Aided Analysis software (SonoView software; GE Healthcare) as described previously[14,26–29] and compared to the expected values for menstrual age (based on a nomogram described previously)[28,30] by calculating the observed-to-expected right lung volume ratio and observed-to-expected total lung volume ratio.

Perinatal Management of Fetuses With CDH

All fetuses with a prenatal diagnosis of isolated CDH were followed in our fetal medicine unit and were delivered in our children's hospital. All neonates were treated according to the same protocol that was described previously.[8] Briefly, all infants immediately underwent intubation and ventilator support in the delivery room and were transferred to the neonatal intensive care unit with high-frequency oscillatory ventilation when necessary, followed by delayed CDH repair after hemodynamic stabilization. The treatment protocol did not include extracorporeal membrane oxygenation (ECMO). Inhaled nitric oxide was administered in cases of persistent pulmonary arterial hypertension.

Statistical Analysis

The size parameters characterized in this study were the right lung volume, total lung volume, observed-to-expected right lung volume ratio, and observed-to-expected total lung volume ratio. The relationship between the right and total lung volume was determined by the Pearson correlation coefficient. All parameters were $\log_e$ transformed to normalize their distributions. Functions of menstrual age were obtained by using the best-fitting fractional polynomials. For each parameter, the model fit was assessed by the significance of the best-fitting fractional polynomial, residual diagnostic test, 2-log likelihood, Akaike information criterion, and Bayesian information criterion. The observed-to-expected total and right lung volume ratios were fitted by using a linear function, whereas for the total and right lung volume, linear and quadratic functions, respectively, gave optimal fits.

We used generalized linear mixed models (Proc Glimmix; SAS Institute Inc, Cary, NC), with random intercepts and slopes, to generate growth curve models in healthy fetuses and those with CDH. The sets of 3 (2 if linear) coefficients for the fitted curves served to represent the mean curve for

each group or subgroup.[31] Sets of coefficients for different curves were compared by the SAS Contrast procedure and the *F* test. Growth curves were compared in the following groups: (1) healthy fetuses versus fetuses with CDH; and (2) survivals versus deaths (mortality at 6 months of age) among neonates with CDH. Adjustments for multiple non-independent comparisons were made by the Bonferroni method (significance, $P < .0167$). Furthermore, we used the Estimate procedure in SAS to examine whether the patterns of the study parameters (right lung volume, total lung volume, observed-to-expected right lung volume ratio, and observed-to-expected total lung volume ratio) within each group (CDH or healthy fetuses) changed significantly over gestational age (if the slope was significantly different from 0). Intraoperator and interoperator variability was evaluated in 30 randomly selected 3D volumetric images by the intraclass coefficient test and Bland-Altman analysis. $P < .05$ was considered significant in independent comparisons. All analyses were performed with SAS version 9.3 software.

Results

Serial fetal lung measurements were obtained in 66 healthy fetuses (total of 284 ultrasound scans; median number of examinations per fetus, 4; range, 3–7; median menstrual age at first sonographic examination, 24 weeks; range, 21–24 weeks) and in 52 fetuses with isolated left-sided CDH (total of 242 ultrasound scans; median number of examination per fetus, 4; range, 3–7; median menstrual age at first sonographic examination, 24 weeks; range, 20–24 weeks).

The mean maternal age ± SD was 24.2 ± 6.5 years; 41 patients (34.8%) were nulliparous, whereas 77 had 2 or more previous children. Regarding fetal sex, 63 fetuses (53.4%) were male, whereas 55 (46.6%) were female.

In this study, 25 fetuses had severe forms of left-sided CDH; 18 had moderate forms; and 9 had mild forms. Twenty-nine neonates with CDH died, whereas 23 survived. As mentioned before, only fetuses with more than 2 measurements starting before 25 weeks were included in this analysis.

Longitudinal Growth of Lung Volumes as a Function of Menstrual Age in Healthy Fetuses and Those With CDH

Fetuses with CDH had significantly smaller fetal lung volumes (total lung volume, right lung volume, observed-to-expected right lung volume ratio, and observed-to-expected total lung volume ratio) than healthy fetuses ($P < .001$; Figure 1). Considering the growth pattern, both healthy fetuses and those with CDH had significant lung growth for right and total lung volumes as a function of menstrual age (Figure 1, A and B). The observed-to-expected right and total lung volume ratios did not vary with menstrual age in the healthy fetuses (observed-to-expected right lung volume ratio: slope estimation, –0.000055; $P = .99$; and observed-to-expected total lung volume ratio: slope estimation, 0.00015; $P = .80$) and in fetuses with CDH (observed-to-expected right lung volume ratio: slope estimation, –0.00015; $P = .82$; and observed-to-expected total lung volume ratio: slope estimation, –0.0008; $P = .89$; Figure 1, C and D). There was no statistical difference when comparing the slopes of observed-to-expected right and total lung volume ratios between the healthy and CDH groups (observed-to-expected right lung volume ratio: $F = 0.17$; $P = .68$; and observed-to-expected total lung volume ratio: $F = 0.03$; $P = .87$). However, the intercepts of observed-to-expected right and total lung volume ratios were significantly different between the healthy group (observed-to-expected right lung volume ratio: 0.9365; and observed-to-expected total lung volume ratio: 0.5585) and CDH group (observed-to-expected right lung volume ratio: 0.5323; observed-to-expected total lung volume ratio: 0.3260; observed-to-expected right lung volume ratio: $F = 238.03$; $P < .0001$; and observed-to-expected total lung volume ratio: $F = 230.74$; $P < .0001$).

Longitudinal Growth of Lung Measurements in Fetuses With CDH Based on Outcome

Figure 2 shows fetal right and total lung volume growth as a function of menstrual age in CDH cases with or without mortality. Fetuses who died had significantly smaller volumes on average than those who survived ($P < .001$). Concerning growth patterns, both right and total lung volumes increased significantly in fetuses who died (Figure 2, A and B). The observed-to-expected right and total lung volume ratios did not vary with menstrual age in fetuses with CDH who died (observed-to-expected right lung volume ratio: slope estimation, –0.0039; $P = .26$; and observed-to-expected total lung volume ratio: slope estimation, 0.0004; $P = .62$) and survived (observed-to-expected right lung volume ratio: slope estimation, 0.00034; $P = .52$; and observed-to-expected total lung volume ratio: slope estimation, –0.0011; $P = .36$; Figure 2, C and D). There was no statistical difference in slope comparison between survivors and nonsurvivors (observed-to-expected right lung volume ratio: $F = 1.60$; $P = .21$; and observed-to-expected total lung volume ratio: $F = 1.17$; $P = .28$). However, the intercepts of observed-to-expected right and total lung volume ratios were significantly differ-

ent between survivors (observed-to-expected right lung volume ratio: 0.5860; and observed-to-expected total lung volume ratio: 0.4029) and nonsurvivors (observed-to-expected right lung volume ratio: 0.5004; observed-to-expected total lung volume ratio: 0.2812; observed-to-expected right lung volume ratio: $F = 22.97$; $P < .0001$; and observed-to-expected total lung volume ratio: $F = 38.90$; $P < .0001$).

A good correlation was observed between right and total lung volumes (Pearson correlation coefficient, =0.972; $P < .001$). Good intraoperator reproducibility was observed for right lung volumes (intraclass correlation coefficient, 0.99 [95% confidence interval, 0.98–0.99]; and bias, 0.10 [limits of agreement, –0.87 to +1.07]) and for total lung volumes (intraclass correlation coefficient, 0.99 [95% confidence interval, 0.98–0.99]; and bias, –0.08 [limits of agreement, –1.82 to +1.65]). Good interoperator reproducibility was observed for right lung volumes (intraclass correlation coefficient, 0.96 [95% confidence interval, 0.95–0.99]; and bias, –0.02 [limits of agreement, –1.94 to +1.90]) and for total lung volumes (intraclass correlation coefficient, 0.95 [95% confidence interval, 0.94–0.98]; and bias, –0.21 [limits of agreement, –1.80 to +1.39]).

Discussion

This longitudinal study provides unique information about growth patterns of fetal lung volumes measured by 3D sonography in healthy fetuses and those with isolated left-sided CDH who did not undergo fetal intervention.

Figure 1. **A**, Growth curves for the observed right lung volume (orlv) in healthy fetuses and those with CDH. **B**, Growth curves for the observed total lung volume (otlv) in healthy fetuses and those with CDH. **C**, Growth curves for the observed-to-expected right lung volume ratio (oerlv) in healthy fetuses and those with CDH. **D**, Growth curves for the observed-to-expected total lung volume ratio (oetlv) in healthy fetuses and those with CDH. GA indicates gestational age.

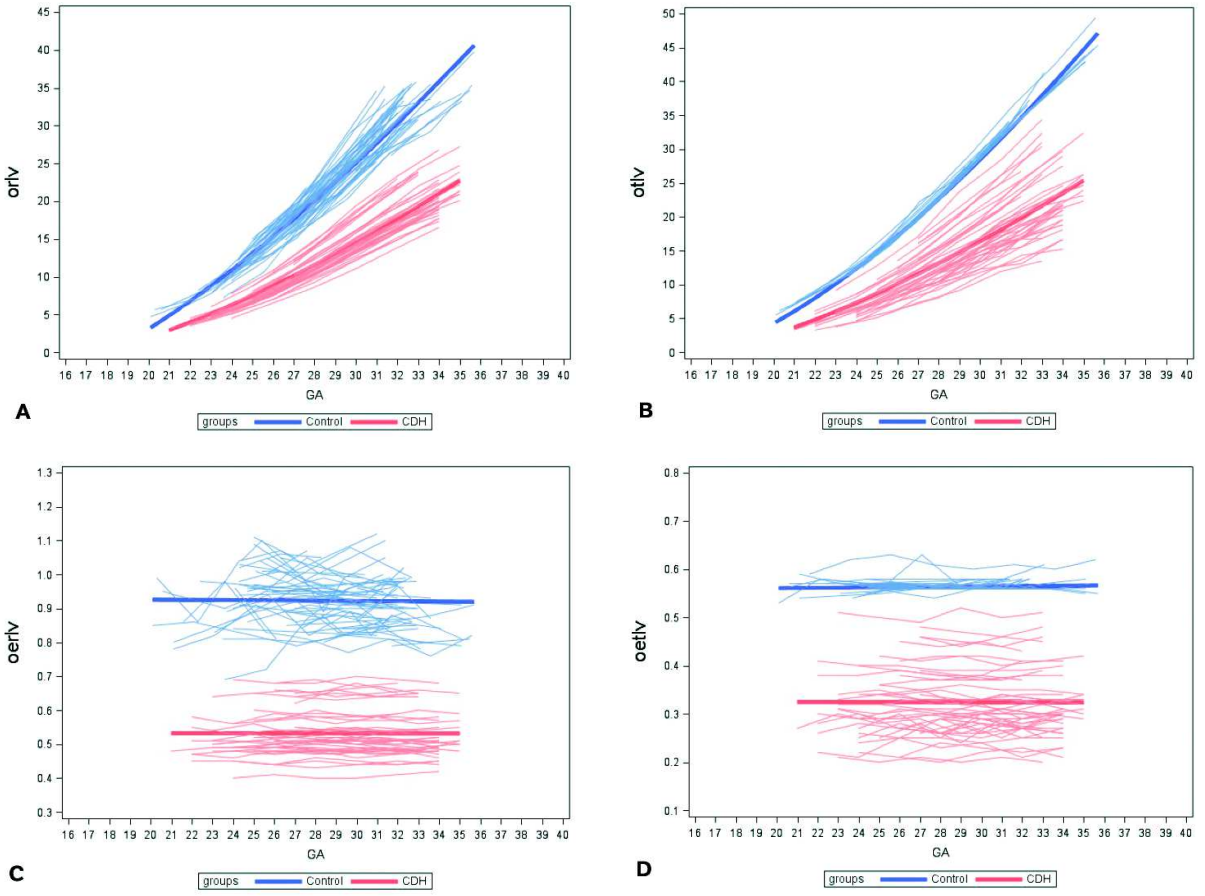

This study demonstrates that fetal right and total lung volumes grow throughout menstrual age in healthy fetuses and those with CDH.

Our study of the observed-to-expected, which is a measure of the difference in average growth rates before the time of measurement in observed and reference populations (expressed as a decimal fraction of the reference growth rate; Appendix), indicated no change with menstrual age during the 20- to 35-week interval for either right or total lung volume. The observed average growth rate of healthy fetuses is much closer to that in the reference sample for right lung volume than it is for total lung volume, even in the same fetuses.

Our findings that the observed-to-expected ratios did not vary as a function of menstrual age confirm the hypothesis that the observed-to-expected right and total lung volume ratios can be used clinically to evaluate fetal lung size and growth independent of fetal age. This study also confirms previous observations reported in the literature that fetuses with CDH have consistently lower values for observed-to-expected right and total lung volume ratios compared to their healthy counterparts, and fetuses with more severe forms of CDH resulting in death had even more significantly reduced observed-to-expected right and total lung volume ratio values. This study did not aim to evaluate cutoffs for the observed-to-expected right and total lung volume ratios to predict survival, since they have been reported previously.[13,26]

In addition to the clinical implications, our results also provide further information regarding the physiopatho-

Figure 2. **A**, Growth curves for the observed right lung volume (orlv) in fetuses with left-sided CDH according to outcome. **B**, Growth curves the observed total lung volume (otlv) in fetuses with left-sided CDH according to outcome. **C**, Growth curves for the observed-to-expected right lung volume ratio (oerlv) in fetuses with left-sided CDH according to outcome. **D**, Growth curves for the observed-to-expected total lung volume ratio (oetlv) in fetuses with left-sided CDH according to outcome. GA indicates gestational age..

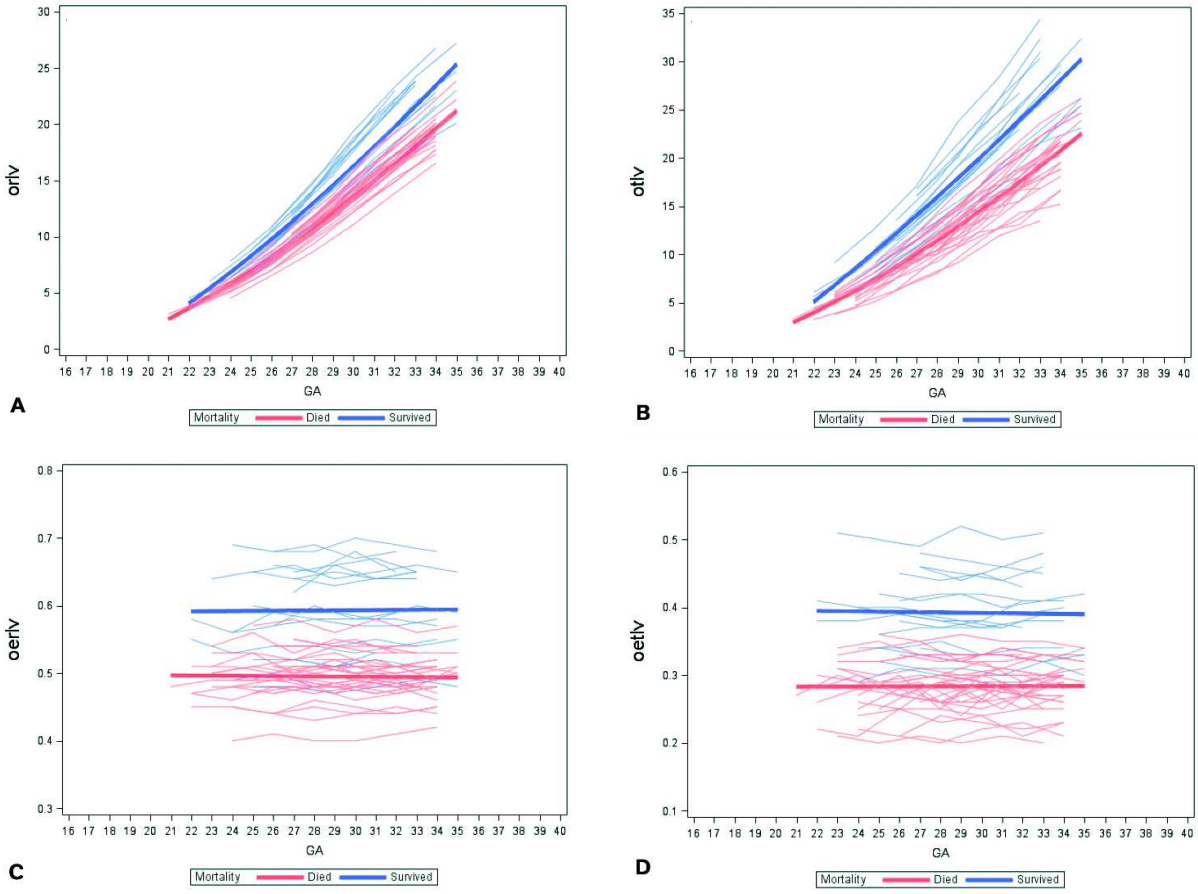

logic characteristics of the disease. The absence of changes in the observed-to-expected right and total lung volume ratios over the 20- to 35-week menstrual age interval suggests that the severity of pulmonary hypoplasia does not progress and that disease severity may be determined very early in pregnancy. A similar observation was reported recently; in 2015, Coleman et al[32] reported a study in which lung volumes were measured in the same fetus twice (initially at 20–30 weeks and then after 30 weeks), and they found that the observed-to-expected total lung volume ratio did not change in these 2 measurements. They clearly stated: "observed-to-expected total lung volume demonstrated no specific change pattern."[32] However, in another recent study, Hagelstein et al[33] showed that the observed-to-expected total lung volume ratio measured on magnetic resonance imaging decreased by an average of 9% in 61% of fetuses, increased by an average of 7% in 26% of the cases, and stayed stable in 13% of cases but without any correlation with survival. These results, different from those reported by Coleman et al[32] and this study, seem to be due to 2 main raisons: (1) different nomograms were used to generate the expected values; and (2) most of the last measurements in fetuses with CDH in the study by Hagelstein et al[33] were after 35 weeks, whereas the nomogram by Rypens et al[34] that was used to generate the observed-to-expected total lung volume ratio had only a few cases after 35 weeks. In addition, both studies only evaluated 2 points on the fetal lung growth trajectory, whereas our study evaluated the fetal lung growth patterns at 4 time points (median, 4; range, 3–7).

To our knowledge, no previously published studies have characterized lung volume growth patterns with serial measurements or have compared observed-to-expected fetal lung volume ratios in healthy fetuses and those with CDH (who did not undergo fetal intervention) using longitudinal measurements. This study also evaluated these ratios in fetuses with CDH who had different outcomes (survival and mortality) for the first time. Further longitudinal investigations beginning in the first trimester (or even before 20 weeks' gestation) will be necessary to evaluate when this process starts and to determine whether earlier intervention is possible.

In our study, we observed a strong correlation between right and total lung volumes, which was expected, since the right lung volume is part of the total lung volume. The reproducibility of fetal lung volume measurements by 3D sonography has also been extensively reported.[14,23,26,28,30,35,36] Although it was not the primary objective of this study, we observed good reproducibility of fetal lung volumes using our method. Measuring the ipsilateral lung volumes is especially challenging with this technique, which requires operator expertise and training.[17,23,35] Fetal magnetic resonance imaging may have less operator variability and may be more reproducible than 3D sonography, despite the fact that previous studies reported by expert operators demonstrated a good level of agreement between these methods.[14,37] Magnetic resonance imaging has more clinical applications in tertiary centers where fetuses with CDH are treated.[14,38–40]

This study provides novel information on the growth patterns of fetal lung volumes measured by 3D sonography. Our results provide novel insight into the variation and growth of the observed-to-expected right and total lung volume ratios in both healthy fetuses and those with CDH. However, this study did not evaluate 2 aspects: (1) fetuses with right-sided CDH were excluded because we believe that our hypothesis should be tested separately in fetuses with right-sided CDH; and (2) the liver position (herniation) was not considered, since our goal was to investigate changes in lung volume in fetuses with isolated left-sided CDH in comparison to healthy fetuses independent of herniated organs. We will investigate the variation in the amount of liver herniation into the fetal chest throughout gestation as well as its impact on fetal lung volume growth. However, further longitudinal studies are necessary to establish whether the amount of liver herniation varies with menstrual age.

One criticism of this study may be the fact that our neonates were not treated with the ECMO after birth. The benefits of ECMO in neonates with CDH still need scientific confirmation. However, this study did not aim to evaluate whether fetal lung growth could predict outcomes but, rather, aimed to evaluate fetal lung growth patterns in healthy fetuses and those with CDH. This study provided evidence that those ratios (observed-to-expected right lung volume ratio and observed-to-expected total lung volume ratio) did not change throughout pregnancy, independent of outcome. Therefore, the results of this study would not be influenced by whether ECMO was used.

In conclusion, the observed-to-expected right lung volume ratio and observed-to-expected total lung volume ratio do not show significant variations between 20 and 35 weeks, so they can be used to evaluate the severity of left-sided CDH independent of fetal age.

Appendix: Ratio of Observed and Expected Measurements as a Measure of the Ratio of Observed and Expected Growth Rates

At some menstrual age after the last menstrual period date (menstrual age = 0), the lung can be identified microscopically. At this age, the lung volume can be considered

equal to 0 (it will not be 0 but very close to it). This menstrual age (MA_0) is called the 0 point or start point.

An estimate of an individual menstrual age (MA_{0i}) can be obtained if one assumes approximate linear growth in the first and second trimesters. A linear function can be fit to the second trimester cube root values of the right lung volume or total lung volume measurements and the resulting line extrapolated back to where it crosses the menstrual age axis. In the reference group, the MA_{0i} values can be determined for each fetus and averaged to give an MA_{0R} value.

At any subsequent time point, say, 30 weeks (MA_{30}) in a given individual, we have a measured observed right lung volume value ($o\text{-}RLV_{30i}$) and an expected right lung volume value ($e\text{-}RLV_{30}$), the latter being the expected value at 30 weeks derived from a reference sample. The $o\text{-}RLV_{30i}$ is the result of a growth process occurring between MA_{0i} and MA_{30}. The $e\text{-}RLV_{30}$ can be considered to be the value obtained from a fetus growing along the 50th percentile line of the reference sample from MA_{0R} to MA_{30}.

The average right lung volume growth rates ($av\,RLV\,gr$) between MA_{0i} or MA_{0R} and MA_{30} are:

$$av\ o\text{-}RLV\ gr_i = (o\text{-}RLV_{30i} - 0)/(MA_{30} - MA_{0i}) = o\text{-}RLV_{30i}/(MA_{30} - MA_{0i});$$

$$av\ e\text{-}RLV\ gr = (e\text{-}RLV_{30} - 0)/(MA_{30} - MA_{0R}) = e\text{-}RLV_{30}/(MA_{30} - MA_{0R}).$$

The ratio of average growth rate is:

$$av\ o\text{-}RLV\ gr_i/av\ e\text{-}RLV\ gr = [o\text{-}RLV_{30i}/(MA_{30} - MA_{0i})]/[e\text{-}RLV_{30}/(MA_{30} - MA_{0R})].$$

If $MA_{0i} = MA_{0R}$:

$$av\ o\text{-}RLV\ gr_i/av\ e\text{-}RLV\ gr = o\text{-}RLV_{30i}/e\text{-}RLV_{30}.$$

Differences between MA_{0i} and MA_{0R} might be expected to have a greater effect early in pregnancy when the $MA\text{-}MA_0$ interval is shorter. However, individual plots of the observed-to-expected values for right lung volume and total lung volume (Figures 1C, 1D, 2C, and 2D) do not show clear evidence of such an effect.

References

1. Langham MR Jr, Kays DW, Ledbetter DJ, Frentzen B, Sanford LL, Richards DS. Congenital diaphragmatic hernia. epidemiology and outcome. *Clin Perinatol* 1996; 23:671–688.
2. Cannie MM, Jani JC, De Keyzer F, Allegaert K, Dymarkowski S, Deprest J. Evidence and patterns in lung response after fetal tracheal occlusion: clinical controlled study. *Radiology* 2009; 252:526–533.
3. Cannie M, Jani J, Meersschaert J, et al. Prenatal prediction of survival in isolated diaphragmatic hernia using observed to expected total fetal lung volume determined by magnetic resonance imaging based on either gestational age or fetal body volume. *Ultrasound Obstet Gynecol* 2008; 32:633–639.
4. Gucciardo L, Deprest J, Doné E, et al. Prediction of outcome in isolated congenital diaphragmatic hernia and its consequences for fetal therapy. *Best Pract Res Clin Obstet Gynaecol* 2008; 22:123–138.
5. Hsieh YY, Chang FC, Tsai HD, Hsu TY, Yang TC. Accuracy of sonography in predicting the outcome of fetal congenital diaphragmatic hernia. *Zhonghua Yi Xue Za Zhi (Taipei)* 2000; 63:751–757.
6. Ishikawa S, Kamata S, Usui N, Sawai T, Nose K, Okada A. Ultrasonographic prediction of clinical pulmonary hypoplasia: measurement of the chest/trunk-length ratio in fetuses. *Pediatr Surg Int* 2003; 19:172–175.
7. Jani JC, Benachi A, Nicolaides KH, et al. Prenatal prediction of neonatal morbidity in survivors with congenital diaphragmatic hernia: a multicenter study. *Ultrasound Obstet Gynecol* 2009; 33:64–69.
8. Ruano R, Takashi E, da Silva MM, Campos JA, Tannuri U, Zugaib M. Prediction and probability of neonatal outcome in isolated congenital diaphragmatic hernia using multiple ultrasound parameters. *Ultrasound Obstet Gynecol* 2012; 39:42–49.
9. Ruano R, Yoshisaki CT, da Silva MM, et al. A randomized controlled trial of fetal endoscopic tracheal occlusion versus postnatal management of severe isolated congenital diaphragmatic hernia. *Ultrasound Obstet Gynecol* 2012; 39:20–27.
10. Askenazi SS, Perlman M. Pulmonary hypoplasia: lung weight and radial alveolar count as criteria of diagnosis. *Arch Dis Child* 1979; 54:614–618.
11. Wigglesworth JS, Desai R. Use of DNA estimation for growth assessment in normal and hypoplastic fetal lungs. *Arch Dis Child* 1981; 56:601–605.
12. Wigglesworth JS, Desai R, Guerrini P. Fetal lung hypoplasia: biochemical and structural variations and their possible significance. *Arch Dis Child* 1981; 56:606–615.
13. Mahieu-Caputo D, Sonigo P, Dommergues M, et al. Fetal lung volume measurement by magnetic resonance imaging in congenital diaphragmatic hernia. *BJOG* 2001; 108:863–868.
14. Ruano R, Joubin L, Sonigo P, et al. Fetal lung volume estimated by 3-dimensional ultrasonography and magnetic resonance imaging in cases with isolated congenital diaphragmatic hernia. *J Ultrasound Med* 2004; 23:353–358.
15. Jani J, Nicolaides KH, Keller RL, et al. Observed to expected lung area to head circumference ratio in the prediction of survival in fetuses with isolated diaphragmatic hernia. *Ultrasound Obstet Gynecol* 2007; 30:67–71.
16. Jani J, Peralta CF, Benachi A, Deprest J, Nicolaides KH. Assessment of lung area in fetuses with congenital diaphragmatic hernia. *Ultrasound Obstet Gynecol* 2007; 30:72–76.
17. Jani JC, Cannie M, Peralta CF, Deprest JA, Nicolaides KH, Dymarkowski S. Lung volumes in fetuses with congenital diaphragmatic hernia: comparison of 3D US and MR imaging assessments. *Radiology* 2007; 244:575–582.

18. Jani JC, Cordier AG, Martinovic J, et al. Antenatal ultrasound prediction of pulmonary hypoplasia in congenital diaphragmatic hernia: correlation with pathology. *Ultrasound Obstet Gynecol* 2011; 38:344–349.
19. Peralta CF, Jani JC, Van Schoubroeck D, Nicolaides KH, Deprest JA. Fetal lung volume after endoscopic tracheal occlusion in the prediction of postnatal outcome. *Am J Obstet Gynecol* 2008; 198:60.e1–60.e5.
20. Britto IS, Tedesco GD, Herbst SR, et al. New anatomical landmarks to study the relationship between fetal lung area and thoracic circumference by three-dimensional ultrasonography. *J Matern Fetal Neonatal Med* 2012; 25:1927–1932.
21. Metkus AP, Filly RA, Stringer MD, Harrison MR, Adzick NS. Sonographic predictors of survival in fetal diaphragmatic hernia. *J Pediatr Surg* 1996; 31:148–152.
22. Lipshutz GS, Albanese CT, Feldstein VA, et al. Prospective analysis of lung-to-head ratio predicts survival for patients with prenatally diagnosed congenital diaphragmatic hernia. *J Pediatr Surg* 1997; 32:1634–1636.
23. Jani JC, Peralta CF, Ruano R, et al. Comparison of fetal lung area to head circumference ratio with lung volume in the prediction of postnatal outcome in diaphragmatic hernia. *Ultrasound Obstet Gynecol* 2007; 30:850–854.
24. Ruano R, Britto IS, Sangi-Haghpeykar H, et al. Longitudinal assessment of lung area measurements by two-dimensional ultrasound in fetuses with isolated left-sided congenital diaphragmatic hernia. *Ultrasound Obstet Gynecol* 2015; 45:566–571.
25. Hadlock FP, Shah YP, Kanon DJ, Lindsey JV. Fetal crown-rump length: reevaluation of relation to menstrual age (5–18 weeks) with high-resolution real-time US. *Radiology* 1992; 182:501–505.
26. Ruano R, Benachi A, Joubin L, et al. Three-dimensional ultrasonographic assessment of fetal lung volume as prognostic factor in isolated congenital diaphragmatic hernia. *BJOG* 2004; 111:423–429.
27. Ruano R, Benachi A, Martinovic J, et al. Can three-dimensional ultrasound be used for the assessment of the fetal lung volume in cases of congenital diaphragmatic hernia? *Fetal Diagn Ther* 2004; 19:87–91.
28. Ruano R, Martinovic J, Dommergues M, Aubry MC, Dumez Y, Benachi A. Accuracy of fetal lung volume assessed by three-dimensional sonography. *Ultrasound Obstet Gynecol* 2005; 26:725–730.
29. Ruano R, Martinovic J, Aubry MC, Dumez Y, Benachi A. Predicting pulmonary hypoplasia using the sonographic fetal lung volume to body weight ratio: how precise and accurate is it? *Ultrasound Obstet Gynecol* 2006; 28:958–962.
30. Ruano R, Joubin L, Aubry MC, et al. A nomogram of fetal lung volumes estimated by 3-dimensional ultrasonography using the rotational technique (virtual organ computer-aided analysis). *J Ultrasound Med* 2006; 25:701–709.
31. Laird NM, Ware JH. Random-effects models for longitudinal data. *Biometrics* 1982; 38:963–974.
32. Coleman A, Phithakwatchara N, Shaaban A, et al. Fetal lung growth represented by longitudinal changes in MRI-derived fetal lung volume parameters predicts survival in isolated left-sided congenital diaphragmatic hernia. *Prenat Diagn* 2015; 35:160–166.
33. Hagelstein C, Weidner M, Kilian AK, et al. Repetitive MR measurements of lung volume in fetuses with congenital diaphragmatic hernia: individual development of pulmonary hypoplasia during pregnancy and calculation of weekly lung growth rates. *Eur Radiol* 2014; 24:312–319.
34. Rypens F, Metens T, Rocourt N, et al. Fetal lung volume: estimation at MR imaging—initial results. *Radiology* 2001; 219:236–241.
35. Ruano R, Aubry MC, Barthe B, Dumez Y, Zugaib M, Benachi A. Ipsilateral lung volumes assessed by three-dimensional ultrasonography in fetuses with isolated congenital diaphragmatic hernia. *Fetal Diagn Ther* 2008; 24:389–394.
36. Ruano R, Aubry MC, Barthe B, Dumez Y, Zugaib M, Benachi A. Three-dimensional sonographic measurement of contralateral lung volume in fetuses with isolated congenital diaphragmatic hernia. *J Clin Ultrasound* 2008; 36:273–278.
37. Gerards FA, Twisk JW, Bakker M, Barkhof F, van Vugt JM. Fetal lung volume: three-dimensional ultrasonography compared with magnetic resonance imaging. *Ultrasound Obstet Gynecol* 2007; 29:533–536.
38. Matsuoka S, Takeuchi K, Yamanaka Y, Kaji Y, Sugimura K, Maruo T. Comparison of magnetic resonance imaging and ultrasonography in the prenatal diagnosis of congenital thoracic abnormalities. *Fetal Diagn Ther* 2003; 18:447–453.
39. Jani J, Cannie M, Doné E, et al. Relationship between lung area at ultrasound examination and lung volume assessment with magnetic resonance imaging in isolated congenital diaphragmatic hernia. *Ultrasound Obstet Gynecol* 2007; 30:855–860.
40. Kehl S, Kalk AL, Eckert S, et al. Assessment of lung volume by 3-dimensional sonography and magnetic resonance imaging in fetuses with congenital diaphragmatic hernias. *J Ultrasound Med* 2011; 30:1539–1545.

5.3. Prematurity and fetal lung response after FETO

Prematurity and fetal lung response after tracheal occlusion in fetuses with severe congenital diaphragmatic hernia.

Sananes N, Rodo C, Peiro JL, Britto IS, Sangi-Haghpeykar H, Favre R, Joal A, Gaudineau A, Silva MM, Tannuri U, Zugaib M, Carreras E, Ruano R.

J Matern Fetal Neonatal Med. 2016 Sep;29(18):3030-4.

THE JOURNAL OF MATERNAL-FETAL & NEONATAL MEDICINE

http://informahealthcare.com/jmf
ISSN: 1476-7058 (print), 1476-4954 (electronic)

J Matern Fetal Neonatal Med, Early Online: 1–5
 DOI: 10.3109/14767058.2015.1114080

Taylor & Francis
Taylor & Francis Group

ORIGINAL ARTICLE

Prematurity and fetal lung response after tracheal occlusion in fetuses with severe congenital diaphragmatic hernia

Nicolas Sananes[1,2], Carlota Rodo[3], Jose Luis Peiro[3], Ingrid Schwach Werneck Britto[1], Haleh Sangi-Haghpeykar[1], Romain Favre[2], Arnaud Joal[2], Adrien Gaudineau[2], Marcos Marques da Silva[4], Uenis Tannuri[4], Marcelo Zugaib[5], Elena Carreras[2], and Rodrigo Ruano[1,5]

[1]Department of Obstetrics and Gynecology, Texas Children's Fetal Center, Baylor College of Medicine, Houston, TX, USA, [2]Service De Gynécologie Obstétrique, CMCO – HUS, Hôpitaux Universitaires De Strasbourg, Strasbourg, France, [3]Fetal Surgery Program, Hospital Universitari Vall D'hebron, Barcelona, Spain, [4]Department of Pediatric Surgery and [5]Department of Obstetrics and Gynecology, Faculdade De Medicina, Universidade De Sao Paulo, Sao Paulo, Brazil

Abstract

Objective: To evaluate the independent association of fetal pulmonary response and prematurity to postnatal outcomes after fetal tracheal occlusion for congenital diaphragmatic hernia.

Methods: Fetal pulmonary response, prematurity (<37 weeks at delivery) and extreme prematurity (<32 weeks at delivery) were evaluated and compared between survivors and non-survivors at 6 months of life. Multivariable analysis was conducted with generalized linear mixed models for variables significantly associated with survival in univariate analysis.

Results: Eighty-four infants were included, of whom 40 survived (47.6%) and 44 died (52.4%). Univariate analysis demonstrated that survival was associated with greater lung response (p=0.006), and the absence of extreme preterm delivery (p=0.044). In multivariable analysis, greater pulmonary response after FETO was an independent predictor of survival (aOR 1.87, 95% CI 1.08–3.33, p=0.023), whereas the presence of extreme prematurity was not statistically associated with mortality after controlling for fetal pulmonary response (aOR 0.52, 95% CI 0.12–2.30, p=0.367).

Conclusion: Fetal pulmonary response after FETO is the most important factor associated with survival, independently from the gestational age at delivery.

Keywords

Congenital diaphragmatic hernia, fetal lung, fetal surgery, fetoscopy, lung-to-head ratio, prematurity

History

Received 4 April 2015
Revised 20 October 2015
Accepted 25 October 2015
Published online 1 December 2015

Introduction

Congenital diaphragmatic hernia (CDH) occurs in ~1 in 2500 live births and is associated with high rates of neonatal mortality, especially in cases with severe pulmonary hypoplasia and abnormal pulmonary vasculature [1–4]. Fetal endoscopic tracheal occlusion (FETO) improves survival due to lung growth and decrease of pulmonary arterial hypertension [5–8].

Fetal lung size and position of the liver relative to the diaphragm are both predictors of neonatal outcome in CDH cases being considered for prenatal assessment for FETO [9,10]. Predicting neonatal survival after FETO is of interest as well for prenatal counseling of the parents and for planning adequate perinatal care. Several studies have suggested that FETO promotes fetal pulmonary growth that seems to be associated with increased survival [7,11,12]. On the other hand, FETO is associated with preterm premature rupture of membranes and prematurity [5,6,8–10]. Prematurity has been associated with poor prognosis in infants with CDH without FETO [13,14]. Recent studies have suggested that prematurity is also associated with increased mortality in fetuses with CDH undergoing FETO [9,15,16]. However, no study has so far evaluated the influence of the fetal pulmonary response and prematurity on postnatal outcomes after FETO.

Our hypothesis is that the survival of fetuses with CDH that undergo FETO is more influenced by the fetal pulmonary response to the procedure than the gestational age at delivery. Therefore, the objective of this study was to evaluate the impact of these two factors simultaneously and independently in a multicenter cohort of fetuses that underwent FETO.

Materials and methods

Study design

This was a retrospective cohort study of all patients who underwent FETO for CDH, between 2002 and 2014, and who delivered in three regional centers (Sao Paulo, Brazil; Barcelona, Spain and Strasbourg, France). Eighty-four fetuses

Address for correspondence: Rodrigo Ruano, Pavilion for Women – Texas Children's Fetal Center, 6651 Main Street, Suite F1020, Houston, TX 77030, USA. E-mail: ruano@bcm.edu; rodrigoruano@hotmail.com

with isolated and severe congenital diaphragmatic hernia that underwent fetal intervention were evaluated {48 fetuses from Sao Paulo, Brazil (43 fetuses were reported in previous studies [6–8]), 30 patients from Barcelona, Spain (20 were reported before [17,18]) and 6 from Strasbourg, France (no cases reported before)}. Inclusion criteria were: absence of chromosomal or major structural anomalies, lung-to-head ratio <1.0 (or observed-to-expected lung-to-head ratio <0.25) and at least one-third of liver herniation into fetal chest based on prenatal imaging [5–9]. The local institutional review boards approved the study and all patients had informed consent.

Fetal endoscopic tracheal occlusion

FETO was performed similarly in all institutions using a previously described technique between 22 and 30 weeks [3,5,6,8]. Briefly, fetal intervention was performed under maternal regional or local anesthesia and fetal systemic anesthesia, using a 1.0-mm (11510A; Karl Storz, Tuttlinglen, Germany), 1.2-mm (11530AA; Karl Storz) or 1.3-mm (11540AA; Karl Storz) fetoscope. Direct visualization of the fetal trachea was achieved in all cases prior to occlusion by a detachable balloon filled with saline (GOLDBAL 2 or 4; Balt, Montmorency, France) [4,6,8,15,16]. Fetal intervention was performed by R. Ruano in Brazil, J.L. Peiro and E. Carreras in Spain and J. Deprest in Belgium (cases from France).

Fetal lung assessment

Fetal lung parameters were evaluated immediately before fetal surgery and every 2 weeks following FETO, using a Voluson 730 or E8 ultrasound machine (GE Medical Systems, Zipf, Austria). Lung-to-head ratio and observed-to-expected lung-to-head ratio were measured for the contralateral lung for all fetuses in the present series, at the level of the four-chamber heart view, using two-dimensional ultrasonography [19,20]. The observed-to-expected lung-to-head ratio was calculated by measuring the ratio between the lung area and the head circumference compared with the expected value for gestational age [21].

Perinatal management

The balloon was removed prenatally or by *ex utero* intrapartum therapy delivery (EXIT procedure). Perinatal management was standardized in all centers. All neonates underwent immediate endotracheal intubation in the delivery room and admitted to the neonatal intensive care unit for ventilator support and high-frequency oscillatory ventilation when necessary. Inhaled nitric oxide was administered in cases of persistent pulmonary arterial hypertension. Extracorporeal membrane oxygenation was available if necessary based on clinical criteria (presence of persistent hypoxia, persistent acidosis and/or inadequate tissue perfusion). The time of surgery repair was managed according to the infant physiologic stability [22,23].

Statistical analysis

The primary study outcome of interest was survival of the neonate at 6 months of life. The following variables were analyzed: primary centers where the patients were followed, gestational age at fetal intervention, duration of the procedure, prophylactic tocolysis during the procedure, side of the defect, lung size immediate before the procedure [initial (observed-to-expected) lung-to-head ratio] and before delivery [latest (observed-to-expected) lung-to-head ratio, that was calculated in the same week of the delivery], lung growth after the procedure (percentage of LHR growth = difference of the latest and initial values divided by initial value and the difference of observed-to-expected lung-to-head ratio = difference between the latest and initial values), gestational at delivery, duration of tracheal occlusion (days between fetal ''plugging'' and ''unplugging'' fetal trachea), interval in days between the removal of the balloon and the delivery and the use of extracorporeal membrane oxygenation. Results were reported as number and percentage for categorical variables and mean ± standard deviation for continuous variables. Fisher's exact test and χ^2 test were used for univariate comparisons. Estimation of odds ratios (OR) and their 95% confidence interval were also computed to predict survival.

Multivariable analysis was then conducted with generalized linear mixed models for variables significantly associated with survival in univariate analysis. The different methods to assess lung size weren't included in the same multivariable model because of their colinearity and therefore several models were built. Correlation between measurements of lung size and gestational age at delivery was assessed using Pearson's coefficient, before multivariable analysis. Adjustment for within-center clustering was performed by including the center as random effect in the GLIMMIX procedure in SAS. The GLIMMIX procedure fits generalized linear mixed models and estimates the parameters by maximum likelihood. A p value <0.05 was considered as statistically significant.

Results

A total of 84 cases of CDH treated by FETO were included, among which 40 survived beyond 6 months of life (47.6%) and 44 died (52.4%). Survival rates were respectively 50.0% (24/48), 40.0% (12/30) and 66.7% (4/6) in Sao Paulo, Barcelona and Strasbourg, without statistically significant difference (p=0.432). The mean duration of the surgery was 19.5 ± 9.5 min. The mean duration of tracheal occlusion in all sites was 52.9 ± 21.1 days.

A total of 52 (61.9%) patients delivered before 37 weeks, 23 (27.4%) patients delivered before 34 weeks and 16 (19.1%) delivered before 32 weeks. Survival rates were 48.1, 30.4 and 25.0%, respectively.

Univariate comparisons between survivors and non-survivors are reported in Table 1. Survivors had statistically greater lung response, based on both percentage of increase of lung-to-head ratio after FETO (157 versus 94%, p=0.006) and difference between observed-to-expected lung-to-head ratio before and after FETO (0.20 versus 0.14, p=0.007). Survival was significantly lower in infants born before 32 weeks than after (p=0.044). None of the other parameters analyzed were significantly associated with survival: side of the defect, lung size before FETO, gestational age at FETO, duration of FETO procedure, type of prophylactic tocolytic agent used, duration

Table 1. Univariate comparison between survivors and non-survivors.

Parameters	Survivors (n=40)	Non-survivors (n=44)	OR (95% CI)	p value
Center				
Sao Paulo	24 (50.0%)	24 (50.0%)	1 (reference)	0.432
Barcelona	12 (40.0%)	18 (60.0%)	0.7 (0.3–1.7)	
Strasbourg	4 (66.7%)	2 (33.3%)	2.0 (0.3–11)	
Side				
Left	31 (50.0%)	31 (50.0%)	1 (reference)	0.737
Right	8 (40.0%)	12 (60.0%)	0.7 (0.2–1.9)	
Bilateral	1 (50.0%)	1 (50.0%)	1 (0.1–17)	
Initial lung-to-head ratio, mean ± SD	0.82 ± 0.15	0.81 ± 0.23	1.1 (0.1–10)	0.903
Initial observed-to-expected lung-to-head ratio, mean ± SD	0.12 ± 0.02	0.12 ± 0.04	1.0 (0.2–4.3)	0.962
Gestational age at FETO (weeks), mean ± SD	26.7 ± 1.8	27.1 ± 1.7	0.9 (0.7–1.1)	0.299
Duration of procedure (minutes), mean ± SD	19.9 ± 7.8	19.1 ± 11.3	1.0 (0.9–1.1)	0.761
Prophylactic tocolysis, N (%)	37 (46.3%)	43 (53.7%)	0.3 (0.0–2.9)	0.261
Latest lung-to-head ratio after FETO, mean ± SD	2.0 ± 0.58	1.6 ± 1.12	1.7 (1.0–2.9)	0.059
Latest observed-to-expected lung-to-head ratio after FETO, mean ± SD	0.32 ± 0.08	0.26 ± 0.14	1.7 (1.1–2.6)	0.018
Percentage of increase of lung-to-head ratio between before and after FETO, mean ± SD	157 ± 104	94 ± 91	1.1 (1.0–1.2)	0.006
Difference between observed-to-expected lung-to-head ratio before and after FETO, mean ± SD	0.20 ± 0.08	0.14 ± 0.12	1.9 (1.2–3.2)	0.007
Prenatal removal of the balloon	14 (41.2%)	20 (58.8%)	0.6 (0.3–1.6)	0.330
Gestational age at delivery (weeks), mean ± SD	35.2 ± 2.4	34.5 ± 3.3	1.1 (0.9–1.3)	0.268
Duration of tracheal occlusion (days), mean ± SD	52.9 ± 21.1	46.2 ± 22.1	1.0 (0.9–1.1)	0.165
Interval between removal of the balloon and delivery (days), mean ± SD	20.6 ± 19.0	18.4 ± 16.3	1.0 (0.9–1.1)	0.737
Interval between FETO and delivery (in days), mean ± SD	60.3 ± 18.7	54.1 ± 23.2	1.0 (0.9–1.1)	0.195
Delivery before 37 weeks, N (%)	25 (48.1%)	27 (51.9%)	1.0 (0.4–2.5)	0.915
Delivery before 34 weeks, N (%)	7 (30.4%)	16 (69.6%)	0.4 (0.1–1.0)	0.053
Delivery before 32 weeks, N (%)	4 (25.0%)	12 (75.0%)	0.3 (0.1–1.0)	0.044
Use of extracorporeal membrane oxygenation	0 (0%)	2 (100.0%)	0.0 (0.0–99)	0.185

SD, standard deviation. OR associated with observed-to-expected lung-to-head ratio and increase of lung-to-head ratio was calculated for each 10% increase.

Table 2. Multivariable analysis of odds for survival.

Model	Parameters	aOR	95% CI	p value
Model 1	Delivery before 32 weeks	0.50	0.12–2.12	0.339
	Percentage of increased lung-to-head ratio after FETO	1.08	1.01–1.15	0.029
Model 2	Delivery before 32 weeks	0.52	0.12–2.30	0.380
	Difference between observed-to-expected lung-to-head ratio before and after FETO	1.87	1.08–3.33	0.023

In each model, correlation within each center is adjusted by including it as a random effect. aOR associated with observed-to-expected lung-to-head ratio and increase of lung-to-head ratio was calculated for each 10% increase.

of tracheal occlusion, prenatal versus EXIT removal of the balloon, time between removal of the balloon and delivery, time between FETO and delivery, the use of extracorporeal membrane oxygenation.

The gestational age at delivery did not significantly correlate with the fetal pulmonary response assessed by percentage of increase of lung-to-head ratio between before and after FETO (r=0.127, p=0.235) and difference between observed-to-expected lung-to-head ratio before and after FETO (r=0.11, p=0.17).

Table 2 provides the results obtained from multivariable analysis including the centers as a random variable in each model. Two models were built, each including extreme prematurity (delivery before 32 weeks) and one of the two fetal pulmonary response variables. In the first multivariable model (Model 1), the percentage of increased lung-to-head ratio after FETO was independently associated with survival (aOR 1.08, 95% CI 1.01 < 1.15, p=0.029) whereas the present of extreme prematurity was not significantly associated with survival (aOR 0.50, 95% CI 0.12–2.12, p=0.339). In a second multivariable model (Model 2), difference of the observed-to-expected lung-to-head ratio from FETO to delivery was significantly associated with survival (aOR 1.87, 95% CI 1.08–3.33, p=0.023) while extreme prematurity was not significantly associated with outcome (aOR 0.52, 95% CI 0.12–2.30, p=0.380).

Discussion

Our data suggest that fetal pulmonary response after FETO is the most important factor associated with survival in fetuses with severe isolated CDH undergoing fetal intervention in our series. Prematurity (especially before 32 weeks gestation) also impacts survival; however, in our cohort after performing a multivariable analysis, this factor became secondary to the fetal pulmonary response.

Different predictive factors of survival in fetuses with CDH undergoing FETO have been previously reported, including lung size before the procedure (the lung-to-head ratio, the observed-to-expected lung-to-head ratio and the observed-to-

expected total lung volume before FETO), gestational age at fetal intervention, fetal pulmonary response after the intervention, duration of the tracheal occlusion, time between balloon removal and delivery, gestational age at delivery and prematurity [7,9,12,15,16,24,25]. However, so far, there are very limited data evaluating the association between adequate pulmonary response after FETO and neonatal survival, especially among those infants that born at extreme premature gestational ages have been limited.

In our study, only fetal lung response and prematurity were associated with outcome. Fetal lung response was found to be associated with survival independently of prematurity. Our findings related to the impact of gestational age at delivery following FETO differ slightly from prior studies. Ali et al. [15] recently suggested that birth before 35 weeks was strongly associated with mortality in patients who underwent FETO for CDH. However, there were no survivors that were born prior to 33 weeks, whereas in our series 4 out of 16 (25%) fetuses that were born before 32 weeks survived. The largest series reported in the literature by Jani et al. [24] demonstrated that gestational age at delivery was a predictor of survival with an odds ratio of 1.024 (95% CI 1.007–1.042, p=0.007). In addition, Done et al. [16] found that the difference of mean gestational age at delivery between survivors and non-survivors was 10 days. In our study, prematurity (birth before 37 weeks) did not impact survival, however extreme prematurity (birth before 32 weeks) was statistically associated with mortality in univariate analysis. Nevertheless, the multivariable analysis revealed that even extreme prematurity became a less important predictor of mortality when considering the adequacy of the fetal pulmonary response. Prior studies have suggested that fetuses who deliver prematurely are less likely to survive because their lungs do not have enough time to grow sufficiently [16]. In our series, we did not observe a significant correlation between lung growth and gestational age at delivery. This result can be explained by the fact that the fetal pulmonary response is achieved significantly within 2 weeks after the procedure with a maximal growth 4 weeks after FETO performed between 26–30 weeks [7]. All of our cases but four were born at least 2 weeks after FETO.

The present study had some limitations, including the retrospective analysis of databases from different centers. In addition, patients were managed in different centers. However, the indication for FETO and the perinatal management were similar in all three centers. In addition, we considered the ''centers'' as a random variable in our analysis and thus took into consideration the similarity (correlation) among patients and procedures within each center, revealing that different 'centers' were not associated with outcome. Another potential limitation of the present study was limited use of ECMO in our patients. In our series, ECMO was used only in eight patients and it was not statistically associated with outcome. In reality, ECMO was used more often in patients that died than in those that survived. It is still controversial if ECMO improves the long-term survival (after 6 months as it was evaluated in the present study) in patients that undergo FETO [26–28]. Further studies are necessary to evaluate this aspect. Finally another limitation of the present study may be the small sample size to demonstrate prematurity to be an independent risk factor of mortality in case of CDH treated by FETO. Clearly, in univariate analysis our study had adequate power to show prematurity, specifically delivery before 32 weeks, to be a risk factor for mortality with an OR of 0.3, p=0.04 (70% reduction in odds for survival in presence of prematurity). However, in multivariable analysis, where other variables were included and adjusted for in the model, influence of prematurity became lessened at aOR = 0.5, $p > 0.05$ (50% reduction in odds for survival). Although, in general the presence of other variables in the model reduces power, our results show that lung response, but not prematurity, is an independent risk factor for mortality.

In conclusion, we found that fetal pulmonary response after FETO is the most important factor associated with survival, independently from the gestational age at delivery. Further prospective studies with larger series are necessary to confirm the present findings.

Acknowledgements

N.S. is a recipient of a scholarship grant from FULBRIGHT Franco-American Commission for Education Exchange (process no. 68141003) and I.S.W.B. is a recipient of post-doctoral scholarship grant from FAPESP (Fundação de Amparo à Pesquisa do Estado de São Paulo, process no. 2013/12493-1). Fetal interventions for cases from Strasbourg, France, were performed in Leuven, Belgium.

Declaration of interest

The authors report no conflicts of interest.

References

1. Samangaya RA, Choudhri S, Murphy F, et al. Outcomes of congenital diaphragmatic hernia: a 12-year experience. Prenat Diagn 2012;32:523–9.
2. Wright JC, Budd JL, Field DJ, Draper ES. Epidemiology and outcome of congenital diaphragmatic hernia: a 9-year experience. Paediatr Perinat Epidemiol 2011;25:144–9.
3. Ruano R, Takashi E, da Silva MM, et al. Prediction and probability of neonatal outcome in isolated congenital diaphragmatic hernia using multiple ultrasound parameters. Ultrasound Obstet Gynecol 2012;39:42–9.
4. Gucciardo L, Deprest J, Done E, et al. Prediction of outcome in isolated congenital diaphragmatic hernia and its consequences for fetal therapy. Best Pract Res Clin Obstet Gynaecol 2008;22:123–38.
5. Deprest J, Gratacos E, Nicolaides KH, Group FT. Fetoscopic tracheal occlusion (FETO) for severe congenital diaphragmatic hernia: evolution of a technique and preliminary results. Ultrasound Obstet Gynecol 2004;24:121–6.
6. Ruano R, Yoshisaki CT, da Silva MM, et al. A randomized controlled trial of fetal endoscopic tracheal occlusion versus postnatal management of severe isolated congenital diaphragmatic hernia. Ultrasound Obstet Gynecol 2012;39:20–7.
7. Ruano R, da Silva MM, Campos JA, et al. Fetal pulmonary response after fetoscopic tracheal occlusion for severe isolated congenital diaphragmatic hernia. Obstet Gynecol 2012;119:93–101.
8. Ruano R, Duarte SA, Pimenta EJ, et al. Comparison between fetal endoscopic tracheal occlusion using a 1.0-mm fetoscope and prenatal expectant management in severe congenital diaphragmatic hernia. Fetal Diagn Ther 2011;29:64–70.
9. Jani JC, Nicolaides KH, Gratacos E, et al. Fetal lung-to-head ratio in the prediction of survival in severe left-sided diaphragmatic hernia treated by fetal endoscopic tracheal occlusion (FETO). Am J Obstet Gynecol 2006;195:1646–50.

10. Dekoninck P, Gratacos E, Van Mieghem T, et al. Results of fetal endoscopic tracheal occlusion for congenital diaphragmatic hernia and the set up of the randomized controlled TOTAL trial. Early Hum Dev 2011;87:619–24.
11. Cannie MM, Jani JC, De Keyzer F, et al. Evidence and patterns in lung response after fetal tracheal occlusion: clinical controlled study. Radiology 2009;252:526–33.
12. Peralta CF, Jani JC, Van Schoubroeck D, et al. Fetal lung volume after endoscopic tracheal occlusion in the prediction of postnatal outcome. Am J Obstet Gynecol 2008;198:60 e61–5.
13. Levison J, Halliday R, Holland AJ, et al. A population-based study of congenital diaphragmatic hernia outcome in New South Wales and the Australian Capital Territory, Australia, 1992-2001. J Pediatr Surg 2006;41:1049–53.
14. Tsao K, Allison ND, Harting MT, et al. Congenital diaphragmatic hernia in the preterm infant. Surgery 2010;148:404–10.
15. Ali K, Grigoratos D, Cornelius V, et al. Outcome of CDH infants following fetoscopic tracheal occlusion – influence of premature delivery. J Pediatr Surg 2013;48:1831–6.
16. Done E, Gratacos E, Nicolaides KH, et al. Predictors of neonatal morbidity in fetuses with severe isolated congenital diaphragmatic hernia undergoing fetoscopic tracheal occlusion. Ultrasound Obstet Gynecol 2013;42:77–83.
17. Cordier AG, Jani JC, Cannie MM, et al. Stomach position in the prediction of survival in left-sided congenital diaphragmatic hernia with or without fetoscopic endoluminal tracheal occlusion. Ultrasound Obstet Gynecol 2015;46:155–61.
18. Cordier AG, Cannie MM, Guilbaud L, et al. Stomach position versus liver-to-thoracic volume ratio in left-sided congenital diaphragmatic hernia. J Matern Fetal Neonatal Med 2015;28: 190–5.
19. Metkus AP, Filly RA, Stringer MD, et al. Sonographic predictors of survival in fetal diaphragmatic hernia. J Pediatr Surg 1996;31: 148–51,discussion 151–42.
20. Jani J, Nicolaides KH, Keller RL, et al. Observed to expected lung area to head circumference ratio in the prediction of survival in fetuses with isolated diaphragmatic hernia. Ultrasound Obstet Gynecol 2007;30:67–71.
21. Britto IS, Araujo Junior E, Sangi-Haghpeykar H, et al. Reference ranges for 2-dimensional sonographic lung measurements in healthy fetuses: a longitudinal study. J Ultrasound Med 2014;33: 1917–23.
22. Datin-Dorriere V, Walter-Nicolet E, Rousseau V, et al. Experience in the management of eighty-two newborns with congenital diaphragmatic hernia treated with high-frequency oscillatory ventilation and delayed surgery without the use of extracorporeal membrane oxygenation. J Intensive Care Med 2008;23:128–35.
23. Mitanchez D. Antenatal treatment of congenital diaphragmatic hernia: an update. Arch Pediatr 2008;15:1320–5.
24. Jani JC, Nicolaides KH, Gratacos E, et al. Severe diaphragmatic hernia treated by fetal endoscopic tracheal occlusion. Ultrasound Obstet Gynecol 2009;34:304–10.
25. Ruano R, Peiro JL, da Silva MM, et al. Early fetoscopic tracheal occlusion for extremely severe pulmonary hypoplasia in isolated congenital diaphragmatic hernia: preliminary results. Ultrasound Obstet Gynecol 2013;42:70–6.
26. Morini F, Goldman A, Pierro A. Extracorporeal membrane oxygenation in infants with congenital diaphragmatic hernia: a systematic review of the evidence. Eur J Pediatr Surg 2006;16: 385–91.
27. Mugford M, Elbourne D, Field D. Extracorporeal membrane oxygenation for severe respiratory failure in newborn infants. Cochrane Database Syst Rev 2008;CD001340.
28. Reiss I, Schaible T, van den Hout L, et al. Standardized postnatal management of infants with congenital diaphragmatic hernia in Europe: the CDH EURO Consortium consensus. Neonatology 2010;98:354–64.

5.4. Sonographic assessment of liver herniation in CDH

Improving the Prediction of Neonatal Outcomes in Isolated Left-Sided Congenital Diaphragmatic Hernia by Direct and Indirect Sonographic Assessment of Liver Herniation.

Sananes N, Britto I, Akinkuotu AC, Olutoye OO, Cass DL, Sangi-Haghpeykar H, Lee TC, Cassady CI, Mehollin-Ray A, Welty S, Fernandes C, Belfort MA, Lee W, Ruano R.

J Ultrasound Med. 2016 Jul;35(7):1437-43.

Improving the Prediction of Neonatal Outcomes in Isolated Left-Sided Congenital Diaphragmatic Hernia by Direct and Indirect Sonographic Assessment of Liver Herniation

Nicolas Sananes, MD, Ingrid Britto, MD, PhD, Adesola C. Akinkuotu, MD, Oluyinka O. Olutoye, MD, PhD, Darrell L. Cass, MD, Haleh Sangi-Haghpeykar, PhD, Timothy C. Lee, MD, Christopher I. Cassady, MD, Amy Mehollin-Ray, MD, Stephen Welty, MD, Caraciolo Fernandes, MD, Michael A. Belfort, MD, PhD, Wesley Lee, MD, Rodrigo Ruano, MD, PhD

Received July 10, 2015, from the Department of Obstetrics and Gynecology (N.S., I.S.W.B., H.S.-H., M.A.B., W.L., R.R.), Michael E. DeBakey Department of Surgery (A.C.A., O.O.O., D.L.C., T.C.L.), Department of Radiology (C.I.C., A.M.-R.), and Department of Pediatrics, Section of Neonatology (S.W., C.F.), Texas Children's Fetal Center and Baylor College of Medicine, Houston, Texas USA. Revision requested September 6, 2015. Revised manuscript accepted for publication October 14, 2015.

Dr Sananes was a recipient of a scholarship grant from the Fulbright Franco-American Commission for Education Exchange (process 68141003), and Dr Britto was a recipient of a postdoctoral scholarship grant from the Fundação de Amparo à Pesquisa do Estado de São Paulo (process 2013/12493-1).

Address correspondence to Rodrigo Ruano, MD, PhD, Pavilion for Women, Texas Children's Fetal Center, 6651 Main St, Suite F1020, Houston, TX 77030 USA.

E-mail: ruano@bcm.edu, rodrigoruano@hotmail.com

Abbreviations

CDH, congenital diaphragmatic hernia; ECMO, extracorporeal membrane oxygenation

doi:10.7863/ultra.15.07020

Objectives—Liver herniation can be assessed sonographically by either a direct (liver-to-thoracic area ratio) or an indirect (stomach position) method. Our objective was to evaluate the utility of those methods to assess liver herniation for the prediction of neonatal outcomes in patients with isolated left-sided congenital diaphragmatic hernia (CDH).

Methods—We conducted a retrospective cohort study of all patients with CDH who had prenatal assessment and were delivered at Texas Children's Hospital between January 2004 and April 2014. The predictive value of sonographic parameters for mortality and the need for extracorporeal membrane oxygenation was evaluated by univariate, multivariate, and factor analysis and by receiver operating characteristics curves.

Results—A total of 77 fetuses with isolated left-sided CDH were analyzed. The lung-to-head ratio, liver-to-thorax ratio, and stomach position (according to the classifications of Kitano et al [*Ultrasound Obstet Gynecol* 2011; 37:277–282] and Cordier et al [*J Matern Fetal Neonatal Med* 2015; 28:190–195]) were significantly associated with both neonatal outcomes ($P < .03$). Significant correlations were observed between all of these sonographic parameters. A combination of the liver-to-thorax ratio and stomach position (Kitano) or stomach position (Cordier) with the lung-to-head ratio increased the area under the receiver operating characteristic curve of the lung-to-head ratio for mortality prediction (0.86 [95% confidence interval, 0.74–0.98], 0.83 [0.72–0.95], and 0.83 [0.74–0.92], respectively).

Conclusions—Sonographic measurements of liver herniation (liver-to-thorax ratio and stomach position) are predictive of neonatal outcomes in isolated left-sided congenital diaphragmatic hernia. Our study shows that the combination of those sonographic measurements of liver herniation and lung size improves the accuracy of predicting mortality in those fetuses.

Key Words—congenital diaphragmatic hernia; liver herniation; lung-to-head ratio; obstetric ultrasound; pulmonary hypoplasia; prenatal predictors; stomach position

Congenital diaphragmatic hernia (CDH) affects approximately 1 per 2500 live births and is associated with substantial morbidity and mortality, mostly because of pulmonary hypoplasia.[1–3] Accurate prenatal determination of

the severity of the CDH is necessary to counsel patients and to provide appropriate perinatal management, including selection of candidates for fetal endoscopic tracheal occlusion.[4–6]

Sonographic measurement of the contralateral lung-to-head ratio is commonly used to assess lung size in CDH.[7–9] Studies have shown that the amount of liver herniation can be measured on magnetic resonance imaging and is an independent prognostic factor.[10–12] A recent study demonstrated that the amount of liver herniation can be assessed directly on 2-dimensional sonography in the same image that is used to measure the lung-to-head ratio (lung size) by calculating the liver-to-thoracic area ratio.[13] Investigators have also shown that the stomach position in the fetal chest can be considered an indirect method to quantify the degree of liver herniation, which also correlates with prognosis.[14–16]

To our knowledge, there is no study comparing direct and indirect methods for quantifying liver herniation using conventional sonography. Conventional sonography is already widely used by maternal-fetal specialists to calculate the lung-to-head ratio, which is the measurement most often used to predict outcomes in fetuses with left-sided CDH.

Therefore, the primary objective of this study was to evaluate the utility of the direct and indirect methods used to quantify the amount of liver herniation by 2-dimensional sonography (liver-to-thorax ratio and stomach position) for predicting outcomes in fetuses with isolated left CDH. The secondary objectives were to evaluate the correlation between the methods and to evaluate the combination of these parameters with the lung-to-head ratio for the prediction of outcomes in these patients.

Materials and Methods

Study Design

We conducted a retrospective cohort study of all fetuses with isolated left-sided CDH who had a prenatal sonographic examination and delivered at Texas Children's Hospital between January 2004 and April 2014. We excluded cases with associated anomalies, fetal intervention, and right-sided CDH. The definition of isolated CDH was based on the absence of other structural anomalies on prenatal examination, a normal fetal karyotype, and absence of a cardiac anomaly on fetal echocardiography. The sonographic parameters were obtained from images derived from video clips of comprehensive fetal sonographic examinations. The local Institutional Review Board approved the study (H-29006).

Sonographic Measurements

Figure 1 shows all of the sonographic evaluations and measurements using single images. The lung-to-head ratio measurements were performed according to a standardized protocol by multiplying the two longest perpendicular diameters of the lung on a 4-chamber view of the heart.[7,17]

Figure 1. Sonograms of different fetuses with mild (**A**), moderate (**B**), and severe (**C**) forms of left-sided CDH at 24, 26, and 25 weeks' gestation, respectively. Stomach position is according to the Cordier classification. LHR indicates lung-to-head ratio; and US-LiTR, sonographic liver-to-thorax ratio.

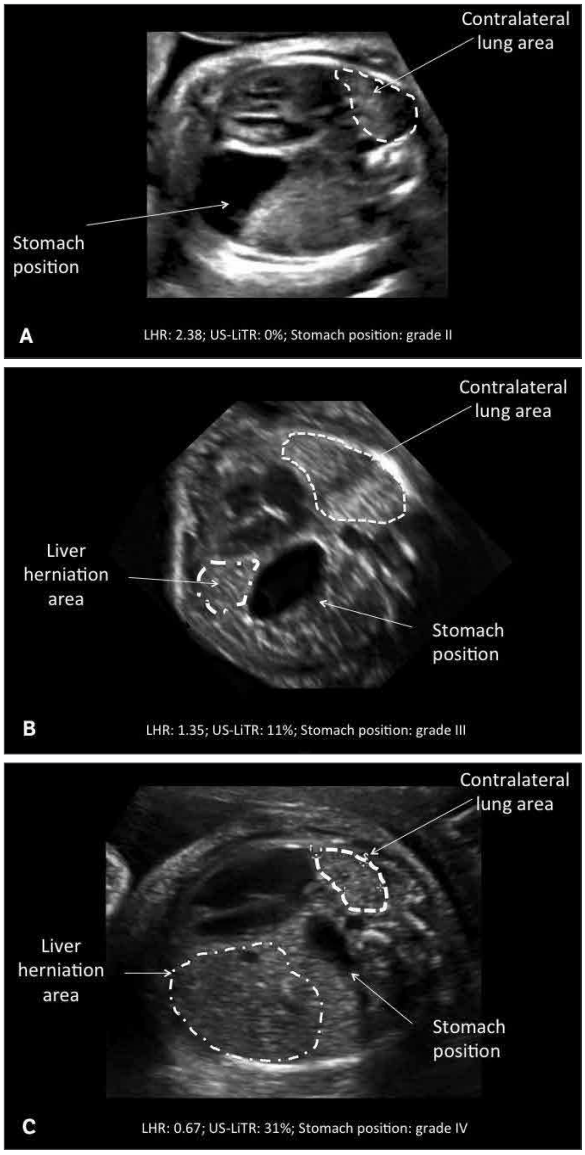

On the same sonogram, the liver herniation area and the fetal thoracic area were measured, and the sonographic liver-to-thoracic area ratio was then calculated.[13] The stomach position was categorized as grades 0 to 3 on a coronal view according to the classification of Kitano et al[14] and as grades 1 to 4 on the 4-chamber view of the heart according to the classification of Cordier et al.[15] The stomach position according to the Cordier classification was evaluated on the same image on which the lung-to-head ratio and liver-to-thorax ratio were measured. Only 1 sonographic examination per patient (the first examination) at our center was considered for analysis. All evaluations of the stomach position were performed by a single investigator (N.S.), whereas the measurements of the lung-to-head ratio and liver-to-thorax ratio were performed by another investigator (I.B.), who were both well trained to perform prenatal sonographic scans and were blinded to postnatal outcomes.

Neonatal Protocol

All neonates were treated according to a standard perinatal protocol.[18] All neonates underwent immediate endotracheal intubation with orogastric decompression and avoidance of bag-mask ventilation by a staff neonatologist. Gentle mechanical ventilation using a permissive hypercapnia protocol was used. Escalation of ventilatory support to a maximal peak inspiratory pressure and positive end-expiratory pressure of 30 and 6 cm H_2O, respectively, and use of high-frequency oscillatory ventilation to a maximum mean airway pressure of 15 cm H_2O were based on preestablished criteria. The need for extracorporeal membrane oxygenation (ECMO) was determined by the presence of persistent hypoxia (oxygenation index >40 or oxygen pressure persistently <40 mm Hg) with persistent acidosis (pH <7.2) or inadequate tissue perfusion (arterial lactate >3 mmol/L and rising). The timing of surgical repair of the CDH was planned with consideration of the infant's physiologic stability and the presence or absence of pulmonary hypertension.

Statistical Analysis

Results were reported as mean ± standard deviation for continuous variables and as number and percentage for categorical variables. The outcomes in this study were survival at 6 months of life and the need for ECMO postnatally. Univariate comparisons were performed by a *t* test and χ^2 square test for continuous and categorical variables, respectively. Correlations between variables were evaluated by the Spearman test. The performances of the different predictors were evaluated by receiver operating characteristic curve analysis, with estimation of areas under the curve with 95% confidence intervals. Multivariable studies were performed using factor analysis (principal component analysis). Statistical comparisons between the areas under the curves of each sonographic variable and multivariate models were performed according to the tests of McNeil et al,[19] Hanley and McNeil,[20] and DeLong et al.[21] Statistical analyses were performed with the software SPSS version 19.0 software package (IBM Corporation, Armonk, NY) and the MedCalc version 11.6 software package (MedCalc, Mariakerke, Belgium). $P < .05$ was considered statistically significant.

Results

A total of 142 cases of CDH were prenatally evaluated and delivered in our institution during the study period. Sixty-five patients were excluded from the study because of associated anomalies (n = 39), right-sided CDH (n = 15), and fetal intervention (n = 11). There was no case of termination of pregnancy. Therefore, a total of 77 patients with isolated left-sided CDH were included in the study (68 patients were reported in our previous study[13]). In the previous study, we described the liver-to-thorax ratio in fetuses with left and right CDH. The mean gestational age at delivery ± SD was 37.6 ± 1.6 weeks (range, 32–40 weeks).

The survival rate within 6 months of life was 79.3%, since 1 fetus died in utero, and 15 died in the neonatal period. Among the 76 fetuses who were born alive, ECMO was needed in 26 cases (34.2%). Table 1 shows sample characteristics and prenatal findings according to mortality at 6 months of life and the need for ECMO. There was a significant association between the lung-to-head ratio, liver-to-thorax ratio, and stomach position (independent of the classification method) and neonatal mortality or need for ECMO ($P < .05$).

Spearman correlation coefficients between variables are reported in Table 2. Significant correlations were observed between the lung-to-head ratio, liver-to-thorax ratio, and stomach position. The liver-to-thorax ratio correlated more with the stomach position according to the Cordier classification than the Kitano classification.

Figures 2 and 3 show receiver operating characteristic curve analyses of all isolated parameters (lung-to-head ratio, liver-to-thorax ratio, and stomach position) to predict mortality and ECMO, respectively. Figures 4 and 5 show receiver operating characteristic curve analyses of different combinations of parameters to predict mortality and ECMO, respectively. Table 3 provides the areas under the curves for each predictor and each combination of parameters. The lung-to-head ratio had the best accuracy

to predict mortality compared to the other parameters when used singly, but the difference was not statistically significant ($P > .05$). The combination of the lung-to-head ratio and liver-to-thorax ratio was the most accurate predictor of mortality when compared to all other parameters when used singly or in combination ($P < .05$). The predictive accuracy of the combination of the lung-to-head ratio and liver-to-thorax ratio was not improved by the addition of stomach grading, whatever it was ($P > .05$). In considering prediction of the need for ECMO, all sonographic parameters when analyzed singly had similar accuracy, with no statistical difference. The combination of parameters slightly improved the accuracy to predict ECMO, but this finding was still not statistically significant.

Discussion

Principal Findings

Our study shows that direct and indirect sonographic assessments of liver herniation are useful tools for predicting mortality in fetuses with isolated left-sided CDH. The accuracy to predict outcomes in those fetuses by the direct or indirect method for quantifying liver herniation improves when combined with the lung-to-head ratio, especially the liver-to-thorax ratio. However, when used individually, all of these parameters were less accurate to predict the need for ECMO (accuracy of 70%), with only a slight improvement when used in combination (lung-to-head ratio and liver-to-thorax ratio: accuracy of 75%).

Strengths and Weaknesses

To our knowledge, a study that evaluated two sonographic methods to quantify fetal liver herniation (liver-to-thorax ratio and stomach position) and compared and combined them with the lung-to-head ratio has not been reported previously. In addition, we provide information about those measurements from one of the largest series. We also provide information about using these sonographic parameters to predict the need for ECMO. We acknowledge that our study had some limitations, such as the retrospective design. To avoid bias, the operator performed the measurements

Table 1. Sample Characteristics and Prenatal Findings of 77 Fetuses With Isolated Left-Sided CDH According to Outcome

	Mortality at 6 mo of Life			ECMO		
	Yes	No		Yes	No	
Parameter	(n = 16)	(n = 61)	*P*	(n = 26)	(n = 50)	*P*
Maternal age, y	27.9 ± 7.4	27.7 ± 6.0	.903	27.5 ± 6.1	27.2 ± 6.3	.78
GA at sonography, wk	26.7 ± 5.4	26.8 ± 5.0	.928	27.2 ± 5.7	26.6 ± 4.7	.631
Lung-to-head ratio	1.12 ± 0.39	1.87 ± 0.75	<.001	1.40 ± 0.68	1.89 ± 0.75	.007
Liver-to-thorax ratio, %	16.92 ± 8.52	8.20 ± 9.05	.001	13.78 ± 8.2	7.89 ± 9.7	.01
Stomach position (Kitano)			.002			.026
0	0 (0.0)	5 (8.2)		0 (0.0)	5 (10.0)	
1	4 (25.0)	30 (49.1)		8 (30.8)	26 (52.0)	
2	4 (25.0)	20 (32.9)		10 (38.4)	14 (28.0)	
3	8 (50.0)	6 (9.8)		8 (30.8)	5 (10.0)	
Stomach position (Cordier)			.018			.008
1	0 (0.0)	7 (11.5)		0 (0.0)	7 (14.0)	
2	1 (6.2)	19 (31.1)		3 (11.5)	17 (34.0)	
3	4 (25.0)	17 (27.9)		8 (30.8)	13 (26.0)	
4	11 (68.8)	18 (29.5)		15 (57.7)	13 (26.0)	
GA at delivery, wk	37.6 ± 1.0	37.6 ± 1.7	.967	37.8 ± 1.2	37.5 ± 1.8	.552

Data are presented as mean ± SD and number (percent). GA indicates gestational age.

Table 2. Correlations Between Lung-to-Head Ratio, Lung-to-Thoracic Ratio, and Stomach Position

Parameter	Lung-to-Head Ratio	Lung-to-Thoracic Ratio	Stomach Position (Kitano)	Stomach Position (Cordier)
Lung-to-head ratio	1.00	–0.54[a]	–0.51[a]	–0.55[a]
Lung-to-thorax ratio	–0.54[a]	1.00	0.49[a]	0.69[a]
Stomach position (Kitano)	–0.51[a]	0.49[a]	1.00	0.65[a]
Stomach position (Cordier)	–0.55[a]	0.69[a]	0.65[a]	1.00

[a]Significant at $P < .001$.

blinded to the neonatal outcome. We did not test the reproducibility of the measurements in this study, as that has been addressed in other publications.[13,15] In this study, we did not include patients who underwent fetal endoscopic tracheal occlusion. This fact could be considered a bias, since fetuses with less severe forms of CDH could have been excluded from the analysis. However, fetal endoscopic tracheal occlusion was performed in only 10 patients with isolated left-sided CDH during the study period, and we included fetuses with severe forms of CDH who did not undergo fetal intervention. In addition, fetal intervention may change the sonographic parameters (lung-to-head ratio, liver-to-thorax ratio, and stomach position), which can also lead to bias. Nevertheless, Cordier et al[16] showed that the stomach position remains a relevant prognostic factor even after fetal endoscopic tracheal occlusion. Further studies are necessary to investigate whether the amount of liver herniation and the stomach position classification change after fetal endoscopic tracheal occlusion.

Figure 2. Receiver operating characteristics curves for the prediction of mortality at 6 months of life using the lung-to-head ratio (LHR), sonographic liver-to-thorax ratio (US-LiTR), and stomach position according to the Kitano and Cordier classifications.

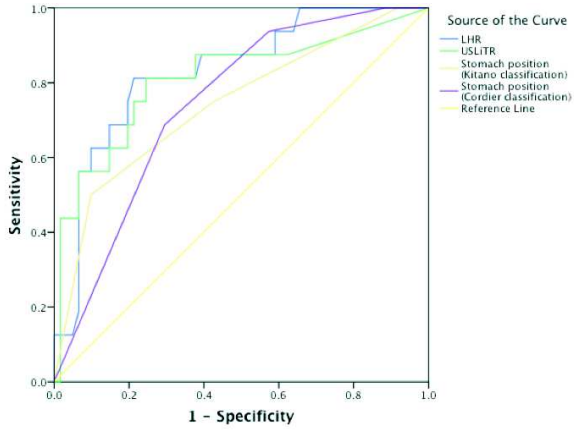

Figure 3. Receiver operating characteristics curves for the prediction of ECMO using the lung-to-head ratio (LHR), sonographic liver-to-thorax ratio (US-LiTR), and stomach position according to the Kitano and Cordier classifications.

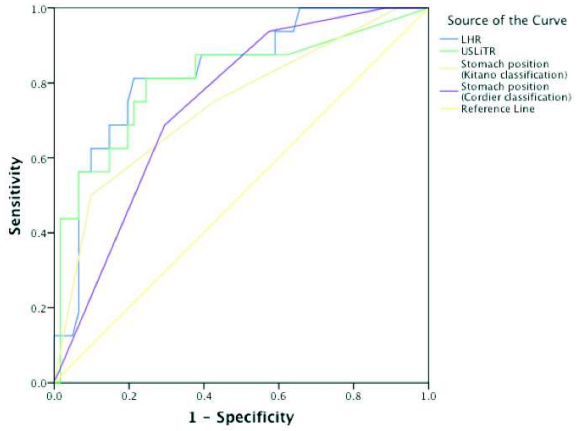

Figure 4. Receiver operating characteristics curves for the prediction of mortality at 6 months of life using combinations of the lung-to-head ratio (LHR), sonographic liver-to-thorax ratio (US-LiTR), and stomach position according to the Kitano and Cordier classifications.

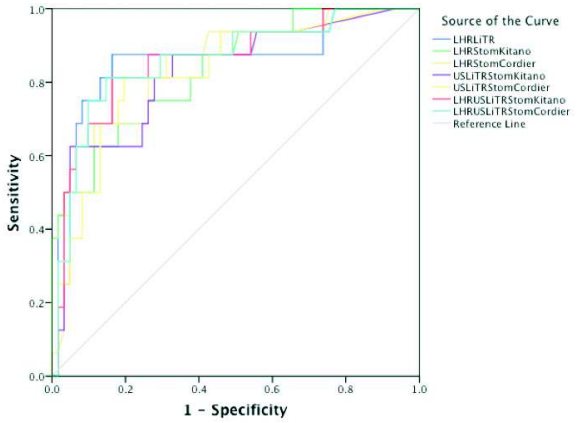

Figure 5. Receiver operating characteristics curves for the prediction of ECMO using combinations of the lung-to-head ratio (LHR), sonographic liver-to-thorax ratio (US-LiTR), and stomach position according to the Kitano and Cordier classifications.

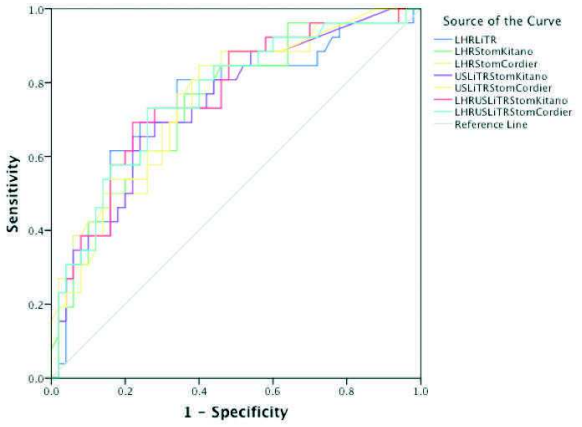

Table 3. Prediction of Neonatal Outcome Using Sonographic Parameters Alone and Combined

Parameter	Mortality at 6 mo of Life		ECMO	
	AUC	95% CI	AUC	95% CI
Lung-to-head ratio	0.80	0.65–0.92	0.72	0.60–0.84
Lung-to-thorax ratio	0.77	0.63–0.90	0.73	0.60–0.80
Stomach position (Kitano)	0.74	0.60–0.89	0.70	0.57–0.82
Stomach position (Cordier)	0.74	0.62–0.87	0.73	0.61–0.84
Lung-to-head ratio + lung-to-thorax ratio	0.86	0.74–0.98	0.76	0.63–0.87
Lung-to-head ratio + stomach position (Kitano)	0.83	0.72–0.95	0.74	0.63–0.86
Lung-to-head ratio + stomach position (Cordier)	0.83	0.74–0.92	0.76	0.64–0.87
Lung-to-thorax ratio + stomach position (Kitano)	0.82	0.70–0.91	0.74	0.62–0.86
Lung-to-thorax ratio + stomach position (Cordier)	0.83	0.71–0.93	0.75	0.64–0.86
Lung-to-head ratio + lung-to-thorax ratio + stomach position (Kitano)	0.86	0.73–0.93	0.76	0.65–0.88
Lung-to-head ratio + lung-to-thorax ratio + stomach position (Cordier)	0.86	0.76–0.93	0.76	0.65–0.88

AUC indicates area under the curve; and CI, confidence interval.

Interpretation

Quantification of liver herniation by magnetic resonance imaging is predictive of neonatal outcomes in left-sided CDH.[10–12] Our study confirms that sonographic assessment of liver herniation, either by a direct or an indirect method, can predict survival at 6 months of life and the need for ECMO.[13–16] Additionally, our results demonstrate that there is a good correlation (correlation coefficient of 0.69) between the liver-to-thorax ratio and evaluation of the stomach position according to Cordier et al.[15] This correlation was expected, since the Cordier method indirectly evaluates the degree of liver herniation. However, only weak correlations were observed between the lung-to-head ratio and liver-to-thorax ratio and between the lung-to-head ratio and stomach position. For these reasons, we recommend using the combination of the lung-to-head ratio (lung size) and one other method to measure the amount of liver herniation (liver-to-thorax ratio or stomach position), but there is no need to use the combination of all parameters. In our experience, the combination of the lung-to-head ratio and liver-to-thorax ratio was statistically more accurate than the lung-to-head ratio and stomach position; however, measuring the liver-to-thorax ratio is more demanding than evaluating the stomach position. Further studies are necessary to confirm our findings.

The ideal situation would be to obtain as much information as possible from as few images as necessary to facilitate the evaluation of a fetus with left-sided CDH. Three of the measurements evaluated can be performed on the exact same sonogram (in a cross section of the fetal chest at the level of the 4-chamber view of the heart). These measurements are the lung-to-head ratio, the liver-to-thorax ratio, and the stomach position according to Cordier et al.[15] Evaluation of the stomach position according to Kitano et al[14] requires a different sonogram; therefore, different sections of the fetus are necessary to obtain that measurement in addition to the lung-to-head ratio.

To test whether the combination of the parameters would improve the accuracy to predict outcomes, principal component analysis was used, instead of multivariate regression. The reason for performing such an analysis was because of the multicollinearity among the variables.

Conclusions

Fetal outcomes in left-sided CDH can be predicted by using a single sonogram by estimating both the lung size and the amount of liver herniation. Our results suggest the liver herniation can be quantified on sonography directly by the liver-to-thorax ratio or indirectly by assessing the stomach position. The combination of sonographic measurements of lung size (lung-to-head ratio) and assessment of the amount of liver herniation (liver-to-thorax ratio or stomach position in the fetal chest) improves the accuracy in predicting outcomes in those fetuses. Future prospective studies with larger numbers of patients are necessary to determine which combination will predict outcomes best in those fetuses.

References

1. Langham MR Jr, Kays DW, Ledbetter DJ, Frentzen B, Sanford LL, Richards DS. Congenital diaphragmatic hernia: epidemiology and outcome. *Clin Perinatol* 1996; 23:671–688.
2. Stege G, Fenton A, Jaffray B. Nihilism in the 1990s: the true mortality of congenital diaphragmatic hernia. *Pediatrics* 2003; 112:532–535.
3. Gallot D, Boda C, Ughetto S, et al. Prenatal detection and outcome of congenital diaphragmatic hernia: a French registry-based study. *Ultrasound Obstet Gynecol* 2007; 29:276–283.

4. Jani JC, Nicolaides KH, Gratacós E, et al. Severe diaphragmatic hernia treated by fetal endoscopic tracheal occlusion. *Ultrasound Obstet Gynecol* 2009; 34:304–310.
5. Peralta CF, Jani JC, Van Schoubroeck D, Nicolaides KH, Deprest JA. Fetal lung volume after endoscopic tracheal occlusion in the prediction of postnatal outcome. *Am J Obstet Gynecol* 2008; 198:60.e1–60.e5.
6. Ruano R, Duarte SA, Pimenta EJ, et al. Comparison between fetal endoscopic tracheal occlusion using a 1.0-mm fetoscope and prenatal expectant management in severe congenital diaphragmatic hernia. *Fetal Diagn Ther* 2011; 29:64–70.
7. Metkus AP, Filly RA, Stringer MD, Harrison MR, Adzick NS. Sonographic predictors of survival in fetal diaphragmatic hernia. *J Pediatr Surg* 1996; 31:148–152.
8. Lipshutz GS, Albanese CT, Feldstein VA, et al. Prospective analysis of lung-to-head ratio predicts survival for patients with prenatally diagnosed congenital diaphragmatic hernia. *J Pediatr Surg* 1997; 32:1634–1636.
9. Laudy JA, Van Gucht M, Van Dooren MF, Wladimiroff JW, Tibboel D. Congenital diaphragmatic hernia: an evaluation of the prognostic value of the lung-to-head ratio and other prenatal parameters. *Prenat Diagn* 2003; 23:634–639.
10. Cannie M, Jani J, Chaffiotte C, et al. Quantification of intrathoracic liver herniation by magnetic resonance imaging and prediction of postnatal survival in fetuses with congenital diaphragmatic hernia. *Ultrasound Obstet Gynecol* 2008; 32:627–632.
11. Lazar DA, Ruano R, Cass DL, et al. Defining "liver-up": does the volume of liver herniation predict outcome for fetuses with isolated left-sided congenital diaphragmatic hernia? *J Pediatr Surg* 2012; 47:1058–1062.
12. Ruano R, Lazar DA, Cass DL, et al. Fetal lung volume and quantification of liver herniation by magnetic resonance imaging in isolated congenital diaphragmatic hernia. *Ultrasound Obstet Gynecol* 2014; 43:662–669.
13. Werneck Britto IS, Olutoye OO, Cass DL, et al. Quantification of liver herniation in fetuses with isolated congenital diaphragmatic hernia using two-dimensional ultrasonography. *Ultrasound Obstet Gynecol* 2015; 46:150–154.
14. Kitano Y, Okuyama H, Saito M, et al. Re-evaluation of stomach position as a simple prognostic factor in fetal left congenital diaphragmatic hernia: a multicenter survey in Japan. *Ultrasound Obstet Gynecol* 2011; 37:277–282.
15. Cordier AG, Cannie MM, Guilbaud L, et al. Stomach position versus liver-to-thoracic volume ratio in left-sided congenital diaphragmatic hernia. *J Matern Fetal Neonatal Med* 2015; 28:190–195.
16. Cordier AG, Jani JC, Cannie MM, et al. Stomach position in the prediction of survival in left-sided congenital diaphragmatic hernia with or without fetoscopic endoluminal tracheal occlusion. *Ultrasound Obstet Gynecol* 2015; 46:155–161.
17. Jani JC, Peralta CF, Nicolaides KH. Lung-to-head ratio: a need to unify the technique. *Ultrasound Obstet Gynecol* 2012; 39:2–6.
18. Lazar DA, Cass DL, Rodriguez MA, et al. Impact of prenatal evaluation and protocol-based perinatal management on congenital diaphragmatic hernia outcomes. *J Pediatr Surg* 2011; 46:808–813.
19. McNeil BJ, Hanley JA, Funkenstein HH, Wallman J. Paired receiver operating characteristic curves and the effect of history on radiographic interpretation: CT of the head as a case study. *Radiology* 1983; 149:75–77.
20. Hanley JA, McNeil BJ. A method of comparing the areas under receiver operating characteristic curves derived from the same cases. *Radiology* 1983; 148:839–843.
21. DeLong ER, DeLong DM, Clarke-Pearson DL. Comparing the areas under two or more correlated receiver operating characteristic curves: a nonparametric approach. *Biometrics* 1988; 44:837–845.

5.5. Ultrasound assessment of lung vasculature in CDH

Original article

Longitudinal ultrasound assessment of lung vasculature in fetuses with congenital diaphragmatic hernia treated or not by endoscopic tracheal occlusion and controls

Short title: lung vasculature in CDH

I. BRITTO [1,2], N. SANANES [1,3], H. SANGI-HAGHPEYKAR [2], R. RUANO [1,2]

[1] Texas Children's Fetal Center and Baylor College of Medicine, Houston, Texas, USA

[2] Department of Obstetrics and Gynecology, Texas Children's Hospital, Houston, Texas, USA

[3] Department of Obstetrics and Gynecology, Strasbourg teaching Hospital, Strasbourg, France

Corresponding author: Rodrigo Ruano, Pavilion for Women – Texas Children's Fetal Center, 6651 Main Street, Suite F1020, Houston, Texas, United States, 77030, ruano@bcm.edu, rodrigoruano@hotmail.com

Acknowledgements:

I.S.W.B. is a recipient of post-doctoral scholarship grant from FAPESP (Fundação de Amparo à Pesquisa do Estado de São Paulo, process n. 2013/12493-1).

N.S. is a recipient of a scholarship grant from FULBRIGHT Franco-American Commission for Education Exchange (process n. 68141003).

ABSTRACT

Objective:

The primary objective of this study was to assess the fetal pulmonary vasculature response after fetal endoscopic tracheal occlusion (FETO) for congenital diaphragmatic hernia (CDH), and to compare with both untreated CDH cases and controls. The secondary objective was to evaluate the correlation between vasculature and survival.

Methods:

In this prospective observational longitudinal study, 3D power Doppler ultrasonography was performed in 33 fetuses divided in 3 groups: 10 normal fetuses, 13 fetuses with isolated left CDH with routine prenatal management and 10 fetuses treated with FETO. Using the same pre-settings for all fetuses, 3 vascular indices were measured throughout pregnancy: vascularization indices (VI), flow indices (FI), and vascularization-flow index (VFI).

Results:

Fetal pulmonary indices showed a constant distribution through pregnancy in normal fetuses and CDH with expectative management. FI and VFI were significantly lower in cases of CDH with no fetal intervention than in controls ($p= 0.0006$ and $p= 0.018$ respectively). FETO resulted in a significant improvement in VFI and VI when compared with controls ($p=0.0003$ and $p<.0001$ respectively). Among FETO cases, the vascular indices VFI and VI were significantly higher in cases that survived compared to fetuses who died ($p= .0005$ and $p= .01$ respectively).

Conclusion:

Vascular indices are altered in CDH in comparison to controls. FETO may restore vascular indices and this response after the procedure can predict neonatal survival.

Keywords: congenital diaphragmatic hernia; fetal endoscopic tracheal occlusion; lung perfusion; three-dimensional power doppler ultrasound; prognosis

INTRODUCTION

Congenital diaphragmatic hernia (CDH) occurs 1 in 2200 newborns and is associated with significant morbidity and mortality due to pulmonary hypoplasia and pulmonary hypertension[1]. Assessment of both lung size and vasculature is of interest, in order to predict accurately the outcome and therefore provide appropriate counseling and perinatal management, including fetal endoscopic tracheal occlusion (FETO) [2-4].

Several parameters have been developed to estimate lung size and predict outcome for isolated CDH, including contralateral lung-to-head ratio (LHR), observed to expected LRH (o/e LHR), o/e total lung volume (O/e TLV) and quantitative lung index (QLI) [5-15]. Even if lung size and vasculature may be partially correlated, accuracy to predict outcome still needs to be improved and direct assessment of pulmonary vasculature is of interest [16].

Pathology studies demonstrated that CDH is associated with decreased number of arterial branches and increased muscular thickness in the pulmonary vessels [18, 19]. Indeed, clinical studies showed that the sonographic fetal pulmonary vascular indices are significantly lower in cases with CDH than in controls [20].

FETO for severe isolated CDH have the potential to increase airway pressure, leading to proliferation, increase alveolar air space and maturation of pulmonary vasculature [21]. Surprinsingly, the only two human pathologic studies didn't show that FETO improved lung vasculature [22, 23]. The few clinical data suggest that pulmonary vasculature correlates with prognosis and that FETO may improve lung tissue perfusion [24, 25]. There is no study comparing the lung vasculature in CDH treated by FETO and lung vasculature in normal fetuses.

Additional studies are therefore necessary because of the paucity of data, and because of the inconsistency in pathology and clinical findings. Moreover, comparison of lung vasculature between FETO cases and controls still need to be investigated.

The primary objective of this study was to assess the fetal pulmonary vasculature response after FETO for CDH, and to compare with both untreated CDH cases and controls. The secondary objective was to evaluate the correlation between vasculature and survival.

METHODS

Study design

This was a single-center cohort prospective observational study conducted in Texas Children's Hospital, that is a tertiary Maternal Fetal Medicine unit. Inclusion period was from February 2011 to September 2014. All patients agreed to participate at this study. The Institutional Review Board from Texas Children's Hospital approved this protocol.

Participants

All consecutive cases of fetal isolated left CDH referred in our center during the study period were included, whether they underwent a FETO or not. The definition of isolated CDH was based on the absence of other structural anomalies on prenatal examination, normal fetal karyotype and absence of cardiac anomaly on fetal echocardiogram.

Assessment of lung vasculature was performed in the right lung using 3-dimensional power Doppler according to methods previously described [20], 24. 3D power Doppler has the advantage of assessing the volume and quantifying the power Doppler signal in the region of interest. A Voluson 730 ultrasound machine (G.E .Health-care, Kretztechnik, Zipf, Austria) was used for 3D volume scanning. Preestableshid settings were used for all cases: angio mode: cent; smooth: 4/5; FRQ: low; quality: 16; density: 6; enhance: 16; balance: G>150; filter: 2; actual power: 2dB; pulse repetition frequency: 0.9 20. In all cases, 3 D power Doppler was performed at the level of four chambers view of the fetal thorax with the pulmonary vessels located proximal to the transducer. The angle of the volumetric box was adjusted to scan entire fetal thorax and the angle of volume sampling varied with gestational age. After obtaining the multiplanar image of 3 orthogonal planes, the right lung volume was measured using VOCAL technique with 30°rotation. 3 D power Doppler histogram was used to determine vascular indices from computer algorithms. The vascular indices analyzed were: vascularization indices (VI), which is related to the color voxel/ total voxel ratio, indicating how many vessels can be detected within the lung; flow indices (FI), which refers to the weighted

color voxel and gives an amplitude value for the color signal, showing how many blood cells are in area of interest (pulmonary blood flow) and vascularization-flow index (VFI), which is related to the weighted color voxel / total voxel ratio, combining the information of vascularity and blood flow.

Each fetus was longitudinally evaluated every two to four weeks and the vascular indices were plotted against gestational age. In the CDH group treated with FETO, measurements were performed before and after the procedure. All measurements were performed by R.R.

Gestational age was established based on the date of the last period and on sonographic measurement of the crown-rump length in the first trimester. The LHR was calculated by measuring the ratio between the longest diameters of the contralateral lung and head circumference at the level of four chambers heart view as described by Metkus [10].

FETO was performed between 24 and 30 weeks using a previously described technique[26]. Briefly, fetal intervention was performed under maternal local anesthesia and fetal systemic anesthesia, using a curved operating sheath with a diameter of 1.3 mm and a 1.0 mm scope. Direct visualization of the fetal trachea was achieved in all cases prior to occlusion by a detachable balloon filled with saline (GOLDBAL 2 or 4; Balt, Montmorency, France). Prophylactic tocolysis and antibiotics were used during the procedure and for 24 hours after fetal intervention. Unplug was planned at around 34 weeks by either fetoscopic approach or ultrasound-guided puncture.

All neonates were managed according to a standard perinatal protocol [27]. All neonates underwent immediate endotracheal intubation with orogastric decompression and avoidance of bag-mask ventilation by a staff neonatologist. Gentle mechanical ventilation using a permissive hypercapnia protocol was used. Escalation of ventilatory support to a maximal peak inspiratory pressure and positive end expiratory pressure of 30 and 6 cm of H20 respectively, and use of high-frequency oscillatory ventilation to a maximum mean airway pressure of 15 were based on pre-established criteria. Need of ECMO was determined by the presence of persistent hypoxia (preductal SaO2<80%), persistent acidosis (pH<7.2), and/or inadequate tissue perfusion. The time of surgery repair was managed according to the infant physiologic stability.

Variables

Fetal pulmonary vasculature was assessed in the right lung using vascular indices (VI, FI, and VFI), which were expressed as continuous variables. The neonatal outcome studied was the 6-month survival.

Data collected included basic demographics and prognosis factors of survival in CDH.

Statistical analysis

Results were reported as mean ± standard deviation for continuous variables and as number and percentage for categorical variables. Vascular indices were plotted against gestational age by regression analysis. P value < 0.05 was considered statistically significant.

RESULTS

A total of 33 patients were included in the study. There were 23 cases of CDH (10 treated with FETO and 13 with expectative management) and 10 controls. The number of evaluations for each patient ranged from 1 to 9, and the median was 4.

Median values of VI, FI and VFI were respectively 37.4; 40.2; 15.1 in controls, 29.5; 29.4; 9.3 in CDH with normal prenatal management and 30.6; 36.3; 10.7 in CDH with FETO.

Fetal pulmonary indices showed a constant distribution throughout pregnancy in controls and CDH with conservative management (Figure 1, 2 and 3).

VFI and FI were significantly lower in cases of CDH with no fetal intervention than in controls (p= .018 and p= .0006 respectively) (Figure 1 and 2). VI indices were lower in cases of CDH with conservative management than in controls, but this result was not statistically significant (p= .06) (Figure 3).

FETO resulted in a significant improvement in VFI (Figure 1) and VI (Figure 3) when compared with controls (p=0.0003 and p<0.0001 respectively). The procedure improved slightly FI indices (Figure 2), however this result was not significant (p=0.26).

Figure 1: VFI indices throughout pregnancy in controls, untreated CDH fetuses, and CDH fetuses treated with FETO.

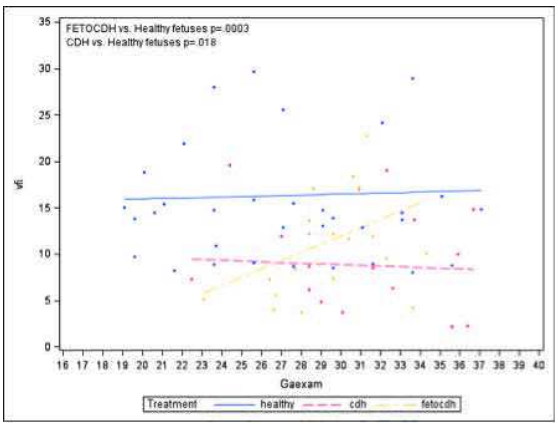

Figure 2: FI indices throughout pregnancy in controls, untreated CDH fetuses, and CDH fetuses treated with FETO.

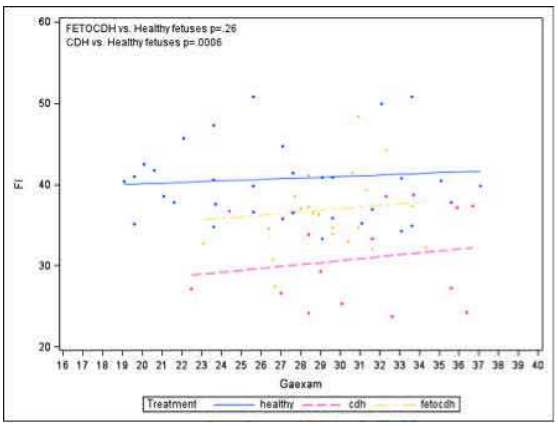

Figure 3: VI indices throughout pregnancy in controls, untreated CDH fetuses, and CDH fetuses treated with FETO.

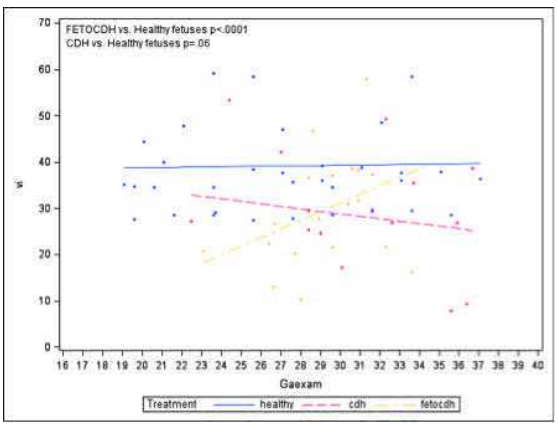

Among 23 cases of CDH, survival rate was 60 % for FETO cases (6 /10 fetuses) and 76.9% for expectant management cases (10/13 fetuses). Maternal and fetal demographics are described in table 1.

Table 1. Baseline characteristics and prognostic factors according to survival, in 23 fetuses with isolated CDH treated by either FETO or expectant management

	FETO			Conservative management		
	Alive (N=6)	**Dead (N=4)**	***Total cases***	**Alive (N=10)**	**Dead (N=3)**	***Total cases***
Maternal age in years (mean ± SD)	30.7±5.6	30.2± 1.9		31.3±6.6	30.6±6.1	
GA at birth in weeks (mean ± SD)	35.0±1.4	37.1±2.1				
LHR <1.0	0.86±0.1	0.78±0.1	*10*	0.77±0.1	0.60±0.1	*2*
LHR 1.0-1.4			*0*	1.20±0.1	1.22±0.1	4
LHR>1.4			*0*	2.05±0.2		*7*

Among FETO cases, the vascular indices VFI and VI increase significantly in cases that survived compared to fetuses who died (p=0.01 and p=0.0005 respectively) (Figure 4 and 5). The same pattern was observed for FI, but the result was not significant (p=0.06).

Figure 4: FVI indices throughout pregnancy

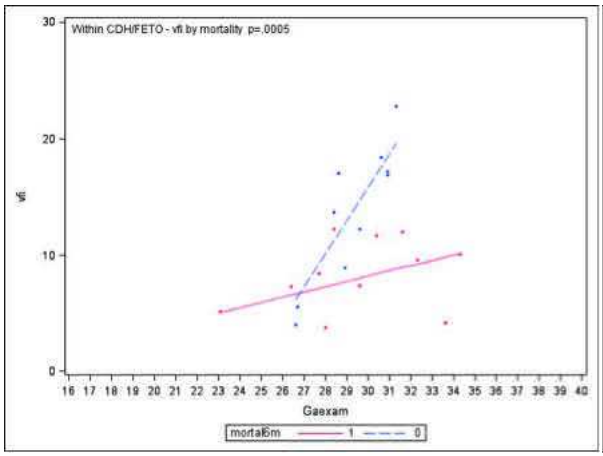

Figure 5: VI indices throughout pregnancy

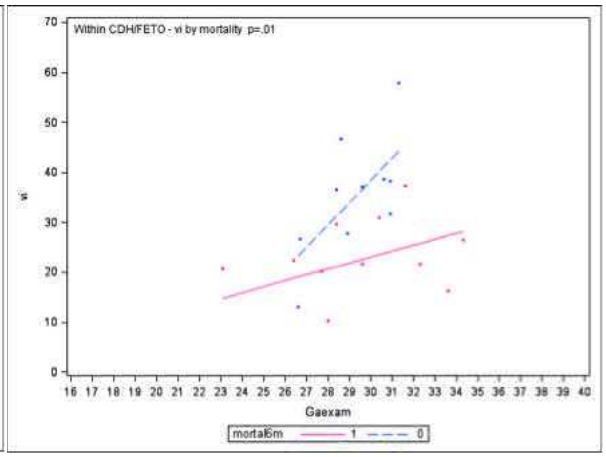

DISCUSSION

Perfusion of the fetal lung can be an important predictor of lung function and neonatal outcome [28]. Many authors already proposed different techniques to study fetal pulmonary vasculature such as pulmonary artery diameter, acceleration time/ejection time ratio of pulmonary arteries, intrapulmonary arterial Doppler velocimetry [29-35]. These studies showed that Doppler of pulmonary artery is a useful tool to predict pulmonary hypoplasia and may help to refine the prediction of survival after FETO in severe CDH [34, 35].

Power Doppler is an interesting technique for analyzing low-velocity blood flows. Power Doppler images have been used by calculating the mean pixel intensity of the signal over the region of interest [28]. 3D power Doppler has the advantage of assessing the volume and quantifying the power Doppler signal in the region of interest [20]. Some limitations related to this technique include difficulty of adjusting gain, depth and attenuation in overlying layers that could interfere with the estimation of lung perfusion [28]. For this reason, pre-settings were determined in our study and each patient was evaluated longitudinally, considering the first evaluation as its own control. The objective of the study was not to define reference values for indices of vascularity, but to analyze the variation of these indices in each case and the response after fetal intervention.

Fractional moving blood volume estimation in the fetal lung using power Doppler is a relevant tool to evaluate blood perfusion. However, this technique also requires experienced operators, using a well-defined region of interest and standard settings to be considered as a reproducible method to quantify fetal lung blood perfusion [36]. Using this method, a study showed that fetuses with CDH have decreased lung tissue perfusion, which is associated with decreased lung growth [37].

Our first observation in this study was the confirmation that fetal pulmonary vascular indices present a constant distribution throughout gestation as already described in the literature [20]. In cases of CDH with conservative management, pulmonary blood flow was significantly lower than controls and remained constant during pregnancy.

Among all cases of CDH, our findings demonstrated that pulmonary vascularization and pulmonary blood flow were significantly lower in cases who died. Pulmonary flow is also reduced but not significantly. A previous study showed that pulmonary vascularization index could be considered as a good predictor of neonatal outcome in CDH cases not treated with fetal intervention [15].

FETO can stimulate lung growth in fetuses with CDH [38] and improve neonatal survival in severe cases [39], leading to changes in pulmonary vascularity and lung size [2]. However, the impact on lung growth occurs differently in each case. A study showed that pulmonary response can be used to predict neonatal outcome in fetuses that undergo fetal intervention[2]. Our study confirms that FETO resulted in a significant improvement of pulmonary vascularization and pulmonary blood flow, by increasing VI and VFI. Moreover, our findings showed that pulmonary response measured by these vascular indices after tracheal occlusion can also be used to predict postnatal outcome.

One of the limitations of our study is the limited number of cases and further longitudinal studies are necessary to evaluate the response of pulmonary indices after fetal intervention.

In conclusion, 3D power Doppler can be used to evaluate fetal pulmonary status. Minimal changes occur in lung vascular indices through pregnancy. Vascular indices are altered in CDH in comparison to controls. FETO may restore vascular indices and this response after the procedure can predict neonatal survival.

REFERENCES

1. R. Keijzer and P. Puri. Congenital diaphragmatic hernia. Seminars in pediatric surgery 2010; 19: 180-185. DOI 10.1053/j.sempedsurg.2010.03.001.
2. R. Ruano, M. M. da Silva, J. A. Campos, R. Papanna, K. Moise, Jr., U. Tannuri and M. Zugaib. Fetal pulmonary response after fetoscopic tracheal occlusion for severe isolated congenital diaphragmatic hernia. Obstet Gynecol 2012; 119: 93-101. DOI 10.1097/AOG.0b013e31823d3aea.
3. C. F. Peralta, J. C. Jani, D. Van Schoubroeck, K. H. Nicolaides and J. A. Deprest. Fetal lung volume after endoscopic tracheal occlusion in the prediction of postnatal outcome. Am J Obstet Gynecol 2008; 198: 60 e61-65. DOI 10.1016/j.ajog.2007.05.034.
4. J. C. Jani, K. H. Nicolaides, E. Gratacos, C. M. Valencia, E. Done, J. M. Martinez, L. Gucciardo, R. Cruz and J. A. Deprest. Severe diaphragmatic hernia treated by fetal endoscopic tracheal occlusion. Ultrasound Obstet Gynecol 2009; 34: 304-310. DOI 10.1002/uog.6450.
5. M. S. Arkovitz, M. Russo, P. Devine, N. Budhorick and C. J. Stolar. Fetal lung-head ratio is not related to outcome for antenatal diagnosed congenital diaphragmatic hernia. Journal of pediatric surgery 2007; 42: 107-110; discussion 110-101. DOI 10.1016/j.jpedsurg.2006.09.010.
6. J. Jani, K. H. Nicolaides, R. L. Keller, A. Benachi, C. F. Peralta, R. Favre, O. Moreno, D. Tibboel, S. Lipitz, A. Eggink, P. Vaast, K. Allegaert, M. Harrison, J. Deprest and C. D. H. R. G. Antenatal. Observed to expected lung area to head circumference ratio in the prediction of survival in fetuses with isolated diaphragmatic hernia. Ultrasound in obstetrics & gynecology : the official journal of the International Society of Ultrasound in Obstetrics and Gynecology 2007; 30: 67-71. DOI 10.1002/uog.4052.
7. J. Jani, C. F. Peralta, A. Benachi, J. Deprest and K. H. Nicolaides. Assessment of lung area in fetuses with congenital diaphragmatic hernia. Ultrasound in obstetrics & gynecology : the official journal of the International Society of Ultrasound in Obstetrics and Gynecology 2007; 30: 72-76. DOI 10.1002/uog.4051.
8. J. A. Laudy, M. Van Gucht, M. F. Van Dooren, J. W. Wladimiroff and D. Tibboel. Congenital diaphragmatic hernia: an evaluation of the prognostic value of the lung-to-head ratio and other prenatal parameters. Prenat Diagn 2003; 23: 634-639. DOI 10.1002/pd.654.
9. G. S. Lipshutz, C. T. Albanese, V. A. Feldstein, R. W. Jennings, H. T. Housley, R. Beech, J. A. Farrell and M. R. Harrison. Prospective analysis of lung-to-head ratio predicts survival for patients with prenatally diagnosed congenital diaphragmatic hernia. J Pediatr Surg 1997; 32: 1634-1636.
10. A. P. Metkus, R. A. Filly, M. D. Stringer, M. R. Harrison and N. S. Adzick. Sonographic predictors of survival in fetal diaphragmatic hernia. Journal of pediatric surgery 1996; 31: 148-151; discussion 151-142.
11. C. F. Peralta, P. Cavoretto, B. Csapo, H. Vandecruys and K. H. Nicolaides. Assessment of lung area in normal fetuses at 12-32 weeks. Ultrasound Obstet Gynecol 2005; 26: 718-724. DOI 10.1002/uog.2651.
12. R. A. Quintero, L. F. Quintero, R. Chmait, L. Gomez Castro, L. M. Korst, M. Fridman and E. V. Kontopoulos. The quantitative lung index (QLI): a gestational age-independent sonographic predictor of fetal lung growth. American journal of obstetrics and gynecology 2011; 205: 544 e541-548. DOI 10.1016/j.ajog.2011.07.031.
13. K. Tsukimori, K. Masumoto, S. Morokuma, T. Yoshimura, T. Taguchi, T. Hara, Y. Sakaguchi, S. Takahashi, N. Wake and S. Suita. The lung-to-thorax transverse area ratio at term and near term correlates with survival in isolated congenital diaphragmatic hernia. Journal of ultrasound in medicine : official journal of the American Institute of Ultrasound in Medicine 2008; 27: 707-713.
14. R. Ruano, M. C. Aubry, B. Barthe, Y. Dumez and A. Benachi. Three-dimensional ultrasonographic measurements of the fetal lungs for prediction of perinatal outcome in isolated congenital diaphragmatic hernia. J Obstet Gynaecol Res 2009; 35: 1031-1041. DOI 10.1111/j.1447-0756.2009.001060.x.
15. R. Ruano, E. Takashi, M. M. da Silva, J. A. Campos, U. Tannuri and M. Zugaib. Prediction and probability of neonatal outcome in isolated congenital diaphragmatic hernia using multiple ultrasound parameters. Ultrasound Obstet Gynecol 2012; 39: 42-49. DOI 10.1002/uog.10095.
16. O. Moreno-Alvarez, R. Cruz-Martinez, E. Hernandez-Andrade, E. Done, O. Gomez, J. Deprest and E. Gratacos. Lung tissue perfusion in congenital diaphragmatic hernia and association with the lung-to-head ratio and intrapulmonary artery pulsed Doppler. Ultrasound Obstet Gynecol 2010; 35: 578-582. DOI 10.1002/uog.7592.
17. A. P. Bos, D. Tibboel, V. C. Koot, F. W. Hazebroek and J. C. Molenaar. Persistent pulmonary hypertension in high-risk congenital diaphragmatic hernia patients: incidence and vasodilator therapy. Journal of pediatric surgery 1993; 28: 1463-1465.
18. K. K. Nobuhara and J. M. Wilson. The effect of mechanical forces on in utero lung growth in congenital diaphragmatic hernia. Clinics in perinatology 1996; 23: 741-752.
19. X. Roubliova, E. Verbeken, J. Wu, H. Yamamoto, T. Lerut, D. Tibboel and J. Deprest. Pulmonary vascular morphology in a fetal rabbit model for congenital diaphragmatic hernia. Journal of pediatric surgery 2004; 39: 1066-1072.
20. R. Ruano, M. C. Aubry, B. Barthe, D. Mitanchez, Y. Dumez and A. Benachi. Quantitative analysis of fetal pulmonary vasculature by 3-dimensional power Doppler ultrasonography in isolated congenital diaphragmatic hernia. Am J Obstet Gynecol 2006; 195: 1720-1728. DOI 10.1016/j.ajog.2006.05.010.

21. P. A. Khan, M. Cloutier and B. Piedboeuf. Tracheal occlusion: a review of obstructing fetal lungs to make them grow and mature. American journal of medical genetics Part C, Seminars in medical genetics 2007; 145C: 125-138. DOI 10.1002/ajmg.c.30127.
22. A. E. Heerema, J. T. Rabban, R. M. Sydorak, M. R. Harrison and K. D. Jones. Lung pathology in patients with congenital diaphragmatic hernia treated with fetal surgical intervention, including tracheal occlusion. Pediatr Dev Pathol 2003; 6: 536-546.
23. E. Danzer, M. G. Davey, P. A. Kreiger, E. D. Ruchelli, M. P. Johnson, N. S. Adzick, A. W. Flake and H. L. Hedrick. Fetal tracheal occlusion for severe congenital diaphragmatic hernia in humans: a morphometric study of lung parenchyma and muscularization of pulmonary arterioles. J Pediatr Surg 2008; 43: 1767-1775. DOI 10.1016/j.jpedsurg.2008.04.033.
24. R. Ruano, M. M. da Silva, J. A. Campos, R. Papanna, K. Moise, Jr., U. Tannuri and M. Zugaib. Fetal pulmonary response after fetoscopic tracheal occlusion for severe isolated congenital diaphragmatic hernia. Obstet Gynecol 2012; 119: 93-101. DOI 10.1097/AOG.0b013e31823d3aea.
25. R. Cruz-Martinez, O. Moreno-Alvarez, E. Hernandez-Andrade, M. Castanon, E. Done, J. M. Martinez, B. Puerto, J. Deprest and E. Gratacos. Contribution of intrapulmonary artery Doppler to improve prediction of survival in fetuses with congenital diaphragmatic hernia treated with fetal endoscopic tracheal occlusion. Ultrasound Obstet Gynecol 2010; 35: 572-577. DOI 10.1002/uog.7593.
26. R. Ruano, C. T. Yoshisaki, M. M. da Silva, M. E. Ceccon, M. S. Grasi, U. Tannuri and M. Zugaib. A randomized controlled trial of fetal endoscopic tracheal occlusion versus postnatal management of severe isolated congenital diaphragmatic hernia. Ultrasound Obstet Gynecol 2012; 39: 20-27. DOI 10.1002/uog.10142.
27. D. A. Lazar, D. L. Cass, M. A. Rodriguez, S. F. Hassan, C. I. Cassady, Y. R. Johnson, K. E. Johnson, A. Johnson, K. J. Moise, B. Belleza-Bascon and O. O. Olutoye. Impact of prenatal evaluation and protocol-based perinatal management on congenital diaphragmatic hernia outcomes. J Pediatr Surg 2011; 46: 808-813. DOI 10.1016/j.jpedsurg.2011.02.009.
28. T. Jansson, E. Hernandez-Andrade, G. Lingman and K. Marsal. Estimation of fractional moving blood volume in fetal lung using Power Doppler ultrasound, methodological aspects. Ultrasound in medicine & biology 2003; 29: 1551-1559.
29. R. Ruano, M. de Fatima Yukie Maeda, J. I. Niigaki and M. Zugaib. Pulmonary artery diameters in healthy fetuses from 19 to 40 weeks' gestation. Journal of ultrasound in medicine : official journal of the American Institute of Ultrasound in Medicine 2007; 26: 309-316.
30. S. Fuke, T. Kanzaki, J. Mu, K. Wasada, M. Takemura, N. Mitsuda and Y. Murata. Antenatal prediction of pulmonary hypoplasia by acceleration time/ejection time ratio of fetal pulmonary arteries by Doppler blood flow velocimetry. American journal of obstetrics and gynecology 2003; 188: 228-233.
31. R. Chaoui, K. Kalache, C. Tennstedt, F. Lenz and M. Vogel. Pulmonary arterial Doppler velocimetry in fetuses with lung hypoplasia. European journal of obstetrics, gynecology, and reproductive biology 1999; 84: 179-185.
32. R. Cruz-Martinez, M. Castanon, O. Moreno-Alvarez, R. Acosta-Rojas, J. M. Martinez and E. Gratacos. Usefulness of lung-to-head ratio and intrapulmonary arterial Doppler in predicting neonatal morbidity in fetuses with congenital diaphragmatic hernia treated with fetoscopic tracheal occlusion. Ultrasound in obstetrics & gynecology : the official journal of the International Society of Ultrasound in Obstetrics and Gynecology 2013; 41: 59-65. DOI 10.1002/uog.11212.
33. R. Cruz-Martinez, E. Hernandez-Andrade, O. Moreno-Alvarez, E. Done, J. Deprest and E. Gratacos. Prognostic value of pulmonary Doppler to predict response to tracheal occlusion in fetuses with congenital diaphragmatic hernia. Fetal diagnosis and therapy 2011; 29: 18-24. DOI 10.1159/000320249.
34. R. Cruz-Martinez, O. Moreno-Alvarez, E. Hernandez-Andrade, M. Castanon, E. Done, J. M. Martinez, B. Puerto, J. Deprest and E. Gratacos. Contribution of intrapulmonary artery Doppler to improve prediction of survival in fetuses with congenital diaphragmatic hernia treated with fetal endoscopic tracheal occlusion. Ultrasound in obstetrics & gynecology : the official journal of the International Society of Ultrasound in Obstetrics and Gynecology 2010; 35: 572-577. DOI 10.1002/uog.7593.
35. S. Yoshimura, H. Masuzaki, K. Miura, K. Muta, H. Gotoh and T. Ishimaru. Diagnosis of fetal pulmonary hypoplasia by measurement of blood flow velocity waveforms of pulmonary arteries with Doppler ultrasonography. American journal of obstetrics and gynecology 1999; 180: 441-446.
36. E. Hernandez-Andrade, A. Thuring-Jonsson, T. Jansson, G. Lingman and K. Marsal. Fractional moving blood volume estimation in the fetal lung using power Doppler ultrasound: a reproducibility study. Ultrasound in obstetrics & gynecology : the official journal of the International Society of Ultrasound in Obstetrics and Gynecology 2004; 23: 369-373. DOI 10.1002/uog.1003.
37. O. Moreno-Alvarez, R. Cruz-Martinez, E. Hernandez-Andrade, E. Done, O. Gomez, J. Deprest and E. Gratacos. Lung tissue perfusion in congenital diaphragmatic hernia and association with the lung-to-head ratio and intrapulmonary artery pulsed Doppler. Ultrasound in obstetrics & gynecology : the official journal of the International Society of Ultrasound in Obstetrics and Gynecology 2010; 35: 578-582. DOI 10.1002/uog.7592.
38. J. C. Jani, K. H. Nicolaides, E. Gratacos, H. Vandecruys, J. A. Deprest and F. T. Group. Fetal lung-to-head ratio in the prediction of survival in severe left-sided diaphragmatic hernia treated by fetal endoscopic tracheal occlusion (FETO). Am J Obstet Gynecol 2006; 195: 1646-1650. DOI 10.1016/j.ajog.2006.04.004.
39. R. Ruano, C. T. Yoshisaki, M. M. da Silva, M. E. Ceccon, M. S. Grasi, U. Tannuri and M. Zugaib. A randomized controlled trial of fetal endoscopic tracheal occlusion versus postnatal management of severe isolated congenital diaphragmatic hernia. Ultrasound Obstet Gynecol 2012; 39: 20-27. DOI 10.1002/uog.10142.

6. PROPERTIES REQUIRED FOR THE POSTNATAL PROSTHESES

Computed Tomographic Study of the Pediatric Diaphragmatic Growth: Application to the Treatment of Congenital Diaphragmatic Hernia.

Schneider A, Koob M, Sananes N, Senger B, Hemmerlé J, Becmeur F.

Eur J Pediatr Surg. 2016 Apr 11.

Computed Tomographic Study of the Pediatric Diaphragmatic Growth: Application to the Treatment of Congenital Diaphragmatic Hernia

Anne Schneider[1,2] Meriam Koob[3] Nicolas Sananes[2,4] Bernard Senger[2] Joseph Hemmerlé[2] Francois Becmeur[1]

[1] Department of Pediatric Surgery, Hôpitaux Universitaires de Strasbourg, Strasbourg, Alsace, France
[2] INSERM UMR 1121 Biomatériaux et Bioingénierie Tissulaire, Universite de Strasbourg, Strasbourg, Alsace, France
[3] Department of Pediatric Radiology, Hôpitaux Universitaires de Strasbourg, Strasbourg, Alsace, France
[4] Department of Fetal Medicine, Hôpitaux Universitaires de Strasbourg, Strasbourg, Alsace, France

Address for correspondence Anne Schneider, MD, Department of Pediatric Surgery, Hôpitaux Universitaires de Strasbourg, Strasbourg, Alsace, France (e-mail: schneider.an@orange.fr).

Eur J Pediatr Surg

Abstract

Background The prosthesis commonly used for the treatment of congenital diaphragmatic hernia (CDH) lacks elasticity to replace the diaphragm's mechanical properties and does not follow the natural growth of the child treated.

Objective To determine the appropriate properties required for the prostheses, a CT study on healthy patients was conducted.

Methods Two methods of diaphragmatic surface analysis are assessed: the diaphragmatic surface is either estimated using surface 2D estimations (method 1), or calculated using length measures on thoracoabdominal CT scans from children (method 2). Patients are divided into two groups depending on their age: group 1: $n = 9$; median age: 2.0 months (0.1–9.5); group 2: $n = 9$; median age: 182.6 months (158.5–235.5). Growth factor between the two groups is calculated and the two methods are statistically compared.

Results The ratio group 2/group 1 of the diaphragmatic surfaces was 4.3 ± 0.2 on the left side and 4.0 ± 0.2 on the right side for method 1, and 5.1 ± 0.2 on the left side and 5.1 ± 0.3 on the right side for method 2. The difference in the median values between both methods is statistically significant for both the left and right sides ($p = 0.022$ and $p = 0.002$, respectively). Hence, the two methods cannot be used exchangeably.

Conclusion The treatment of CDH with large defect remains a challenge because of the high incidence of hernia recurrence probably due to prosthesis defect; thus it is important to estimate the diaphragmatic surface precisely. We aim to develop a prosthesis material that can be commonly used and found a mean diaphragmatic growth factor of approximately 4 to 5 from early childhood to adolescence.

Keywords
- congenital diaphragmatic hernia
- diaphragmatic growth
- pediatrics

received
January 5, 2016
accepted after revision
February 26, 2016

DOI http://dx.doi.org/10.1055/s-0036-1582242.
ISSN 0939-7248.

Introduction

Congenital diaphragmatic hernia (CDH) is a rare congenital disease, which requires neonatal surgical treatment. The diaphragmatic replacement is justified when more than half of the diaphragmatic dome is absent.[1,2] The most frequently used prosthesis is composed of "expanded polytetrafluoroethylene" (ePTFE, Gore-Tex [W.L. Gore and Associates, Flagstaff, Arizona, United States]),[3] which lacks elasticity to replace the diaphragm's mechanical properties. Indeed, the prosthesis will be inserted at birth in a growing child and will lead to major traction on the anchoring stitches. Those can result in thoracic deformations, scoliosis,[4] or hernia recurrence through prosthesis leakage (28–50%).[1,5–8]

To design a prosthesis with better accuracy in shape and size to the anatomical features of the neonatal diaphragm, we aimed to determine the normal diaphragmatic growth from early childhood to adolescence, to define the required mechanical properties of prosthesis. To our best knowledge, there are no data published in the English literature regarding the diaphragmatic growth.[9]

Material and Methods

This retrospective monocentric study included patients with a median age of 2.0 months (0.1–9.5) (group 1, $n = 9$) and with a median age of 182.6 months (158.5–235.5) (group 2, $n = 9$). Those patients had previously undergone a thoracoabdominal computed tomographic (CT) scan for other reasons (traumatology, oncology follow-up, etc.) and did not have any diaphragmatic pathology or severe cardiac and/or pulmonary anomalies.

Two methods of evaluation of the surface of the diaphragm were followed and the results compared. The first method (method 1) consisted of a 2D surface estimation of each diaphragmatic dome using a cross-sectional imaging (►Fig. 1a, 1b). The second method (method 2) considered the diaphragmatic dome as a part of an ellipsoid on a sagittal plane (►Fig. 2) and consisted of a surface calculation using the formula $A = \pi b^2 + \pi ab \arcsin(e)/e$ where a is the half major axis of the ellipsoid, b is the half minor axis of the ellipsoid, and e the eccentricity defined by $\sqrt{a^2 - b^2}/a$.

Following the two methods, we obtained the surface area for each nine realizations of the left-part and nine realizations of the right-part diaphragmatic surface for both children and adolescents. Thereby we harvested eight samples of nine measurements each.

Statistical data analysis was performed using the Mann-Whitney rank sum test from the software SigmaPlot 11.0 (Systat Software Inc., San Jose, California, United States).

Informed consent was obtained to perform this study from the patients and the study was authorized by the local ethical board.

Results

Combining the samples corresponding to the same method and the same side of the diaphragm, we computed $9 \times 9 = 81$ surface ratios that give the relative surface growth from childhood to adolescence. The four distributions obtained this way are shown in ►Fig. 3a, 3b. In each panel, we compared method 1 with method 2. It is readily seen that method 2 (gray bars) leads to a distribution shifted toward the larger ratios if compared with the histogram derived from method 1 (black bars). More precisely, the ratio group 2/group 1 is for method 1 4.3 ± 0.3 on the left side and 4.0 ± 0.3 on the right side, and for method 2 5.1 ± 0.5 on the left side and 5.1 ± 0.5 on the right side (mean ± sem; see ►Table 1).

To compare the ratios from method 1 with those from method 2, we tried to perform the usual *t*-test. However, because the distributions are non-normal (see ►Figs. 3a, 3b), this test could not be applied. Instead, we performed the Mann-Whitney rank sum test. This test showed that the difference in the median values between the two methods (1L vs. 2L; 1R vs. 2R) is statistically significant for both the left and the right sides ($p = 0.022 < 0.05$ and $p = 0.002 < 0.05$, respectively). Thus,

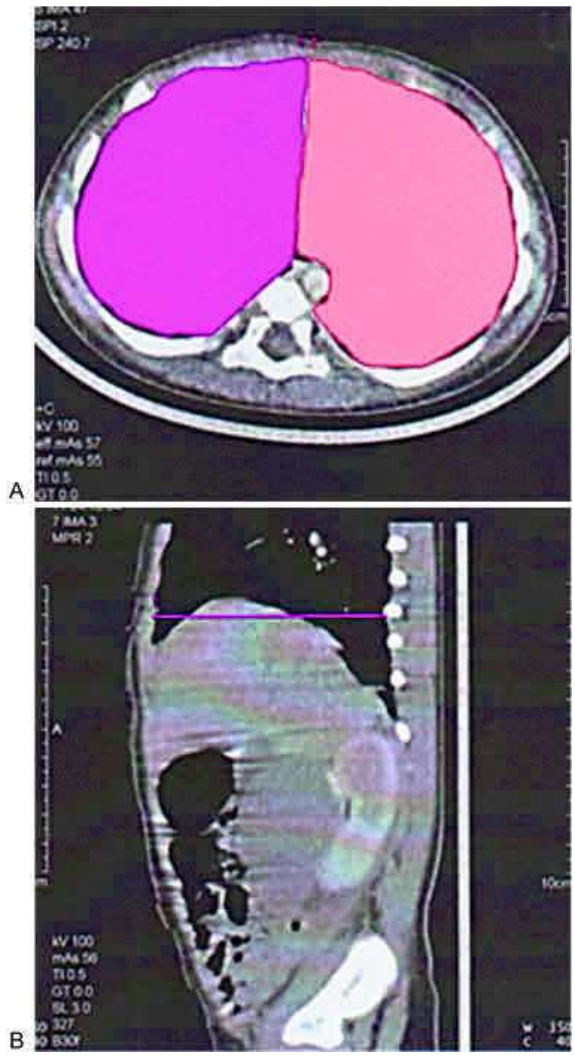

Fig. 1 (a, 1b) Method 1: 2D diaphragmatic surface estimation using a CT cross-sectional imaging; (1a) transverse section at the level of the diaphragmatic area; (1b) sagittal view.

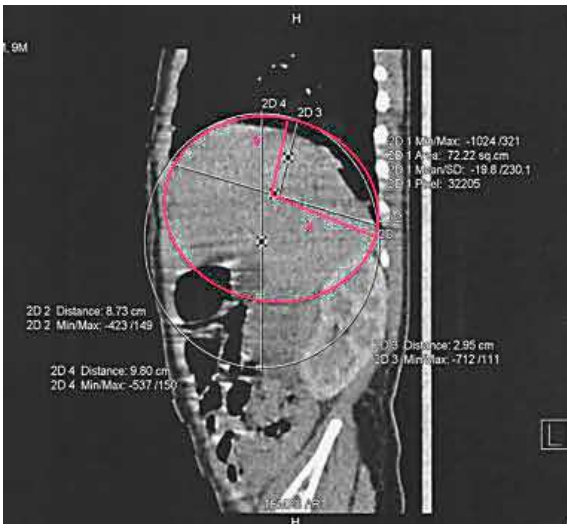

Fig. 2 Method 2: Diaphragmatic surface calculation. Sagittal view of the ellipsoid following the diaphragmatic dome on a CT scan with a = half major axis of the ellipsoid and b = half minor axis of the ellipsoid.

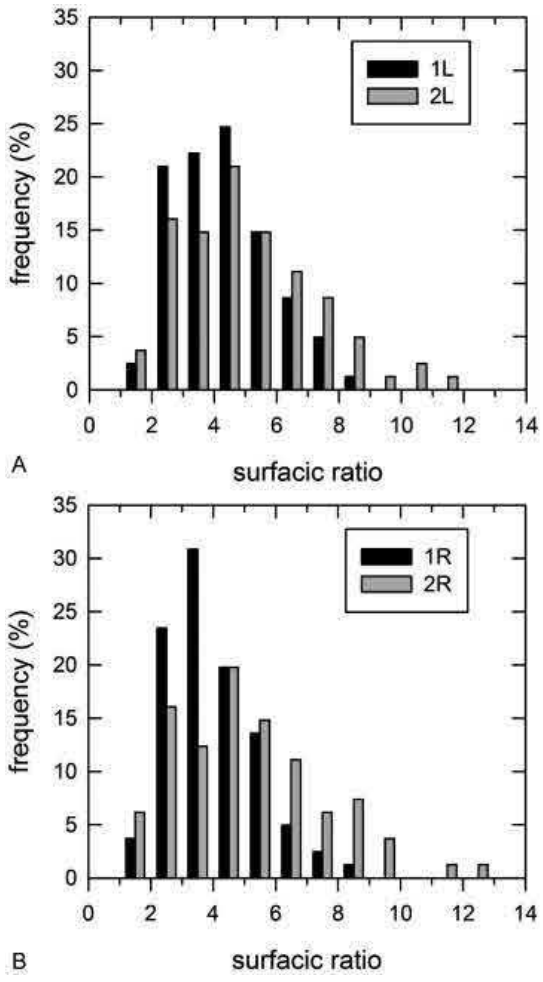

Fig. 3 Distribution of the group 2/group 1 ratio for left (3a) and right (3b) diaphragmatic domes. 1L, method 1 left side; 2L, method 2 left side; 1R, method 1 right side; 2R, method 2 right side.

Table 1 Characteristics of the distributions of the group 2/group 1 ratios

	Mean ± sem	Median	1st–3rd quartiles
1L	4.3 ± 0.2	4.1	3.0–5.3
2L	5.1 ± 0.2	4.7	3.5–6.4
1R	4.0 ± 0.2	3.9	2.9–4.7
2R	5.1 ± 0.3	4.8	3.3–6.4

Abbreviations: 1L, method 1 left side; 2L, method 2 left side; 1R, method 1 right side; 2R, method 2 right side; sem, standard error on the mean.

the two methods are assumed to be not equivalent when the risk of first kind is fixed to 0.05.

Discussion

Human diaphragmatic development has not been extensively studied. Precise determination of diaphragm geometry is difficult as the shapes are complex and the structure of the diaphragm is both anisotropic and variable from one part to another.[9] To our knowledge, there are no published data or anatomical studies regarding normal diaphragmatic growth. The only published work mentioned that the diaphragmatic growth is proportional to the child's growth. In 2001 Rehan et al conducted an ultrasound study on 15 newborns and concluded that the diaphragmatic thickness is significantly associated with weight, height, and head circumference, but not to gestational age.[9] One study, based on posteroanterior plain chest radiographic measures, revealed a significant association between age and diaphragmatic diameter in 89 children aged 9.0 ± 5.5 years.[10]

Our study aimed to define the normal diaphragmatic growth ratio from early childhood to adolescence. As the failure of the diaphragmatic prosthesis currently used for the treatment of CDH is due to its lack of elasticity required to replace the fluid movements of the diaphragm and the natural growth,[11] the present findings are of utmost interest to establish the specifications of an ideal prosthesis.

The present study reveals diaphragmatic surface growth factors ranging from 4.0 to 5.1 from early childhood to adolescence. Nevertheless, to be more accurate, our results should be related to weight, height, and sex at the time when the CT scan is performed, particularly for the group of adolescents. This information is often unavailable. Two methods of surface estimation were assessed: with method 1, it was easier to obtain the surface area thanks to the specific CT software, whereas method 2 required manual measures and time-consuming mathematical calculations. However, despite the practical problems it poses, in our opinion method 2 suits better to evaluate the diaphragmatic surface because it follows the anatomical landmarks. Statistical difference between methods 1 and 2 was more significant for the right side ($p = 0.002$), probably due to the presence of the leaver. Indeed, the right dome is placed higher than the left dome with a better evaluation using the 3D surface calculation than the 2D cross-sectional imaging.

Our study presents several problems. This is a biased sampling because our patients are a group having CT scans and are not randomly chosen and nor completely healthy. We could not include patients as their own controls, which could be a method more valid to follow changes in the diaphragm in single patients. However, patients who have had CT studies separated by several years are unfortunately rare. Both methods to estimate the diaphragmatic size are arbitrary, because this organ has a complex 3D structure. It is also problematic to estimate how a diaphragm grows sagittally, axially, coronally, and also how the muscular part grows in relation to the central tendon area as this part represents a sizeable and important portion of the normal diaphragm. The importance of this tendon area has been suggested in diaphragmatic tissue engineering methods.[12] However, the complex structure of the diaphragm is not accessible to actual imaging investigations with the current technologies.

Although the present methodology cannot be directly implemented in daily clinical practice for CDH patients, it provides original data of utmost importance for the design of appropriate biomaterials. First, we clearly demonstrate that the way of calculating area of the diaphragm can be improved, and we suggest a different calculation method to do so. Following this preliminary study, we aim to include in the future more patients using a diaphragmatic surface 3D modeling that provides more accurate measurements of the surface. Second, this paper discloses for the first time the precise growing factor of the diaphragm in relation to age.

Nevertheless, on behalf of these two points, we can say that our findings can obviously be implemented in the development of biomaterials that properly fit to the CDH defect, and thus are highly beneficial, although indirectly, in daily clinical practice for CDH patients.

References

1 Moss RL, Chen CM, Harrison MR. Prosthetic patch durability in congenital diaphragmatic hernia: a long-term follow-up study. J Pediatr Surg 2001;36(1):152–154
2 Turner CG, Klein JD, Steigman SA, et al. Preclinical regulatory validation of an engineered diaphragmatic tendon made with amniotic mesenchymal stem cells. J Pediatr Surg 2011;46(1): 57–61
3 Clark RH, Hardin WD Jr, Hirschl RB, et al. Current surgical management of congenital diaphragmatic hernia: a report from the Congenital Diaphragmatic Hernia Study Group. J Pediatr Surg 1998;33(7):1004–1009
4 Chiu P, Hedrick HL. Postnatal management and long-term outcome for survivors with congenital diaphragmatic hernia. Prenat Diagn 2008;28(7):592–603
5 Grethel EJ, Cortes RA, Wagner AJ, et al. Prosthetic patches for congenital diaphragmatic hernia repair: Surgisis vs Gore-Tex. J Pediatr Surg 2006;41(1):29–33, discussion 29–33
6 Jancelewicz T, Vu LT, Keller RL, et al. Long-term surgical outcomes in congenital diaphragmatic hernia: observations from a single institution. J Pediatr Surg 2010;45(1):155–160, discussion 160
7 Laituri CA, Garey CL, Valusek PA, et al. Outcome of congenital diaphragmatic hernia repair depending on patch type. Eur J Pediatr Surg 2010;20(6):363–365
8 Mitchell IC, Garcia NM, Barber R, Ahmad N, Hicks BA, Fischer AC. Permacol: a potential biologic patch alternative in congenital diaphragmatic hernia repair. J Pediatr Surg 2008;43(12):2161–2164
9 Rehan VK, Laiprasert J, Wallach M, Rubin LP, McCool FD, McCool FD. Diaphragm dimensions of the healthy preterm infant. Pediatrics 2001;108(5):E91
10 Kamata S, Usui N, Sawai T, Nose K, Kamiyama M, Fukuzawa M. Radiographic changes in the diaphragm after repair of congenital diaphragmatic hernia. J Pediatr Surg 2008;43(12):2156–2160
11 Gasior AC, St Peter SD. A review of patch options in the repair of congenital diaphragm defects. Pediatr Surg Int 2012;28(4): 327–333
12 Fauza DO. Tissue engineering in congenital diaphragmatic hernia. Semin Pediatr Surg 2014;23(3):135–140

7. PATENT, PAPERS AND COMMUNICATIONS

7.1. Patent

A patent application has been filed on May 2nd 2016 (request #1653954 / submission #1000345616): 'BALLONNET GONFLABLE ET DÉTACHABLE, DESTINÉ À ÊTRE IMPLANTÉ DANS UNE CAVITÉ CORPORELLE, NÉCESSAIRE DE TRAITEMENT ET PROCÉDÉ DE VIDANGE ASSOCIÉS'. We applied for an international extension of our patent on May 2017.

7.2. Papers

Sananès N, Ruano R, Weingertner AS, Regnard P, Salmon Y, Kohler A, Miry C, Mager C, Guerra F, Schneider A, Becmeur F, Leroy J, Dimarcq JL, Debry C, Favre R. Experimental fetal endoscopic tracheal occlusion in rhesus and cynomolgus monkeys: nonhuman primate models. J Matern Fetal Neonatal Med. 2015;28(15):1822-7.

Britto IS, Sananes N, Olutoye OO, Cass DL, Sangi-Haghpeykar H, Lee TC, Cassady CI, Mehollin-Ray A, Welty S, Fernandes C, Belfort MA, Lee W, Ruano R. Standardization of Sonographic Lung-to-Head Ratio Measurements in Isolated Congenital Diaphragmatic Hernia: Impact on the Reproducibility and Efficacy to Predict Outcomes. J Ultrasound Med. 2015 Oct;34(10):1721-7.

Ruano R, Britto IS, Sananes N, Lee W, Sangi-Haghpeykar H, Deter RL. Growth Patterns of Fetal Lung Volumes in Healthy Fetuses and Fetuses With Isolated Left-Sided Congenital Diaphragmatic Hernia. J Ultrasound Med. 2016 Jun;35(6):1159-66.

Sananes N, Rodo C, Peiro JL, Britto IS, Sangi-Haghpeykar H, Favre R, Joal A, Gaudineau A, Silva MM, Tannuri U, Zugaib M, Carreras E, Ruano R. Prematurity and fetal lung response after tracheal occlusion in fetuses with severe congenital diaphragmatic hernia. J Matern Fetal Neonatal Med. 2016 Sep;29(18):3030-4.

Sananes N, Britto I, Akinkuotu AC, Olutoye OO, Cass DL, Sangi-Haghpeykar H, Lee TC, Cassady CI, Mehollin-Ray A, Welty S, Fernandes C, Belfort MA, Lee W, Ruano R. Improving the Prediction of Neonatal Outcomes in Isolated Left-Sided Congenital Diaphragmatic Hernia by Direct and Indirect Sonographic Assessment of Liver Herniation. J Ultrasound Med. 2016 Jul;35(7):1437-43.

Britto IS, Sananes N, Sangi-Haghpeykar H, Ruano R. Longitudinal ultrasound assessment of lung vasculature in fetuses with congenital diaphragmatic hernia treated by endoscopic tracheal occlusion and controls. (to be submitted)

Schneider A, Koob M, Sananes N, Senger B, Hemmerlé J, Becmeur F. Computed Tomographic Study of the Pediatric Diaphragmatic Growth: Application to the Treatment of Congenital Diaphragmatic Hernia. Eur J Pediatr Surg. 2016 Apr 11.

7.3. Oral communications

Journée annuelle du Centre de Référence sur les hernies de coupole diaphragmatiques, 2017, Paris. Occlusion trachéale réversible par champ magnétique. N Sananès, R Favre, C Debry.

35th Annual Meeting of International Fetal Medicine and Surgery Society, 2016, Botswana. Ongoing development of a new balloon for Fetal Endoscopic Tracheal Occlusion. N Sananès, R Favre, C Debry.

15th World Congress in Fetal Medicine, 2016, Palma de Majorque. Ongoing development of a new balloon for Fetal Endoscopic Tracheal Occlusion. N Sananès, R Favre, C Debry.

Club Francophone de Médecine Fœtale, 2016, Strasbourg. Développement d'un ballonnet innovant pour l'occlusion trachéale par foetoscopie. N Sananès, R Favre, C Debry.

‘Meet and Match’ day: smart implants – new devices and innovative technologies, Strasbourg, 2016. Développement d’un ballonnet innovant pour l’occlusion trachéale par foetoscopie. N Sananès, R Favre, C Debry.

Club Francophone de Médecine Fœtale, 2014, Marrakech. Développement du modèle du singe dans l’occlusion trachéale par endoscopie fœtale. N Sananès, R Ruano, AS Weingertner, P Regnard, I Nisand, R Favre.

34th Annual Meeting of International Fetal Medicine and Surgery Society, 2015, Hersonissos. Fetal surgery for diaphragmatic hernia. Prediction of outcome by ultrasound. N Sananes, I Britto, A Akinkuotu, O Olutoye, D Cass, H Sangi-Hagheykar, T Lee, C Cassady, A Mehollin-Ray, S Welty, C Fernandes, M Belfort, W Lee, R Ruano.

Annual Convention of American Institute of Ultrasound in Medicine, 2015, Lake Buena Vista. Standardization of the Lung-To-Head Ratio in the prediction of prognosis in isolated congenital diaphragmatic hernia: a single center experience. I Britto, N Sananes, D Cass, C Cassady, A Mehollin-Ray, S Welty, J Mastrobattista, O Olutoye, W Lee, M Belfort, R Ruano.

World Federation for Ultrasound in Medicine and Biology, World Congress 2014, Sao Paulo. Standardization of the Lung-To-Head Ratio in the prediction of prognosis in isolated congenital diaphragmatic hernia: a single center experience. I Britto, N Sananes, D Cass, C Cassady, A Mehollin-Ray, S Welty, J Mastrobattista, O Olutoye, W Lee, M Belfort, R Ruano.

7.4. Posters

Britto Ingrid Swach Werneck; SANANES, N. ; OLUTOYE, O. ; SANGI-HAGHPEYKAR, H. ; CASSADY, C. ; MEHOLLIN-RAY, A. ; WELTY, S. ; LEE, W. ; RUANO, R. . Longitudinal ultrasound assessment of lung vasculature in fetuses with congenital diaphragmatic hernia treated by endoscopic tracheal occlusion and controls. In: 26th World Congress on Ultrasound in Obstetrics and Gynecology, 2016, Roma. J Ultra Obstet Gynecol, 2016. v. 48. p. 121.

Britto, Ingrid Schwach Werneck; SANANES, N. ; CASS, D. ; ZAMORRA, I. ; LEE, T. ; OLUTOYE, O. ; MEHOLLIN-RAY, A. ; WELTY, S. ; FERNANDES, C. ; BELFORT, M. ; LEE, W. ; CASSADY, C. ; RUANO, R. . Quantification of liver herniation in fetuses with isolated congenital diaphragmatic hernia using two-dimensional ulstrasonography. In: 25th World Congress on Ultrasound in Obstetrícs and Gynecology, 2015, Montreal. Ultrasound in Obstetrics & Gynecology, 2215. v. 46. p. 30-31.

RUANO, R. ; SANANES, N. ; Britto, Ingrid Schwach Werneck ; MASTROBATTISTA, J. ; SILVA, M. ; TANNURI, U. ; ZUGAIB, M. . Impact of fetal endoscopy tracheal occlusion on postnatal outcome according to the severity of congenital diaphragmatic hernia. In: 25th World Congress on Ultrasound in Obstetrícs and Gynecology, 2015, Montreal. Ultrasound in Obstetrics & Gynecology, 2015. v. 46. p. 31-31.

RUANO, R. ; Britto, Ingrid Schwach Werneck ; SANANES, N. ; SANGI-HAGHPEYKAR, H. ; SILVA, M. ; BELFORT, M. ; LEE, W. ; TANNURI, U. ; ZUGAIB, M. ; DETEX, R. . Lung growth in fetuses with left-sided congenital diaphragmatic hernia evaluated by there tridimensional ultrasonography. In: 25th World Congress on Ultrasound in Obstetrícs and Gynecology, 2015, Montreal. Ultrasound in Obstetrics & Gynecology, 2015. v. 46. p. 180.

19th International Conference on Prenatal Diagnosis and Therapy, 2015, Washington DC. Lung-to-head ratio, ultrasound liver herniation-to-thoracic ratio and stomach position in isolated left congenital diaphragmatic hernia to predict outcome. N Sananes, I Britto, A Akinkuotu, O Olutoye, D Cass, H Sangi-Haghpeykar, T Lee, C Cassady, A Mehollin-Ray, S Welty, C Fernandes, M Belfort, W Lee, R Ruano.

19th International Conference on Prenatal Diagnosis and Therapy, 2015, Washington DC. Longitudinal measurements of fetal lung volumes in healthy fetuses and fetuses with isolated left-sided congenital diaphragmatic hernia. R Ruano, I Britto, N Sananes, H Sangi-Haghpeykar, MM da Silva, M Belfort, W Lee, U Tannuri, R Deter.

8. APPENDICES

8.1. Patent filed

BREVET D'INVENTION
CERTIFICAT D'UTILITE

Réception électronique de la soumission

Il est certifié par la présente qu'une demande de brevet (ou d'un certificat d'utilité) a été reçue par le biais du dépôt électronique sécurisé de l'INPI. Après réception, un numéro d'enregistrement et une date de réception ont été automatiquement attribués.

Numéro de demande	1653954	
Numéro de soumission	1000345616	
Date de réception	02 mai 2016	
Vos références	BFF 14P0800AH	
Demandeur	Université de Strasbourg	
Pays	FR	
Titre de l'invention	BALLONNET GONFLABLE ET DÉTACHABLE, DESTINÉ À ÊTRE IMPLANTÉ DANS UNE CAVITÉ CORPORELLE, NÉCESSAIRE DE TRAITEMENT ET PROCÉDÉ DE VIDANGE ASSOCIÉS	
Documents envoyés	package-data.xml	requetefr.xml
	application-body.xml	fr-fee-sheet.xml
	requetefr.pdf (5 p.)	validation-log.xml
	comment.pdf (2 p.)	indication-bio-deposit.xml
	fr-office-specific-info.xml	textebrevet.pdf (17 p.)
	dessins.pdf (5 p.)	
Déposé par	EMAIL=paris@lavoix.eu,CN=Philippe BLOT,O=CABINET LAVOIX,C=FR	
Méthode de dépôt	Dépôt électronique	
Date et heure de réception électronique	02 mai 2016, 16:53:59 (CEST)	
Empreinte officielle du dépôt	6D:15:90:CE:25:66:77:46:88:D5:88:91:8D:DD:C4:49:5E:E6:42:D3	

/INPI, section dépôt/

Ballonnet gonflable et détachable, destiné à être implanté dans une cavité corporelle, nécessaire de traitement et procédé de vidange associés

La présente invention concerne un ballonnet gonflable, destiné à être implanté dans une cavité corporelle, comportant :

- une poche formée d'une paroi étanche délimitant un espace intérieur ;
- une vanne de remplissage de l'espace intérieur par un fluide, propre à être obturée après remplissage de l'espace intérieur.

Le ballonnet est propre à être inséré à l'extrémité d'un dispositif de largage et de gonflage et à être détaché du dispositif.

Un tel ballonnet est destiné notamment à être implanté dans la trachée d'un fœtus pour réaliser une occlusion trachéale fœtale lorsque le fœtus est atteint de hernie diaphragmatique congénitale. Le ballonnet peut également être utilisé dans le cadre d'indications potentielles, comme la rupture prématurée des membranes ou toute autre affection associée à une hypoplasie pulmonaire fœtale. La hernie diaphragmatique congénitale est une maladie affectant sporadiquement les fœtus, avec une incidence généralement comprise entre 1/3000 et 1/5000 parmi les nouveau-nés.

Cette hernie se traduit par une invasion d'organes de l'abdomen, tels que l'intestin, l'estomac et/ou le foie dans la cavité thoracique en raison du défaut diaphragmatique. Ceci applique une pression sur les poumons en développement et provoque une hypoplasie pulmonaire susceptible d'engendrer une insuffisance respiratoire, voire parfois la mort du nouveau-né. La mortalité actuelle résultant d'une hernie diaphragmatique congénitale isolée est estimée à 30 % environ par certaines études. L'hypoplasie pulmonaire est plus ou moins sévère en fonction de l'importance de la hernie. Les conséquences une fois l'enfant né sont l'insuffisance respiratoire, mais aussi l'hypertension artérielle pulmonaire.

Pour pallier ce problème, il est connu notamment de l'article « Technical Aspects of Fetal Endoscopic Tracheal Occlusion for Congenital Diaphragmatic Hernia », Journal of Pediatric Surgery, (2011) 46, 22-32, d'implanter un ballon par voie endoscopique dans la trachée du fœtus et de remplir ce ballon de fluide afin de bloquer dans les poumons des sécrétions pulmonaires en amont du ballon entraînant une hyperpression qui stimule le développement pulmonaire.

Lorsqu'une telle technique est appliquée, les études montrent une amélioration significative du développement pulmonaire, augmentant notablement les chances de survie du nouveau-né après la naissance.

Pour être efficace, l'implantation d'un ballon dans la trachée du fœtus doit donc obstruer les voies respiratoires naturelles du fœtus. Il est cependant nécessaire de

dégonfler le ballon, en réalisant une nouvelle endoscopie ou alors en perçant la paroi du ballon, afin de désobstruer les voies respiratoires naturelles.

Cette opération est réalisée in utero vers 34 semaines d'aménorrhée ou avant en cas de rupture de la poche des eaux ou de début de travail. En effet, le retrait du ballon avant la naissance est crucial pour achever une maturation cellulaire adéquate des poumons, qui augmente les chances de survie néonatale. Le retrait in utero facilite en outre la gestion néonatale, et permet d'envisager dans certains cas un accouchement par voie vaginale.

Des difficultés résultent du fait qu'une telle opération ne peut être faite que par une équipe spécialisée, que cette opération n'est pas toujours techniquement réalisable et qu'elle est associée à une morbi-mortalité périnatale élevée.

Par ailleurs, il existe toujours un risque que l'accouchement se produise avant le dégonflage du ballon. Ceci peut avoir des conséquences dramatiques pour le nouveau-né, si l'équipe en charge de l'accouchement ne parvient pas à retirer le ballon lors du travail, ou rapidement après la délivrance.

Les patientes portant un fœtus ayant un ballon dans la trachée sont ainsi astreintes à rester à proximité ou au sein d'un centre hospitalier apte à effectuer une telle intervention rapidement et de manière la plus sûre.

Ceci est fastidieux et coûteux, dans les cas où la patiente n'habite pas au voisinage d'un tel centre hospitalier.

Un but de l'invention est d'obtenir un ballonnet gonflable facile et pratique à implanter dans une cavité corporelle, notamment dans la trachée d'un fœtus, et qui peut néanmoins être simplement dégonflé lorsque cela est souhaité.

À cet effet, l'invention a pour objet un ballonnet du type précité, caractérisé en ce que la poche délimite un orifice de vidange de fluide débouchant dans l'espace intérieur, le ballonnet comportant un organe d'obturation de l'orifice de vidange, l'organe d'obturation étant propre à libérer l'orifice de vidange sous l'effet d'un champ magnétique, pour permettre la vidange au moins partielle du fluide contenu dans l'espace intérieur, l'organe d'obturation étant déplaçable suivant au moins deux axes distincts par rapport à la poche.

Le ballonnet selon l'invention peut comprendre l'une ou plusieurs des caractéristiques suivantes, prise(s) isolément ou suivant toute combinaison techniquement possible :

- l'organe d'obturation est disposé dans l'espace intérieur ;
- l'organe d'obturation est librement déplaçable dans l'espace intérieur défini par la poche sous l'effet d'un champ magnétique ;

- l’organe d’obturation est propre à être maintenu dans une position d’obturation de l’orifice de vidange par aimantation, l’organe d’obturation étant propre à être déplacé à l’écart de l’orifice de vidange sous l’effet d’un champ magnétique propre à vaincre l’aimantation maintenant l’organe d’obturation dans la position d’obturation de l’orifice de vidange ;

- le ballonnet comporte un siège de retenue de l’organe d’obturation, disposé au voisinage de l’orifice de vidange, l’organe d’obturation coopérant par aimantation avec le siège de retenue dans une position d’obturation de l’orifice de vidange ; le siège de retenue étant préférentiellement un anneau, rapporté sur la paroi étanche autour de l’orifice de vidange

- le siège de retenue est couvert d’une couche d’un matériau souple, l’organe d’obturation étant disposé en appui sur la couche de matériau souple dans une position d’obturation de l’orifice de vidange ;

- l’organe d’obturation est une bille ;

- l’organe d’obturation présente une aimantation permanente ;

- l’organe d’obturation est propre à être déplacé jusqu’à au moins deux positions distinctes de libération de l’orifice de vidange sur deux axes sécants passant par l’orifice de vidange ;

- la paroi étanche de la poche est réalisée à partir d’un polymère choisi parmi le silicone, le latex, le polyuréthane, et/ou le polyisoprène ;

- l’orifice de vidange est défini par la vanne de remplissage, l’organe d’obturation étant propre à fermer la vanne de remplissage après remplissage de l’espace intérieur ;

- la vanne de remplissage comporte une bague de guidage d’un tube de gonflage du ballonnet, la bague de guidage et/ou l’organe d’obturation présentant un revêtement biocompatible.

L'invention a également pour objet un nécessaire de traitement d’un patient comportant :

- une ballonnet tel que défini plus haut ;

- un dispositif de gonflage et de largage du ballonnet, comprenant un tuteur de support du ballonnet, le ballonnet étant monté de manière libérable sur le tuteur de support, et un tube de gonflage du ballonnet, propre à être inséré de manière libérable dans la vanne de remplissage.

L'invention a aussi pour objet un procédé de vidange d’un ballonnet tel que défini plus haut, le ballonnet étant implanté dans une cavité corporelle, l’espace intérieur du ballonnet contenant du fluide, l’organe d’obturation obturant l’orifice de vidange. Le procédé comprenant les étapes suivantes :

- soumission du ballonnet à un champ magnétique externe, avantageusement produit par un appareil de résonance magnétique nucléaire, suivant au moins une première direction ;

- déplacement de l'organe d'obturation suivant au moins un axe sous l'effet du champ magnétique externe, pour libérer l'orifice de vidange ;

- vidange au moins partielle du fluide contenu dans l'espace intérieur à travers l'orifice de vidange.

Le procédé selon l'invention peut comprendre l'une ou plusieurs des caractéristiques suivantes, prise(s) isolément ou suivant toute combinaison techniquement possible :

- une étape de soumission du ballonnet à un champ magnétique externe, avantageusement produit par l'appareil de résonance magnétique nucléaire, suivant au moins une deuxième direction, distincte de la première direction.

L'invention a plus généralement pour objet un procédé d'ouverture d'un orifice de vidange d'un fluide dans un implant, l'implant comportant un organe d'obturation de l'orifice de vidange, propre à libérer l'orifice de vidange sous l'effet d'un champ magnétique pour permettre le passage au moins partiel du fluide présent dans l'implant à travers l'orifice de vidange, le procédé comprenant les étapes suivantes :

- soumission de l'implant à un champ magnétique externe issu d'un appareil de résonance magnétique nucléaire suivant au moins une première direction ;

- déplacement de l'organe d'obturation suivant au moins un axe sous l'effet du champ magnétique externe, pour libérer l'orifice de vidange ;

- passage de fluide à travers l'orifice de vidange.

Le procédé d'ouverture peut comprendre une étape de soumission de l'implant au champ magnétique externe produit par l'appareil de résonance magnétique nucléaire, suivant au moins une deuxième direction, distincte de la première direction.

L'invention a également pour objet une méthode de traitement chirurgical comprenant les étapes suivantes :

- fourniture d'un nécessaire tel que défini plus haut ;

- amenée, avantageusement par endoscopie, du ballonnet dans une cavité corporelle, à l'aide du dispositif de largage et de gonflage ;

- gonflage du ballonnet dans la cavité corporelle ;

- largage du ballonnet dans la cavité corporelle et retrait du dispositif de gonflage et de largage hors de la cavité corporelle.

La méthode de traitement chirurgical peut comprendre la caractéristique suivante :

- l'étape d'amenée comporte le convoyage du ballonnet dans la cavité amniotique d'une patiente, puis son introduction dans la trachée d'un fœtus présent dans la cavité amniotique.

L'invention sera mieux comprise à la lecture de la description qui va suivre, donnée uniquement à titre d'exemple, et faite en se référant aux dessins annexés, sur lesquels :

- la figure 1 est une vue schématique d'un premier nécessaire de traitement selon l'invention, avant l'implantation du ballonnet dans une cavité corporelle ;

- la figure 2 est un détail illustrant l'orifice de vidange du ballonnet, et l'organe d'obturation de l'orifice dans une position d'obturation, vu depuis l'intérieur du ballonnet ;

- les figures 3 à 6 illustrent les étapes successives d'introduction du ballonnet dans la cavité corporelle ;

- la figure 7 est une vue en perspective du ballonnet gonflé, lors de son largage ;

- la figure 8 est une vue analogue à la figure 7, lors du déplacement de l'organe d'obturation du ballonnet pour libérer l'orifice de vidange, sous l'effet d'un champ magnétique extérieur à la patiente ;

- la figure 9 est une vue en perspective de trois-quarts face d'un deuxième ballonnet selon l'invention, avant son gonflage ;

- la figure 10 est une vue prise en coupe suivant un plan axial médian du ballonnet de la figure 9, lors de son gonflage ;

- la figure 11 est une vue analogue à la figure 9, après gonflage du ballonnet ;

- la figure 12 est une vue analogue à la figure 10, lors du dégonflage ;

- la figure 13 est une vue analogue à la figure 12 d'un troisième ballonnet selon l'invention ;

- la figure 14 est une vue d'un détail d'une variante de ballonnet selon l'invention.

Un premier nécessaire de traitement 10 selon l'invention est illustré schématiquement sur la figure 1.

Le nécessaire de traitement 10 comporte un ballonnet gonflable 12 selon l'invention, destiné à être implanté dans une cavité corporelle 14, visible sur les figures 4 à 6. Le nécessaire 10 comporte en outre un dispositif 16 de gonflage et de largage du ballonnet gonflable 12 dans la cavité 14, illustré en particulier sur les figures 1 et 3.

Dans l'application particulière représentée sur les figures 3 à 6, la cavité 14 est la trachée d'un fœtus 18, présent dans la cavité amniotique 20 d'une patiente 22. Le fœtus 18 souffre par exemple d'une hernie diaphragmatique congénitale.

En référence aux figures 1 et 2, le ballon 12 comporte une poche 24 gonflable par un fluide, une vanne 26 de remplissage de la poche 24, et selon l'invention, une vanne 28

de vidange, libérable sous l'effet d'un champ magnétique extérieur à la patiente 22. La vanne de vidange 28 est ici distincte de la vanne de remplissage 26.

La poche 24 est formée d'une paroi étanche 30 déformable au toucher, délimitant un espace intérieur 32 de volume variable en fonction de la quantité de fluide qu'il contient.

La paroi étanche 30 est par exemple réalisée à partir d'un matériau polymère tel que du silicone, du latex, ou d'un caoutchouc ou tel que le polyisoprène.

L'épaisseur de la paroi étanche 30 est inférieure à 1 mm et est généralement comprise entre 0,1 mm et 0,5 mm.

La poche 24 présente généralement une forme allongée le long d'un axe A-A', visible sur la figure 2.

En référence à la figure 1, la poche 24 définit un orifice 34 de remplissage de l'espace intérieur 32, obturé sélectivement par la vanne de remplissage 26 et un orifice 36 de vidange, distinct de l'orifice de remplissage 34, obturé de manière sélective par la vanne de vidange 28.

Dans cet exemple, l'orifice de remplissage 34 est situé à une extrémité proximale de la poche 24, prise le long de l'axe A-A'. L'orifice 34 est délimité à sa périphérie par un manchon 38 de montage de la vanne 26 faisant saillie le long de l'axe A-A' par rapport à la paroi 30. Le manchon 38 est d'un seul tenant avec la paroi 30

L'orifice de vidange 36 est ménagé de manière traversante dans une région périphérique distale 40 de la paroi 30, située à l'opposé de l'orifice de remplissage 34 dans cet exemple.

L'étendue transversale de l'orifice de vidange 36 est avantageusement inférieure à 1,5 mm et est comprise par exemple entre 1 mm et 1,5 mm.

L'espace intérieur 32 de la poche 24 est propre à être rempli par un fluide, de préférence par un liquide, à travers la vanne de remplissage 26, pour passer la poche 24 d'une configuration dégonflée, contractée radialement (visible sur la figure 1 ou sur la figure 5) à une configuration gonflée, dilatée radialement (visible sur la figure 7).

Dans la configuration dégonflée, la poche 24 présente avantageusement une étendue transversale maximale et, prise perpendiculairement à l'axe A-A', avantageusement inférieure à 1,5 mm et comprise généralement entre 1 mm et 1,5 mm.

La longueur de la poche 24, prise le long de l'axe A-A', est avantageusement comprise entre 5 mm et 10 mm.

Le volume de l'espace intérieur 32 est alors compris avantageusement entre 3 mm^3 et 10 mm^3.

Dans la configuration gonflée, la poche 24 présente avantageusement une étendue transversale maximale Et, prise perpendiculairement à l'axe A-A', avantageusement inférieure à 10 mm et comprise par exemple entre 5 mm et 9 mm.

La longueur de la poche 24 dans la configuration gonflée, prise le long de l'axe A-A' est supérieure à la longueur de la poche 24 dans la configuration dégonflée. Cette longueur est avantageusement comprise entre 15 mm et 25 mm.

Le volume de l'espace intérieur 32 est alors compris avantageusement entre 250 mm^3 et 1600 mm^3.

Le fluide de gonflage de la poche est par exemple un liquide, notamment un liquide physiologique. Ce liquide contient éventuellement un agent de contraste propre à être visible par radiographie.

En référence à la figure 1, la vanne de remplissage 26 est normalement fermée. Elle définit une lumière centrale 50 d'injection de fluide dans l'espace intérieur 32.

Dans cet exemple, la vanne de remplissage 26 fait saillie axialement par rapport à la paroi 30. Elle est montée autour du manchon 38.

Elle comporte, à l'intérieur du manchon 38, un joint annulaire déformable 52 définissant la lumière centrale 50, et une bague périphérique 54 montée autour du manchon 38 pour enserrer le manchon 38 et le joint 52.

Le joint annulaire 52 est disposé dans l'orifice de remplissage 34. Il est déformable radialement par compression, pour permettre l'introduction d'un élément de remplissage de l'espace intérieur 32. Il est propre à revenir spontanément vers une configuration d'obturation de l'orifice de remplissage 34.

En référence à la figure 2, la vanne de vidange 28 comporte un siège 60 fixé sur la paroi étanche 30, sur la région périphérique 40 autour de l'orifice de vidange 36, et un organe d'obturation 62 de l'orifice de vidange 36, déplaçable suivant au moins deux axes A-A', B-B' distincts, sous l'effet d'un champ magnétique extérieur à la patiente 22.

Dans cet exemple, le siège 60 est rapporté sur la région périphérique 40, à l'extérieur de la paroi étanche 30. Il est par exemple collé sur la région périphérique 40.

Le siège 60 présente ici une forme d'anneau entourant l'orifice de vidange 36.

Le siège 60 est réalisé à l'aide d'un matériau métallique ferromagnétique, propre à être aimanté par un aimant permanent.

L'organe d'obturation 62 est disposé ici dans l'espace intérieur 32. Comme visible sur la figure 2, il présente une étendue transversale maximale e2 supérieure à l'étendue transversale maximale e1 de l'orifice de vidange 36. Dans cet exemple, l'organe d'obturation 62 est une bille.

L'organe d'obturation 62 présente une aimantation permanente. Il est ainsi propre à coopérer magnétiquement avec le siège 60 pour être maintenu dans une position d'obturation de l'orifice de vidange 36, dans laquelle il est appliqué contre la région périphérique 40 en regard du siège 60.

Dans cette position, l'organe d'obturation 62 obture totalement l'orifice 36, et empêche le passage de fluide depuis le volume intérieur 32 vers l'extérieur de la poche 24.

L'étanchéité autour de l'orifice de vidange 36 est renforcée par la présence de la région périphérique 40, sur laquelle s'appuie l'organe d'obturation 62, qui forme une couche intermédiaire déformable.

Sous l'effet d'un champ magnétique extérieur, propre à engendrer une force d'attraction de l'organe d'obturation 62 supérieure à la force de coopération entre l'organe d'obturation 62 et le siège 60, l'organe d'obturation 62 est propre à se déplacer à l'écart de l'orifice de vidange 36 dans l'espace intérieur 32 suivant au moins deux axes A-A', B-B'.

L'intensité du champ magnétique propre à libérer l'organe d'obturation 62 est par exemple supérieure à 0,1 T et est notamment comprise entre 0,5 T et 2 T.

En pratique, lorsqu'il se détache de la position d'obturation, l'organe d'obturation 62 est propre à se déplacer librement suivant une multitude d'axes dans un cône 64 centré sur l'axe A-A' de l'orifice de vidange 36, au niveau de l'orifice 36. Le cône 64 présente un angle d'ouverture vers l'espace intérieur 32 supérieur à 30°, de préférence supérieur à 90°, et avantageusement égal à 180°.

Aucun moyen mécanique de retenue ne raccorde l'organe d'obturation 62 à la poche gonflable 24 et/ou au siège 60.

Une fois détachée de la position d'obturation, l'organe d'obturation 62 est propre à atteindre au moins une position de libération de l'orifice 36, cette position dépendant de l'orientation de la patiente 22, et de celle du champ magnétique extérieur.

En particulier, l'organe d'obturation 62 est propre à occuper une pluralité de positions de libération distinctes, dans l'espace intérieur 32, après avoir quitté la position d'obturation, dont une est illustrée sur la figure 8.

En référence aux figures 1 et 3, le dispositif 16 de gonflage et de largage du ballonnet 12 comporte un tuteur souple 70 portant à son extrémité distale 71 le ballonnet 12, un tube de gonflage 72 disposé dans le tuteur 70, et avantageusement, une tige mandrin 74 disposée dans le tube de gonflage 72 pour le rigidifier.

Le dispositif 16 comporte en outre un embout proximal 76, pour sa manipulation par un praticien, et avantageusement, une gaine amovible 78 de protection du ballonnet 12.

Le tuteur 70 s'étend entre l'embout proximal 76 et l'extrémité distale 71. Il est propre à être déformé pour être introduit dans la patiente 22 avantageusement par voie endoscopique, et atteindre la cavité 14.

Le tube de gonflage 72 s'étend à travers le tuteur 70. Il est raccordé en amont à un réservoir 80 d'injection de fluide.

Le tube de gonflage 72 présente une partie distale 82 qui fait saillie par rapport à l'extrémité distale 71 du tuteur 70 pour être introduite dans la lumière centrale 50 de la vanne de remplissage 26.

La gaine amovible 78 est propre à couvrir le ballonnet 12 lors de son introduction jusqu'à la cavité 14. Elle est mobile longitudinalement autour du tuteur 70 pour découvrir le ballonnet 12, à son point d'implantation dans la cavité 14.

Le fonctionnement du nécessaire de traitement 10 dans le cadre d'une implantation dans une cavité corporelle 14 va maintenant être décrit.

Cette implantation est par exemple réalisée dans la trachée d'un fœtus 18 présent dans la cavité amniotique 20 d'une patiente 22.

Initialement, le ballonnet 12 est monté à l'extrémité distale 71 du tuteur 70 du dispositif de gonflage et de largage 16. La partie distale 82 du tube de gonflage 72 est introduite dans la vanne de remplissage 26, par déformation radiale du joint annulaire 52.

L'organe d'obturation 62 est plaqué en regard du siège 60 contre la région périphérique 40. Il occupe sa position d'obturation de l'orifice 36.

La poche 24 occupe alors sa configuration dégonflée, d'étendue radiale minimale, visible sur les figures 1 et 5.

Le dispositif 16, muni du ballonnet 12 à son extrémité est alors introduit dans la patiente 22, par voie endoscopique. Dans l'exemple représenté sur la figure 3, le praticien l'introduit dans la cavité amniotique 20, puis l'amène à travers les voies respiratoires du fœtus 18 jusqu'à la trachée, en passant à travers les cordes vocales (figure 4).

Une fois l'extrémité distale 71 dans la cavité 14, le praticien extrait le ballonnet 12 hors de la gaine 78, en tirant la gaine 78 vers l'embout proximal 76, comme visible sur la figure 5.

La poche gonflable 24 occupe toujours sa configuration dégonflée.

Le praticien injecte alors du fluide de gonflage dans l'espace intérieur 32 à travers le tube de gonflage 72 introduit dans la vanne de remplissage 26. La poche 24 se dilate

radialement pour atteindre sa configuration gonflée, en appui sur la paroi délimitant la cavité 14, comme visible sur la figure 6.

Puis, le praticien détache le ballonnet 12 du dispositif de gonflage et de largage 16, en extrayant le tube de gonflage 72 hors de la vanne de remplissage 26. La vanne de remplissage 26 se referme par dilatation radiale du joint annulaire 52.

Le praticien retire alors le dispositif 16 de la patiente 22.

Durant le gonflage, et après celui-ci, l'organe d'obturation 62 reste dans sa position d'obturation. Le fluide de gonflage reste donc confiné dans le volume intérieur 32.

La cavité 14 est alors obturée. Dans le cas d'un fœtus 18 souffrant d'hernie diaphragmatique congénitale, le développement pulmonaire du fœtus est amélioré, grâce à la présence du ballonnet 12 gonflé dans la trachée.

Lorsque le ballonnet 12 doit être retiré, la patiente est soumise à un champ magnétique extérieur de forte intensité, par exemple d'intensité supérieure à 0,1 T.

Ce champ magnétique est par exemple produit par un appareil d'imagerie par résonance magnétique. Selon les circonstances, la patiente se positionne dans l'appareil lors d'une acquisition d'image ou de préférence sans acquisition d'images dans l'appareil. Préférentiellement, la patiente n'a pas besoin de se positionner dans l'appareil, le champ de fuite de l'appareil allumé ou à l'entrée du tunnel est avantageusement suffisant pour produire un champ magnétique adéquat pour libérer l'organe d'obturation 62, auquel cas la patiente se tient simplement debout devant la machine.

De préférence, comme illustré par la figure 8, l'orientation relative entre le champ magnétique et la patiente 22 est modifié, par exemple en déplaçant la patiente, pour que le champ magnétique soit appliqué suivant au moins deux axes H1 et H2 distincts, comme illustré par la figure 8.

Le champ magnétique extérieur engendre une force d'attraction sur l'organe d'obturation 62 qui surmonte la force de coopération entre l'organe d'obturation 62 et le siège 60.

Sous l'effet du champ magnétique extérieur, l'organe d'obturation 62 se déplace à l'écart de l'orifice de vidange 36, jusqu'à une position de libération de l'orifice 36, représentée par exemple sur la figure 8.

Au moins une partie du fluide présent dans l'espace intérieur 32 s'écoule alors depuis l'espace intérieur 32 vers l'extérieur, à travers l'orifice de vidange 36, provoquant le dégonflage rapide du ballonnet 12.

Les voies respiratoires du fœtus sont alors à nouveau dégagées. Le ballonnet 12 est alors apte à être expulsé hors du fœtus par la libération du fluide pulmonaire en surpression, ou est retiré quelques jours après la naissance.

La libération de l'organe d'obturation 62 est immédiate et très facile à réaliser. Aucune liaison mécanique n'existant entre d'une part, l'organe d'obturation 62 et d'autre part, la poche gonflable 24 ou le siège 60, cette libération est très fiable et ne dépend pas d'un mécanisme mécanique ou électrique. Au contraire, le dégagement de l'orifice de vidange 36 est exclusivement provoqué par le champ magnétique extérieur appliqué, combiné aux forces de gravité s'appliquant sur l'organe d'obturation 62.

Cette libération est en outre non invasive pour la patiente 22, puisqu'elle peut être réalisée à distance, sans avoir à inciser la patiente 22, voire à pénétrer dans la cavité amniotique 20.

La vanne de vidange 28 ainsi obtenue est peu coûteuse à réaliser, tout en assurant un fonctionnement adéquat, quelles que soient les circonstances.

Les risques pour le fœtus 18 sont donc totalement écartés, puisque le retrait du ballonnet 12 est facilité par son dégonflage immédiat, et son expulsion hors de la trachée, au moment souhaité et sans procédure invasive.

La patiente 22 bénéficie d'un traitement adéquat, assurant le bon développement de son fœtus 18, sans nécessairement être maintenue au voisinage ou au sein d'un centre hospitalier spécialisé, ce qui limite les coûts en maintenant la qualité de soins.

Un deuxième nécessaire de traitement 110 selon l'invention est illustré par les figures 9 à 13.

Le ballonnet 12 du deuxième nécessaire 110 est formé de manière similaire au ballonnet 12 du premier nécessaire 10. En particulier, les dimensions du ballonnet 12 du deuxième nécessaire 110 sont analogues à celles du ballonnet 12 du premier nécessaire 10.

Toutefois, à la différence du premier nécessaire 10, le ballonnet 12 comporte une vanne unique formant à la fois une vanne de remplissage 26 et une vanne de vidange 28.

L'orifice de vidange 36 est constitué par l'orifice de remplissage 34 à l'extrémité de la vanne 26, 28. La poche 24 est donc munie d'un orifice 34, 36 unique permettant le remplissage de l'espace intérieur 32 en fluide et la vidange du fluide contenu dans l'espace intérieur 32.

L'organe d'obturation 62 obture par défaut la vanne de remplissage 26. Ainsi, la bague périphérique 54 délimitant la vanne de remplissage 26 est dépourvue de joint annulaire. Elle définit donc une lumière centrale 50 dégagée en permanence.

Comme pour le ballonnet 12 du premier nécessaire 10, la poche 24 se prolonge par un manchon 38 inséré dans la bague périphérique 54 et délimitant la périphérie de la lumière centrale 50.

Dans cet exemple, le manchon 38 se prolonge au-delà de la bague 54, à l'opposé de la poche 24, par un embout annulaire 112 s'ouvrant vers l'extérieur.

La bague périphérique 54 est ici en matériau métallique ferromagnétique. Elle définit le siège 60, sur lequel s'appuie l'organe d'obturation 62 dans la position d'obturation, sur la région périphérique 40.

L'organe d'obturation 62 présente ici une aimantation permanente. Il s'applique donc au repos sur le siège 60, dans la position d'obturation.

Le fonctionnement du deuxième nécessaire 110 selon l'invention est analogue à celui du premier nécessaire 10.

Toutefois, à la différence du premier nécessaire 10, le tube de gonflage 72 est introduit dans la bague périphérique 54 de la vanne de remplissage 26, sans ouvrir l'orifice de remplissage 34, puisque l'organe d'obturation 62 reste appliqué sur le siège 60.

Comme illustré par la figure 10, la force hydraulique générée par la pression du fluide injecté par le tube de gonflage 72, pousse l'organe d'obturation 62 à l'écart du siège 60 et surmonte au moins partiellement la force magnétique retenant l'organe d'obturation 62 sur le siège 60.

Un interstice se forme alors entre le siège 60 et l'organe d'obturation 62 permettant l'entrée de fluide dans l'espace intérieur 32 et le gonflage de la poche 24.

Lorsque le gonflage s'achève, l'organe d'obturation 62 reprend sa position d'obturation sous l'effet de la force magnétique. L'espace intérieur 32 de fluide est obturé de manière étanche, comme l'illustre la figure 11. Une pression induite, par exemple supérieure à 0,5 bars relatifs, et notamment de l'ordre de 1 bar relatifs subsiste dans l'espace intérieur 32 du ballonnet 12.

Cette pression est nécessaire au démarrage du gonflage (amorçage de l'élasticité du ballonnet 12). Cette pression baisse dans la deuxième phase du gonflage. La pression induite dépend de l'élasticité du matériau, de l'épaisseur de paroi, de la longueur initiale du ballonnet, etc. Elle favorise l'étanchéité de la vanne.

Pour dégonfler le ballonnet 12, la patiente est soumise à un champ magnétique extérieur de forte intensité, comme décrit précédemment.

Comme visible sur la figure 12, ceci engendre la libération de l'organe d'obturation 62 au moins temporairement à l'écart du siège 60 et le passage de fluide autour de l'organe d'obturation 62 vers la lumière centrale 50 pour dégonfler la poche 24.

Le déplacement de l'organe d'obturation 62 à l'écart du siège 60 est avantageusement très limité, par exemple limitée à quelques centièmes, voir quelques dixièmes de millimètres.

L'organe d'obturation 62 est cependant déplaçable suivant au moins deux axes distincts par rapport à la poche 24, comme pour le ballonnet 12 du premier nécessaire 10, ce qui ne nécessite pas de contrôler l'orientation du champ magnétique suivant une direction spécifique pour libérer l'organe d'obturation 62.

Avantageusement, pour chacun des ballonnets 12 décrits précédemment, l'organe d'obturation 62 et/ou la bague périphérique 54 sont munis d'un revêtement biocompatible 114.

Ce revêtement est par exemple un revêtement en titane, en carbone, en polymère fluoré (notamment en polytétrafluoroéthylène), ou/et en parylène. En variante, le revêtement est un film, notamment un film polymère, par exemple en polyisoprène, ou en polyuréthane.

Dans l'exemple représenté sur la figure 13, au moins une surface périphérique extérieure 116 de la bague 54 est munie du revêtement biocompatible. Avantageusement, une surface périphérique intérieure 118 de la bague 54 et la surface extérieure de l'organe d'obturation 62 sont également munies de ce revêtement,

Dans encore une autre variante, visible sur la figure 14, la bague 54 présente un chanfrein 201 à son extrémité formant le siège 60 de l'organe d'obturation 62.

L'organe d'obturation 62 est ainsi apte à entrer plus dans le diamètre intérieur de la bague 54. Ceci augmente la surface de contact et donc l'étanchéité entre l'organe d'obturation 62 et la bague 54, prise au niveau du siège 60.

Dans une variante (non représentée), l'organe d'obturation 62 après avoir quitté la position d'obturation n'est pas nécessairement déplaçable librement dans tout l'espace intérieur 32, mais uniquement dans une région limitée de l'espace intérieur 32. Par exemple, un compartiment de réception de l'organe d'obturation 62 est monté dans l'espace intérieur 32 autour de l'orifice de vidange 36.

Dans une autre variante (non représentée), l'organe d'obturation 62 est disposé dans sa position d'obturation à l'extérieur de l'espace intérieur 32. Un compartiment de réception de l'organe d'obturation 62 est monté sur la poche 24, à l'extérieur de celle-ci, autour de l'orifice de vidange 36. Ce compartiment de réception est de préférence ajouré pour permettre l'écoulement du fluide provenant de l'espace intérieur 32.

Dans d'autres variantes, l'organe d'obturation 62 ne présente pas une forme sphérique mais présente une autre forme, par exemple polyédrique.

REVENDICATIONS

1.- Ballonnet (12) gonflable, destiné à être implanté dans une cavité (14) corporelle, comportant :

- une poche (24) formée d'une paroi étanche (30) délimitant un espace intérieur (32) ;

- une vanne de remplissage (26) de l'espace intérieur (32) par un fluide, propre à être obturée après remplissage de l'espace intérieur (32) ;

caractérisé en ce que la poche (24) délimite un orifice de vidange (36) de fluide débouchant dans l'espace intérieur (32), le ballonnet (12) comportant un organe d'obturation (62) de l'orifice de vidange (36), l'organe d'obturation (62) étant propre à libérer l'orifice de vidange (36) sous l'effet d'un champ magnétique, pour permettre la vidange au moins partielle du fluide contenu dans l'espace intérieur (32), l'organe d'obturation (62) étant déplaçable suivant au moins deux axes distincts par rapport à la poche (24).

2. - Ballonnet (12) selon la revendication 1, dans lequel l'organe d'obturation (62) est disposé dans l'espace intérieur (32).

3. - Ballonnet (12) selon la revendication 2, dans lequel l'organe d'obturation (62) est librement déplaçable dans l'espace intérieur (32) défini par la poche (24) sous l'effet d'un champ magnétique.

4. - Ballonnet (12) selon l'une quelconque des revendications précédentes, dans lequel l'organe d'obturation (62) est propre à être maintenu dans une position d'obturation de l'orifice de vidange (36) par aimantation, l'organe d'obturation (62) étant propre à être déplacé à l'écart de l'orifice de vidange (36) sous l'effet d'un champ magnétique propre à vaincre l'aimantation maintenant l'organe d'obturation (62) dans la position d'obturation de l'orifice de vidange (36).

5. - Ballonnet (12) selon l'une quelconque des revendications précédentes, comprenant au moins un siège de retenue (60) de l'organe d'obturation (62), disposé au voisinage de l'orifice de vidange (36), l'organe d'obturation (62) coopérant par aimantation avec le siège de retenue (60) dans une position d'obturation de l'orifice de vidange (36), le siège de retenue (60) étant préférentiellement un anneau, rapporté sur la paroi étanche (30) autour de l'orifice de vidange (36).

6. - Ballonnet (12) selon la revendication 5, dans lequel le siège de retenue (60) est couvert d'une couche d'un matériau souple, l'organe d'obturation (62) étant disposé en appui sur la couche de matériau souple dans une position d'obturation de l'orifice de vidange (36).

7. - Ballonnet (12) selon l'une quelconque des revendications précédentes, dans lequel l'organe d'obturation (62) est une bille.

8. - Ballonnet (12) selon l'une quelconque des revendications précédentes, dans lequel l'organe d'obturation (62) présente une aimantation permanente.

9. - Ballonnet (12) selon l'une quelconque des revendications précédentes, dans lequel l'organe d'obturation (62) est propre à être déplacé jusqu'à au moins deux positions distinctes de libération de l'orifice de vidange (36) sur deux axes sécants passant par l'orifice de vidange.

10. - Ballonnet (12) selon l'une quelconque des revendications précédentes, dans lequel la paroi étanche (30) de la poche (24) est réalisée à partir d'un polymère choisi parmi le silicone, le latex, le polyuréthane, et/ou le polyisoprène.

11. - Ballonnet (12) selon l'une quelconque des revendications précédentes, dans lequel l'orifice de vidange (36) est défini par la vanne de remplissage (26), l'organe d'obturation (62) étant propre à fermer la vanne de remplissage (26) après remplissage de l'espace intérieur (32).

12. - Ballonnet (12) selon l'une quelconque des revendications précédentes, dans lequel la vanne de remplissage (26) comporte une bague de guidage (54) d'un tube (72) de gonflage du ballonnet (12), la bague de guidage (54) et/ou l'organe d'obturation (62) présentant un revêtement biocompatible (114).

13. - Nécessaire (10) de traitement d'un patient, comportant :

- un ballonnet (12) selon l'une quelconque des revendications précédentes ;

- un dispositif (16) de gonflage et de largage du ballonnet (12), comprenant un tuteur (70) de support du ballonnet (12), le ballonnet (12) étant monté de manière libérable sur le tuteur de support (70), et un tube (72) de gonflage du ballonnet (12), propre à être inséré de manière libérable dans la vanne de remplissage (26).

14. - Procédé de vidange d'un ballonnet (12) selon l'une quelconque des revendications 1 à 12, le ballonnet (12) étant implanté dans une cavité corporelle (14), l'espace intérieur (32) du ballonnet (12) contenant du fluide, l'organe d'obturation (62) obturant l'orifice de vidange (36), le procédé comprenant les étapes suivantes :

- soumission du ballonnet (12) à un champ magnétique externe, avantageusement produit par un appareil de résonance magnétique nucléaire, suivant au moins une première direction (H1) ;

- déplacement de l'organe d'obturation (62) suivant au moins un axe sous l'effet du champ magnétique externe, pour libérer l'orifice de vidange (36) ;

- vidange au moins partielle du fluide contenu dans l'espace intérieur (32) à travers l'orifice de vidange (36).

15. - Procédé selon la revendication 14, comprenant une étape de soumission du ballonnet (12) à un champ magnétique externe, avantageusement produit par l'appareil de résonance magnétique nucléaire, suivant au moins une deuxième direction (H2), distincte de la première direction (H1).

ABREGE

Ballonnet gonflable et détachable, destiné à être implanté dans une cavité corporelle, nécessaire de traitement et procédé de vidange associés

Le ballonnet (12) comporte :

- une poche (24) formée d'une paroi étanche (30) délimitant un espace intérieur (32) ;

- une vanne de remplissage de l'espace intérieur (32) par un fluide, propre à être obturée après remplissage de l'espace intérieur (32).

La poche (24) délimite un orifice de vidange (36) de fluide débouchant dans l'espace intérieur (32). Le ballonnet (12) comporte un organe d'obturation (62) de l'orifice de vidange (36), l'organe d'obturation (62) étant propre à libérer l'orifice de vidange (36) sous l'effet d'un champ magnétique, pour permettre la vidange au moins partielle du fluide contenu dans l'espace intérieur (32). L'organe d'obturation (62) est déplaçable suivant au moins deux axes distincts par rapport à la poche (24).

Figure 2

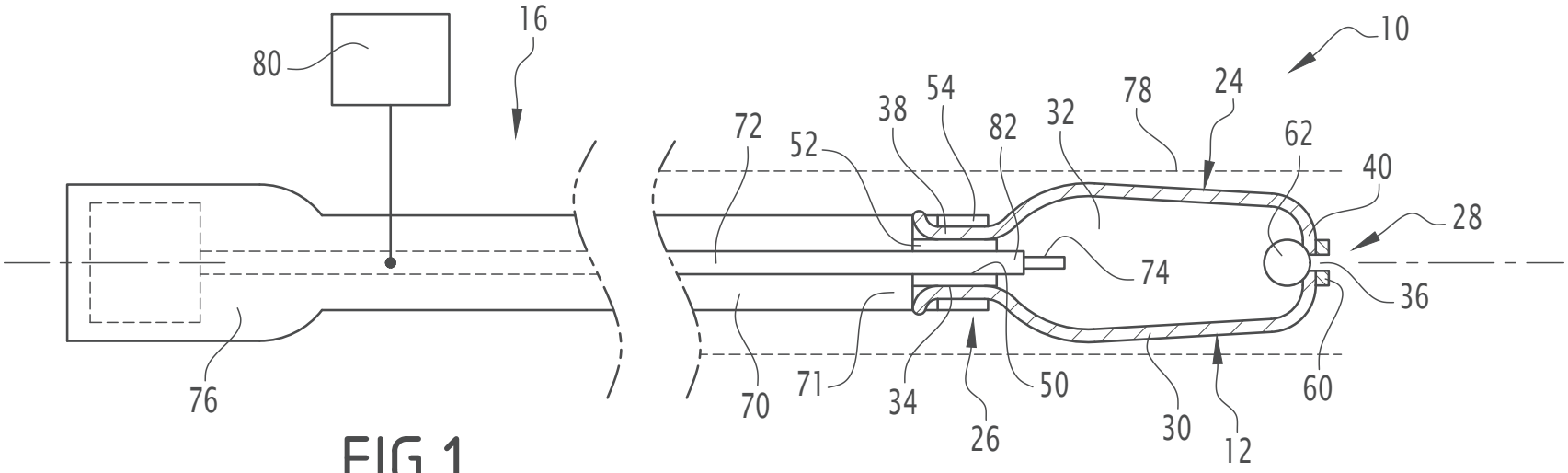
16
80
10
72
52
38
54
82
32
78
24
62
40
28
74
36
76
70
71
34
26
50
30
12
60

FIG.1

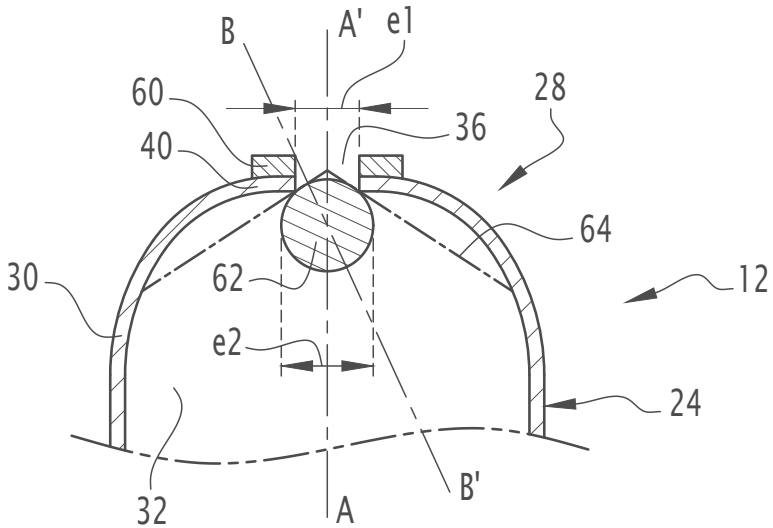
B
A'
e1
60
28
36
40
64
30
62
12
e2
24
32
A
B'

FIG.2

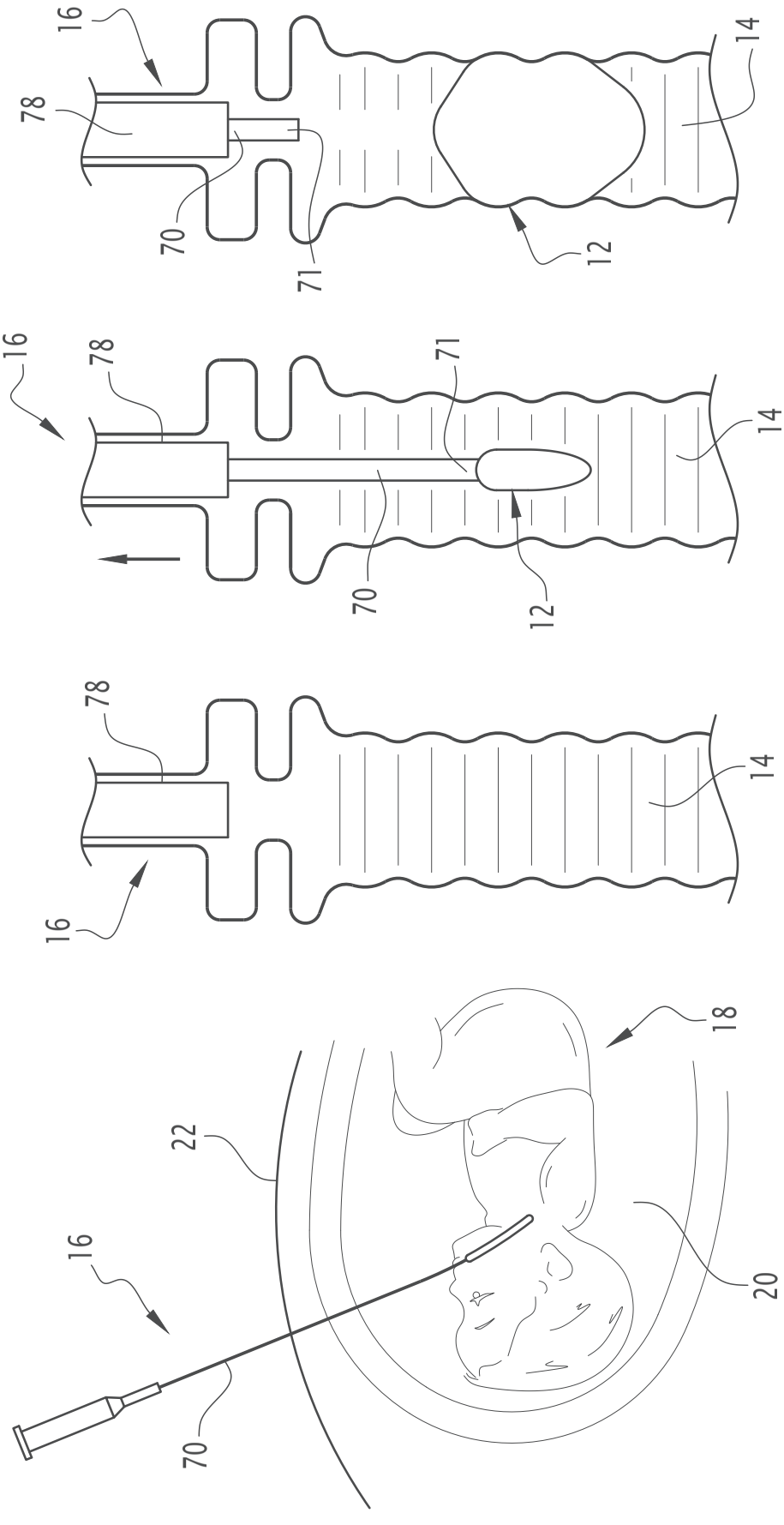

FIG.6

FIG.5

FIG.4

FIG.3

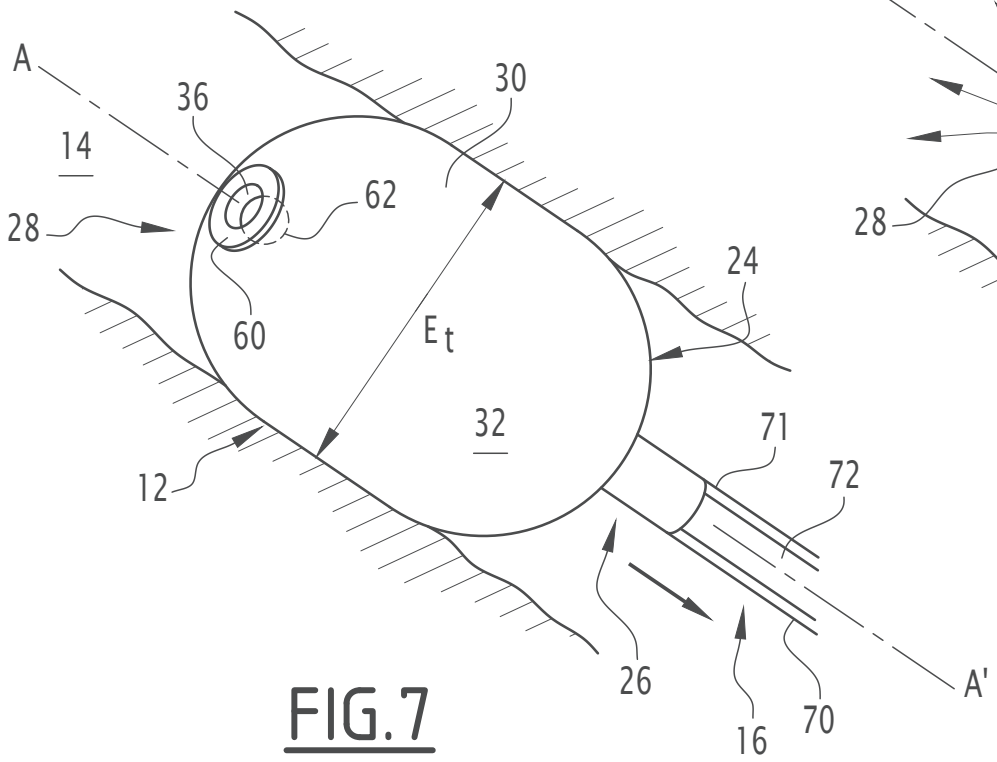
A
36
14
28
62
60
30
24
E_t
32
12
71
72
26
16
70
A'

FIG.7

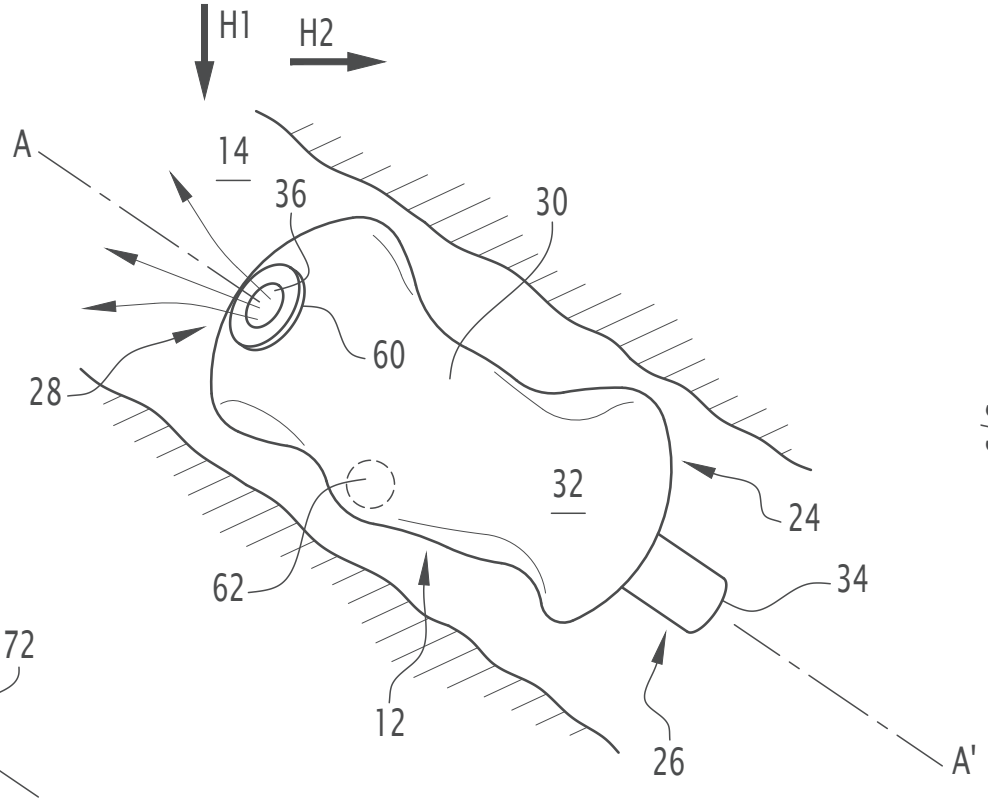
H1
H2
A
14
36
30
60
28
32
24
62
34
12
26
A'

FIG.8

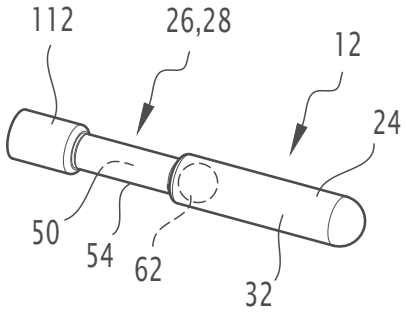

FIG.9

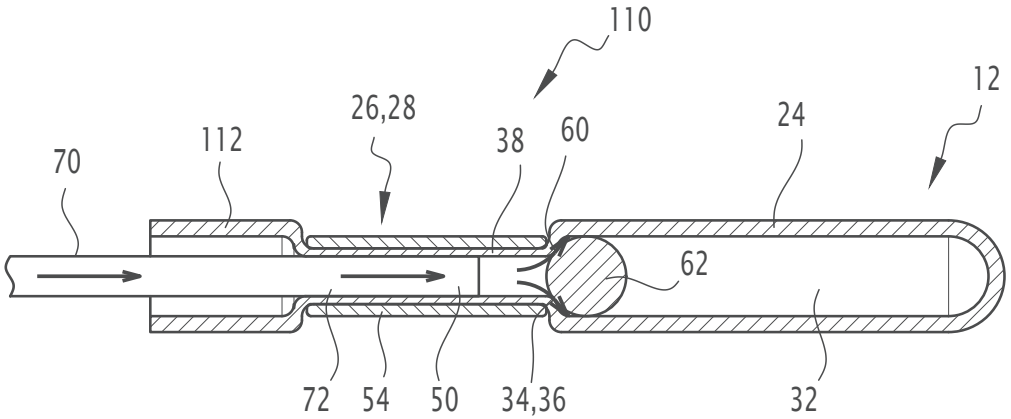

FIG.10

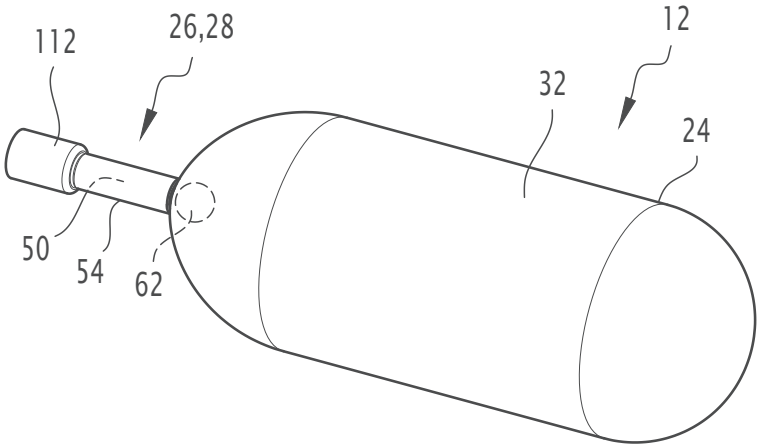

FIG.11

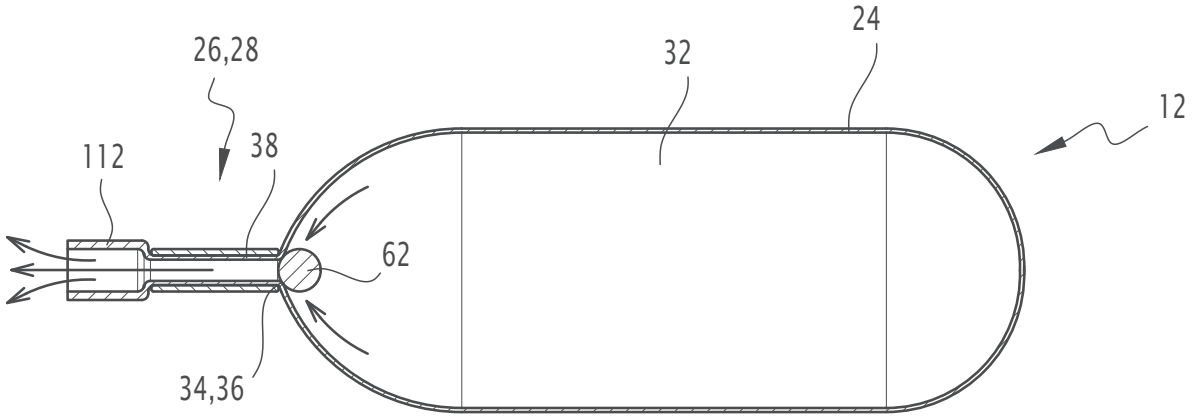

FIG.12

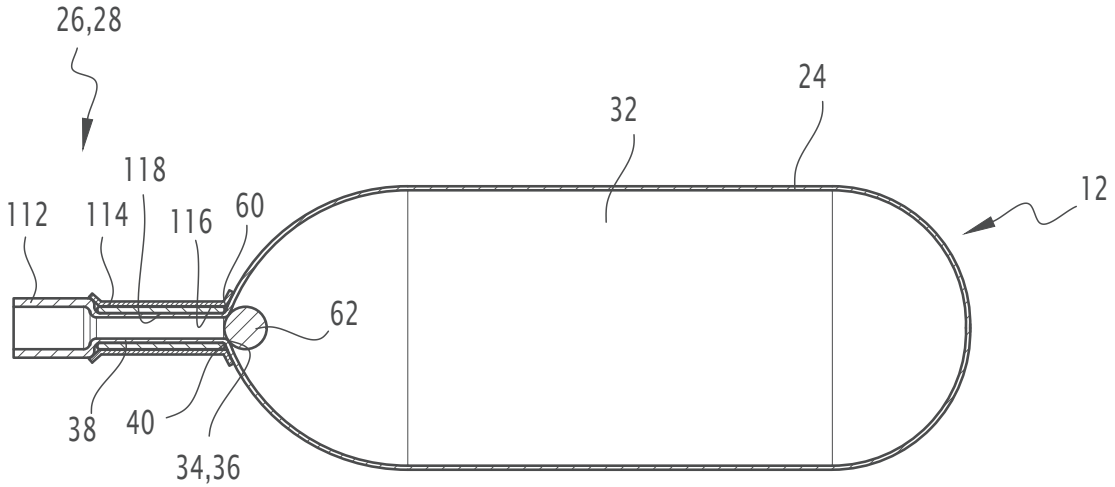

FIG.13

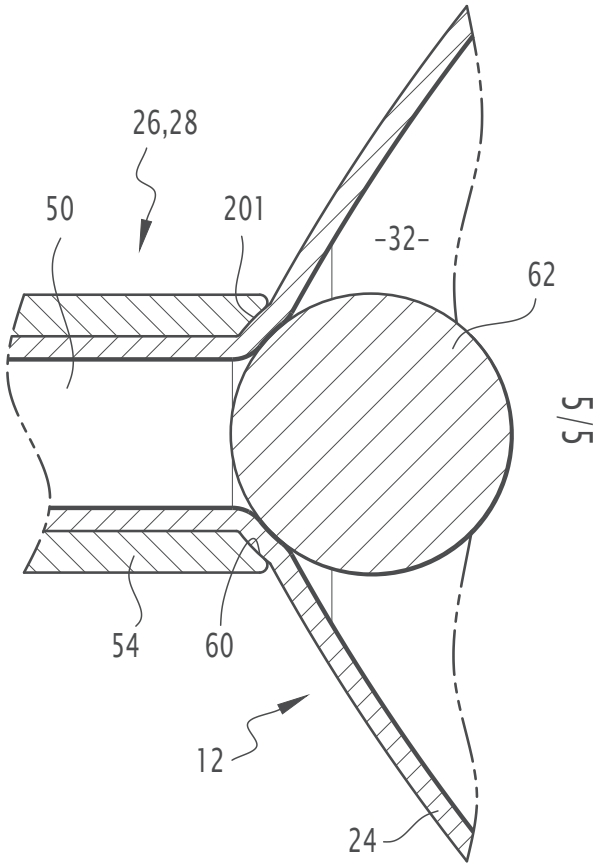

FIG.14

8.2. Instruction for use

Smart-TO balloon and delivery system
Instruction for use

1 – Description

Detachable Smart-TO balloon and delivery system include different components listed below.
Delivery system (length 935 mm) equipped with Luer Lock valve and delivered in a dispenser,
Stylet Ø0.2 mm x 937 mm equipped with a pod and delivered in a dispenser,
Luer Lock 1 ml Syringe,
Smart-TO balloon equipped with magnetic valve, Ø 7x 20 mm, delivered in a dedicated pouch.

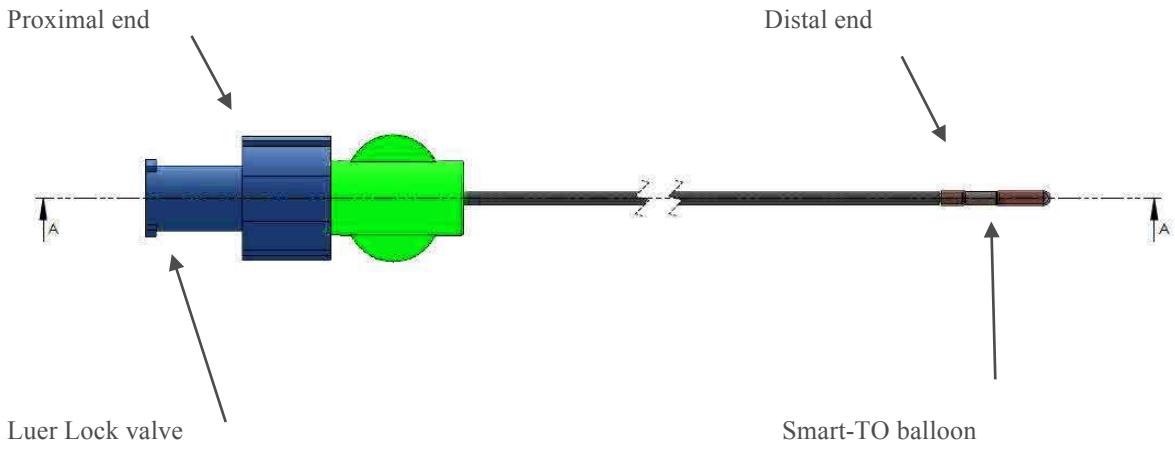

2 – Indication

BS-MTI delivery systems for detachable balloon allow the introduction of Smart-TO balloons and are indicated for the use in the fetal endoscopic tracheal occlusion (FETO) for congenital diaphragmatic hernia (CDH) treatment.

3 – Additional precautions

Precautions for use listed below must be scrupulously followed to ensure the proper functioning of the device and the safety of the patient.
- Do not use if the pouch is open and/or damaged, thus compromising the sterility and/or the integrity of the kit.
- Carefully respect the instruction for use.
- Respect instruction for use of products injected in the delivery system and balloon.
- Wet the delivery system distal tip before mounting the balloon.
- Do not infuse with any other syringe as the one provided with the delivery system.

- Respect the recommended inflate volume of the Smart-TO balloon as indicated on the product label: 0.7 ml max.
- Never inflate the balloon with air.
- Fit the balloon on the catheter just before its use (do not leave it dry out).
- Be careful not to pierce or damage the balloon during mounting.
- Do not use the balloon if its connection to the delivery system is difficult or if it does not perfectly fit the delivery system.
- These products must be used by expert physician in interventional fetal surgery.
- Delivery system and balloons are single use. Delivery system and balloons are sterile when the packaging is not damaged. Do not re-use and/or re-sterilize delivery system.
- Any re-use of the device or part is strictly prohibited because it causes a high risk of microbiological contamination for the patient and a loss of the performance of the device.
- Store in a dry place at room temperature and away from light.
- Do not use the product after expiry date.

4 – Instruction for use

4-1 – Delivery system preparation

Carefully inspect the sterile pouch: it must be unopened and undamaged. Carefully open the sterile pouch, remove the delivery system from the dispenser. Inspect the catheter prior to use in order to verify that is it undamaged and unfolded.
Fill the syringe with sterile physiological solution.
Introduce the delivery system into one of the side-ports of the fetoscope and move it forward until it goes out of the distal side of the endoscopic sheath. When the distal end of delivery system is out from a few centimeters, connect the syringe to the Luer Lock valve at the proximal end of the delivery system.
Control flow through delivery system using syringe and saline solution and flush the catheter.

4-2 – Smart-TO balloon control and connection

Carefully inspect the sterile pouch of the balloon: it must be unopened and undamaged. Carefully open the sterile pouch and remove the Smart-TO balloon. Inspect the balloon prior to use in order to verify it is undamaged.
Wet the proximal end of the balloon and mount it on the distal end of the delivery system. The black part of the tube must be completely inserted into the metal ring of the balloon.
Fill in the balloon with recommended volume of 0.7 ml physiological solution to test balloons inflation.
Disconnect the syringe from the delivery system and introduce the stylet into the black tube visible at the proximal end of the delivery system. Place the stylet in the delivery system until the pod reach the stop from the black tube.
Drain the Smart-TO balloon: a simple pressure on the magnetic ball inside the balloon allows fluid to flow. Please watch that at the end of emptying that the magnetic ball returns in contact with the metal ring.
Slowly remove the stylet from the delivery system.
Back up the delivery system in the endoscopic sheath until the balloon is inside (at the edge of the distal part of the endoscopic sheath).

4-3 – Delivery system introduction and balloon positioning
According to the protocol in force, introduce the fetoscope to reach the trachea of the fetus and position the balloon in its optimal position *i.e.* approximately at the carena level. Inject recommended volume of 0.7 ml of sterile physiological solution.
In case of incorrect positioning of the balloon in the trachea, remove the syringe and introduce the stylet in the black tube at the proximal end of the delivery system. Push the stylet into the tube until the pod comes against the black tube.
Drain the Smart-TO balloon: a simple pressure on the magnetic ball inside the balloon allows fluid to flow. Emptying can take up to a minute. After complete deflating of the balloon, slowly remove the stylet from the balloon and then from the delivery system.
Refill the syringe with sterile physiological solution and connect the syringe to the delivery system. Inflate the balloon again by injecting recommended volume of 0.7 ml of sterile physiological solution.

4-4 – Balloon release
Pull gently on the delivery system to release the balloon.

5 – Recommendations for patient

The patient must be under close surveillance conducted at pre-set time intervals and according to established protocols.
At the end of the appropriate period (or before, in case of spontaneous labor or preterm premature rupture of membranes), occlusive Smart-TO balloon should be deflated by presenting the patient in front of an MRI scanner, according to established protocol.

Deflation protocol description:

Deflation protocol takes place in an MRI examination room. To be noted that the fringe field operates near the MRI since the machine is on, with no need for an imaging acquisition. The patient must be positioned in front of the MRI scanner, with her abdomen facing the tunnel. Then she needs to make a quarter turn on herself in front of the middle of the tunnel and turn around the MRI scanner staying close to the machine. On the other side of the machine, once again she will need to position her abdomen facing the tunnel, make a quarter turn in front of the middle of the tunnel and turn around the MRI machine on the other side until the other side of the tunnel. The patient shall then leave the MRI room.
An ultrasound scan should be performed after this procedure to control the balloon deflation. In case the balloon has not been completely emptied, a second surgery should be considered with the patient in order to remove the balloon before the birth.

6 – Complications

The possible complications associated with the use of delivery system for the detachable balloons or treatment procedures by fetal endoscopy include:
- occasional minor access site complication
- occasional preterm premature rupture of the membranes
- occasional premature birth

- improbable allergic reaction due to latex
- unimaginable death of the fetus

7 – Warnings

This device must only be used by a physician or specialist staff members, with the pre-requisite training as well as the experience and training in the technique of fetal endoscopic tracheal occlusion.

8 – Disposal

After use, dispose product and packaging in accordance with hospital, administration and/or local government policy.

9 – Product information disclosure

BS-MTI cannot be sued for damages for improper use of its material.
If the products are damaged or destroyed before use, or if they have a defect during use, keep the product and inform the BS-MTI company.
The return of goods, after agreement from the BS-MTI company, must be in their original packaging.
In case of dispute or appeal, the Court of the head office of BS-MTI is the only competent and the French law is applicable.

Smart-

Delivery system and Smart-TO balloon exclusively made in France

BS-MTI

Medical Tech Industry, 2 rue de l'avenir 67470 Niederroedern France

Certifié DIN en ISO 13485 :2012

Directive 93/42/CEE Medical Device – Annexe II

CE

Date of first CE marking…

Sommaire du résumé étendu en français

1. INTRODUCTION

1.1. Hernie de coupole diaphragmatique

1.1.1. Définition

Le diaphragme se développe chez l'embryon entre la 4ème et la 10ème semaines d'aménorrhée. La hernie de coupole diaphragmatique (HDC) correspond à l'absence de développement de tout ou partie d'une coupole diaphragmatique, avec comme conséquence l'ascension des viscères abdominaux dans le thorax, entrainant la compression des poumons. Les HDC sont le plus souvent gauches (87% gauches, 11% droites, 2% bilatérales) et postérieures. Les défects dorsaux sont appelées hernies de Bochdalek tandis que les défects antérieurs sont appelés hernies de Morgagni (4).

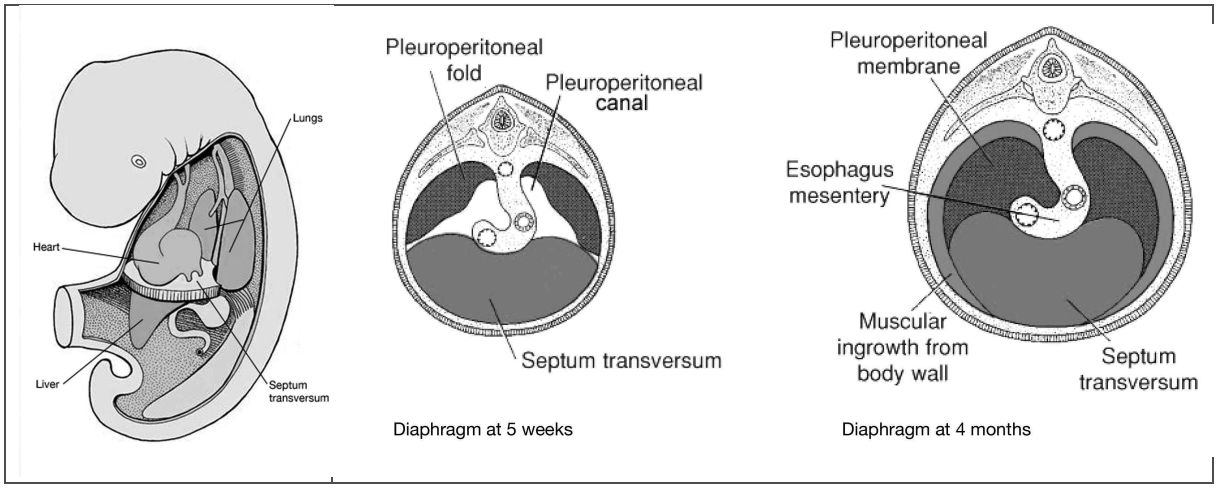

Figure 1: Embryologie du diaphragme (5)
http://www.bionalogy.com/respiratory_system.htm

1.1.2. Épidémiologie

La HDC compte parmi les malformations fœtales les plus classiques et se retrouve dans environ 1/3000 à 1/5000 naissances vivantes (6). Cela n'inclut pas la mortalité prénatale

(fausses couches, morts in utero et interruptions médicales de grossesse) ni les cas de morts néonatales précoces avant transfert dans une maternité de niveau III (7). Ainsi, on estime que la HCD concerne environ 542 à 2168 nouveau-nés chaque année en Europe (8) et 1114 aux États-Unis (9). Les programmes de dépistages anténataux par échographie ont permis de diagnostiquer cette malformation dans la période prénatale dans environ 2 cas sur 3 (10). Il y a environ 40% de hernies qui sont associées à des malformations, des syndromes ou des problèmes génétiques (11, 12). Ces cas-là nécessitent alors une prise en charge spécifique et sont associés à un mauvais pronostic, indépendamment du problème de HCD.

1.1.3. Pronostic

La HCD est associée à une hypoplasie pulmonaire qui touche les voies aériennes elles-mêmes mais aussi les vaisseaux, avec comme conséquence une hypertension pulmonaire. C'est pourquoi il y a environ 30% de mortalité, même dans les centres de niveaux 3, malgré le fait que le diaphragme peut être réparé chirurgicalement après la naissance (19, 20). C'est pourquoi la promotion de la croissance pulmonaire pendant la vie fœtale présente un intérêt.

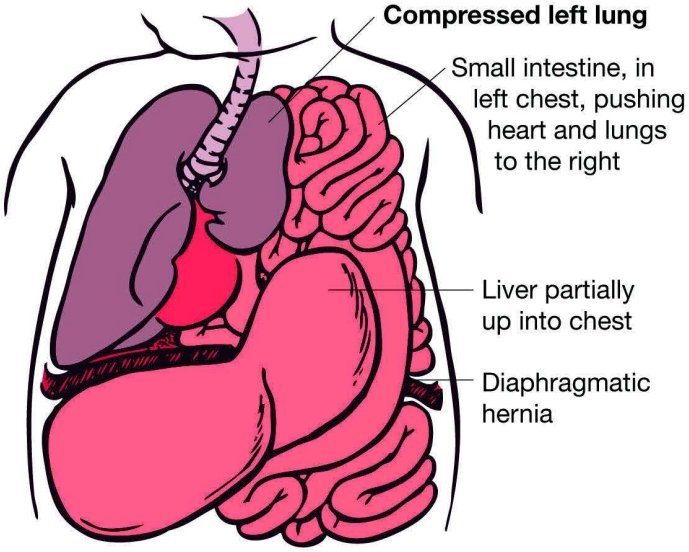

Figure 2: HCD avec compression pulmonaire (21)

https://fetus.ucsfmedicalcenter.org/cdh

Plusieurs facteurs pronostiques prénataux ont été développés. Le principal est le rapport de la mesure du poumon controlatéral sur le périmètre crânien, idéalement rapporté à l'âge gestationnel : observed on expected lung-to-head ratio (O/E LHR) (23, 24). L'existence de foie hernié est également un facteur pronostique(26, 27). Les taux de survie néonatale en fonction du O/E LHR et de la position du foie sont illustrés dans la figure 5. D'autres facteurs pronostiques existent, telles que le volume pulmonaire total ou encore les indices de vascularisation (29). Enfin, le fait de savoir si les hernies droites ont un pronostic similaire ou moins favorable que les hernies gauches est controversé (30-33).

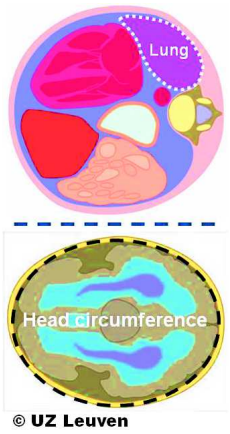

Figure 3: LHR (34)

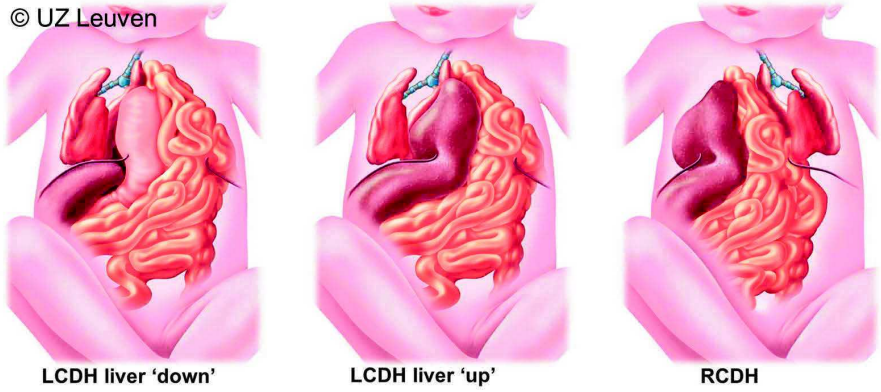

Figure 4: Position du foie et côté de la HCD (34)

http://www.totaltrial.eu/?id=13

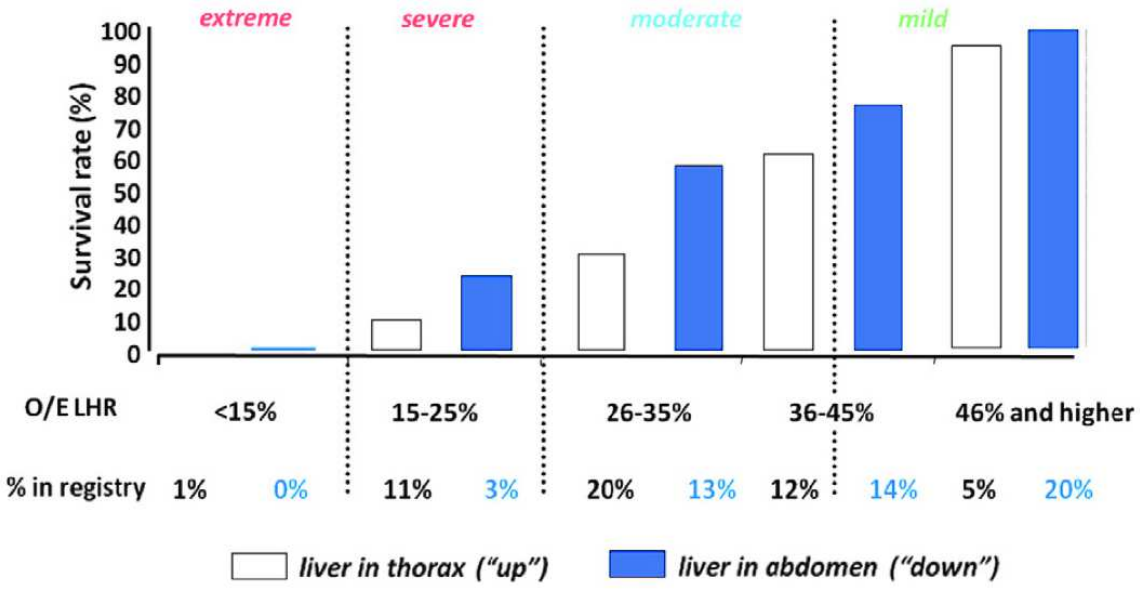

Figure 5: Taux de survie des foetus atteints de HCD gauche, en fonction du O/E LHHR et de la position du foie (28)

1.2. Chirurgie foetale

1.2.1. Occlusion trachéale par endoscopie foetale : aspects techniques

L'occlusion trachéale par endoscopie fœtale (FETO) combine un guidage échographique et une chirurgie endoscopique percutanée. Les aspects techniques ont été décrits par l'équipe de Jan Deprest (49). Cette procédure est réalisée sous anesthésie locale maternelle, sédation et curarisation fœtale. Un endoscope de 1,3 mm dans une gaine de 3 mm est introduit de façon percutanée dans la cavité amniotique puis, sous contrôle de la vue, est introduit dans la bouche du fœtus, jusqu'à la trachée de celui-ci. Un ballonnet gonflable détachable (Goldbal 2, Balt ®) est ensuite mis en place dans la trachée fœtale, entre les cordes vocales et la carène.

Deux essais randomisés internationaux évaluant l'intérêt de la FETO pour les formes sévères et modérées de HCD sont actuellement en cours (NCT01240057 et NCT00763737). L'acronyme utilisé pour cet essai est « TOTAL » (Tracheal Occlusion To Accelerate Lung growth). Dans les formes sévères, la FETO est réalisée entre 20 et 30 semaines, tandis qu'elle est réalisée entre 30 et 32 semaines dans les cas modérés. Le retrait du ballon est prévu vers 34 semaines mais ce point critique est discuté plus tard.

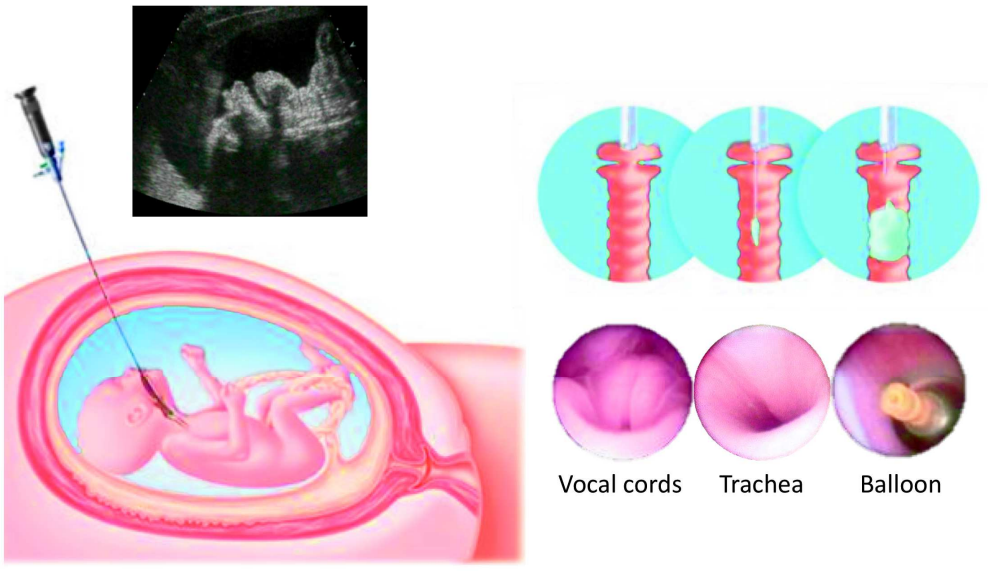

Figure 6: Illustration de la procédure FETO (49)

Instrument	Physical properties	Other specific features
Insertion instruments		
Fetal tracheoscope, 11540AA, Karl Storz	Outer diameter = 1.3 mm Working length = 30.6 cm Opening angle = 70° Angle of view = 0° 17,000 pixels	Deported eye piece (lighter weight) Autoclavable Fiber optic endoscope (allows bending)
Tracheoscopic sheath with 3 side ports, 11540KE, Karl Storz	Outer diameter = 3.3 mm With 2 connections for instruments Working length = 30.6 cm Precurved 30°	Sandblasted tip for increased echogenicity Autoclavable Blunted tip to avoid direct trauma
Balloon removal instruments		
Inner sheath for postnatal tracheoscope, 26161CN, Karl Storz	Outer diameter = 4.3 mm Working channel = 1.7 mm, with stopcock and Luer lock connection	Together with outer sheath, it forms a continuous-flow sheath. Tip is blunted as to avoid trauma.
Continuous-flow fetoscope sheath, 26161CD, Karl Storz	Outer diameter = 5 mm With Luer lock connection	
Third-trimester tracheoscope, 26008FUA, Karl Storz	Outer diameter = 2.0 mm Opening angle = 60° Angle of view = 12° Working length = 26 cm	Autoclavable Rod lens telescope (comes also as 0° [26008AA] or 30° [26008BUA]
Retrieval forceps, 11510C, Karl Storz	Outer diameter = 1.0 mm Length = 35 cm	Semirigid Double-action jaws
Adjustable puncture stylet, 11506P, Karl Storz	Length = 50 cm Outer diameter = 0.4 mm Single use	Movable torquer allows adjustment of length to avoid overintroduction
Other instruments that are generic to fetoscopy		
Trocar, 11650TG	Pyramidal trocar, for introduction of cannula Length = 170 mm	For introduction of cannula
Cannula RCF-10.0, Check-Flo Performer Set, Cook	Outer diameter flexible cannula = 10 Fr Working length = 13 cm	
Single-use balloon and catheter systems (as used by the FETO consortium)		
GVB 16 detachable balloon, Nfocus Neuromedical (Palo Alto, CA) (off-label use)	Latex balloon, with radiopaque inclusion Outer diameter* = 1.5/8.0 mm Length* = 6.5/21 mm	Earlier marketed by Cathnet Science, and before by Nycomed. Recommended filling volume = 0.8 mL
Goldbal 2 detachable balloon, Balt (Montmorency, France) (off-label use)	Latex balloon, with radiopaque inclusion Outer diameter* = 1.5/7.0 mm Length* = 5.0/20.0 mm	Recommended filling volume = 0.6 mL
CIFN Mini-Torquer catheter, Nfocus Neuromedical (off-label use)	Length = 130 cm, tapered microcatheter supple section 20 cm Outer diameter = maximum, 0.X mm Tapered to ward the tip Guiding catheter inner diameter = 0.066"	Comes with mandrel and Toohy-Borst connection. Different lengths available
BALTACCI-BDPE catheter, Balt (off-label use)	Length = 160 cm, tapered microcatheter Outer diameter = maximum, 0.9 mm; minimum, 0.4 mm (tapered toward the tip) with guiding catheter	Comes with mandrel. Toohy-Borst (11510V, Karl Storz) Y- connection can be added. A coaxial double catheter system can be used as well.

Tableau 1 : Instrumentation pour la procédure FETO (49)

Figure 7 : Ballonnets Goldbal (50)

1.2.2. Pronostic après FETO

Un groupe européen a publié les résultats des 210 premiers cas de HCD sévère traités par occlusion trachéale par foetoscopie (51). Alors que la survie attendue des fœtus atteints de HCD gauche sévère est de 24,1%, la survie après chirurgie fœtale par occlusion trachéale était de 49.1% ($p < 0,001$). De même, la survie était significativement augmentée pour les cas de hernies droites, 0% contre 35.3% ($p < 0,001$). Un même effet bénéfique a été rapporté dans d'autres études (52-54). Le premier essai randomisé conduit par Ruano *et al*. a retrouvé également une augmentation du taux de survie, de 4,8% à 50,0% ($p < 0,001$) (55). Deux méta-analyses ont retrouvé également que la FETO permettait d'améliorer la survie en cas de HCD sévère(56, 57). Enfin, la morbidité néonatale des cas sévères traités par occlusion trachéale serait comparable aux cas modérés non traités (70).

1.2.3. Modalités de retrait du ballon

Le rétablissement des voies aériennes fœtales doit être réalisé idéalement avant la naissance, vers 34 semaines. Tout d'abord, le fait de lever l'occlusion trachéale *in utero* a un effet crucial sur la maturation pulmonaire, avec une correction du déficit en pneumocytes de type II et de la sécrétion de surfactant (49, 59, 61-63, 71). La séquence d'occlusion puis de levée de l'occlusion in utero (« plug-unplug sequence ») améliore donc la survie néonatale et est devenue un standard (62, 64, 65). Aussi et surtout, en cas naissance d'un enfant avec la trachée obstruée, la prise en charge néonatale est périlleuse.

La levée de l'occlusion trachéale en prénatal est réalisée au cours d'une autre foetoscopie ou, plus rarement, par ponction écho-guidée du ballonnet (28, 49, 51). La foetoscopie est réalisée selon les mêmes modalités que lors de la pose du ballonnet et consiste au retrait du ballonnet après l'avoir ponctionné sous contrôle de la vue au moyen d'un stylet. Lorsque le ballonnet est ponctionné sous contrôle échographique, il est par la suite spontanément recraché par le fœtus dans le liquide amniotique, en raison de l'hyperpression régnant dans les poumons.

Dans certains cas, la patiente se met en travail et/ou rompt la poche des eaux avant que le ballonnet ait été retiré. Un retrait du ballonnet peut parfois encore être tenté en prénatal, lorsque cela apparaît comme étant techniquement réalisable et sans risque important. Sinon, le ballonnet peut être extrait en *per partum*, lors d'une césarienne conventionnelle ou de façon plus classique, lors d'une procédure EXIT (« ex utero intrapartum treatment ») (49, 66, 67). Cela revient à extraire le ballonnet par trachéoscopie, sur un fœtus partiellement extrait de l'utérus, mais toujours oxygéné via le cordon ombilical, avant de procéder véritablement à l'accouchement. Enfin, lorsque l'enfant naît avec la trachée obstruée, ce qui est la pire des situations, le ballonnet doit être retiré le plus rapidement possible, par trachéoscopie ou par ponction au travers du cou du nouveau-né (49).

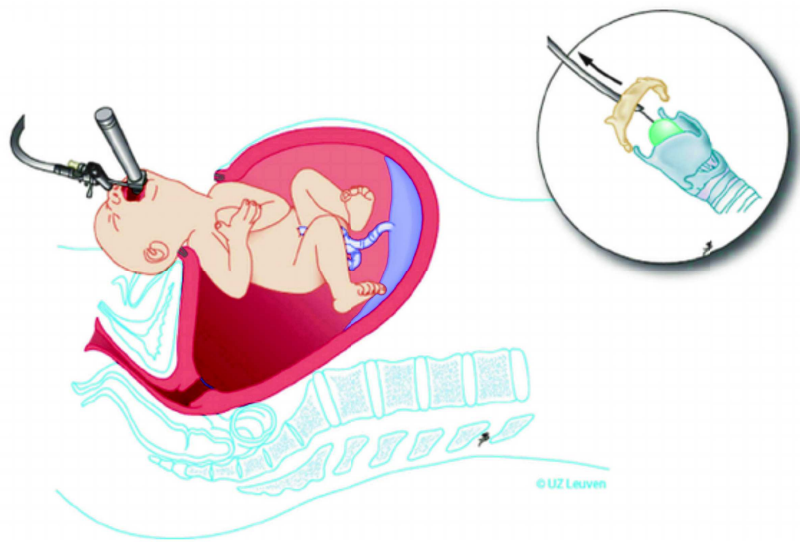

Figure 8 : Retrait du ballonnet sous circulation placentaire (UZ Leuven)

Dans la série historique belge de 210 procédures FETO, le ballonnet avait été retiré *in utero* dans 69% des cas et en *perpartum* dans 23% des cas(49, 51). À noter que dans 8% des cas, il n'y avait pas eu de nécessité de retrait du ballonnet en raison d'une mauvaise insertion de celui-ci, d'une mort in utero, d'une interruption médicale de grossesse, ou encore d'un dégonflement spontané du ballonnet. Dans 56% des cas, le rétablissement des voies aériennes était réalisé dans un contexte d'urgence. L'expérience de retrait du ballonnet de trois centres d'expertise a été récemment publiée avec un total de 302 procédures chez 292 fœtus (2 procédures avaient été nécessaires dans 10 cas) (68). Le ballonnet avait été retiré *in utero* dans 87.4% des cas et en *perpartum* dans 12.3% des cas. Dans 28.1% des cas, le rétablissement des voies aériennes était réalisé dans un contexte d'urgence.

Balloon removal procedure	Elective (n=217; 71.9%)	Emergency (n=85; 28.1%)	Difference of proportions % (95% CI)	Total (n=302)
Ultrasound guided puncture	45 (20.7%)	18 (21.2%)	0.5 (-0.1-0.1)	**63 (20.8%)**
Fetoscopic	171 (78.8%)	30 (35.3%)	43.5 (0.3-0.5)	**201 (66.6%)**
On placental circulation	1 (0.5%)	33 (38.8%)	38.3 (0.3-0.5)	**34 (11.3%)**
Postnatal	0 (0%)	4 (4.7%)	4.8 (-0.03-0.09)	**4 (1.3%)**

Tableau 2 : Techniques de retrait du ballonnet dans 3 centres d'expertise (68)

Dans 9 cas, le rétablissement des voies aériennes a été tenté en dehors d'un centre d'expertise de FETO. Dans trois cas, cela a été impossible, ce qui a conduit au décès du nouveau-né.

1.2.4. Problèmes posés par le retrait du ballonnet

Il s'agit d'une procédure difficile qui requiert une expertise spécifique. Le retrait du ballonnet n'est pas possible in utero dans 12.6 à 24.7% des cas, même dans un centre d'expertise. De plus, le rétablissement des voies aériennes doit être fait dans une situation d'urgence dans 28.1 à 56% des cas. Cela implique que les patientes restent à proximité d'un centre d'expertise pendant toute la durée d'occlusion trachéale, ce qui est souvent difficile en pratique. Les difficultés de retrait du ballonnet peuvent même conduire au décès néonatal, en particulier quand la procédure n'est pas réalisée dans un centre d'expertise. Enfin, le fait de réaliser une procédure prénatale invasive pour retirer le ballonnet est associé à un risque d'accouchement prématuré dans la semaine qui suit l'intervention dans 25% des cas.

1.3. Objectifs

1.3.1. Développement d'un nouveau ballonnet pour l'occlusion trachéale

Notre objectif principal était de développer un dispositif médical intelligent pour l'occlusion trachéale fœtale, permettant un retrait du ballonnet qui soit à la fois simple, non-invasif et actionné par contrôle externe.

Un dispositif avec de telles caractéristiques permettrait de pallier ainsi à chacune des difficultés liées au retrait du ballonnet et donc d'améliorer la survie néonatale :

- RETRAIT SIMPLE DU BALLONNET : Les patientes résidant à distance d'un centre de référence et dont le fœtus est atteint de HCD pourraient bénéficier également d'une occlusion trachéale, à partir du moment où une expertise limitée serait nécessaire à la libération des voies aériennes.

- NON-INVASIF : Une procédure de retrait chirurgical serait alors évitée, ainsi que les conséquences en termes de prématurité induite et de mortalité.

- ACTIONNÉ PAR CONTRÔLE EXTERNE : Le moment de la levée de l'occlusion trachéale pourrait être adapté à chaque situation, en particulier en cas de rupture prématurée des membranes et/ou de début de travail alors que le ballonnet est encore en place.

1.3.2. Modèle du singe pour la FETO

Notre objectif secondaire était de developer le modèle du singe pour la pratique de la FETO, dans l'idée de tester le nouveau ballonet sur un modèle animal le plus proce possible de l'Homme.

1.3.3. Facteurs prédictifs de survie néonatale

L'identification de facteurs pronostiques pertinents est indispensable afin de sélectionner les candidats à la FETO. Nos objectifs secondaires incluaient l'analyse de facteurs prédictifs en lien avec la croissance pulmonaire, la position du foie et de la vascularisation pulmonaire.

1.3.4. Propriétés requises pour les prothèses post-natales

Enfin, nous avons cherché à déterminer la croissance du diaphragme après la naissance, ce qui est un pré-requis indispensable à la conception de prothèses adaptées.

1.4. Références

1. Labbe A, Coste K, Dechelotte PJ. [Congenital diaphragmatic hernia - mechanisms of pulmonary hypoplasia]. Rev Mal Respir. 2011;28(4):463-74.
2. Ackerman KG, Greer JJ. Development of the diaphragm and genetic mouse models of diaphragmatic defects. Am J Med Genet C Semin Med Genet. 2007;145C(2):109-16.
3. Babiuk RP, Zhang W, Clugston R, Allan DW, Greer JJ. Embryological origins and development of the rat diaphragm. J Comp Neurol. 2003;455(4):477-87.
4. Irish MS, Holm BA, Glick PL. Congenital diaphragmatic hernia. A historical review. Clin Perinatol. 1996;23(4):625-53.
5. Dryden R. Formation of respiratory system http://www.bionalogy.com/respiratory_system.htm.
6. Butler N, Claireaux AE. Congenital diaphragmatic hernia as a cause of perinatal mortality. Lancet. 1962;1(7231):659-63.
7. Harrison MR, Bjordal RI, Langmark F, Knutrud O. Congenital diaphragmatic hernia: the hidden mortality. J Pediatr Surg. 1978;13(3):227-30.
8. The EU-27 population continues to grow. [Internet]. Eurostat 2009. 2010.
9. Langham MR, Jr., Kays DW, Ledbetter DJ, Frentzen B, Sanford LL, Richards DS. Congenital diaphragmatic hernia. Epidemiology and outcome. Clin Perinatol. 1996;23(4):671-88.
10. Garne E, Haeusler M, Barisic I, Gjergja R, Stoll C, Clementi M. Congenital diaphragmatic hernia: evaluation of prenatal diagnosis in 20 European regions. Ultrasound Obstet Gynecol. 2002;19(4):329-33.
11. Slavotinek AM. The genetics of congenital diaphragmatic hernia. Semin Perinatol. 2005;29(2):77-85.

12. Stoll C, Alembik Y, Dott B, Roth MP. Associated malformations in cases with congenital diaphragmatic hernia. Genet Couns. 2008;19(3):331-9.
13. Keijzer R, Liu J, Deimling J, Tibboel D, Post M. Dual-hit hypothesis explains pulmonary hypoplasia in the nitrofen model of congenital diaphragmatic hernia. Am J Pathol. 2000;156(4):1299-306.
14. Featherstone NC, Connell MG, Fernig DG, Wray S, Burdyga TV, Losty PD, et al. Airway smooth muscle dysfunction precedes teratogenic congenital diaphragmatic hernia and may contribute to hypoplastic lung morphogenesis. Am J Respir Cell Mol Biol. 2006;35(5):571-8.
15. Jesudason EC, Smith NP, Connell MG, Spiller DG, White MR, Fernig DG, et al. Peristalsis of airway smooth muscle is developmentally regulated and uncoupled from hypoplastic lung growth. Am J Physiol Lung Cell Mol Physiol. 2006;291(4):L559-65.
16. Jesudason EC. Small lungs and suspect smooth muscle: congenital diaphragmatic hernia and the smooth muscle hypothesis. J Pediatr Surg. 2006;41(2):431-5.
17. Areechon W, Eid L. Hypoplasia of lung with congenital diaphragmatic hernia. Br Med J. 1963;1(5325):230-3.
18. Nakamura Y, Yamamoto I, Fukuda S, Hashimoto T. Pulmonary acinar development in diaphragmatic hernia. Arch Pathol Lab Med. 1991;115(4):372-6.
19. Gallot D, Boda C, Ughetto S, Perthus I, Robert-Gnansia E, Francannet C, et al. Prenatal detection and outcome of congenital diaphragmatic hernia: a French registry-based study. Ultrasound Obstet Gynecol. 2007;29(3):276-83.
20. Stege G, Fenton A, Jaffray B. Nihilism in the 1990s: the true mortality of congenital diaphragmatic hernia. Pediatrics. 2003;112(3 Pt 1):532-5.
21. University of California SF-TRotUoC. Congenital diaphragmatic hernia. In: https://fetus.ucsfmedicalcenter.org/sites/fetus.ucsfmedicalcenter.org/files/wysiwyg/cdh.jpg, editor. https://fetus.ucsfmedicalcenter.org/cdh2013
22. Metkus AP, Filly RA, Stringer MD, Harrison MR, Adzick NS. Sonographic predictors of survival in fetal diaphragmatic hernia. J Pediatr Surg. 1996;31(1):148-51; discussion 51-2.
23. Jani J, Nicolaides KH, Keller RL, Benachi A, Peralta CF, Favre R, et al. Observed to expected lung area to head circumference ratio in the prediction of survival in fetuses with isolated diaphragmatic hernia. Ultrasound Obstet Gynecol. 2007;30(1):67-71.
24. Jani JC, Benachi A, Nicolaides KH, Allegaert K, Gratacos E, Mazkereth R, et al. Prenatal prediction of neonatal morbidity in survivors with congenital diaphragmatic hernia: a multicenter study. Ultrasound Obstet Gynecol. 2009;33(1):64-9.
25. Knox E, Lissauer D, Khan K, Kilby M. Prenatal detection of pulmonary hypoplasia in fetuses with congenital diaphragmatic hernia: a systematic review and meta-analysis of diagnostic studies. J Matern Fetal Neona. 2010;23(7):579-88.
26. Mayer S, Klaritsch P, Petersen S, Done E, Sandaite I, Till H, et al. The correlation between lung volume and liver herniation measurements by fetal MRI in isolated congenital diaphragmatic hernia: a systematic review and meta-analysis of observational studies. Prenat Diagn. 2011;31(11):1086-96.
27. Cannie M, Jani J, Chaffiotte C, Vaast P, Deruelle P, Houfflin-Debarge V, et al. Quantification of intrathoracic liver herniation by magnetic resonance imaging and prediction of postnatal survival in fetuses with congenital diaphragmatic hernia. Ultrasound Obstet Gynecol. 2008;32(5):627-32.
28. Deprest J, De Coppi P. Antenatal management of isolated congenital diaphragmatic hernia today and tomorrow: ongoing collaborative research and development. Journal of Pediatric Surgery Lecture. J Pediatr Surg. 2012;47(2):282-90.

29. Ruano R, Takashi E, da Silva MM, Campos JA, Tannuri U, Zugaib M. Prediction and probability of neonatal outcome in isolated congenital diaphragmatic hernia using multiple ultrasound parameters. Ultrasound Obstet Gynecol. 2012;39(1):42-9.
30. Skari H, Bjornland K, Haugen G, Egeland T, Emblem R. Congenital diaphragmatic hernia: a meta-analysis of mortality factors. J Pediatr Surg. 2000;35(8):1187-97.
31. Nagata K, Usui N, Kanamori Y, Takahashi S, Hayakawa M, Okuyama H, et al. The current profile and outcome of congenital diaphragmatic hernia: a nationwide survey in Japan. J Pediatr Surg. 2013;48(4):738-44.
32. DeKoninck P, Toelen J, Zia S, Albersen M, Lories R, Coppi PD, et al. Routine isolation and expansion late mid trimester amniotic fluid derived mesenchymal stem cells in a cohort of fetuses with congenital diaphragmatic hernia. European journal of obstetrics, gynecology, and reproductive biology. 2014;178:157-62.
33. Bryner BS, Kim AC, Khouri JS, Drongowski RA, Bruch SW, Hirschl RB, et al. Right-sided congenital diaphragmatic hernia: high utilization of extracorporeal membrane oxygenation and high survival. J Pediatr Surg. 2009;44(5):883-7.
34. Leuven U. http://www.totaltrial.eu/.
35. Harrison MR, Adzick NS, Longaker MT, Goldberg JD, Rosen MA, Filly RA, et al. Successful repair in utero of a fetal diaphragmatic hernia after removal of herniated viscera from the left thorax. N Engl J Med. 1990;322(22):1582-4.
36. Harrison MR, Adzick NS, Bullard KM, Farrell JA, Howell LJ, Rosen MA, et al. Correction of congenital diaphragmatic hernia in utero VII: a prospective trial. J Pediatr Surg. 1997;32(11):1637-42.
37. Harrison MR, Adzick NS, Flake AW, Jennings RW, Estes JM, MacGillivray TE, et al. Correction of congenital diaphragmatic hernia in utero: VI. Hard-earned lessons. J Pediatr Surg. 1993;28(10):1411-7; discussion 7-8.
38. Khan PA, Cloutier M, Piedboeuf B. Tracheal occlusion: a review of obstructing fetal lungs to make them grow and mature. Am J Med Genet C Semin Med Genet. 2007;145C(2):125-38.
39. Luks FI, Wild YK, Piasecki GJ, De Paepe ME. Short-term tracheal occlusion corrects pulmonary vascular anomalies in the fetal lamb with diaphragmatic hernia. Surgery. 2000;128(2):266-72.
40. Kitano Y, Von Allmen D, Kanai M, Quinn TM, Davies P, Kitano Y, et al. Fetal lung growth after short-term tracheal occlusion is linearly related to intratracheal pressure. J Appl Physiol (1985). 2001;90(2):493-500.
41. Hashim E, Laberge JM, Chen MF, Quillen EW, Jr. Reversible tracheal obstruction in the fetal sheep: effects on tracheal fluid pressure and lung growth. J Pediatr Surg. 1995;30(8):1172-7.
42. Alcorn D, Adamson TM, Lambert TF, Maloney JE, Ritchie BC, Robinson PM. Morphological effects of chronic tracheal ligation and drainage in the fetal lamb lung. Journal of anatomy. 1977;123(Pt 3):649-60.
43. DiFiore JW, Fauza DO, Slavin R, Peters CA, Fackler JC, Wilson JM. Experimental fetal tracheal ligation reverses the structural and physiological effects of pulmonary hypoplasia in congenital diaphragmatic hernia. J Pediatr Surg. 1994;29(2):248-56; discussion 56-7.
44. Hedrick MH, Estes JM, Sullivan KM, Bealer JF, Kitterman JA, Flake AW, et al. Plug the lung until it grows (PLUG): a new method to treat congenital diaphragmatic hernia in utero. J Pediatr Surg. 1994;29(5):612-7.

45. Wilson JM, DiFiore JW, Peters CA. Experimental fetal tracheal ligation prevents the pulmonary hypoplasia associated with fetal nephrectomy: possible application for congenital diaphragmatic hernia. J Pediatr Surg. 1993;28(11):1433-9; discussion 9-40.
46. Benachi A, Dommergues M, Delezoide AL, Bourbon J, Dumez Y, Brunnelle F. Tracheal obstruction in experimental diaphragmatic hernia: an endoscopic approach in the fetal lamb. Prenat Diagn. 1997;17(7):629-34.
47. Harrison MR, Keller RL, Hawgood SB, Kitterman JA, Sandberg PL, Farmer DL, et al. A randomized trial of fetal endoscopic tracheal occlusion for severe fetal congenital diaphragmatic hernia. N Engl J Med. 2003;349(20):1916-24.
48. Deprest J, Gratacos E, Nicolaides KH. Fetoscopic tracheal occlusion (FETO) for severe congenital diaphragmatic hernia: evolution of a technique and preliminary results. Ultrasound Obstet Gynecol. 2004;24(2):121-6.
49. Deprest J, Nicolaides K, Done E, Lewi P, Barki G, Largen E, et al. Technical aspects of fetal endoscopic tracheal occlusion for congenital diaphragmatic hernia. J Pediatr Surg. 2011;46(1):22-32.
50. BALT. Goldballoon. In: BALT, editor.
51. Jani JC, Nicolaides KH, Gratacos E, Valencia CM, Done E, Martinez JM, et al. Severe diaphragmatic hernia treated by fetal endoscopic tracheal occlusion. Ultrasound Obstet Gynecol. 2009;34(3):304-10.
52. Ruano R, Duarte SA, Pimenta EJ, Takashi E, da Silva MM, Tannuri U, et al. Comparison between fetal endoscopic tracheal occlusion using a 1.0-mm fetoscope and prenatal expectant management in severe congenital diaphragmatic hernia. Fetal Diagn Ther. 2011;29(1):64-70.
53. Peralta CF, Sbragia L, Bennini JR, de Fatima Assuncao Braga A, Sampaio Rousselet M, Machado Rosa IR, et al. Fetoscopic endotracheal occlusion for severe isolated diaphragmatic hernia: initial experience from a single clinic in Brazil. Fetal Diagn Ther. 2011;29(1):71-7.
54. Kohl T, Gembruch U, Filsinger B, Hering R, Bruhn J, Tchatcheva K, et al. Encouraging early clinical experience with deliberately delayed temporary fetoscopic tracheal occlusion for the prenatal treatment of life-threatening right and left congenital diaphragmatic hernias. Fetal Diagn Ther. 2006;21(3):314-8.
55. Ruano R, Yoshisaki CT, da Silva MM, Ceccon ME, Grasi MS, Tannuri U, et al. A randomized controlled trial of fetal endoscopic tracheal occlusion versus postnatal management of severe isolated congenital diaphragmatic hernia. Ultrasound Obstet Gynecol. 2012;39(1):20-7.
56. Al-Maary J, Eastwood MP, Russo FM, Deprest JA, Keijzer R. Fetal Tracheal Occlusion for Severe Pulmonary Hypoplasia in Isolated Congenital Diaphragmatic Hernia: A Systematic Review and Meta-analysis of Survival. Ann Surg. 2016;264(6):929-33.
57. Junior EA, Tonni G, Martins WP, Ruano R. Procedure-Related Complications and Survival Following Fetoscopic Endotracheal Occlusion (FETO) for Severe Congenital Diaphragmatic Hernia: Systematic Review and Meta-Analysis in the FETO Era. Eur J Pediatr Surg. 2016.
58. Benachi A, Delezoide AL, Chailley-Heu B, Preece M, Bourbon JR, Ryder T. Ultrastructural evaluation of lung maturation in a sheep model of diaphragmatic hernia and tracheal occlusion. Am J Respir Cell Mol Biol. 1999;20(4):805-12.
59. Benachi A, Chailley-Heu B, Delezoide AL, Dommergues M, Brunelle F, Dumez Y, et al. Lung growth and maturation after tracheal occlusion in diaphragmatic hernia. Am J Respir Crit Care Med. 1998;157(3 Pt 1):921-7.

60. H IJ, Tibboel D. The lungs in congenital diaphragmatic hernia: do we understand? Pediatr Pulmonol. 1998;26(3):204-18.
61. Antunes MJ, Greenspan JS, Cullen JA, Holt WJ, Baumgart S, Spitzer AR. Prognosis with preoperative pulmonary function and lung volume assessment in infants with congenital diaphragmatic hernia. Pediatrics. 1995;96(6):1117-22.
62. Flageole H, Evrard VA, Piedboeuf B, Laberge JM, Lerut TE, Deprest JA. The plug-unplug sequence: an important step to achieve type II pneumocyte maturation in the fetal lamb model. J Pediatr Surg. 1998;33(2):299-303.
63. Bin Saddiq W, Piedboeuf B, Laberge JM, Gamache M, Petrov P, Hashim E, et al. The effects of tracheal occlusion and release on type II pneumocytes in fetal lambs. J Pediatr Surg. 1997;32(6):834-8.
64. Ruano R, Ali RA, Patel P, Cass D, Olutoye O, Belfort MA. Fetal endoscopic tracheal occlusion for congenital diaphragmatic hernia: indications, outcomes, and future directions. Obstetrical & gynecological survey. 2014;69(3):147-58.
65. Snowise S, Johnson A. Tracheal occlusion for fetal diaphragmatic hernia. American journal of perinatology. 2014;31(7):605-16.
66. Morris LM, Lim FY, Crombleholme TM. Ex utero intrapartum treatment procedure: a peripartum management strategy in particularly challenging cases. J Pediatr. 2009;154(1):126-31 e3.
67. Liechty KW. Ex-utero intrapartum therapy. Semin Fetal Neonatal Med. 2010;15(1):34-9.
68. Jimenez JA, Eixarch E, DeKoninck P, Bennini JR, Devlieger R, Peralta CF, et al. Balloon removal after fetoscopic endoluminal tracheal occlusion for congenital diaphragmatic hernia. Am J Obstet Gynecol. 2017.
69. Ali K, Grigoratos D, Cornelius V, Davenport M, Nicolaides K, Greenough A. Outcome of CDH infants following fetoscopic tracheal occlusion - influence of premature delivery. J Pediatr Surg. 2013;48(9):1831-6.
70. Done E, Gratacos E, Nicolaides KH, Allegaert K, Valencia C, Castanon M, et al. Predictors of neonatal morbidity in fetuses with severe isolated congenital diaphragmatic hernia undergoing fetoscopic tracheal occlusion. Ultrasound Obstet Gynecol. 2013;42(1):77-83.
71. Benachi A, Delezoide AL, Chailley-Heu B, Preece M, Bourbon JR, Ryder T. Ultrastructural evaluation of lung maturation in a sheep model of diaphragmatic hernia and tracheal occlusion. Am J Respir Cell Mol Biol. 1999;20(4):805-12.

2. DÉVELOPPEMENT D'UN NOUVEAU BALLON POUR LA FETO

2.1. Solution technique

Une valve de remplissage et de vidange est composée d'un tube métallique ferromagnétique et d'une bille aimantée libre de mouvement à l'intérieur du ballonnet. L'injection de sérum physiologique au travers de la valve repousse légèrement la bille magnétique ce qui permet le remplissage du ballon. Une fois que l'injection est terminée, la bille aimantée se plaque à nouveau sur le tube métallique, garantissant alors l'étanchéité. Quad le ballonnet est placé dans un champ magnétique assez puissant, la bille aimantée est attirée en dehors du tube cylindrique, ce qui provoque la vidange du ballonnet. À noter que quelque soit la direction du champ magnétique dans un hémi-champ de l'espace, l'attraction de la bille en dehors du tube est assurée.

Le champ magnétique utilisé est le camp de fuite d'un appareil d'IRM. Il existe en effet un champ de fuite important autour du cœur de l'IRM, dès lors que la machine est allumée et sans qu'il n'y ait besoin de réaliser une acquisition d'image.

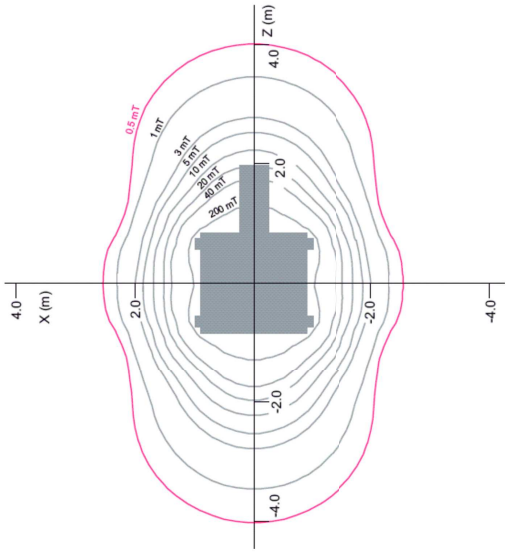

Figure 9 : Champ de fuite d'une IRM Siemens 1.5 T Avanto®

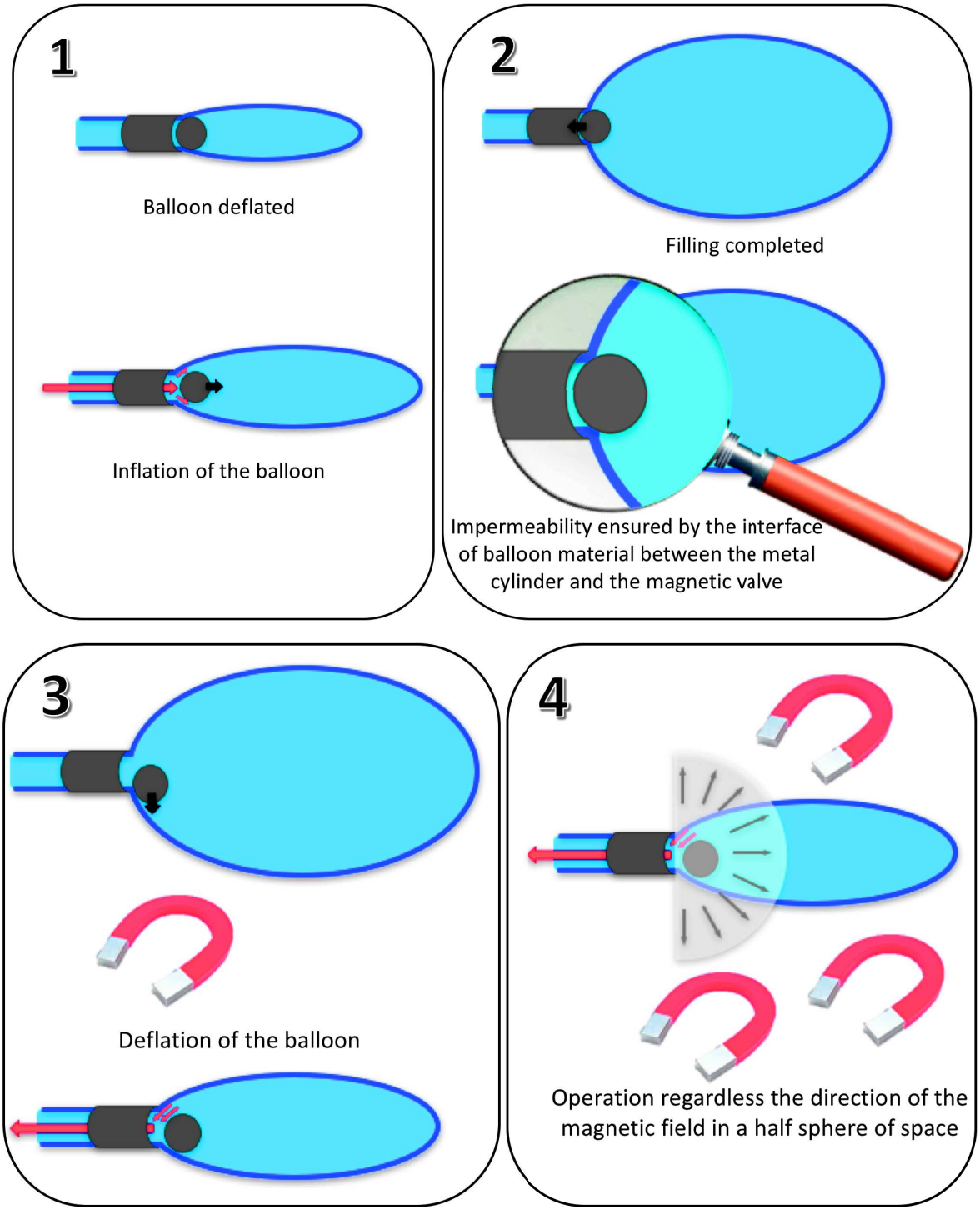

Figure 10 : Principe du fonctionnement du ballon

2.2. Prototypage du ballonnet et du système de pose

2.2.1. Prototypage du ballonnet

Le prototypage du ballonnet a été réalisé en partenariat avec BS Medical Tech Industry (BSMTI), Niedorroedern.

Le ballon est fait de latex et ses dimensions sont de 1.42mm x 6mm lorsqu'il est vide et 7mm x 20mm lorsqu'il est rempli avec 0.7 mL de sérum physiologique. La bille magnétique est incluse dans le ballon et est libre de mouvement. Elle est composée de Neodyme NdFeB / N35 et son diamètreest de 1mm. Le tube cylindrique cylindrique est composé d'un métal ferromagnétique de type 430 et ses dimensions sont de 1.3mm x 3mm. Le tube métallique et la bille aimanté sont tous les deux recouverts de parylène afin d'assurer la biocompatibilité.

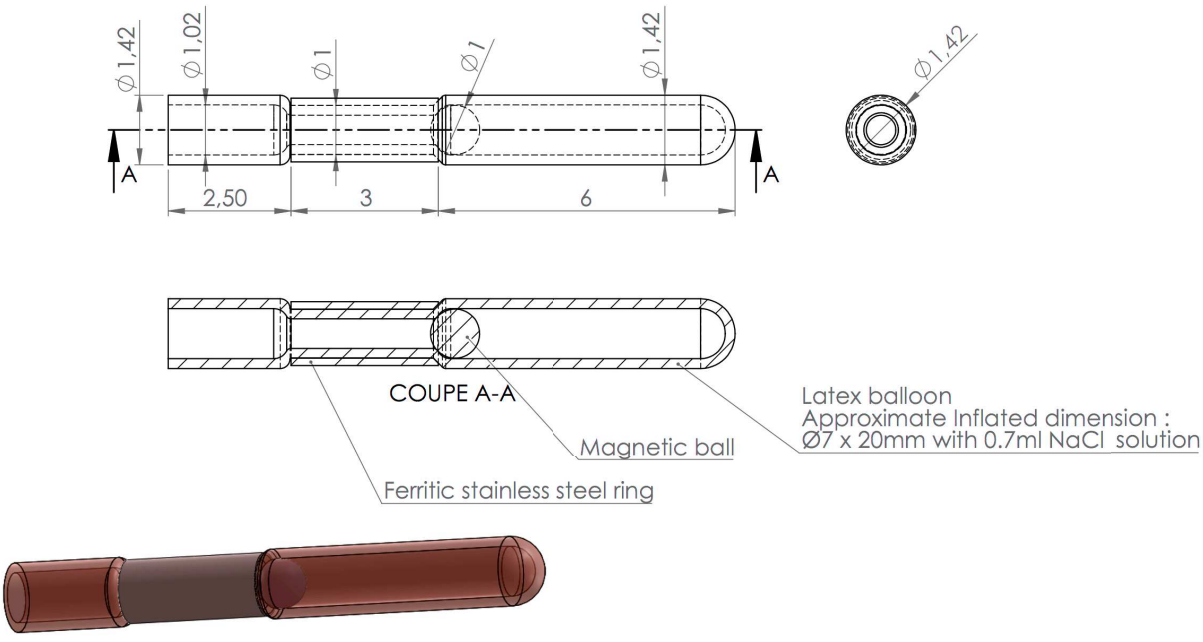

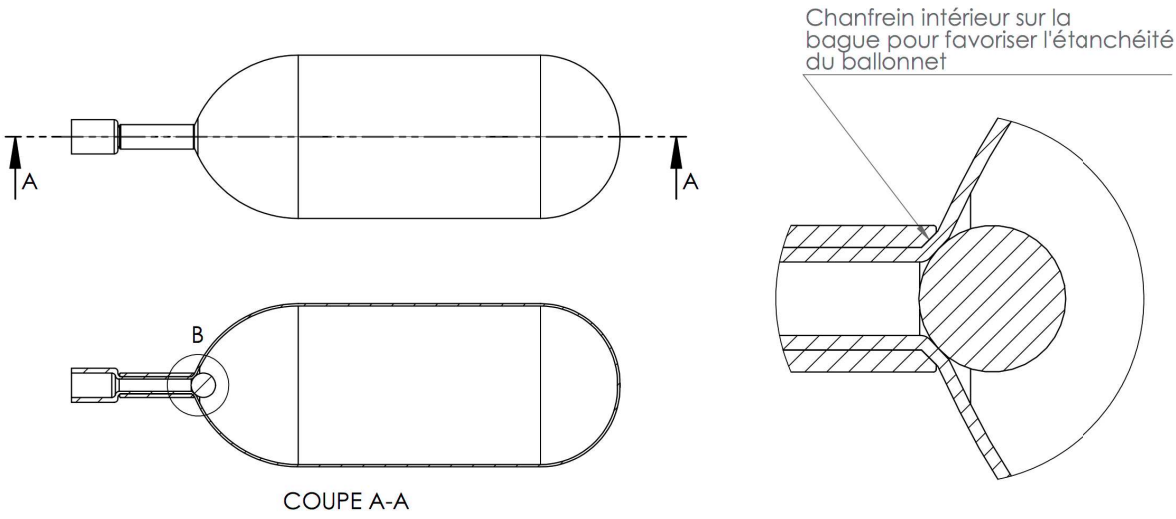

Figure 11 : Schémas du nouveau ballonnet

2.2.2. Preuve de concept

Une preuve de concept avec un premier prototype à l'échelle 1/1 a été conduite devant des machines d'IRM de 1.5 et 2 Teslas. Le positionnement du ballonnet à environ 30-40 cm devant le cylindre de l'IRM (soit environ 40 mT) provoquait sa vidange immédiate. Le prototype a aussi été testé sur simulateur et un aimant de 40 mT avec les mêmes résultats.

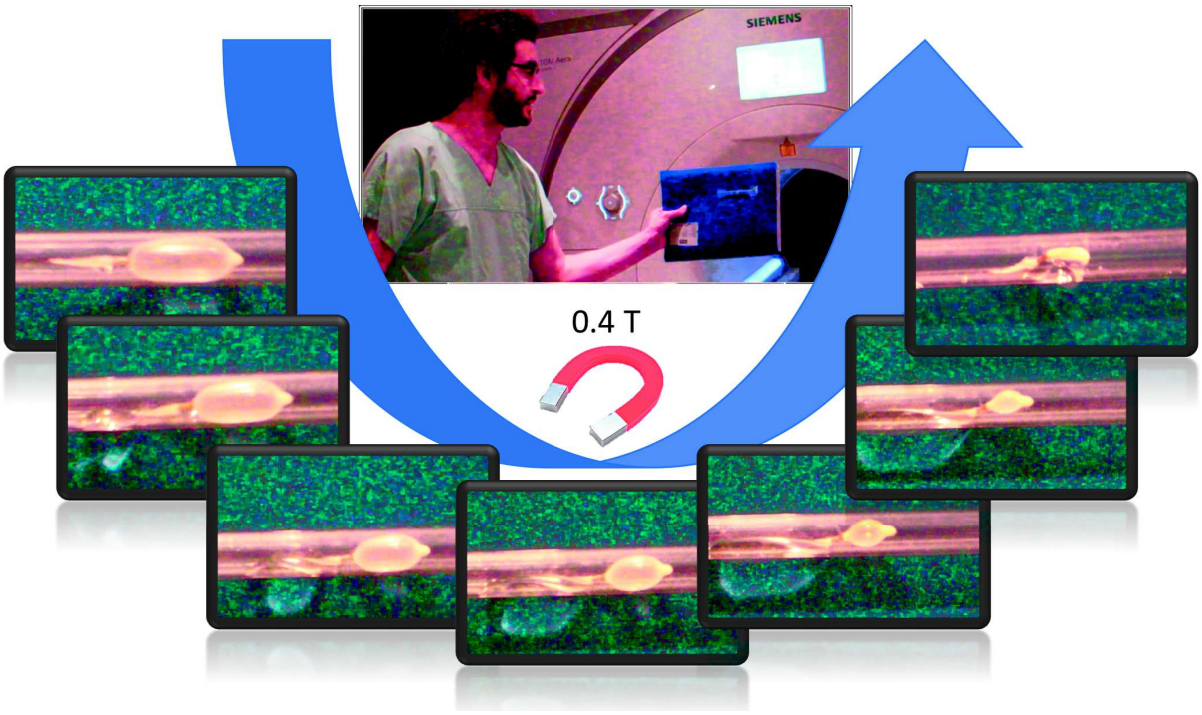

Figure 12: Preuve de concept devant l'IRM

Placement of the balloon on the catheter before moving back inside the fetoscope

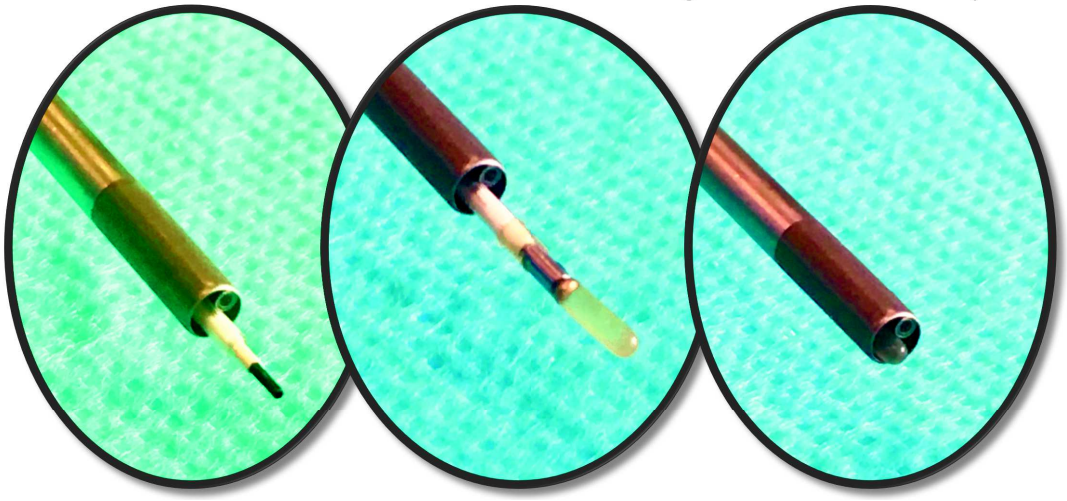

High-fidelity simulator for FETO, endoscopic instruments, balloon and delivery catheter

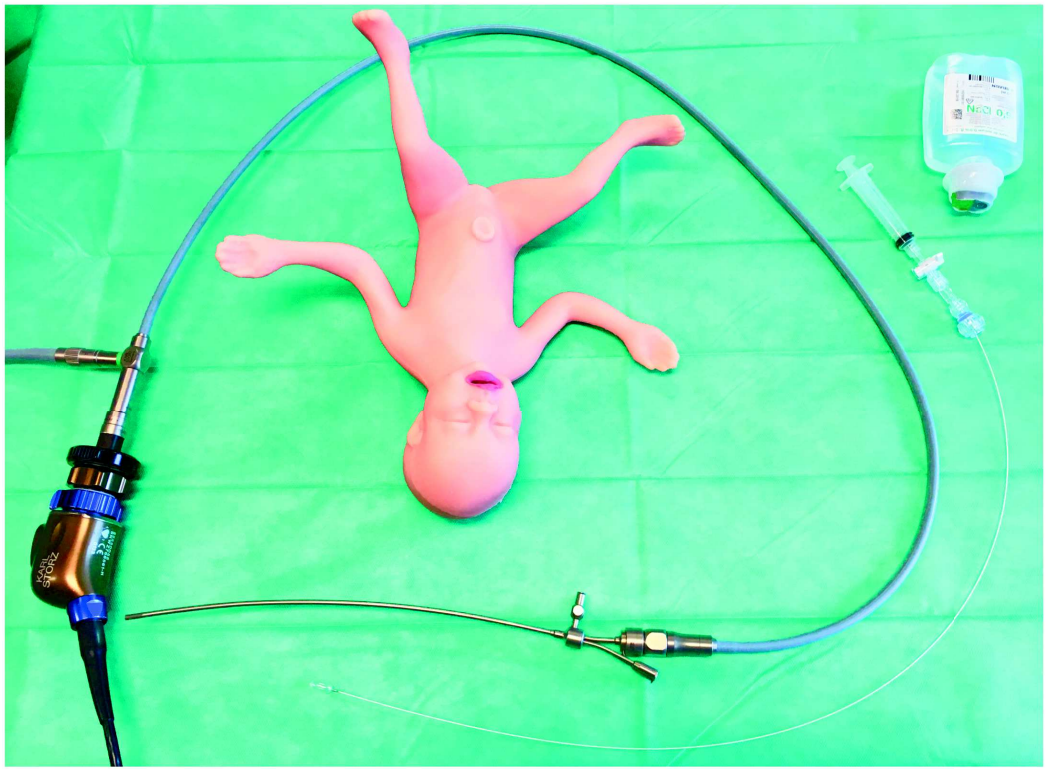

Balloon inflated inside the trachea

Saline coming out from the balloon

Balloon deflated inside the trachea

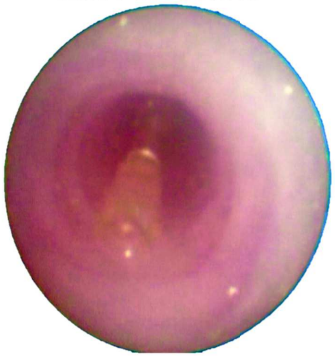

Figure 13 : Preuve de concept sur simulateur

2.2.3. Prototypage du système de pose

Le système de pose est composé d'un triple tube. Un tube interne au travers duquel le sérum physiologique est injecté. Un tube intermédiaire bloquant le tube métallique afin que le tube interne ne pénètre pas dans le ballonnet lui-même. Un tube externe ayant le même diamètre que le ballonnet afin d'éviter que le ballonnet ne se désinsère au moment où le système est reculé dans la chemise du foetoscope.

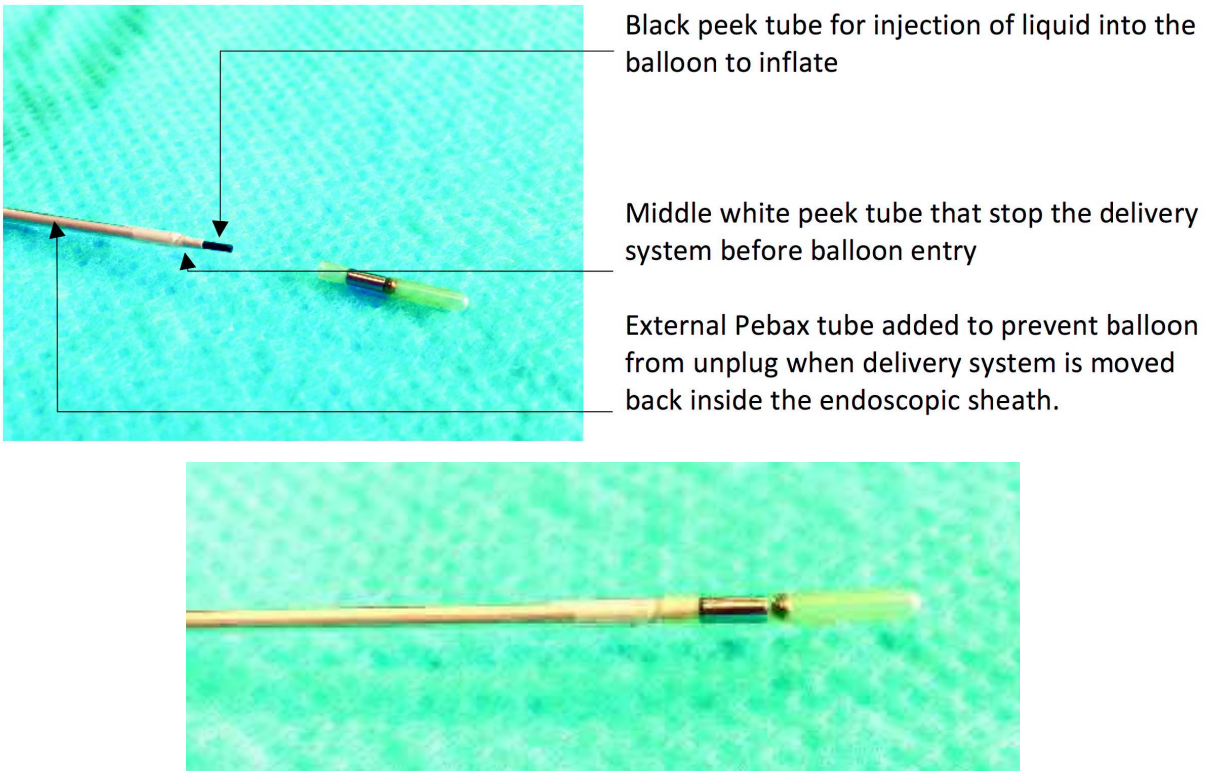

Figure 14 : Système de pose

2.3. Propriété intellectuelle

Un dépôt de brevet a été réalisé en mai 2016 (demande 1653954 / soumission 1000345616): 'BALLONNET GONFLABLE ET DÉTACHABLE, DESTINÉ À ÊTRE IMPLANTÉ DANS UNE CAVITÉ CORPORELLE, NÉCESSAIRE DE TRAITEMENT ET PROCÉDÉ DE VIDANGE ASSOCIÉS'.

2.4. Tests

2.4.1. Tests in vitro.

Des tests d'étanchéité et d'occlusion ont été réalisés. Ils ont montré que les ballonnets étaient bien étanches et conservaient leur caractère d'occlusion sur au moins 6 semaines d'observation.

Des tests de fonctionnement devant une IRM 1,5 T ont été réalisés. Un total de 40 tests ont été réalisés selon 3 différentes hauteurs et 4 angles différents (β=0°, 30°, 60°, and 90°). Le fait présenter le ballonnet devant le tunnel de l'IRM puis de tourner autour provoquait la vidange dans 100% des cas.

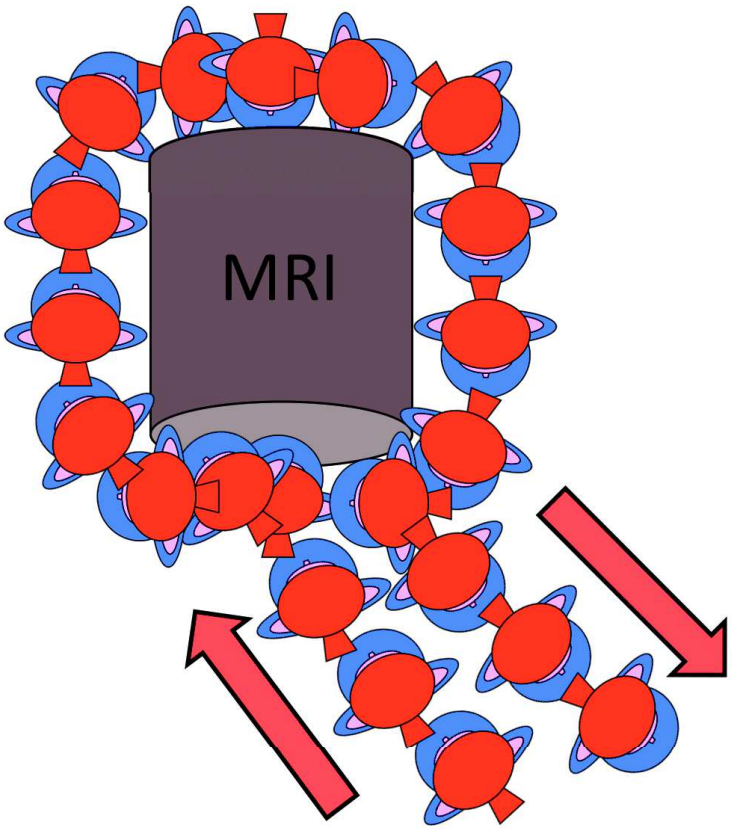

Figure 15 : Rotation de la patiente autour de l'IRM necessaire à induire la vidange

2.4.2. Tests animaux

Une première expérimentation a été réalisée sur le modèle du singe macaque rhésus au sein de la plateforme SILABE. Un ballonnet a été posé par foetoscopie chez une guenon à 139 jours de gestation. Une semaine après le ballonnet était toujours en place, sans modification substantielle de sa forme. La guenon a été positionné devant une IRM de 1.5 T de la plateforme d'imagerie. Le ballonnet n'était plus visible en échographie et la radiographie standard de contrôle a mis en évidence que le ballonnet avait bien été expulsé dans la poche des eaux par le fœtus.

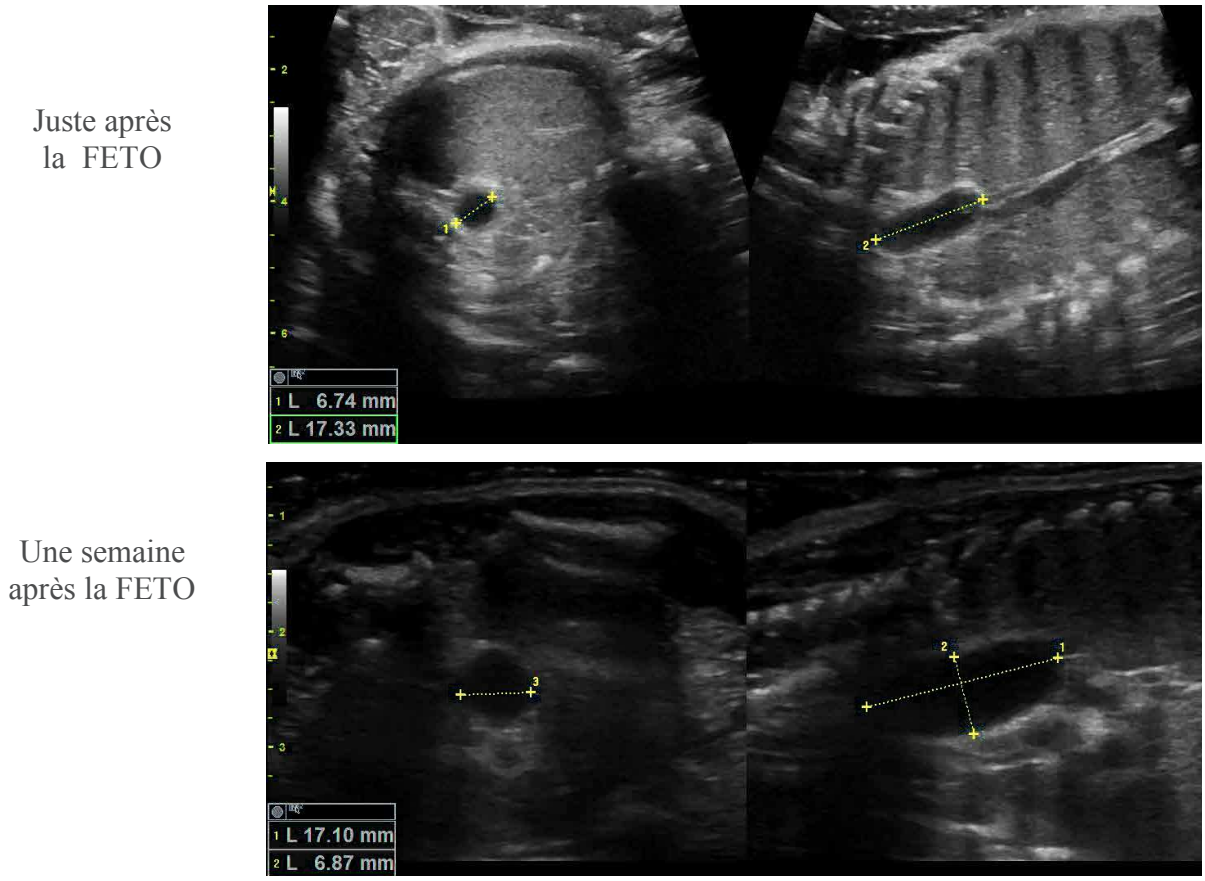

Figure 16 : Ballonnet dans la trachée juste après et une semaine après la FETO

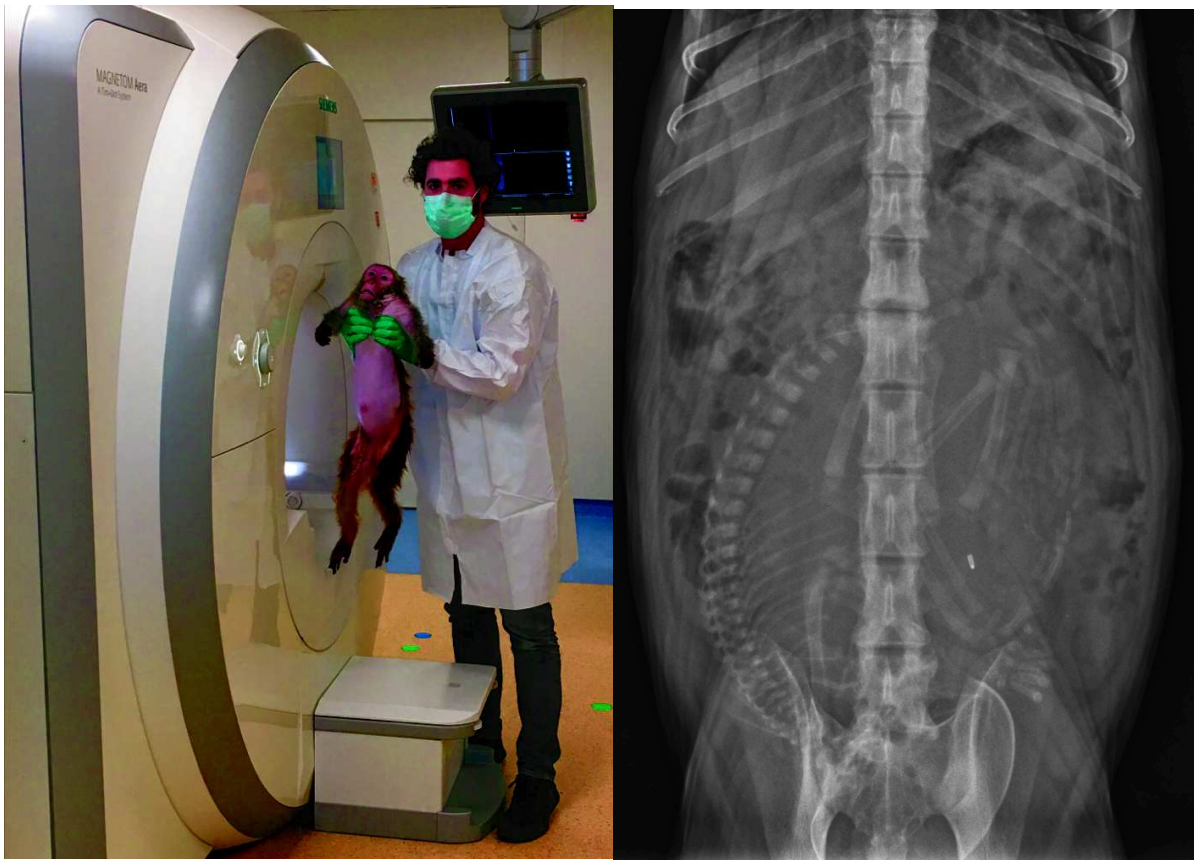

Figure 17 : Singe devant l'IRM et contrôle radiographique

2.5. Conclusion

Nous avons pu développer un ballonnet avec les spécifications que nous avions préalablement définies. Les premiers tests sont encourageants. Des tests avancés sur la brebis sont prévus ainsi qu'une analyse du chemin réglementaire nécessaire à une commercialisation.

Nicolas SANANÈS

Développement d'un dispositif médical innovant pour la prise en charge prénatale de la hernie de coupole diaphragmatique

Development of a new device for the prenatal care of congenital diaphragmatic hernia

Résumé

Nous avons développé un nouveau ballonnet pour l'occlusion trachéale fœtale par endoscopie (FETO) qui permet une levée de l'occlusion facile, par contrôle externe et non-invasive. Ce ballonnet « Smart-TO » permet d'éviter les problèmes liés au rétablissement des voies aériennes. La solution technique est basée sur une valve magnétique dont l'ouverture est contrôlée par le champ de fuite d'une IRM. L'ouverture de la valve provoque la vidange du ballonnet, qui est ensuite expulsé par les sécrétions pulmonaires.

Les tests d'imperméabilité, d'occlusion et de fonctionnement sont prometteurs. Une toute première expérimentation sur le modèle du singe a montré la bonne fonctionnalité et fonctionnement du ballonnet « Smart-TO ». D'autres tests *in vitro* ainsi que d'autres tests animaux sont prévus. Un brevet a été déposé en 2016.

Une analyse de risques préliminaire, une exploration des chemins réglementaires et une étude de marché ont été initiés mais sont encore en cours.

Mots-clés : Hernie de coupole diaphragmatique, occlusion trachéale fœtale par endoscopie, ballonnet.

Abstract

We developed a new balloon for Fetal Endoscopic Tracheal Occlusion (FETO) which allows an easy, remotely controlled, and non-invasive reversal occlusion. This 'Smart-TO' balloon allows to overcome issues related to the airway reestablishment. The technology solution is based on a magnetic valve whose opening is actuated by the fringe field of an MRI scanner. The opening of the valve induces the deflation of the balloon, which is then washed out by the fluid coming out from the lungs.

The impermeability, occlusion, and operation tests are promising. A very first experimentation on the monkey model showed appropriate functionality and operation of the 'Smart-TO' balloon. Further *in vitro* and animal tests are planned. A patent has been filed in 2016.

Preliminary risk analysis, regulatory routes exploration, and market study have been started but are still ongoing.

Key-words: Congenital diaphragmatic hernia, Fetal Endoscopic Tracheal Occlusion, balloon.